Title
Molecular mechanisms of organic cation transport in ephithelia

Author
Zhang, Lei,

Publication Date
1998

Peer reviewed|Thesis/dissertation

Molecular Mechanisms of Organic Cation Transport in Epithelia

by

Lei Zhang

DISSERTATION

Submitted in partial satisfaction of the requirements for the degree of

DOCTOR OF PHILOSOPHY

in

Pharmaceutical Chemistry

in the

GRADUATE DIVISION

of the

UNIVERSITY OF CALIFORNIA SAN FRANCISCO

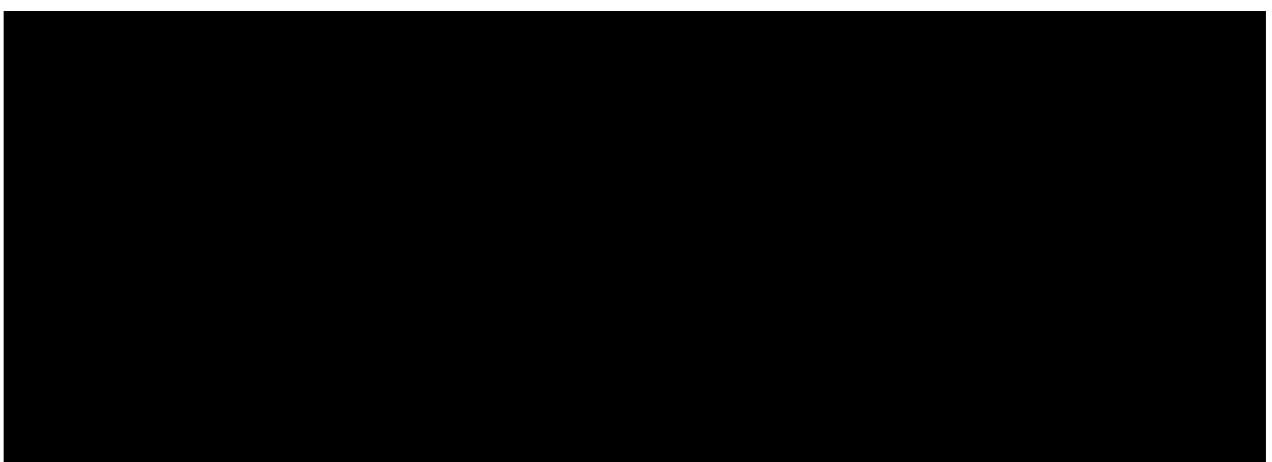

Date University Librarian

Degree Conferred: .....

To my parents and my husband

ACKNOWLEDGMENTS

As I reflect on my challenging and rewarding graduate life at UCSF, I am struck by how quickly the time has passed. Now that I have finished, I have so many people to acknowledge. First of all, I would like to convey my sincerest thanks to my research advisor, Dr. Kathleen M. Giacomini, for her great mentorship, support and friendship. Without her, my graduate experience at UCSF would have been very different. Kathy has been an incredible role model for me, and I could not ever wish for a better advisor. During my graduate studies at UCSF, especially in Dr. Giacomini's research group, I had the unique opportunity to receive an excellent education in molecular biology, drug transport and pharmacokinetics, as well as a broad basic understanding in diverse disciplines, such as medicinal chemistry, structural biology, clinical pharmacology, etc.

I would also like to thank Drs. Leslie Z. Benet and Wolfgang Sadee, members of my thesis and orals committees, for their timely and critical review of this dissertation. I would like to give special thanks to Dr. Benet who was the Chairman of my orals committee. Dr. Benet not only offered great help during my orals, but also carefully reviewed my thesis and gave me great suggestions. Heartfelt thanks to my other orals committee members, Drs. Harlan E. Ives, Lily Y. Jan, and Martin D. Shetlar, each gave me the benefit of their insight and knowledge. I thank the UCSF Chancellor's Research Fellowship for the financial support during the last academic year.

I thank Dr. Claire M. Brett for her mentorship, friendship and warm gifts. Claire has been a wonderful collaborator, mentor and friend. I shall miss the banana cakes she made. Thanks also to Drs. Deanna L. Kroetz, Svein Øie, and Jelveh Lameh for fruitful

discussions, advice and useful help especially during my orals. Thanks to Dr. Christine Guthrie for critical review of my manuscript (Chapter 4).

I have been fortunate to share a laboratory with the nicest people. Specifically, I would like to thank Dr. Joanne K. Chun, Mark J. Dresser, Dr. Marci E. Schaner, Carlo E. Bello, Dr. Shigeyuki Terashita, Wenche Gorset, Ernest K. Lau, and Dr. Micheline Piquette-Miller for helping me with my thesis projects. Special thanks also to numerous members (past and present) of the KMG group and the Department whom I have worked with and learned from for the last four years: Karin M. Gerstin, Dr. Vikram Ramanathan, Silja Thomassen, Juan Wang, Dr. Carla B. Washington, Dr. Shoshana Zevin, Philip Yook, Dr. Laurent Salphati, Dr. Mark Grillo, Dr. Ming Covitz and many others. Special thanks also to Alan Lee who scanned most of the nice gel pictures for me. I also thank Liza Crosse, Judi Mozesson, Vivian Tucker, Kim Bivens, and Gloria Johnson for all their help through my years here. They are wonderful.

Special thanks to Dr. Norman J. Oppenheimer for providing me with the opportunity to work in his laboratory before attending the Ph.D. program at UCSF. He taught me a lot and broadened my views.

Heartfelt thanks also to my family members, Mom, Dad, Brother, Sister-in-Law and my little nephew whom I haven't met yet, for their love, encouragement and unyielding support across the Pacific Ocean from Shanghai, China. Thanks to my friends, Chengnong Shao, Jin Xu, and Ying Wu for the friendship we have held for all these years.

Last but not least, I would like to thank Yuanchao (Derek) Zhang, my wonderful husband, for his love, support, encouragement and friendship.

Lei Zhang

July, 1998

Annual Reviews

4139 El Camino Way
P.O. Box 10139
Palo Alto, CA 94303-0139
Telephone: (650) 493-4400
FAX: (650) 855-9815
URL: http://www.AnnualReviews.org

FAX

Date: June 29, 1998

Number of pages including cover sheet 3

TO:	Lei Zhang
	UC San Francisco
	Dept. of Bipharmaceutical Sciences
Phone	
Fax	415-476-8258 0681

FROM:	Jeanne M. Kunz Permissions Department
	Annual Reviews, Inc.
	4139 El Camino Way
	P.O. Box 10139
	Palo Alto, CA 94303-0139
	USA
Phone	(650) 843-6635
Fax Phone	(650) 855-9815
e-mail	JKunz@annurev.org

CC:

REMARKS: ☐ Urgent ☐ For your review ☐ Reply ASAP ☐ Please Comment

To: Lei Zhang Re your permission request

I emailed the following response to your email this morning. I just received your fax, so in case my reply is lost in cyberspace, I am faxing this to you now.

Permission is granted to use the referenced material in your dissertation, provided you use the following acknowledgment: "With permission, from the Annual Review of Pharmacology and Toxicology, Volume 38, copyright 1998, by Annual Reviews."

We do, however, need you to email us with the specific pages or portions that you plan to use in your dissertation for our records here.

FYI: When Annual Reviews copyright materials are placed on a web site, the above acknowledgment must be shown as indicated along with a hypertext link showing our URL: http://AnnualReviews.org

Good luck on your dissertation!

Sincerely,

Jeanne M. Kunz
Permissions Department

The Journal of Biological Chemistry
9650 Rockville Pike
Bethesda, MD 20814
301-530-7150 (TEL)
301-571-1824 (FAX)
Email: lwest@asbmb.faseb.org.

FACSIMILE TRANSMISSION

DATE: June 30, 1998

TO: Lei Zhang

FAX #: 415-476-0688

Please note your recent request for copyright permission has been granted for the following: Cloning and functional Characterization of a rat renal organic cation transporter isoform (rOCT1A), JBC 272(26): 16548-16554, 1997).

Please note your original will follow by mail only if requested. For future requests. I can be contacted by email at lwest@asbmb.faseb.org. If you have any questions concerning this matter, please contact me at the number listed above.

Sincerely yours,

PERMISSION GRANTED
contingent upon obtaining that of the author

Lanette West

for the copyright owner
THE AMERICAN SOCIETY FOR BIOCHEMISTRY
& MOLECULAR BIOLOGY

Lanette West
Office Manager

AMERICAN SOCIETY FOR PHARMACOLOGY AND EXPERIMENTAL THERAPEUTICS

9650 Rockville Pike **Bethesda, Maryland 20814-3995**

Phone: (301) 530-7060
Fax: (301) 530-7061

Email: aspetinfo@faseb.org
Internet: http://www.faseb.org/aspet/

June 12, 1998

Ms. Lei Zhang
Dept of Biopharmaceutical Sciences
Univ of California, San Francisco
513 Parnassus Ave
Box 0446
San Francisco, CA 94143-0446

Dear Ms. Zhang:

We are pleased to grant you non-exclusive permission to reproduce the material from our publication as stated in your request (copy attached).

Please cite the source.

Sincerely yours,

Richard Dodenhoff
Journals Director

Attachment

RD:av

UCSF

University of California, San Francisco...A Health Sciences Campus

Lei Zhang
Department of Biopharmaceutical Sciences
513 Parnassus Avenue
Box 0446
San Francisco, California
94143-0446

415/476-6756
FAX: 415/476-0688
E-mail: leizhang@cgl.ucsf.edu

May 14, 1998

Debbie Heise
Rights and Permissions
Williams & Wilkins
351 W. Camden St
Baltimore, MD 21201-2436

Dear Ms. Heise,

I am writing to obtain copyright permission to reprint two articles which appeared in *Molecular Pharmacology* in 1997 and *The Journal of Pharmacology and Experimental Therapeutics* in 1998 (in press) as part of my Ph.D. dissertation at the University of California, San Francisco. The titles of the articles are "Cloning and functional expression of a human liver organic cation transporter" (*Molecular Pharmacology* 51:913-921, 1997) and "Functional characterization of an organic cation transporter (hOCT1) in a transiently-transfected human cell line (HeLa)" (*The Journal of Pharmacology and Experimental Therapeutics*, in press, 1998), respectively.

Please write or fax the permission to me. My fax number is 415-476-0688.

Thank you very much for your assistance.

Sincerely,

Lei Zhang

ABSTRACT

Molecular Mechanisms of Organic Cation Transport in Epithelia

Lei Zhang

Polyspecific organic cation transporters are critical in the absorption, targeting, and elimination of many endogenous bioactive amines and cationic drugs. It has become increasingly clear that multiple mechanisms are involved in organic cation transport in the key tissues responsible for drug absorption and disposition: the kidney, liver and intestine. With the availability of cloned organic cation transporters, it is possible to delineate the functional characteristics of various transporters. The major goals of my thesis work were to determine the mechanisms of organic cation transport in the kidney, to clone organic cation transporters and to elucidate their functional characteristics in heterologous expression systems. I found that the mechanisms of guanidine transport in rat renal brush-border membrane vesicles differed from those of TEA transport suggesting that different guanidine and TEA transporters are present in the kidney. In addition, I cloned the first organic cation transporter splice variant, rOCT1A, from rat kidney and the first human organic cation transporter, hOCT1, from liver. I found that hOCT1 differs from rOCT1 both in terms of the tissue distribution and intrinsic function. I developed a mammalian expression system in a human epitheloid carcinoma cell line, HeLa, to carry out detailed functional studies. Because of the clinical importance of hOCT1, I focused on studying the role of hOCT1 in the elimination of therapeutically important drugs and its structure-function relationships in predicting potential drug-drug interactions. I found that HIV protease inhibitors are potent inhibitors but poor substrates of hOCT1. hOCT1 may not

play a role in the elimination of these agents. To study the structural requirements for interacting with and being translocated by hOCT1, I used a series of n-tetraalkylammonium (n-TAA) compounds. I found that with increasing alkyl chain length (≥ 2), n-TAA compounds are more poorly translocated by hOCT1 although their potency of inhibition increases. Similar findings were obtained for nonaliphatic organic cations. The results suggest that small hydrophilic cationic drugs will be translocated by hOCT1 whereas large hydrophobic drugs will be potent inhibitors but will not be translocated. Potential drug-drug interactions at the level of transport may occur between hydrophilic and hydrophobic compounds. The results of my thesis have greatly advanced our understanding of the role of organic cation transporters in the elimination of drugs. The functional characterization of cloned organic cation transporters is critical in the development of *in vitro* functional assays for candidate drug screening in early drug discovery and development. Such information is essential in predicting pharmacokinetics and pharmacodynamics and in the design and development of cationic drugs.

Kathleen M. Giacomini

TABLE OF CONTENTS

ACKNOWLEDGMENTS iv

ABSTRACT x

LIST OF TABLES xxii

LIST OF FIGURES xxv

CHAPTER 1

ROLE OF ORGANIC CATION TRANSPORTERS IN DRUG ABSORPTION AND ELIMINATION

1.1 Introduction 1

1.2 Characteristics of Epithelia, Transporters and Transport 4

1.2.1 Epithelia and Transporters 4

1.2.2 Mechanisms of Transport 6

1.3 Organic Cation Transport 10

1.3.1 Kidney 12

1.3.1.1 General Structure and Function 12

1.3.1.2 Processes Involved in Renal Handling of Drugs 13

1.3.1.3 Organic Cation Transport 14

1.3.2 Liver 19

1.3.2.1 General Structure and Function 19

1.3.2.2 Organic Cation Transport 22

1.3.3 Intestine 26

1.3.3.1 General Structure and Function 26

1.3.3.2 Organic Cation Transport 30

1.4 Aims and Outline of This Thesis 33

1.4.1 Chapter 2 34

1.4.2 Chapter 3 35

1.4.3 Chapter 4 36

1.4.4 Chapter 5 36

1.4.5 Chapter 6 37

1.4.6 Chapter 7 38

1.4.7 Chapter 8 39

CHAPTER 2

TRANSPORT OF GUANIDINE IN RAT RENAL BRUSH-BORDER MEMBRANE VESICLES

2.1 Introduction 40

2.2 Materials and Methods 42

2.2.1 Preparation of Brush-Border Membrane Vesicles (BBMV) 42

2.2.2 Transport Studies 42

2.2.3 Analytical Methods 43

2.2.4 Data Analysis 43

2.2.5 Materials 43

2.3 Results 44

2.3.1 Effect of an Outwardly-Directed Proton Gradient on Guanidine and TEA Uptake 44

2.3.2 Effect of Membrane Potential on Guanidine Uptake 49

2.3.3 Concentration Dependence of Guanidine Uptake 49

2.3.4 *Trans*-Stimulation Effect on Guanidine and TEA Uptake 51

2.4 Discussion 59

CHAPTER 3

EXPRESSION OF RAT RENAL GUANIDINE TRANSPORT ACTIVITY IN XENOPUS LAEVIS OOCYTES

3.1 Introduction 61

3.2 Materials and Methods 63

3.2.1 Isolation and Size-Fractionation of Poly(A)$^+$ RNA 63

3.2.2 Molecular Cloning 63

3.2.3 Oocyte Preparation and Functional Assay 64

3.2.4 Data Analysis 66

3.2.5 Materials 66

3.3 Results 66

3.3.1 Initial Characterization of Expression of Guanidine Transport Activity 66

3.3.2 Inhibition Studies 67

3.3.3 Kinetics of Guanidine Transport 71

3.3.4 Effect of pH and Potential on Guanidine Transport in Rat Kidney mRNA-Injected Oocytes 71

3.3.5 Uptake of ^{14}C-Guanidine in Oocytes Expressing rOCT1 and rOCT2 75

3.3.6 Effects of pH and Potential on Guanidine Transport in rOCT2 cRNA-Injected Oocytes 75

3.4 Discussion 81

CHAPTER 4

CLONING AND FUNCTIONAL CHARACTERIZATION OF A RAT RENAL ORGANIC CATION TRANSPORTER ISOFORM (rOCT1A)

4.1 Introduction 84

4.2 Materials and Methods 86

4.2.1 cDNA Cloning 86

4.2.2 Genomic DNA Cloning 87

4.2.3 Mutagenesis of rOCT1A 88

4.2.4 Sequence Analysis 88

4.2.5 *Xenopus Laevis* Oocytes and ^{14}C-TEA Transport Measurements 89

4.2.6 *In Vitro* Translation and SDS-Polyacrylamide Gel Electrophoresis Analysis 89

4.2.7 RNase Protection Assay 90

4.2.8 Data Analysis 90

4.2.9 Materials 90

4.3 Results and Discussion 91

4.3.1 Detection of a Novel Isoform of the mRNA Transcript of rOCT1 in the Rat Kidney 91

4.3.2 Functional Expression in *Xenopus Laevis* Oocytes 93

4.3.3 DNA Sequencing and Primary Amino Acid Sequence 96

4.3.4 Genomic DNA Cloning 101

4.3.5 *In Vitro* Translation 103

4.3.6 Functional Expression of Synthetic Constructs 105

4.3.7 RNA Expression of rOCT1A and Its Tissue Distribution 109

CHAPTER 5

MOLECULAR CLONING AND FUNCTIONAL EXPRESSION OF A HUMAN LIVER ORGANIC CATION TRANSPORTER

5.1 Introduction 113

5.2 Materials and Methods 115

5.2.1 Isolation and Subcloning of OCT1-Like Homologous PCR Fragments From Human Liver cDNA 115

5.2.2 DNA Amplification of the cDNA 5'- and 3'-Ends and the Full-Length cDNA 116

5.2.3 Sequence Analysis 117

5.2.4 Expression of hOCT1 in *Xenopus Laevis* Oocytes and ^{3}H-MPP^{+} and ^{14}C-TEA Transport Measurements 118

5.2.5 *In Vitro* Translation and Sodium Dodecyl Sulfate-Polyacrylamide Gel Electrophoresis (SDS-PAGE) Gel Analysis 119

5.2.6 Northern Blot Analysis 119

5.2.7 Data Analysis 120

5.2.8 Materials 120

5.3 Results 121

5.3.1 Molecular Cloning of the Full-Length hOCT1 cDNA 121

5.3.2 DNA Sequencing and Primary Amino Acid Sequence 121

5.3.3 Functional Expression and Characterization in *Xenopus Laevis* Oocytes 124

5.3.4 *In Vitro* Translation of hOCT1 mRNA 133

5.3.5 Tissue Distribution and Expression of hOCT1 mRNA 133

5.3.6 Homology of hOCT1 to Other Organic Cation Transporters 136

5.4 Discussion 138

CHAPTER 6

FUNCTIONAL CHARACTERIZATION OF AN ORGANIC CATION TRANSPORTER (hOCT1) IN A TRANSIENTLY TRANSFECTED HUMAN CELL LINE (HeLa)

6.1 Introduction 143

6.2 Materials and Methods 145

6.2.1 Construction and Isolation of Plasmid DNA for Transfection 145

6.2.2 HeLa Cell Culture and Transfection 146

6.2.3 Uptake Measurements 147

6.2.4 Protein Assay 147

6.2.5 Data Analysis 148

6.2.6 Materials 149

6.3 Results 149

6.3.1 Initial Characterization of hOCT1 Expression in Transiently-Transfected HeLa Cells 149

6.3.2 Permeant Studies 150

6.3.3 Inhibition Studies 156

6.3.4 *Trans*-Stimulation Studies 162

6.4 Discussion 167

CHAPTER 7

INTERACTIONS OF HIV PROTEASE INHIBITORS WITH A HUMAN ORGANIC CATION TRANSPORTER IN A MAMMALIAN EXPRESSION SYSTEM

7.1 Introduction 172

7.2 Materials and Methods 175

7.2.1 DNA Isolation 175

7.2.2 HeLa Cell Culture and Transfection 175

7.2.3 Uptake Measurements 176

7.2.4 RT-PCR 176

7.2.5 Data Analysis 177

7.2.6 Materials 177

7.3 Results 178

7.3.1 *Cis*-Inhibition Studies 178

7.3.2 *Trans*-Stimulation Studies 181

7.3.3 Permeant (Substrate) Studies 184

7.3.4 Expression of hOCT1, MDR1, MRP1 in MOLT-4 Cells 186

7.4 Discussion 189

CHAPTER 8

THE INTERACTION OF n-TETRAALKYLAMMONIUM COMPOUNDS WITH A HUMAN ORGANIC CATION TRANSPORTER, hOCT1

8.1 Introduction 192

8.2 Materials and Methods 194

8.2.1 DNA Isolation 194

8.2.2 RT-PCR 194

8.2.3 Maintenance of Cell Culture and Transfection 195

8.2.4 Uptake Measurements 195

8.2.5 Partition Coefficient Determinations 196

8.2.6 Data Analysis 196

8.2.7 Materials 197

8.3 Results 197

8.3.1 Tissue Distribution of hOCT1 197

8.3.2 Expression of hOCT1 in HeLa Cells 198

8.3.3 Inhibition Studies 198

8.3.4 *Trans*-Stimulation Studies 208

8.4 Discussion 211

CHAPTER 9

SUMMARY/CONCLUSIONS AND FUTURE PERSPECTIVES

9.1 Introduction 215

9.2 Molecular and Functional Characteristics of Cloned Organic Cation Transporters (OCT) 216

9.2.1 OCT Family: OCT1 218

9.2.1.1 rOCT1 218

9.2.1.2 rOCT1A 219

9.2.1.3 hOCT1 222

9.2.1.4 rbOCT1 225

9.2.2 OCT Family: OCT2 227

9.2.2.1 rOCT2 227

9.2.2.2 pOCT2 227

9.2.2.3 hOCT2 228

9.2.3 OCT Family: OCT3 229

9.2.3.1 rOCT3 and mOCT3 229

9.2.4 OCT Family: OCTN1 229

9.2.4.1 OCTN1 229

9.2.5 OCT Family: OCTN2 230

9.2.5.1 OCTN2 230

9.2.6 Other Members of the OCT Family 231

9.3 Future Directions 232

REFERENCES 238

APPENDIX

INTERACTIONS OF VARIOUS COMPOUNDS WITH hOCT1 IN TRANSFECTED HeLa CELLS

A.1 Objectives 270

A.2 Materials and Methods 270

A.2.1 Construction and Isolation of Plasmid DNA for Transfection 270

A.2.2 HeLa Cell Culture and Transfection 271

A.2.3 Uptake Measurements 272

A.2.4 Protein Assay 272

A.2.5 Data Analysis 273

A.2.6 Materials 273

A.3 Results 274

A.3.1 Inhibition Studies 274

A.3.2 *Trans*-Stimulation Studies 277

LIST OF TABLES

Chapter 1

Table 1.1 Properties of various regions of the gastrointestinal tract as compared to other organs 29

Chapter 2

Table 2.1 Kinetic parameters of guanidine uptake in rat kidney BBMV 50

Table 2.2 Effect of clinically used drugs on ^{14}C-guanidine and ^{14}C-TEA uptake in rat renal brush border membrane vesicles 54

Chapter 3

Table 3.1 Effect of inhibitors on ^{14}C-guanidine and ^{14}C-TEA uptake in rat kidney mRNA-injected oocytes 70

Table 3.2 Kinetics of organic cation transport in rOCT2 cRNA-injected oocytes 78

Chapter 4

Table 4.1 Sequences of primers and their positions in the rOCT1 cDNA 87

Chapter 5

Table 5.1 Primers used for PCR cloning of hOCT1 cDNA 117

Table 5.2 Uptake of ^{3}H-MPP^{+} in the presence of non-classic organic cation transport inhibitors 132

Chapter 6

Table 6.1 Comparison of K_i values of organic cations determined from experiments conducted in *X. laevis* oocytes or transfected HeLa cells 161

Table 6.2 K_i values of various compounds in inhibiting TEA uptake mediated by hOCT1 163

Chapter 7

Table 7.1 IC_{50} values of HIV protease inhibitors inhibiting ^{14}C-TEA uptake in hOCT1 DNA-transfected HeLa cells 180

Chapter 8

Table 8.1 Partition coefficients and IC_{50} values of n-tetraakylammonium compounds 202

Table 8.2 Partition coefficients and IC_{50} values of non-aliphatic organic cations 207

Chapter 9

Table 9.1 Pairwise comparison of amino acid sequences of selected members of the OCT family 217

Table 9.2 General characteristics of cloned organic cation transporters 220

Table 9.3 Interactions of various compounds with rOCT1, hOCT1, rOCT2 and hOCT2 221

Table 9.4 Kinetics of TEA transport mediated by wild-type and mutant hOCT1 (ΔMet420) 236

Appendix

Table A.1 IC_{50} values of β-blockers in inhibiting ^{14}C-TEA uptake in hOCT1 DNA-transfected HeLa Cells 274

Table A.2 IC_{50} values of azole compounds in inhibiting ^{14}C-TEA uptake in hOCT1 DNA-transfected HeLa Cells 275

Table A.3 IC_{50} values of stereoisomers in inhibiting ^{14}C-TEA uptake in hOCT1 DNA-transfected HeLa Cell 276

LIST OF FIGURES

Chapter 1

Figure 1.1 Structures of various organic cations 2

Figure 1.2 Secondary structure of a representative organic cation transporter 5

Figure 1.3 Kinetics of passive diffusion and facilitated diffusion (carrier-mediated) processes 8

Figure 1.4 Model of organic cation secretion across the epithelium of the proximal tubule 16

Figure 1.5 Liver lobule 20

Figure 1.6 Model of organic cation secretion across the epithelium of the hepatocyte 24

Figure 1.7 Site of absorption of various molecules in the gastrointestinal tract 28

Figure 1.8 Model of organic cation transport across the epithelium of the intestine 32

Chapter 2

Figure 2.1a Uptake of ^{14}C-guanidine (50 μM) in rat kidney BBMV in the presence or absence of an outwardly-directed proton gradient in HK buffer 45

Figure 2.1b Uptake of ^{14}C-TEA (50 μM) in rat kidney BBMV in the presence or absence of an outwardly-directed proton gradient in HK buffer 46

Figure 2.2a Uptake of ^{14}C-guanidine (50 μM) in rat kidney BBMV in the presence or absence of an outwardly-directed proton gradient in K^+-free buffer 47

Figure 2.2b Uptake of ^{14}C-TEA (50 μM) in rat kidney BBMV in the presence or absence of an outwardly-directed proton gradient in the K^+-free buffer 48

Figure 2.3a pH-gradient stimulated 30 sec uptake of ^{14}C-guanidine (50 μM) in rat kidney BBMV in the presence of various inhibitors (5 mM) in HK buffer 52

Figure 2.3b pH-gradient stimulated 30 sec uptake of ^{14}C-TEA (50 μM) in rat kidney BBMV in the presence of various inhibitors (5 mM) in HK buffer 53

Figure 2.4a Uptake at 60 sec of 50 μM ^{14}C-guanidine in BBMV pre-incubated with 5 mM guanidine or TEA in HK buffer for one hour 55

Figure 2.4b Uptake at 60 sec of 50 μM ^{14}C-TEA in BBMV pre-incubated with 5 mM guanidine or TEA in HK buffer for one hour 56

Figure 2.5a Uptake of 50 μM ^{14}C-guanidine (15 sec) in BBMV pre-incubated with 5 mM guanidine or TEA for one hour in K^+-free buffer 57

Figure 2.5b Uptake of 50 μM ^{14}C-TEA (15 sec) in BBMV pre-incubated with 5 mM guanidine or TEA for one hour in K^+-free buffer 58

Chapter 3

Figure 3.1 Expression of guanidine transport activity *in Xenopus laevis* oocytes injected with rat kidney total mRNA and different size fractions of mRNA 68

Figure 3.2 1% Agarose/1.1% formaldehyde gel of total and size-fractionated rat kidney mRNA 69

Figure 3.3 Kinetics of guanidine transport in oocytes injected with rat kidney total mRNA or water 72

Figure 3.4a Effect of pH on ^{14}C-guanidine (500 μM) uptake in oocytes injected with rat kidney mRNA or water 73

Figure 3.4b Effect of membrane potential on ^{14}C-guanidine (500 μM) uptake in oocytes injected with rat kidney mRNA or water 74

Figure 3.5a ^{14}C-Guanidine (500 μM) and ^{14}C-TEA (500 μM) uptake in oocytes injected with rOCT1 cRNA or water 76

Figure 3.5b ^{14}C-Guanidine (500 μM) and ^{14}C-TEA (500 μM) uptake in oocytes injected with rOCT2 cRNA or water 77

Figure 3.6a Effect of pH on ^{14}C-guanidine (500 μM) uptake in oocytes injected with rOCT2 cRNA or water 79

Figure 3.6b Effect of membrane potential on ^{14}C-guanidine (500 μM) uptake in oocytes injected with rOCT2 cRNA or water 80

Chapter 4

Figure 4.1 Results of RT-PCR 92

Figure 4.2a Functional expression of rOCT1A in *Xenopus laevis* oocytes 94

Figure 4.2b Effect of various organic cations and the organic anion on ^{14}C-TEA (500 μM) uptake by oocytes injected with water or rOCT1A cRNA 95

Figure 4.2c Kinetics of TEA transport in rOCT1A cRNA-injected oocytes 97

Figure 4.3a cDNA sequence of the 1.5-kb (rOCT1A) clone and the corresponding three possible translational reading frames 100

Figure 4.3b Kyte-Doolittle hydropathy analysis of rOCT1A (the protein encoded from bp 312 to bp 1601) 100

Figure 4.4a Diagram of rOCT1 gene showing the alternative splicing sites 102

Figure 4.4b Partial nucleotide sequences flanking the splicing sites 102

Figure 4.5 Autoradiograph of an SDS-polyacrylamide gel electrophoresis showing *in vitro* translation product 106

Figure 4.6a Schematic diagram showing the construction of Pro 1, 2 and 3 107

Figure 4.6b ^{14}C-TEA uptake in Pro 1, 2 and 3 cRNA-injected oocytes compared to water, rOCT1 and rOCT1A cRNA-injected oocytes 108

Figure 4.7 Expression of rOCT1 and rOCT1A transcripts detected by RPA 110

Figure 4.8 Expression of rOCT1 and rOCT1A transcripts detected by RT-PCR 111

Chapter 5

Figure 5.1a Nucleotide and deduced amino acid sequences of hOCT1 cDNA 122

Figure 5.1b Kyte-Doolittle hydropathy analysis of hOCT1 123

Figure 5.2a Functional expression of hOCT1 in *X. laevis* oocytes 125

Figure 5.2b Kinetics of MPP^+ transport in hOCT1 cRNA-injected oocytes 127

Figure 5.3a Effect of various organic cations (5 mM) on ^{3}H-MPP^+ uptake in oocytes injected with hOCT1 cRNA or water 128

Figure 5.3b Effect of various organic cations (1 mM) on ^{3}H-MPP^+ uptake in oocytes injected with hOCT1 cRNA or water 129

Figure 5.3c Study of the effects of the organic cations, decynium-22, vecuronium, and TEA on ^{3}H-MPP^+ uptake 130

Figure 5.3d Effect of membrane potential on ^{3}H-MPP^+ uptake in oocytes injected with hOCT1 cRNA or water 131

Figure 5.4 Autoradiograph of an SDS-polyacrylamide gel electrophoresis showing *in vitro* translation products of rOCT1 and hOCT1 cDNA 134

Figure 5.5 Northern blot analysis of hOCT1 mRNA in various human tissues 135

Figure 5.6 Alignment of amino acid sequence of rOCT1, Lx1, hOCT1, and rOCT2 using Pileup program 137

Chapter 6

Figure 6.1 Transient expression of transfected hOCT1 plasmid DNA in HeLa cells over time 151

Figure 6.2 Temperature dependence of ^{14}C-TEA transport in pTargeT-hOCT1 and empty vector-transfected HeLa cells 152

Figure 6.3 Concentration dependence of ^{14}C-TEA transport in pTargeT-hOCT1 and empty vector-transfected HeLa cells 153

Figure 6.4 Time course of ^{3}H-cimetidine (5 μM) uptake in the pTargeT-hOCT1-transfected and empty vector-transfected HeLa cells 155

Figure 6.5a Inhibition of ^{14}C-TEA uptake 157

Figure 6.5b Inhibition of ^{14}C-TEA uptake 158

Figure 6.5c Inhibition of ^{14}C-TEA uptake 159

Figure 6.5d Inhibition of ^{14}C-TEA uptake 160

Figure 6.6a Concentration-dependent inhibition of ^{14}C-TEA uptake by quinine and quinidine in HeLa cells transfected with pTargeT-hOCT1 164

Figure 6.6b Concentration-dependent inhibition of ^{14}C-TEA uptake by S-(+)-disopyramide and R-(-)-disopyramide in HeLa cells transfected with pTargeT-hOCT1 165

Figure 6.7 *Trans*-stimulation of ^{14}C-TEA uptake in pTargeT-hOCT1 transfected HeLa cells 166

Chapter 7

Figure 7.1 Chemical structures of HIV protease inhibitors 173

Figure 7.2 Concentration-dependent inhibition of ^{14}C-TEA uptake by ritonavir in HeLa cells transfected with pTargeT-hOCT1 179

Figure 7.3 *Trans*-stimulation of ^{14}C-TEA uptake in pTargeT-hOCT1 transfected HeLa cells 182

Figure 7.4 *Trans*-stimulation of ^{14}C-TEA uptake in pTargeT-hOCT1 transfected HeLa cells 183

Figure 7.5 Uptake of ^{14}C-saquinavir (26 μM) in the pTargeT-hOCT1-transfected and empty vector-transfected HeLa cells 185

Figure 7.6a RT-PCR analysis of hOCT1 mRNA transcript expression in various tissues and cells 187

Figure 7.6b RT-PCR analysis of MDR1 and MRP1 mRNA transcript expression in MOLT-4 cells 188

Chapter 8

Figure 8.1 RT-PCR analysis of hOCT1 mRNA transcript expression in various tissues 199

Figure 8.2 Inhibition of ^{14}C-TEA uptake by n-TAA compounds 200

Figure 8.3 Concentration-dependent inhibition of ^{14}C-TEA uptake by TPeA in HeLa cells transfected with pTargeT-hOCT1 201

Figure 8.4 Relationship between IC_{50} values in inhibiting ^{14}C-TEA uptake in HeLa cells expressing hOCT1 and alkyl chain length (N) of n-TAA compounds 204

Figure 8.5 Relationship between molecular weight (MW) of quaternary ammonium compounds and partition coefficient (P) 205

Figure 8.6 Relationship between IC_{50} values in inhibiting ^{14}C-TEA uptake in HeLa cells expressing hOCT1 and partition coefficient (P) values of n-TAA compounds 206

Figure 8.7 *Trans*-stimulation of ^{14}C-TEA uptake in pTargeT-hOCT1 transfected HeLa cells 209

Figure 8.8 *Trans*-stimulation of ^{14}C-TEA uptake in pTargeT-hOCT1 transfected HeLa cells 210

Chapter 9

Figure 9.1 Expression of hOCT1 and its splice variants in different human tissues and cells detected by PCR 226

Figure 9.2 Uptake of 4-Di-ASP$^+$ (10 μM) at 15 min in hOCT1 DNA-transfected HeLa cells 234

Appendix

Figure A.1 *Trans*-stimulation of ^{14}C-TEA uptake in pTargeT-hOCT1 transfected HeLa cells 278

Figure A.2 *Trans*-stimulation of ^{14}C-TEA uptake in pTargeT-hOCT1 transfected HeLa cells 279

CHAPTER 1

ROLE OF ORGANIC CATION TRANSPORTERS IN DRUG ABSORPTION AND ELIMINATION [1]

1.1 Introduction

A large number of drugs as well as endogenous metabolites are compounds with one or more primary, secondary, tertiary or quaternary amines. Quaternary amines are always positively charged, whereas other amines can be protonated and become positively charged depending on their pKa values. Collectively, these compounds are termed organic cations (Figure 1.1). Drugs from a wide array of clinical classes including antihistamines, skeletal muscle relaxants, antiarrhythmics and beta-adrenoceptor blocking agents are organic cations. In addition, a number of endogenous bioactive amines such as dopamine, choline, and N^1-methylnicotinamide (NMN) are organic cations. Since many of these molecules (pKa usually 8-12) are polar and positively charged at physiologic pH, membrane transporters generally are involved in the absorption, distribution and elimination of these compounds.

For many years, it has been clear that facilitated transporters in the kidney, liver and intestine play a major role in the absorption and elimination of a number of basic drugs and organic cations; however, the molecular events involved in the transport processes have not been fully elucidated. Recently, several organic cation transporters have been cloned from

[1] Part of this chapter was published in *Annual Review of Pharmacology and Toxicology* 38:431-460, 1998. Permission from the publisher is included in "Acknowledgments". I would like to thank Drs. Claire M. Brett and Kathleen M. Giacomini for their contribution to this chapter.

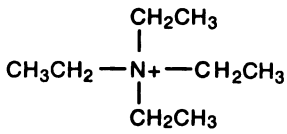

Tetraethylammonium (TEA)

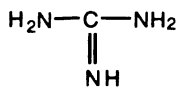

Guanidine

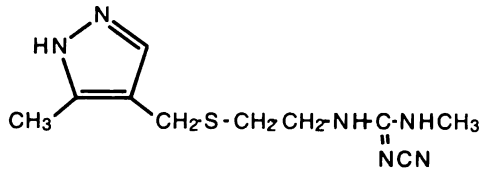

Cimetidine

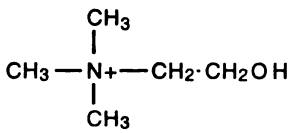

Choline

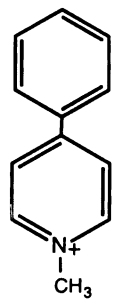

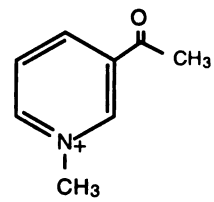

***N*[1]-methylnicotinamide (NMN)**

1-Methyl-4-phenylpridinium (MPP^+)

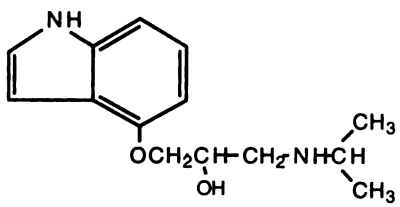

Pindolol

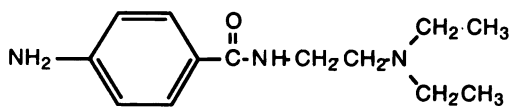

Procainamide

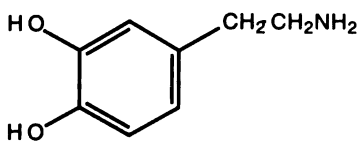

Dopamine

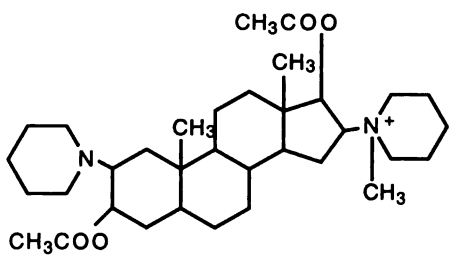

Vecuronium

Figure 1.1 Structures of various organic cations.

various species and are members of a family of transporters termed OCT (Gorboulev *et al.*, 1997; Grundemann *et al.*, 1994 and 1997; Kekuda *et al.*, 1998; Lopez-Nieto *et al.*, 1997; Okuda *et al.*, 1996; Tamai *et al.*, 1997; Terashita *et al.*, 1998; Walsh *et al.*, 1996; Wu *et al.*, 1998a and 1998b; Zhang *et al.*, 1997a and 1997b). Transporters from the OCT family are expressed in epithelial tissues including kidney, liver and intestine and function in the transport of both endogenous amines as well as various xenobiotics including a number of clinically important drugs (Busch *et al.*, 1996a and 1996b; Gorboulev *et al.*, 1997; Grundemann *et al.*, 1994 and 1997; Martel *et al.*, 1996a; Okuda *et al.*, 1996; Pritchard, *et al.*, 1997; Terashita *et al.*, 1998; Zhang *et al.*, 1997a and 1997b). Transporters from families other than the OCT family also transport organic cations in various epithelia (Bonisch and Bruss, 1994; Bossuyt *et al.*, 1996; Gottesman and Pastan, 1993; Gottesman *et al.*, 1996; Higgins, 1992; Kitayama and Dohi, 1996).

This introductory chapter will focus on the mechanisms of transport of organic cations in epithelia. I first discuss the general properties of epithelia relevant to drug absorption and elimination. Second, a brief background of the kinetics of transport processes is provided followed by a detailed discussion of the cellular and molecular mechanisms of organic cation transport in the kidney, liver and intestine. Molecular and functional characteristics of cloned organic cation transporters including my thesis work, the current status of the field and future directions will be discussed in the summary/ conclusions and future perspective chapter.

1.2 Characteristics of Epithelia, Transporters and Transport

1.2.1 Epithelia and Transporters

In general, for a substance to enter or exit the body, it must cross an epithelial barrier. Epithelia are thin layers of polarized cells which line body cavities and isolate various fluid compartments from each other and from the external environment. The plasma membrane of epithelial cells is a polarized structure. That is, such cells characteristically have an apical or brush border (facing a lumen) and basolateral (facing a capillary) domain. Each domain has specialized functions in part defined by the presence of various proteins and the absence of others. This polarized structure is vital to achieve the main function of epithelia: vectorial movement of molecules.

Absorption, distribution and elimination of both endogenously-produced and exogenously-administered substances require transport across one or more epithelial barrier(s). For absorption to occur, a substance first crosses the apical membrane from the lumen into the intracellular compartment. To move into the blood from the intracellular compartment, the substance must move across the basolateral surface. For secretion to occur, the movement of a substance is in the opposite direction: first across the basolateral membrane into the cytosol and then across the brush border membrane to reach the lumen.

Transporters are one type of integral (transmembrane) protein and exist in both the apical and basolateral membranes. Specifically, transporters facilitate the transmembrane flux of substances. As integral proteins, they are embedded in and span across the phospholipid bilayer and have multiple membrane-spanning domains. The hydrophobic segments of the protein are embedded within the membrane, often in α-helical structures, and the hydrophilic segments extend into the extracellular and cytosolic environments. For a typical secondary structure of an organic cation transporter, see Figure 1.2.

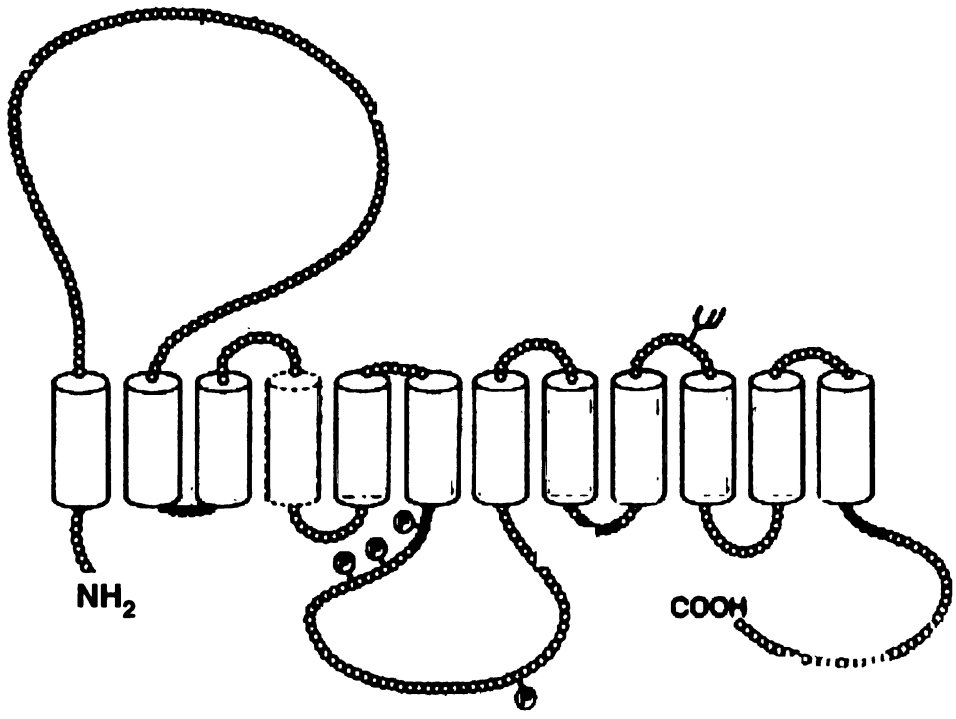

Figure 1.2 Secondary structure of a representative organic cation transporter. (Adapted from Grundemann *et al.*, 1994)

1.2.2 Mechanisms of Transport

Transepithelial flux of solutes including drugs and other xenobiotics generally involves three steps: transport across the apical membrane; intracellular transport which may involve sequestration in vesicles; and transport across the basolateral membrane. The net direction of transepithelial flux, i.e., secretory from lumen to blood or absorptive from blood to lumen, is determined by the relative kinetics of the three steps.

The transport of a compound across either the basolateral or apical membrane of an epithelial cell can occur by four mechanisms: simple diffusion, facilitated diffusion, primary active transport and secondary active transport. Simple diffusion involves the movement of compounds across the phospholipid bilayer. More lipophilic compounds diffuse through the membrane bilayer (transcellular route) whereas more hydrophilic compounds diffuse through aqueous pathways between cells (paracellular route). The paracellular route is more highly dependent upon the size of the molecule. However, in many epithelia paracellular transport is restricted because of the tight junctions between cells. The diffusion rate can be described kinetically by Fick's first law of diffusion which basically states that the rate of flux of a compound is proportional to its chemical gradient across the cell membrane:

$$J = P (C)$$

where J is the rate of transport of the compound, P is the permeability coefficient for the compound in the membrane and C is the concentration gradient across the membrane. The permeability coefficient is based on a number of factors including the hydrophobicity, molecular weight of the compound and the thickness and surface area of the membrane. Two opposing forces, the influx and the efflux, determine the net direction of flux. At steady-state, the concentration of the compound is equal on both sides of the membrane and net flux is zero. Because interaction with a protein is not involved in diffusion, the

movement of one compound is not influenced by the presence of another nor is the process saturable.

For charged molecules such as organic cations or anions, the law of electroneutrality, which states that the sum of the positive charges on each side of the membrane is equal to the sum of the negative charges, must be obeyed. Thus, at steady-state, the concentration of a charged compound is not equal on both sides of the membrane, but is determined by the electrical potential difference. The driving force for transport in this situation is defined as the electrochemical potential. The Nernst equation describes the steady-state situation for charged molecules and for a monovalent compound (at 25°C), a ratio of 10:1 (concentration inside the cell to concentration outside the cell) balances a -60 mV electrical potential difference (inside negative) across the membrane. An inside negative electrical potential is usual in all cells and is created and maintained by the potassium channel and Na^+/K^+ATPase.

Facilitated diffusion differs from simple diffusion in terms of both the molecular events and the kinetics involved in the transport of a compound. The molecular events of a facilitated diffusion process consists of the interaction and binding of a compound with a transporter. (Channels may also be involved in facilitated diffusion, but are generally involved in ion flux and less relevant to the transport of most drugs.) After binding, the compound is translocated to the other side of the membrane. The exact mechanism of translocation is not known, but may involve formation of a pore by the transporter. Finally, the compound is released to the other side of the membrane.

The molecular events determine the kinetic characteristics of a facilitated diffusion process. Kinetically, the rate of transport of a compound by facilitated diffusion is faster than predicted by the permeability coefficient and is saturable (Figure 1.3), i.e., it is not linearly proportional to the concentration gradient. The rate of transport of a compound by facilitated diffusion (J) can be described by a hyperbolic, Michaelis-Menten equation:

$$J = J_{max} \bullet C / (K_t + C)$$

where J_{max} is the maximal transport rate observed for the compound and K_t is the concentration of the compound which produces half the maximal rate of transport (J_{max}). The J_{max} represents the product of the actual number of transporters in a membrane and their turnover rate constant (or how efficient the transporter is in making a complete cycle--binding to a compound, translocation and release of the compound to the other side of the membrane). The affinity (inverse of the K_t) of a compound for a transport protein is an index of how well it binds to the transporter. In contrast to simple diffusion, competitive inhibition of transport by structurally-similar compounds can occur.

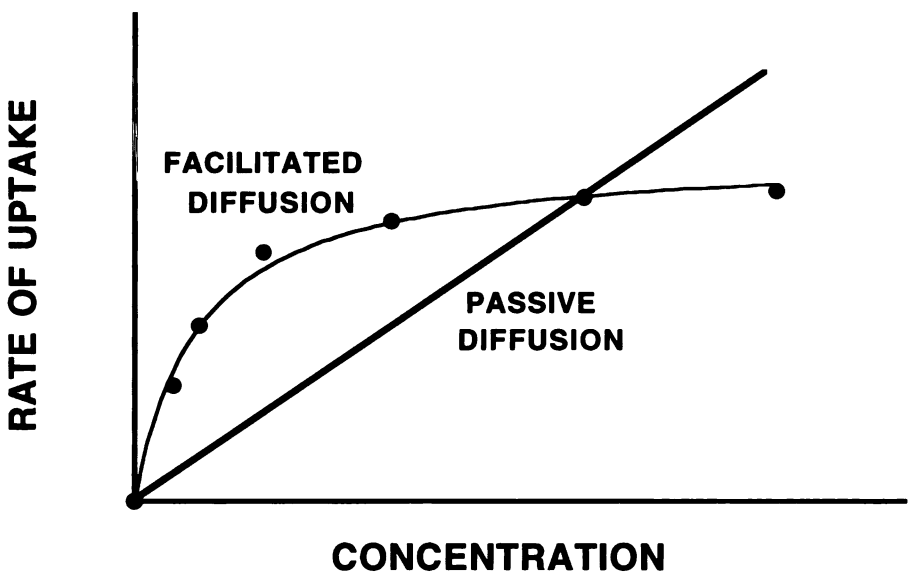

Figure 1.3 Kinetics of passive diffusion and facilitated diffusion (carrier-mediated) processes.

The transport of the organic cation, tetraethylammonium (TEA), in basolateral membrane vesicles from kidney fulfills all of the requirements of a facilitated diffusion mechanism (see details in section 1.3 Organic Cation Transport). TEA is transported down its electrochemical gradient at a rate greater than predicted by its permeability coefficient. TEA transport is sensitive to membrane potential, consistent with the transport of a charged molecule. The transport of TEA is saturable and inhibited by other organic cations.

Active transport exhibits characteristics similar to facilitated diffusion except that the transport occurs against the concentration gradient and requires cellular energy. Two major types of active transport systems, primary and secondary active, have been described. In animal cells, primary active systems are directly coupled to the breakdown of ATP. An important primary active transporter is P-glycoprotein, the product of the *mdr* gene, which transports drugs and other xenobiotics out of cells and thereby confers drug resistance to various neoplasms. P-glycoprotein is also present in normal cells and is involved in both the intestinal and renal secretion of a number of clinically relevant drugs (Germann *et al.*, 1993; Gottesman *et al.*, 1996; Higgins, 1992).

Secondary active transport mechanisms involve the uphill transport of one substance against its concentration gradient coupled to the downhill transport of another substance down its concentration gradient. The substance which moves down its concentration gradient, is termed the activator and supplies the energy for the uphill transport of the second substance, which is termed the substrate of the transporter. Typically in mammalian cells, the activator is Na^+ or H^+. If the activator moves in the same direction as the substrate, the transporter is termed a co-transporter or symporter and if the activator moves in the opposite direction the transporter is termed an antiporter or countertransporter. Important transporters which are secondary active are the Na^+-dependent nucleoside transporters. These transporters move various nucleosides and nucleoside analogs into cells and are coupled to the Na^+-gradient. Na^+-dependent

nucleoside transporters are important in the absorption and elimination of many therapeutic nucleoside analogs (Cass, 1995; Griffith and Jarvis, 1996; Wang *et al.*, 1997).

To mediate the transepithelial flux of a compound, two distinct transporters in series are usually involved. In general, one transporter is facilitated and the other is active. For the model organic cation, TEA, secretory flux from blood to tubule fluid in the proximal tubule is mediated by a facilitated transporter at the basolateral membrane and a secondary active transporter, *i.e.*, an organic cation proton antiporter, at the apical membrane (Pritchard and Miller, 1993).

1.3 Organic Cation Transport

Transport of organic cations has been studied in various epithelia such as: kidney (Chun *et al.*, 1997a; Gorboulev *et al.*, 1997; Groves and Wright, 1995; Grundemann *et al.*, 1994 and 1997; Hohage *et al.*, 1996; Nabekura *et al.*, 1996; Okuda *et al.*, 1996; Somogyi *et al.*, 1996; Terashita *et al.*, 1998; Ullrich and Rumrich, 1996; Zhang *et al.*, 1997a), liver (Martel *et al.*, 1996a and 1996b; Moseley and Van Dyke, 1995; Moseley *et al.*, 1996a, 1996b and 1997; Nakamura *et al.*, 1994; Zhang *et al.*, 1997b), intestine (Iseki *et al.*, 1993; Miyamoto *et al.*, 1988; Saitoh and Aungst, 1995; Takahashi *et al.*, 1993; Turnheim and Lauterbach, 1977a, 1977b and 1980; Zhang *et al.*, 1996), choroid plexus (Miller *et al.*, 1995; Suzuki and Sugiyama, 1994; Villalobos *et al.*, 1997; Whittico *et al.*, 1990 and 1991), and placenta (Ganapathy *et al.*, 1988; Grassl, 1994; Prasad *et al.*, 1992; Van der Aa *et al.*, 1995; van der Aa *et al.*, 1996) (for current reviews see Meijer *et al.*, 1990; Oude Elferink *et al.*, 1995; Pritchard and Miller, 1993 and 1996; Roch-Ramel *et al.*, 1992; Somogyi, 1996; Wright, 1996) using a variety of experimental techniques including perfused or nonperfused tissue, isolated apical and basolateral membrane vesicles, primary cell culture and continuous cell lines. From these studies, the functional characteristics of

organic cation transport in the various epithelia have been elucidated. However, because the tissues used in characterizing organic cation transport mechanisms contain multiple carriers with overlapping driving forces and substrate selectivities, the precise mechanisms involved in the transport of organic cations via a particular transporter are largely unknown.

The isolation of transporters and their expression in heterologous expression systems is essential to understanding the mechanisms of transport of organic cations. However, the approach of isolating the transport proteins by affinity chromatography and photoaffinity labelling (Gilsdorf *et al.*, 1997; Holohan *et al.*, 1992; Kimura *et al.*, 1995; Meijer *et al.*, 1990) has been hindered by a number of intrinsic problems, many of which are related to the development of specific ligands to the native transport proteins. In addition the low abundance of transport proteins poses a major problem in their isolation and purification. Recently, an organic cation transporter from rat kidney, rOCT1, was cloned using expression cloning methods in *Xenopus laevis* oocytes (Grundemann *et al.*, 1994). Subsequent studies using homology cloning have identified other related organic cation transporters (Gorboulev *et al.*, 1997; Grundemann *et al.*, 1994 and 1997; Lopez-Nieto *et al.*, 1997; Okuda *et al.*, 1996; Terashita *et al.*, 1998; Walsh *et al.*, 1996; Zhang *et al.*, 1997a and 1997b).

Excretory organs such as kidney, liver and intestine are equipped with detoxifying mechanisms which include secretory systems for potentially toxic compounds as well as metabolic conversion processes. Most characterization of organic cation transport has been carried out in the kidney (for recent reviews see Bendayan, 1996; McKinney, 1993; Pritchard and Miller, 1993 and 1996; Roch-Ramel, 1992; Somogyi *et al.*, 1996; Ullrich, 1994; Wright, 1996) and to a lesser extent in the liver (for reviews see Groothuis and Meijer, 1996; Meijer, 1987; Meijer and Molema, 1995; Meijer *et al.*, 1990; Oude Elferink *et al.*, 1995). In contrast, limited information is available on the mechanisms of organic cation transport in the intestine (Elsenhans *et al.*, 1985; Grundemann *et al.*, 1994; Iseki *et*

al., 1993; Miyamoto *et al.*, 1988; Saitoh and Aungst, 1995; Takahashi *et al.*, 1993; Turnheim and Lauterbach, 1977a, 1977b and 1980; Zhang *et al.*, 1996).

1.3.1 Kidney

1.3.1.1 General Structure and Function

The primary function of the renal epithelium is to excrete metabolic by-products, salvage various nutrients (e.g., glucose, amino acids, nucleosides), and regulate extracellular fluid volume and electrolyte concentration. Similar to the processes in the gastrointestinal tract, the kidney necessarily concentrates the glomerular filtrate to avoid water, electrolyte, and nutrient loss. The large volume of the initial filtrate is reduced by 98-99% via various channels and transporters along the renal tubules.

Different segments of the renal tubular system are involved to a variable degree in the absorption and secretion of nutrients and ions, and the anatomy of the tubules reflects these differences in function. Analogous to the gastrointestinal tract, various nutrients are transported in the proximal sites and water is reabsorbed more distally. In fact, about 65% of all reabsorption and secretion takes place in the proximal tubule via multiple active transport processes. The proximal tubules have an extensive brush border, and leaky "tight junctions." Glucose, amino acids, proteins, and vitamins are almost completely reabsorbed by the active transport processes at this site.

Of particular relevance to this discussion, organic cation carriers seem to have the highest activity in the proximal tubules. The capacity of many of these carriers is greater on the basolateral membrane than on the apical membrane. Since many xenobiotic by-products are organic cations, this may result in high concentrations of potentially toxic solutes in the proximal tubule cells (e.g., the nephrotoxicity of some cephalosporins such as cephaloridine) (Dekant and Vamvakas, 1996). In addition, because of the reabsorption of water distally, a "passive" concentrative phenomenon occurs as a non-absorbed solute passes along the tubule. This factor along with the potential for intracellular accumulation

of xenobiotics secondary to various transport systems at the brush border and basolateral membranes may explain, in part, their nephrotoxicity.

The thin segment of the loop of Henle has no brush border, is highly permeable to water and moderately permeable to solutes such as urea. Thus, diffusion is prominent at this site. In contrast, the thick segment of the loop of Henle does have a "rudimentary" brush border and "tighter" tight junctions. This is the site of active transport of sodium and potassium, but this area is virtually impermeable to water. The anatomic characteristics of the thick loop of Henle continue into the diluting segment (first half) of the distal tubule.

The late distal tubule and the cortical collecting tubule are similar. The epithelium at these sites is practically impermeable to urea. The absorption of sodium at these sites is under the control of aldosterone and permeability to water is under the control of antidiuretic hormone. The cuboidal epithelia of the collecting ducts is devoid of brush border configuration.

1.3.1.2 Processes Involved in Renal Handling of Drugs

For any compound, the renal excretion rate is determined by three complex processes: filtration at the glomeruli, tubular reabsorption and tubular secretion. Thus, the rate of renal excretion can be defined as follows:

rate of renal excretion = rate of filtration - rate of reabsorption + rate of secretion

The rate of filtration is dependent upon the glomerular filtration rate (GFR) and the unbound drug concentration. Because the nephron does not allow the passage of plasma proteins into the ultrafiltrate, bound drug is generally not available for filtration. The GFR can be experimentally determined by measuring the renal clearance of inulin, a compound that is eliminated only by filtration in the glomerulus (Rowland and Tozer, 1995). The rate of reabsorption is the rate at which a drug is reabsorbed from the tubule fluid. Therefore, the reabsorption of a compound reduces its overall excretion rate. The rate of secretion is the rate at which a drug is secreted from the blood through the renal tubule into the tubule

fluid. Secretion of a compound increases the overall exrcetion rate of the drug by the kidney. Both reabsorption and secretion may involve transporters localized to the brush border or basolateral membrane of the renal tubules.

1.3.1.3 Organic Cation Transport

Organic cation secretion by the mammalian kidney was first demonstrated by Rennick *et al.* in 1947 (Rennick *et al.*, 1947). Subsequently, various techniques have been adapted to study renal transport mechanisms of organic cations including: *in vivo* and *in vitro* clearance techniques (Levinsky and Levy, 1973; Maack, 1980), the Sperber technique (Sperber, 1946), stop-flow analysis (Malvin and Wilde, 1973), renal slices (Cacini *et al.*, 1982; Holm, 1977), renal tubule suspensions (Burg and Orloff, 1962; Groves *et al.*, 1994), *in vivo* micropuncture and microperfusion (Gottschalk and Lassiter, 1973), *in vitro* microperfusion (Burg, 1972), membrane vesicles (Murer and Gmaj, 1986; Ross and Holohan, 1983) and continuous cell lines (Fauth *et al.*, 1988 and 1991; Fouda *et al.*, 1990; Inui *et al.*, 1985; McKinney *et al.*, 1990 and 1992; Ott and Giacomini, 1993; Ott *et al.*, 1992 and 1994; Saito *et al.*, 1992; Yuan *et al.*, 1991). More recently, molecular cloning techniques and heterologous expression systems have been used to elucidate the function of organic cation transporters (Busch *et al.*, 1996a and 1996b; Gorboulev *et al.*, 1997; Grundemann *et al.*, 1994 and 1997; Kekuda *et al.*, 1998; Okuda *et al.*, 1996; Tamai, *et al.*, 1997; Terashita *et al.*, 1998; Wu *et al.*, 1998a and 1998b; Zhang *et al.*, 1997a and 1997b).

In general, radiolabeled model organic cations have been used as substrates to study transport; however, recently, organic cation transport processes in LLC-PK_1 cells have been dynamically monitored by fluorescence measurements using the permeant cationic fluorescent probe 4-(4-dimethylaminostyryl)-N-methylpyridinium (4-Di-ASP^+) (Stachon *et al.*, 1996). Using this model compound with fluorescent microscopy allows the direct monitoring of organic cation transport rate as well as interactions of drugs with the transporter (Pietruck and Ullrich, 1995; Stachon *et al.*, 1996). For electrogenic organic

cation transporters, electrophysiologic techniques such as voltage clamping methods, have been used (Busch *et al.*, 1996a and 1996b).

Stop flow, micropuncture, and microperfusion analysis and studies in isolated perfused and non-perfused tubules have demonstrated that organic cations are transported in the proximal tubule of the nephron and that the transport differs in various segments of the proximal tubule (McKinney, 1982; Rennick, 1981; Schali *et al.*, 1983; Weiner, 1985). With the recent advance in the molecular cloning, it will be possible to understand whether the regional specific organic cation transport is related to the different distribution of the individual organic cation transporters in the various proximal tubule segments.

Using isolated and purified brush border and basolateral membrane vesicles prepared from the kidney of the dog, a two-step model was initially proposed by Holohan and Ross (1980 and 1981) for the renal secretion of the model organic cation, NMN. NMN entered the cell from the blood by facilitated and electrogenic diffusion processes at the basolateral membrane, and then exited from inside of the cell into the tubule lumen across the apical membrane by a proton or organic cation exchange mechanism. Both brush border and basolateral membrane transporters were observed to be broadly selective for many organic cations including NMN and TEA. The model is consistent with *in vivo* clearance data suggesting that organic cations such as NMN and TEA undergo net secretion (Peters, 1960). Subsequent studies in various animal species generally supported the initial model proposed by Holohan and Ross (Dantzler *et al.*, 1989 and 1991; Gisclon *et al.*, 1987; Hsyu and Giacomini, 1987; Katsura *et al.*, 1993; Miyamoto *et al.*, 1989; Ott *et al.*, 1991; Rafizadeh *et al.*, 1986 and 1987; Takano *et al.*, 1984; Wright, 1985; Wright and Wunz, 1987 and 1988).

In more recent studies other renal transport mechanisms for organic cations across the brush border membrane have been characterized (Figure 1.4). Although secretion appears to be the predominant direction of flux, possible reabsorptive mechanisms have

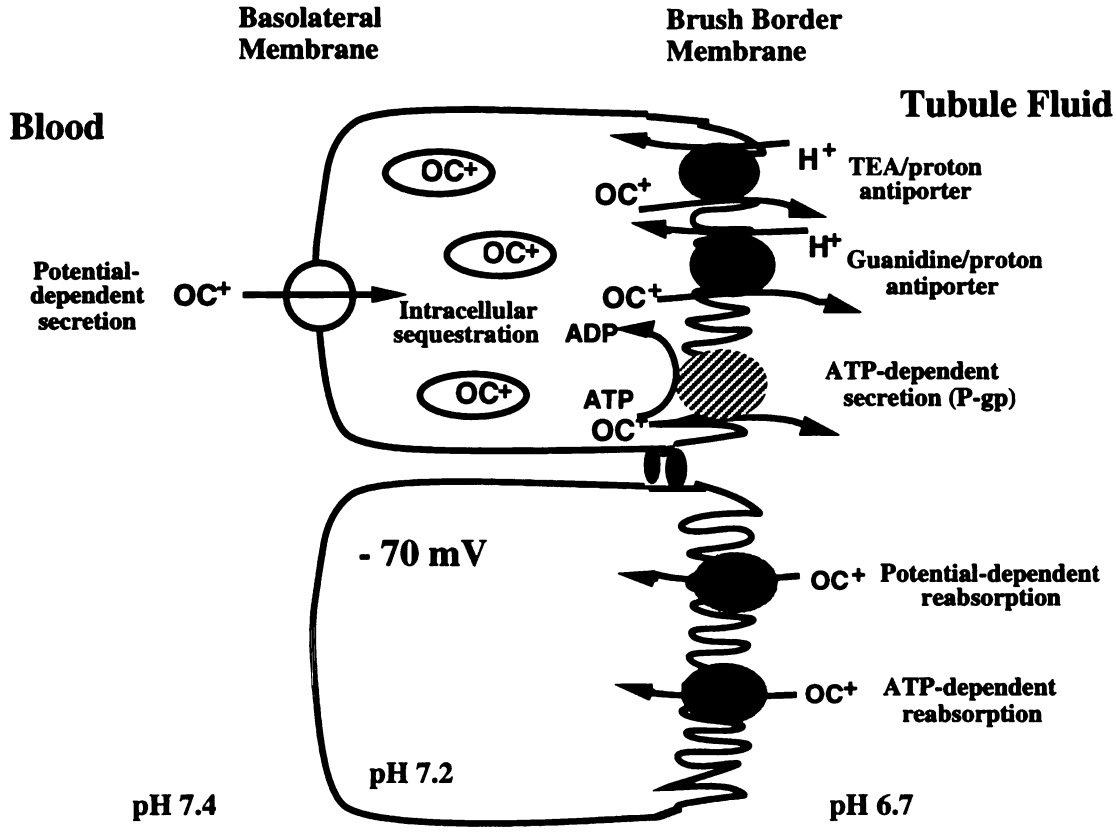

Figure 1.4 Model of organic cation secretion across the epithelium of the proximal tubule involving three steps: *(a)* potential-dependent facilitative diffusion across the basolateral membrane, *(b)* intracellular sequestration, and *(c)* secretion across the apical membrane. Two putative reabsorption pathway are also shown.

also been described. These studies together with the studies of secretion are briefly discussed below:

(1) An organic cation/proton exchange mechanism (antiporter), selective for TEA and NMN, has been identified in brush border membrane vesicles prepared from the kidney and proximal tubule cell lines of a number of species (Dantzler *et al.*, 1989; Gisclon *et al.*, 1987; Holohan and Ross, 1980 and 1981; Hsyu and Giacomini, 1987; Inui *et al.*, 1985; Miyamoto *et al.*, 1989; Ott *et al.*, 1991; Rafizadeh *et al.*, 1986 and 1987; Takano *et al.*, 1984; Wright, 1985; Wright and Wunz, 1987 and 1988; Yuan *et al.*, 1991).

(2) An organic cation/proton exchanger, selective for guanidine, has been characterized in brush border membrane vesicles prepared from rabbit (Miyamoto *et al.*, 1989) and human (Chun *et al.*, 1997a) kidney. The exchanger excludes NMN and TEA. Other substrate and inhibitor selectivity differences between this exchanger and the organic cation/proton exchange mechanism for TEA and NMN have been observed.

(3) The ATP-driven luminal transporter, P-glycoprotein (multidrug resistance transporter) plays a role in the renal elimination of more hydrophobic organic cations (Dudley and Brown, 1996; Dutt *et al.*, 1994; Ford and Hait, 1990; Homolya *et al.*, 1993).

(4) An electrogenic transporter for the organic cation, choline, which may mediate reabsorption has been characterized in rabbit renal brush border membrane vesicles (Wright *et al.*, 1992).

(5) An ATP-stimulated TEA transporter has been characterized in rabbit renal brush border membrane vesicles (McKinney and Hosford, 1993). This transporter appears to function in the reabsorptive direction.

Multiple mechanisms for organic cation transport across the basolateral membrane have also been proposed (Figure 1.4) and are described below:

(1) A potential dependent facilitated diffusion mechanism with broad substrate selectivity for organic cations has been characterized in basolateral membrane vesicles and isolated renal tubules from a number of species (Dantzler, 1991; Katsura *et al.*, 1993; Sokol and McKinney *et al.*, 1990; Takano *et al.*, 1984; Wright and Wunz, 1987).

(2) An organic cation/organic cation exchange mechanism has been characterized in isolated basolateral membrane vesicles from rabbit; however, this exchange mechanism may represent the potential dependent mechanism operating in a different mode (Sokol and McKinney, 1990).

(3) A distinct transporter for paraquat has been characterized in isolated tubules from rabbit kidney. Inhibitors of this transporter include the synthetic polyamine methylglyoxal bis(guanyl-hydrazone)dihydrochloride (MGBG) (Groves *et al.*, 1995).

The mechanisms listed above for both the brush border and basolateral membrane involve cation specific transporters. However, drug-drug interactions in the renal tubule between organic cations and anions have been observed (e.g., probenecid and NMN (Hsyu *et al.*, 1988), levofloxacin and TEA (Ohtomo *et al.*, 1996)), suggesting that non-charge selective transport mechanisms may also play a role in organic cation transport in the

kidney. Such mechanisms have been described for the hepatic transport of organic cations (see below).

In addition to the transporters on the apical and basolateral membranes, an intracellular process has been identified (Pritchard and Miller, 1996; Pritchard *et al.*, 1994). Organic cations can be sequestered by intracellular organelles (e.g., endosomes), which may explain the observed higher than predicted (by the Nernst equation) intracellular concentrations of TEA. This process advances the two-step model to a three-step model (Figure 1.4).

1.3.2 Liver

1.3.2.1 General Structure and Function

The liver has diverse and complex functions including a myriad of metabolic and synthetic processes. This organ also has vital phagocytic and hematopoetic functions. Particularly relevant to this discussion, vital secretory and excretory systems in the liver result in the formation of bile providing a pathway for excretion of various xenobiotics and endogenous compounds into the duodenum.

The liver lobule is considered to be a functional hepatic unit. To understand hepatic epithelial absorption and secretion, the essential anatomy of the lobule needs to be appreciated. A lobule is comprised of a central vein (which eventually empties into the inferior vena cava via the hapatic veins) surrounded by hepatic plates (Figure 1.5). Each of the plates is comprised of an epithelia surrounding bile canaliculi. Between the hepatic plates are liver sinusoids, small blood vessels that receive blood from the portal vein via portal venules. The endothelium of the sinusoids is leaky secondary to its large pores, so that solutes in the plasma of the portal circulation pass freely into the space between the endothelial cells and the hepatocytes (space of Disse), but often carrier-mediated transporters are necessary for movement into the hepatocyte.

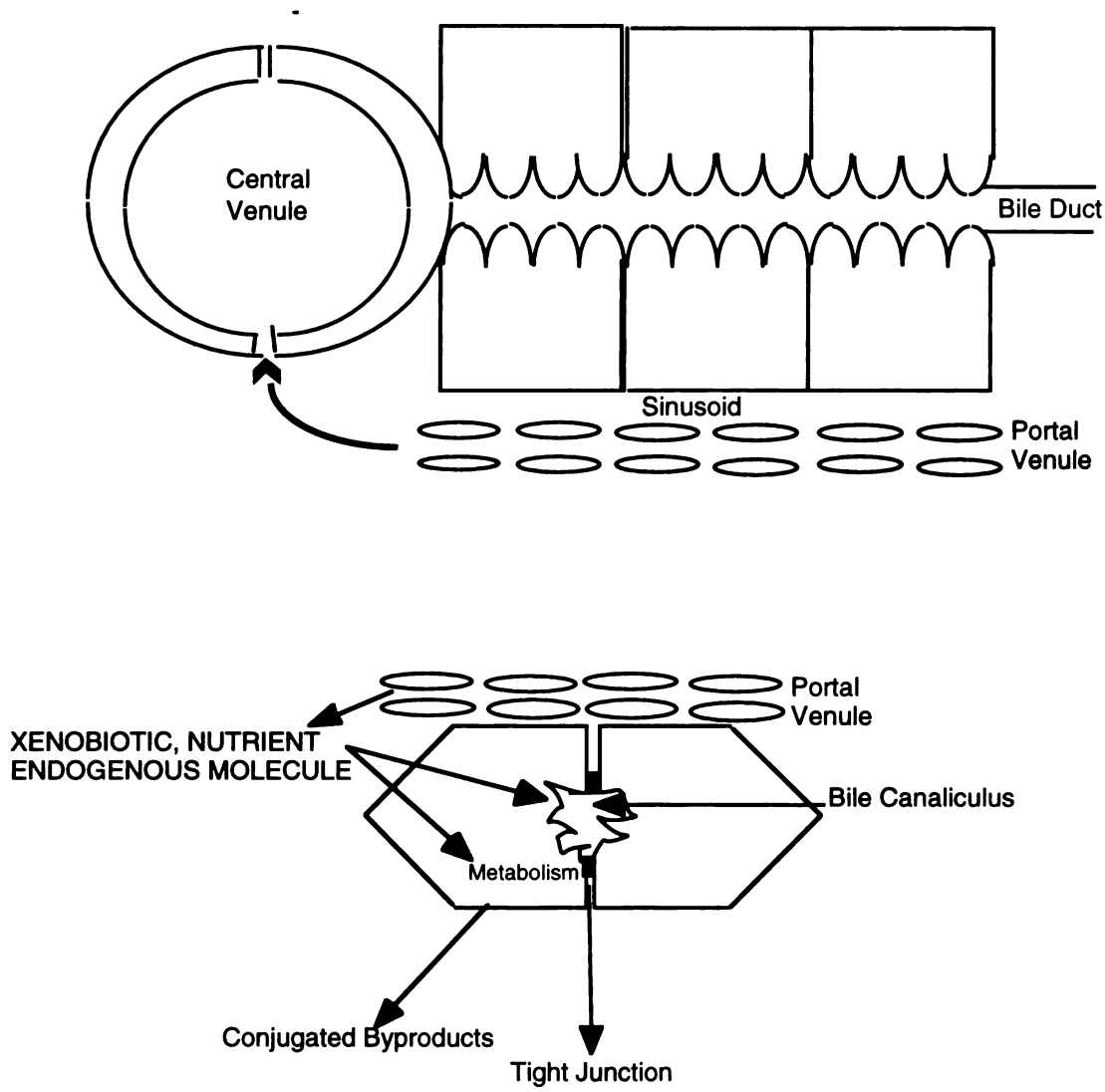

Figure 1.5 Liver lobule. Two views (sagittal and cross sectional) showing the relationship between the blood, the bile, and the epithelial cell. The bottom panel illustrates that molecules contacting the epithelial cell of the liver from the portal circulation may be metabolized and released into the blood as a conjugated byproduct or may enter the bile unchanged or as a conjugated by-product. (Adapted from Schwenk, 1987)

Thus, drugs and other molecules absorbed from the intestinal lumen may enter the liver via the portal venous drainage, eventually enter into the sinusoids, and come into close contact with the hepatocyte. Some drugs will be transported into the hepatocyte either by simple diffusion or a carrier-mediated system and then undergo metabolism with subsequent release into the blood or bile. Other drugs are released into the bile or blood unchanged.

The sinusoidal membrane is a basolateral membrane (facing the circulation) and the canalicular membrane is a brush border membrane (facing the lumen of the bile duct) (Figure 1.5). The brush border membranes of the hepatocyte are oriented between adjacent cells rather than in the configuration of "sheets" that characterize the renal and intestinal epithelia. Because of this anatomy, it is essential that tight junctions isolate the canaliculi from the intercellular space and the sinusoidal lumen. The tight junction complex completely surrounds the canalicular membrane.

Bile, produced in large amounts (0.5-1.0 liters/day), is a complex mixture of bile salts, phospholipids, cholesterol and protein that functions to emulsify fat in the intestine. Most of the bile salts (95%) are reabsorbed in the intestine and returned to the liver via the portal vein. The vast majority of bile salts are transported in the hepatocytes by active transport processes at both the basolateral and apical membranes.

1.3.2.2 Organic Cation Transport

Drugs are carried in the portal blood to the liver, where they move from the periportal region of the lobules to the pericentral region. As noted above, the specific architecture of the hepatic sinusoids brings the drugs in close contact with the hepatocytes. For polar molecules such as organic cations, movement from blood to bile (secretion) will rely largely on specific carrier-mediated systems. Thus, the transport process resembles in some respects organic cation transport processes in the kidney, and membrane transport may dictate the overall efficiency for hepatic elimination. To mediate elimination, transporters on the sinusoidal membrane of the hepatocyte function in the uptake of organic cations from the blood into intracellular space. Once in the hepatocyte, organic cations may be sequestered, metabolized or transported across either the canalicular membrane into the biliary tract or the sinusoidal membrane into the blood. Because of its numerous metabolic and synthetic functions, the handling of organic cations by the liver may show some differences from that in the kidney.

Similar to studies of drug transport in the kidney, various techniques, some of which are unique, are utilized to study organic cation transport in the liver. These include isolated perfused liver (Gores *et al.*, 1986; Meijer *et al.*, 1981; Reichen, 1991; Wolkoff *et al.*, 1987), liver slices (Krumdieck *et al.*, 1980), isolated hepatocytes (Berry *et al.*, 1991 and 1992; Blom *et al.*, 1982), isolated plasma membrane vesicles (McKinney and Hosford, 1992; Moseley *et al.*, 1992) and expression and cloning of the genes for the relevant transporters (Gorboulev *et al.*, 1997; Grundemann *et al.*, 1994; Takeda *et al.*, 1994; Zhang *et al.*, 1997b).

Functional studies of organic cation transport in the liver have been carried out mostly in rats (Groothuis and Meijer, 1996; Grundemann *et al.*, 1994; Martel *et al.*, 1996a and 1996b; McKinney and Hosford, 1992; Meijer *et al.*, 1990; Meijer and Molema, 1995; Moseley, 1997; Moseley *et al.*, 1992, 1996a and 1996b; Muller *et al.*, 1994; Neef *et al.*,

1984a; Oude Elferink *et al.*, 1995; Steen *et al.*, 1991 and 1992), and little information is available on interspecies differences in transport mechanisms (Groothuis and Meijer, 1996; Oude Elferink *et al.*, 1995; Sandker *et al.*, 1994; Steen and Meijer, 1991). Although primarily cleared in the kidney, TEA has been used as a model compound to study organic cation transport in the liver (McKinney and Hosford, 1992; Moseley *et al.*, 1992). In some studies, tributylmethylammonium (TBuMA), which is eliminated by the liver, has also been used (Moseley *et al.*, 1996a; Steen *et al.*, 1991). Accordingly, a model similar to the renal model of organic cation transport, has been proposed for hepatic transport of organic cations (Groothuis and Meijer, 1996; Meijer, 1987; Meijer and Molema, 1995; Meijer *et al.*, 1990; Oude Elferink *et al.*, 1995). That is, an electrogenic organic cation transport process is located on the basolateral side and a proton-dependent transport process is found on the apical side of the cell. However, unlike organic cation transporters in the kidney, NMN does not inhibit the hepatic transport of TEA at either the sinusoidal or canalicular membrane (McKinney and Hosford, 1992; Moseley *et al.*, 1990 and 1992). Besides the transport processes in the sinusoidal (basolateral) and canalicular (apical) plasma membrane, intracellular transport sites have also been identified in organelles such as endosomes, lysomes and mitochondria (Moseley and Van Dyke, 1995; Van Dyke *et al.*, 1992).

Similar to the kidney, there appear to be multiple mechanisms involved in the transport of organic cations in the liver (Figure 1.6). At least five distinct transport processes have been postulated for exogenous cations at the sinusoidal and canalicular level of the hepatocyte (Groothuis and Meijer, 1996; Oude Elferink *et al.*, 1995): a type I (small organic cation) carrier system, a type II (divalent, bulky organic cation) carrier system, a noncharge-selective multispecific carrier system, the multi-drug resistance carrier-protein (P-glycoprotein) and a carrier transporting both type I and type II compounds on the canalicular membrane. These mechanisms for sinusoidal transport of organic cations are briefly described below (Figure 1.6):

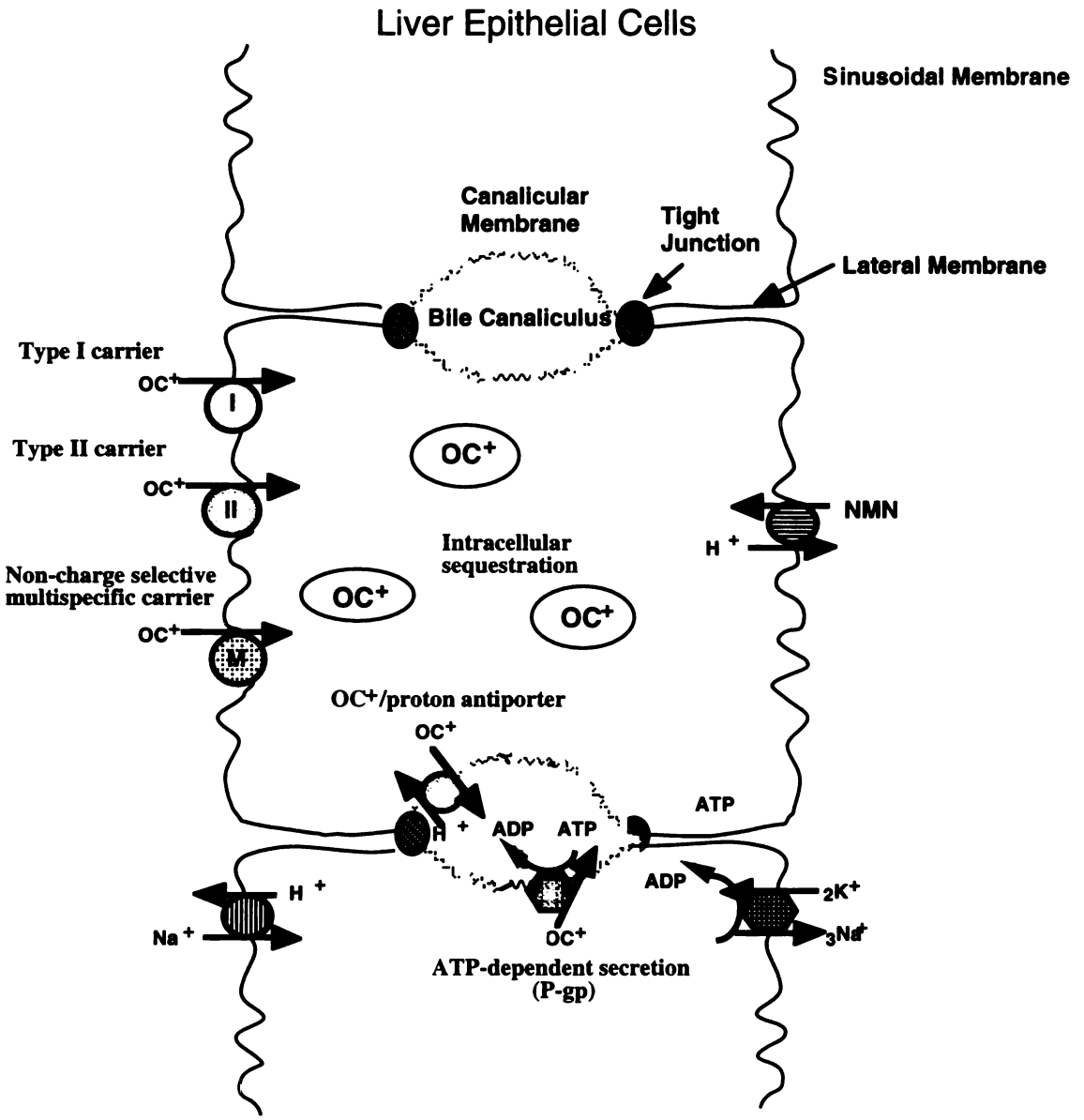

Figure 1.6 Model of organic cation secretion across the epithelium of the hepatocyte.

(1) The type I carrier system accepts small, monovalent organic cations such as TEA and has considerable overlap in specificity with the electrogenic renal basolateral membrane organic cation transporter except that NMN is not a substrate for the type I carrier in the liver. Bulkier organic cations are inhibitors, but it is not clear whether they are also substrates of the type I carrier system (McKinney and Hosford, 1992; Mol *et al.*, 1992; Moseley *et al.*, 1992; Steen *et al.*, 1991; Vonk *et al.*, 1978a).

(2) The type II carrier system accepts bulkier and/or multi-valent organic cations such as the muscle relaxants, vecuronium and pancuronium, and excludes small organic cations (Bencini *et al.*, 1988; Meijer *et al.*, 1970; Mol *et al.*, 1988). Furthermore, cardiac glycosides and bile acids exert potent inhibitory effects on the type II, but not the type I, carrier (Vonk *et al.*, 1978a and 1978b). Although proposed to be on the sinusoidal membrane, the precise location of the type II transporter has not been identified.

(3) A noncharge-selective multispecific transport system has recently been characterized in rat hepatocytes (Steen *et al.*, 1992). This system accepts both type I and type II organic cations plus neutral molecules such as digoxin and anions such as taurocholate. Similar to the type II transporter, the precise location of the noncharge selective multispecific transporter has not been identified.

(4) An organic cation proton antiporter selective for NMN has been characterized on the sinusoidal membrane of the hepatocyte (Moseley *et al.*, 1990). Unlike the renal organic cation proton antiporter which is selective for both TEA and NMN, this transporter excludes TEA. Its location on the basolateral membrane of the hepatocyte also distinguishes it from the renal brush border membrane organic cation proton antiporter.

Transport of organic cations across the canalicular membrane appears to involve two distinct mechanisms (Figure 1.6):

(1) A proton-dependent transport process accepts both type I and type II organic cations but NMN shows no inhibition (Moseley *et al.*, 1992). However, it is not clear what role this proton antiporter plays in overall secretion of cationic drugs into bile because there is no apparent bile-to-cell proton gradient to provide a driving force. (In the hepatocyte, the Na^+/H^+ antiporter is localized to the sinusoidal membrane).

(2) An ATP-dependent process (P-glycoprotein mediated transport process) transports bulky, amphiphilic cations such as quinidine and ajmalinium (Ford and Hait, 1990; Homolya *et al.*, 1993; Kamimoto *et al.*, 1989; Martel *et al.*, 1996b; Muller *et al.*, 1994).

Although data are limited, notable species differences have been observed in the rate of transport of the organic cation, vecuronium, in human and rat hepatocytes (Sandker *et al.*, 1994). Namely, the influx rate constant (k_{in}) of vecuronium in isolated rat hepatocytes was a factor of 10 greater than in human hepatocytes, and similar differences were also observed in the intact organ. These data suggest that transporters among various mammalian species may have different intrinsic functional characteristics.

1.3.3 Intestine

1.3.3.1 General Structure and Function

The primary function of the intestinal epithelium is to absorb molecules that are produced from digestion of food. In addition, this epithelium has been recently recognized as an important site of secretion of many substances. The quantity of fluid that is absorbed per day in the entire gastrointestinal tract is enormous—approximately 9 liters (1.5 liters from ingested material and approximately 7-8 liters of intestinal secretions). The small

intestine absorbs all but 1.5 liters which is presented to the large intestine where additional reabsorptive processes occur.

The entire gastrointestinal tract is lined by a continuous sheet of epithelia. However, the epithelial morphology as well as function of different segments of the gastrointestinal tract is variable (Figure 1.7). Some areas are primarily involved in selective absorption of various nutrients but not others. Other sites are primarily involved in secretion, and others perform both functions.

The stomach lacks the villus structure characteristic of other areas of the gastrointestinal tract. The gastric epithelium is characterized by tight junctions. This epithelia is not a primary site of solute absorption. In contrast, the apical surface of the small intestinal epithelium is characterized by the presence of villi (0.5-1.0 mm long), which have a single layer of columnar epithelial cells along the surface. These cells have microvilli (100 nm in diameter), which form the "brush border" of the cell. These projections of the cell surface extend into the lumen and increase the surface area available for transfer of substances. This anatomy of villi and microvilli expands the surface area of the small intestine to about 250 square meters. The average life span of mucosal cells is 2-5 days. The human small intestine sheds about 17 billion of these cells per day.

The main function of the colon is absorption of water and sodium but essentially no significant amount of nutrients. Consistent with this, there are no villi on the mucosa of the colon, and the tight junctions are more like those in the stomach than those in the small intestine. This site reduces the content of water in stool by 90%. That is, 1-2 liters is converted into ~100-200 ml of stool.

As with all epithelia, some degree of tight junctions are necessary between the gastrointestinal cells. However, some of the intestinal epithelia are 'leaky' (resistance less than 100 Ω cm^2) while other sites are 'tight' (~500 Ω cm^2) (Table 1.1). Leaky epithelia cannot maintain, while tight epithelia do maintain, steep concentration gradients.

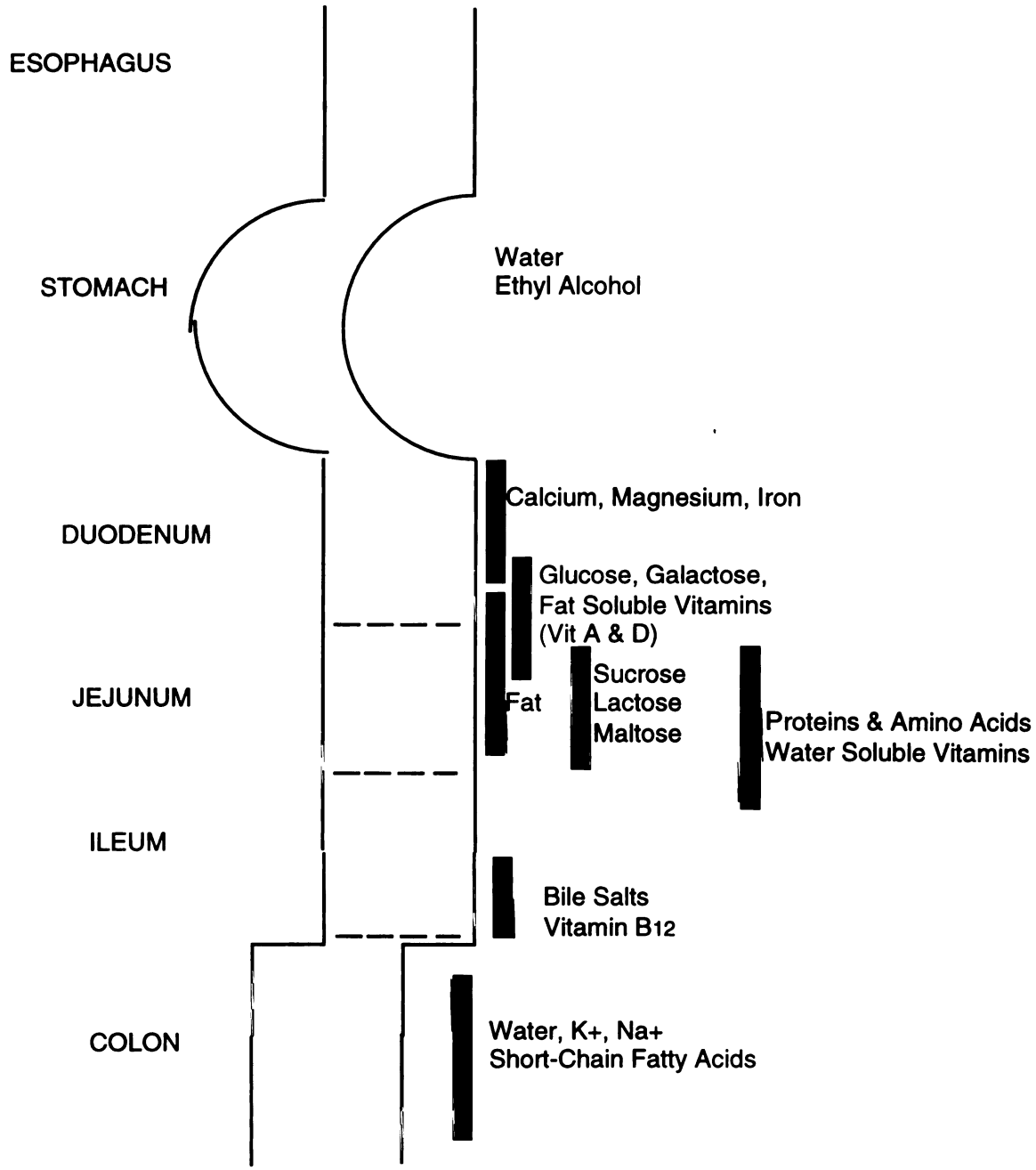

Figure 1.7 Site of absorption of various molecules in the gastrointestinal tract. (Adapted from Hunt and Groff, 1990)

Table 1.1 Properties of various regions of the gastrointestinal tract as compared to other organs[a]

	Potential Difference (*mV*)	Resistance ($\Omega \bullet cm^2$)	pH	Brushborder Microvilli	Primary Function
Stomach	10-60	100-600	1-3	None	Food storage HCl secretion
Liver	~5			++	Metabolic Hematopoetic Bile secretion
Gall bladder	0-3	30-100		++	Bile storage
Small intestine	1-3	30-70	5-7	++++	Reabsorption of nutrients
Large intestine	10-50	100-500	7-8	None	Reabsorption of water
Urinary bladder		50,000			

[a] Adapted from Steward and Case, 1989.

1.3.3.2 Organic Cation Transport

The small intestine is the major route for drug entry. However, the single layer of epithelial cells connected by tight junctions forms the barrier between the lumen and capillaries. Especially for polar drugs, specific proteins in the membrane of epithelial cells will control the entry and exit of drugs depending on the substrate selectivity of these carriers.

Intestinal organic cation transport has been investigated using techniques such as isolated membrane vesicles (Miyamoto *et al.*, 1988; Ruifrok, 1981; Saitoh *et al.*, 1992), analogous to transport studies performed in the kidney and liver . Other *in vivo* and *in vitro* techniques (everted intestinal sacs and Ussing chambers mounted with isolated intestinal mucosa) (Acra and Ghishan, 1991; Grass and Sweetana, 1988; Lennernas *et al.*, 1997; Leppert and Fix, 1994) were developed specifically to study intestinal transport. In particular, Ussing chambers allow the investigator to monitor the substrate composition on either side of a membrane, and in that way, define the directional transport of a compound.

A number of organic cations are incompletely absorbed after oral administration and may also be actively secreted in the intestine (Hardman *et al.*, 1996). Intestinal transporters may play a critical role in limiting and/or promoting the absorption or secretion of a number of clinically important drugs. Improving absorption of some drugs or understanding how the intestine functions as an organ of elimination for other drugs (i.e., secretion) might prove to be an important therapeutically-relevant goal.

In comparison to the kidney and liver, fewer data are available regarding the mechanisms of organic cation transport in the intestine. The limited studies of intestinal organic cation transport have focused primarily on the mechanisms across the brush border membrane; virtually nothing is known about the mechanisms of organic cation transport across the intestinal basolateral membrane. Consequently, the model for organic cation

transport in the intestine is incompletely defined. Furthermore, many studies have focused on individual drugs rather than on model organic cations such as TEA or NMN.

Lauterbach and coworkers first demonstrated active secretion of quaternary ammonium compounds in the intestine of the rat and guinea pig using both *in vivo* and *in vitro* methods (Turnheim and Lauterbach, 1977a, 1977b and 1980; Turnheim *et al.*, 1977). Based upon the data obtained in their studies, secretion of organic cations appears to involve two carrier-mediated processes in series with one located on the seroal (basolateral) side and one on the mucosal (apical) side (Turnheim *et al.*, 1977). Recently, active secretion of a specific class of organic cations, the β-blockers, has been demonstrated in both human (Gramatte *et al.*, 1996) and rat intestine (Kuo *et al.*, 1994; Lennernas and Regardh, 1993a and 1993b).

Similar to the liver and kidney, multiple mechanisms of organic cation transport have been characterized in the intestinal brush border membrane (Figure 1.8). These are enumerated below:

(1) A proton antiporter for guanidine has been demonstrated in isolated brush border membrane vesicles prepared from rabbit intestine which would presumably mediate secretion (Miyamoto *et al.*, 1988). Interestingly, neither TEA nor NMN interact with this guanidine selective transporter. Furthermore, in contrast to the kidney and liver, a proton antiporter for TEA is absent in the rabbit intestine (Miyamoto *et al.*, 1988).

(2) The involvement of P-glycoprotein in the secretion of certain organic cations such as verapamil and celiprolol has been demonstrated in both rat intestine (Saitoh and Aungst, 1995), human Caco-2 cells (Karlsson *et al.*, 1993), and in a multidrug-resistant leukemic cell line variant (K562/ADM) (Terao *et al.*, 1996).

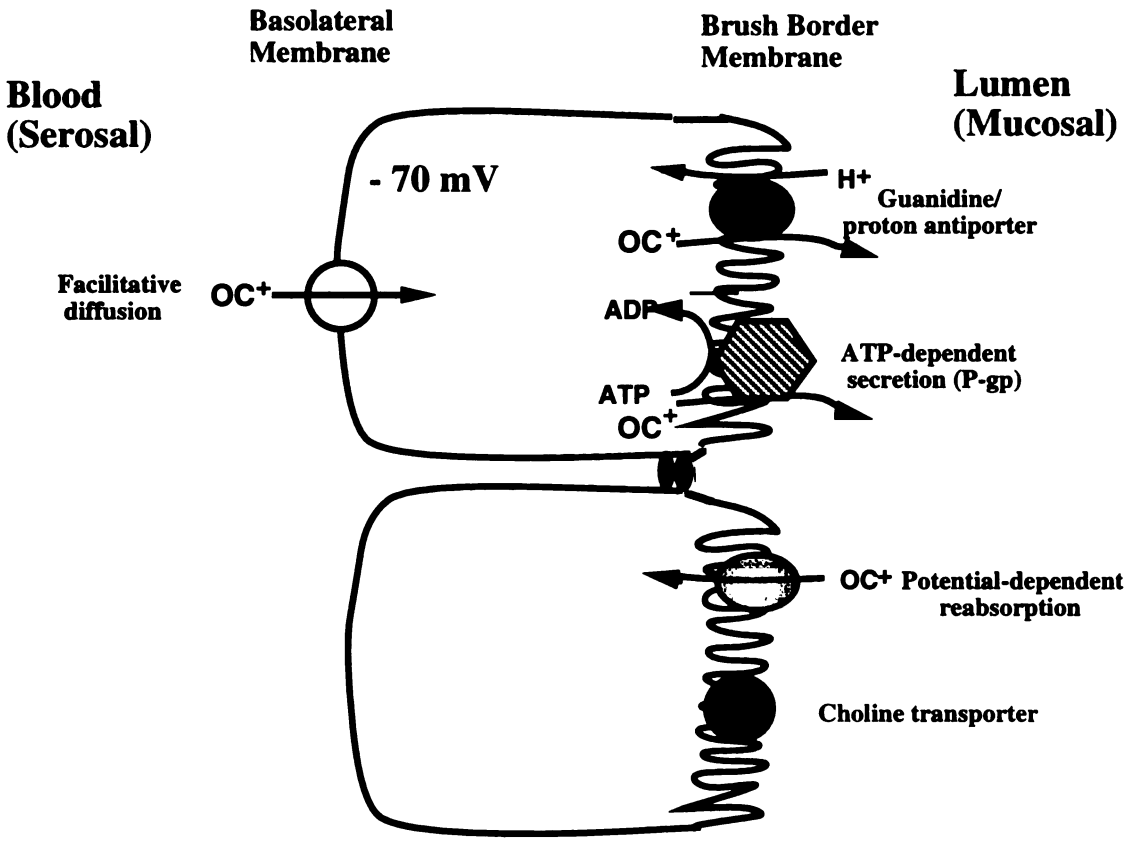

Figure 1.8 Model of organic cation transport across the epithelium of the intestine.

(3) Transport of various organic cations (e.g., disopyramide, tyramine) across the rat intestinal brush-border membrane involves a potential dependent mechanism (Iseki *et al.*, 1993; Takahashi *et al.*, 1993). This mechanism, which is distinct from the electroneutral organic cation proton-antiporters found in the apical membrane of various epithelia, may mediate absorption.

(4) Finally, a choline transport process with no driving force has been characterized in rat intestinal brush-border membrane vesicles (Saitoh *et al.*, 1992). TEA did not affect choline transport.

As discussed above, the regional specific absorption and secretion of fluid and electrolytes in the intestine is well-established. In contrast, little is known about regional differences in intestinal absorption and secretion of drugs. Recently, regional specific intestinal transport of several β-blockers has been demonstrated (Gramatte *et al.*, 1996; Lennernas and Regardh, 1993b). It will be interesting to learn whether the observed transport characteristics are related to the differences in the distribution of the the transport proteins for organic cations.

1.4 Aims and Outline of This Thesis

Polyspecific organic cation transporters in the epithelia mediate the transport of many clinically used drugs as well as endogenous metabolites. To understand the mechanism of organic cation transport in epithelia and the role of organic cation transporters in drug absorption and elimination, it is critical to elucidate the multiplicity of the transport mechanisms using different organic cations as model compounds, to clone the individual organic cation transporters and to study their functions, especially drug interactions in heterologous expression systems. These are overall aims of my thesis.

When I started my thesis research, two organic cation transporters (rOCT1 and rOCT2) had been cloned from rat kidney (Grundemann *et al.*, 1994; Okuda *et al.*, 1996; Walsh *et al.*, 1996). Subsequently, I used homology cloning methods and cloned two new organic cation transporters (Zhang *et al.*, 1997a and 1997b; Chapters 4 and 5). In the mean time, other organic cation transporters have been cloned in our and other laboratories (Gorboulev *et al.*, 1997; Grundemann *et al.*, 1997; Kekuda *et al.*, 1998; Lopez-Nieto *et al.*, 1997; Taimi *et al.*, 1997; Terashita *et al.*, 1998; Wu *et al.*, 1998a and 1998b).

The outline of my thesis is as follows:

1.4.1 Chapter 2

A proton-antiporter on the brush-border membrane using TEA as a model compound has been characterized in various species. However, studies in rabbit and human kidney preparations suggest that guanidine, an endogenous organic cation, is actively transported by mechanisms distinct from those described for TEA. The goal of this study was to determine the mechanisms of guanidine transport across rat renal brush-border membrane. Rat renal brush-border membrane vesicles (BBMV) were prepared by divalent cation precipitation and ultracentrifugation. The uptake of ^{14}C-guanidine in the BBMV, determined by rapid vacuum filtration, was saturable with a K_m of 3.59 ± 1.12 mM and a V_{max} of 94.4 ± 15.9 pmol/mg protein/sec in buffer containing 150 mM KCl. Uptake was *trans*-stimulated by 5 mM guanidine or TEA. The uptake of guanidine was also *cis*-inhibited by various organic cations including guanidine, TEA, cimetidine and N^1-methylnicotinamide (NMN). Proton gradient-stimulated ^{14}C-guanidine uptake was observed in the absence but not in the presence of KCl. In contrast, proton gradient-stimulated ^{14}C-TEA uptake was observed in either the presence or absence of KCl (150 mM). Transport of guanidine exhibited both higher affinity and capacity in the absence of KCl. In addition, an outwardly-directed proton gradient increased both the K_m and V_{max} (0.32 ± 0.13 mM and 147 ± 20 pmol/mg protein/sec without proton gradient vs. 0.61 ±

0.16 mM and 345 ± 36 pmol/mg protein/sec with proton gradient). The data suggest that the mechanisms of guanidine transport are distinct from those of TEA transport in rat BBMV.

1.4.2 Chapter 3

We studied the expression of guanidine transport activity in *Xenopus laevis* oocytes to develop a functional assay for expression cloning of a renal "guanidine-selective" transporter. *X. laevis* oocytes were injected with rat kidney mRNA and uptake studies were carried out four days post-injection. In mRNA-injected oocytes, the uptake of ^{14}C-guanidine was significantly increased ($p < 0.05$) compared to that in water-injected oocytes (36.7 ± 5.4 vs. 12.2 ± 3.9 pmol/oocyte/hr, mean ± SD). Further enhancement of guanidine uptake was achieved in oocytes injected with an enriched size-fraction of mRNA ranging between 1.4 and 3.7 kb (average size of 2.2 kb) (9-fold greater in comparison to water-injected oocytes). The uptake of ^{14}C-guanidine was saturable (K_m of 254 ± 76 μM) and was inhibited by a number of organic cations including TEA, guanidine, cimetidine, choline, and NMN. Uptake studies in oocytes injected with the cRNA of a recently cloned rat renal organic cation transporter, rOCT1, revealed a less than two-fold enhancement of ^{14}C-guanidine uptake in comparison to that obtained in water-injected oocytes (15.0 ± 3.9 vs. 8.8 ± 1.5 pmol/oocyte/hr, mean ± SD). In contrast, a greater than 6-fold enhancement (range 6-60 fold) of ^{14}C-guanidine uptake in comparison to that obtained in water-injected oocytes was observed in oocytes injected with the cRNA of rOCT2. K_m values of guanidine transport obtained in oocytes injected with total rat kidney mRNA and rOCT2 cRNA were comparable (254 μM vs. 234 μM). These data suggest that the expressed activity of guanidine transport in mRNA-injected oocytes can be accounted for, at least in part, by expression of rOCT2 which translocates both guanidine and TEA. These studies provide further evidence for the involvement of multiple polyspecific organic cation transporters in the renal elimination of cationic drugs.

1.4.3 Chapter 4

In this study, we report the cloning and functional expression of an rOCT1 isoform, rOCT1A, from rat kidney. Genomic DNA cloning and sequencing demonstrated that rOCT1A is an alternatively spliced variant of rOCT1 with a deletion of 104 bp near the 5'-end. The uptake of ^{14}C-TEA in oocytes injected with the cRNA encoding rOCT1A was increased 16-fold over that in water-injected oocytes (29 ± 3 pmol/oocyte/hr vs 1.8 ± 0.1 pmol/oocyte/hr, mean ± SE, $p < 0.05$). ^{14}C-TEA uptake in the cRNA injected oocytes was saturable ($K_m = 42 \pm 11$ μM) and was inhibited significantly by organic cations including cimetidine and NMN. The amino acid sequence was deduced from the cDNA after examination of all three reading frames. Two overlapping open reading frames were found. Studies with synthetic constructs suggest that a functional organic cation transporter is encoded by the larger open reading frame. The larger open reading frame encodes a 430 amino-acid protein (termed rOCT1A) which is 92% identical to rOCT1 and 57% identical to rOCT2. From hydropathy analysis, rOCT1A is predicted to have ten transmembrane domains with both the amino and carboxy termini intracellular. RNase protection assays demonstrate the presence of rOCT1A mRNA transcripts in rat kidney cortex and medulla and in the intestine. These studies demonstrate the presence of a functional, alternatively spliced organic cation transporter (rOCT1A) in rat kidney.

1.4.4 Chapter 5

Polyspecific organic cation transporters in the liver mediate the elimination of a wide array of endogenous amines and xenobiotics. In contrast to our understanding of the mechanisms of organic cation transport in rat liver, little is known about the mechanisms of organic cation transport in the human liver. In this study, we report the cloning, sequencing and functional characterization of the first human polyspecific organic cation

transporter from liver (termed hOCT1). hOCT1 (554 amino acids) is 78% identical to the previously cloned organic cation transporter from rat, rOCT1. In *Xenopus laevis* oocytes injected with the cRNA of hOCT1, the specific uptake of the organic cation, ^{3}H-MPP$^+$, was significantly enhanced (8-fold) over that in water injected oocytes. Uptake of ^{3}H-MPP$^+$ was saturable (K_m = 14.6 ± 4.4 μM) and sensitive to membrane potential. Both small monovalent organic cations such as TEA and NMN and bulkier organic cations (e.g., vecuronium and decynium-22) inhibited the uptake of ^{3}H-MPP$^+$. In addition, the bile acid taurocholate inhibited the uptake of ^{3}H-MPP$^+$ in oocytes expressing hOCT1. Northern analysis demonstrated that the mRNA transcript of hOCT1 is expressed primarily in the human liver whereas the mRNA transcript of rOCT1 is found in rat kidney, liver, intestine and colon, In comparison to rOCT1, hOCT1 exhibits notable differences in its kinetic characteristics and tissue distribution. The functional expression of hOCT1 will provide a powerful tool for elucidating the mechanisms of organic cation transport in the human liver and understanding the mechanisms involved in the disposition and hepatotoxicity of drugs.

1.4.5 Chapter 6

The purpose of this study was to develop a mammalian expression system for hOCT1 and to characterize the interactions of various compounds with the cloned transporter. Lipofection was used to transiently transfect the hOCT1 plasmid DNA in a human cell line, HeLa. We tested the interaction of an array of organic cations and other compounds with hOCT1 by determining K_i values in inhibiting ^{14}C-TEA transport in the transfected cells. Transient expression of hOCT1 activity was observed between 24 and 72 hours post-transfection, with maximal expression at approximately 40 hours. TEA transport was temperature dependent and saturable with V_{max} and K_m values of 2.89 ± 0.45 nmol/mg protein/30 min and 229 ± 78 μM, respectively. ^{14}C-TEA uptake in hOCT1

plasmid DNA-transfected HeLa cells was *trans*-stimulated by unlabeled TEA and MPP^+. Organic cations including clonidine, quinine, quinidine and verapamil (0.1 mM) significantly inhibited ^{14}C-TEA uptake, whereas the organic anion, *p*-aminohippuric acid (PAH) (5 mM), did not. The neutral compounds, corticosterone (K_i of 7.0 μM) and midazolam (K_i of 3.7 μM) potently inhibited ^{14}C-TEA uptake. K_i values of several compounds interacting with hOCT1 differed substantially from the corresponding values for the rat organic cation transporter, rOCT1, and the human kidney-specific organic cation transporter, hOCT2, as determined in previous studies. Transiently transfected HeLa cells represent a useful tool in the study of the interactions and kinetics of organic cations and other xenobiotics with hOCT1 and in understanding the molecular events involved in organic cation transport.

1.4.6 Chapter 7

HIV protease inhibitors are a new class of therapeutic agents. The purpose of this study was to elucidate the interactions of HIV protease inhibitors with hOCT1 and to determine whether hOCT1 is involved in the elimination of these compounds. We studied the interactions of HIV protease inhibitors with hOCT1 in a transiently transfected human cell line, HeLa. Uptake studies were carried out 40 hours post-transfection using radiolabeled model organic cation, ^{14}C-TEA, under different experimental conditions. In *cis*-inhibition studies, all the HIV protease inhibitors, i.e., indinavir (IC_{50} of 62 μM), nelfinavir (IC_{50} of 22 μM), ritonavir (IC_{50} of 5.2 μM), and saquinavir (IC_{50} of 8.3 μM) potently inhibited TEA uptake in HeLa cells expressing hOCT1. However, none of the HIV protease inhibitors *trans*-stimulated ^{14}C-TEA uptake suggesting that they are poorly translocated by hOCT1. Nelfinavir, ritonavir, and saquinavir demonstrated an apparent "*trans*-inhibition" effect. No enhanced uptake of ^{14}C-saquinavir was observed in hOCT1

DNA -transfected cells versus empty vector-transfected cells. These data suggest that HIV protease inhibitors are potent inhibitors but are poor substrates of hOCT1. hOCT1 does not appear to play a role in the elimination of these agents. However, HIV protease inhibitors may potently inhibit the elimination of cationic drugs which are substrates for hOCT1 leading to potential drug-drug interactions.

1.4.7 Chapter 8

The purpose of this study was to determine the effect of molecular size and hydrophobicity on the transport of organic cations by hOCT1. We studied the interaction of a series of n-tetraalkylammonium (n-TAA) compounds (alkyl chain length, N, ranging from 1 to 6 carbons) with hOCT1 in a transiently transfected human cell line, HeLa. ^{14}C-TEA uptake was measured under different experimental conditions. Both *cis*-inhibition and *trans*-stimulation studies were carried out. With the exception of tetramethylammonium (TMA), all the n-TAAs significantly inhibited ^{14}C-TEA uptake. A reversed correlation of IC_{50} values (range 3.0 to 260 μM) with alkyl chain lengths or partition coefficients (LogP) was observed. *Trans*-stimulation studies revealed that TEA, tetrapropylammonium (TPrA), tetrabutylammonium (TBA) as well as tributylmethylammonium (TBuMA) *trans*-stimulated TEA uptake mediated by hOCT1. In contrast, TMA and tetrapentylammonium (TPeA) did not *trans*-stimulate ^{14}C-TEA uptake, and tetrahexylammonium (THA) demonstrated an apparent "*trans*-inhibition" effect. These data indicate that with increasing alkyl chain length ($N \geq 2$), n-TAA compounds are more poorly translocated by hOCT1 although their potency of inhibition increases. These data suggest that a balance between hydrophobic and hydrophilic properties is necessary for binding and subsequent translocation by hOCT1.

CHAPTER 2

TRANSPORT OF GUANIDINE IN RAT RENAL BRUSH-BORDER MEMBRANE VESICLES [1]

2.1 Introduction

Many clinically used cationic drugs as well as endogenous metabolites are organic cations which carry at least one positively-charged amine moiety under physiological pH. Many organic cations are actively secreted from blood to urine. Transepithelial movement of organic cations is mediated by organic cation transporters located on both the basolateral and brush-border membrane of the renal proximal tubule (see reviews McKinney, 1993; Pritchard and Miller, 1993; Roch-Ramel *et al.*, 1992; Zhang *et al.*, 1998a). Using TEA as a model compound, a three-step model has been proposed: a potential-dependent, facilitated process at the basolateral membrane, intracellular sequestration, and a proton/organic cation exchanger at the brush-border membrane (Pritchard and Miller, 1993).

The proton/organic cation exchange mechanism (also termed organic cation proton antiporter 1, OCPA1), using TEA and NMN as model compounds, has been demonstrated in brush-border membrane vesicles (BBMV) from the kidneys of various species including rats, rabbits, dogs and humans (Dantzler *et al.*, 1989; Holohan and Ross, 1981; Hsyu and Giacomini, 1987; Ott *et al.*, 1991; Rafizadeh *et al.*, 1987; Sokol *et al.*, 1985; Takano *et al.*, 1984; Wright, 1985; Wright and Wunz, 1987). This process is electroneutral with an

[1] This study was presented in part at the 11th Annual Meeting of American Association of Pharmaceutical Scientists in November 2-6, 1997 in Boston, MA.

organic cation:H^+ stoichiometry of 1:1, and the inwardly-directed proton gradient is proposed to be generated largely by the Na^+-H^+ exchanger located on the brush-border membrane (Aronson, 1985). This mechanism has a broad substrate-selectivity and is considered to be the transporter that functions in the excretion of a wide array of organic cations in the kidney.

More recently, data suggest that a second organic cation transporter (termed organic cation proton antiporter 2, OCPA2), is involved in the renal elimination of organic cations (Chun *et al.*, 1997a; Miyamoto *et al.*, 1989). This transporter differs from the TEA-proton antiporter in substrate selectivities and kinetic parameters. Namely, OCPA2 is selective for guanidine, interacts with 5-(*N*-methyl-*N*-isobutyl)amiloride (MIBA), but generally excludes TEA and NMN. The goals of the current investigation are to determine whether there is a guanidine transporter, distinct from the TEA transporter, in the rat kidney.

In the present study, we provide evidence for a guanidine-selective transport mechanism in the renal brush border membrane of the rat. The transport mechanism is distinct from both OCPA1 and OCPA2. Namely, guanidine transport in rat renal BBMV was pH-independent in KCl containing buffer whereas both OCPA1 and OCPA2 are pH-sensitive in the presence of KCl. In comparison to TEA transport in rat renal BBMV, guanidine transport demonstrates potency rank order differences from that of TEA transport consistent with two distinct pathways for organic cation transport in the rat kidney. Furthermore, substrate selectivity for guanidine transport in rat kidney is different from that of OCPA2 described in rabbit and human kidney, i.e., TEA and NMN also interact with guanidine transport.

2.2 Materials and Methods

2.2.1 Preparation of Brush-Border Membrane Vesicles (BBMV)

BBMV were isolated from the renal cortex of male Sprague-Dawley rats (280-300g) by the Mg^{2+}/EGTA precipitation method as modified in our laboratory (Chun *et al.*, 1997a; Ott *et al.*, 1991). All steps were performed on ice or at 4°C. Briefly, the rat renal cortex was homogenized in ice-cold HK-EGTA buffer (150 mM KCl, 10 mM HEPES, 5 mM EGTA, pH 7.4). The homogenate was stirred in $MgSO_4$ (16 mM) on ice for 20 min. After a series of centrifugations, the vesicles were resuspended in HK buffer (150 mM KCl, 10 mM HEPES, pH 7.4). For pH-dependent studies, the vesicles were pre-incubated in MK buffer (150 mM KCl, 10 mM MES, pH 6.0) for an hour before uptake studies. For counter-flux studies, the vesicles were preincubated (1 hr) in HK buffer containing 5 mM unlabeled guanidine or TEA as mentioned in the legend of the relavent figures. The transport studies were performed using freshly-prepared BBMV.

2.2.2 Transport Studies

Uptake of ^{14}C-guanidine (50 μM) in vesicles (200-400 μg) was measured by a rapid filtration technique using Millipore pH-type filters (0.3 μm, Millipore, Bedford, MA)at room temperature as previously described (Chun *et al.*, 1997a). At the end of the incubation time, the uptake was stopped by adding ice-cold buffer and filtering the suspension under vacuum through the filter. The filter was washed three times with ice-cold buffer and placed into 5ml of scintillant. The radioactivity associated with the filter was determined by liquid scintillation counting (LS-1801, Beckman Instruments, Fullerton, CA).

2.2.3 Analytical Methods

The protein concentration was determined by the Bradford method using a Bio-Rad protein assay kit (Bio-Rad, Herculus, CA) with bovine serum albumin (BSA) as standard. The purity of the BBMV was monitored by measuring the enrichment of enzyme markers. The activity of alkaline phosphatase (Sigma, St. Louis, MO), an enzyme marker for the brush-border membrane, and Na^+-K^+ ATPase, an enzyme marker for the basolateral membrane, was determined in the final suspension and compared to the activity in the initial homogenate.

2.2.4 Data Analysis

Data are presented as mean ± Standard Deviation (SD). In Michaelis-Menten studies, kinetic parameters were calculated by nonlinear regression from the following equation: $V=V_{max}\cdot[S]/(K_m+[S])$, where V is the initial uptake rate, V_{max} is the maximal transport rate, K_m is the concentration needed to reach half of V_{max}, [S] is the concentration of guanidine in the extravesicular solution. Student *t*-test were used for statistical analysis and $p < 0.05$ was considered significant.

2.2.5 Materials

^{14}C-Guanidine hydrochloride (56 mCi/mmol) was purchased from Moravek (Brea, CA) and ^{14}C-TEA bromide (53 mCi/mmol) was purchased from American Radiolabeled Chemicals, Inc. (St. Louis, MO). All other chemicals used were of the highest purity available and were from Sigma.

2.3 Results

2.3.1 Effect of an Outwardly-Directed Proton Gradient on Guanidine and TEA Uptake

The time course of guanidine uptake in BBMV in the presence ($[H^+]_i > [H^+]_o$) and absence ($[H^+]_i = [H^+]_o$) of an outwardly directed proton gradient is shown in Figure 2.1a. The uptake of guanidine (50 μM) in the vesicles was not affected by the proton gradient at all time points. However, proton-coupled uphill transport of TEA via the organic cation-proton antiporter was observed (Figure 2.1b).

Since potassium was shown to inhibit the uptake of guanidine uptake in BBMV isolated from rabbit kidney and human placenta (Ganapathy *et al.*, 1988; Miyamoto *et al.*, 1989), 150 mM KCl was replaced with 300 mM mannitol. "Overshoot phenomena" were observed for both TEA and guanidine uptake in the presence of the pH-gradient (Figures 2.2a and 2.2b).

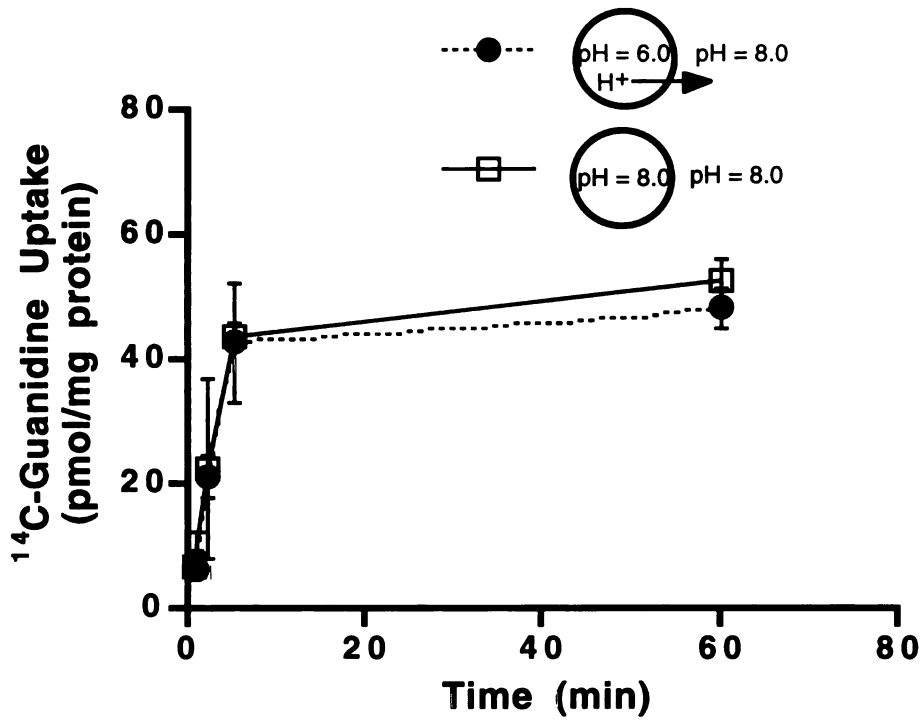

Figure 2.1a Uptake of ^{14}C-guanidine (50 μM) in rat kidney BBMV in the presence (pH_{in}:pH_{out} = 6.0:8.0) or absence (pH_{in}:pH_{out} = 8.0:8.0) of an outwardly-directed proton gradient in HK buffer. Data are from one representative experiment (mean ± SD), n = 3.

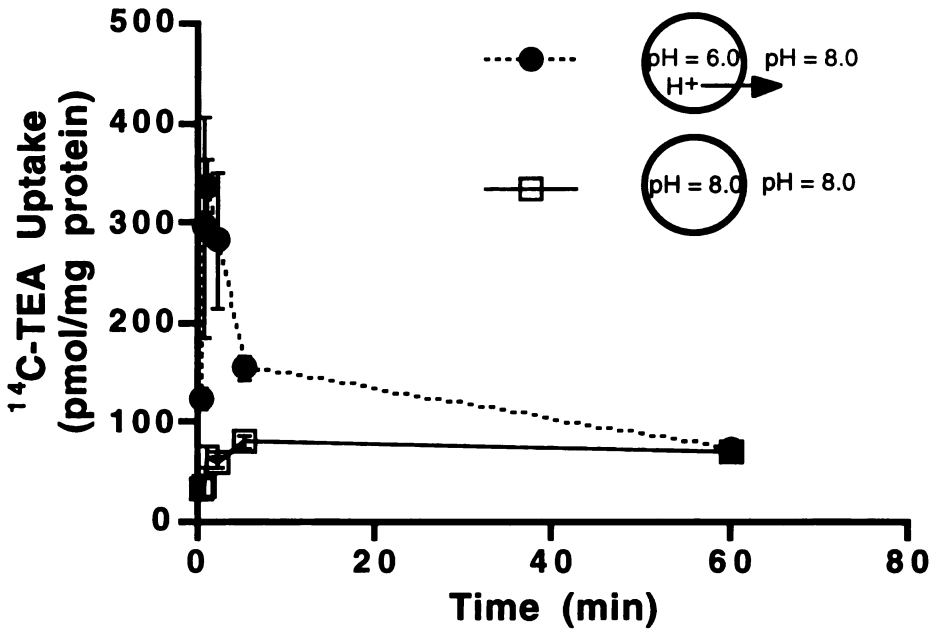

Figure 2.1b Uptake of ^{14}C-TEA (50 μM) in rat kidney BBMV in the presence (pH_{in}:pH_{out} = 6.0:8.0) or absence (pH_{in}:pH_{out} = 8.0:8.0) of an outwardly-directed proton gradient in HK buffer. Data are from one representative experiment (mean ± SD), n = 3.

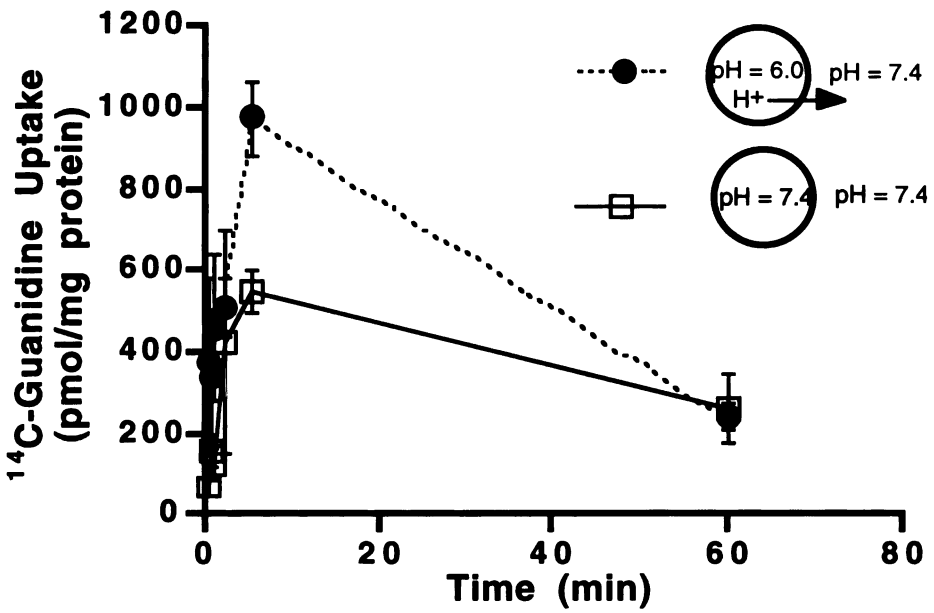

Figure 2.2a Uptake of ^{14}C-guanidine (50 μM) in rat kidney BBMV in the presence (pH_{in}:pH_{out} = 6.0:7.4) or absence (pH_{in}:pH_{out} = 7.4:7.4) of an outwardly-directed proton gradient in K^+-free (replaced with mannitol) buffer. Data are from one representative experiment (mean ± SD), n = 3.

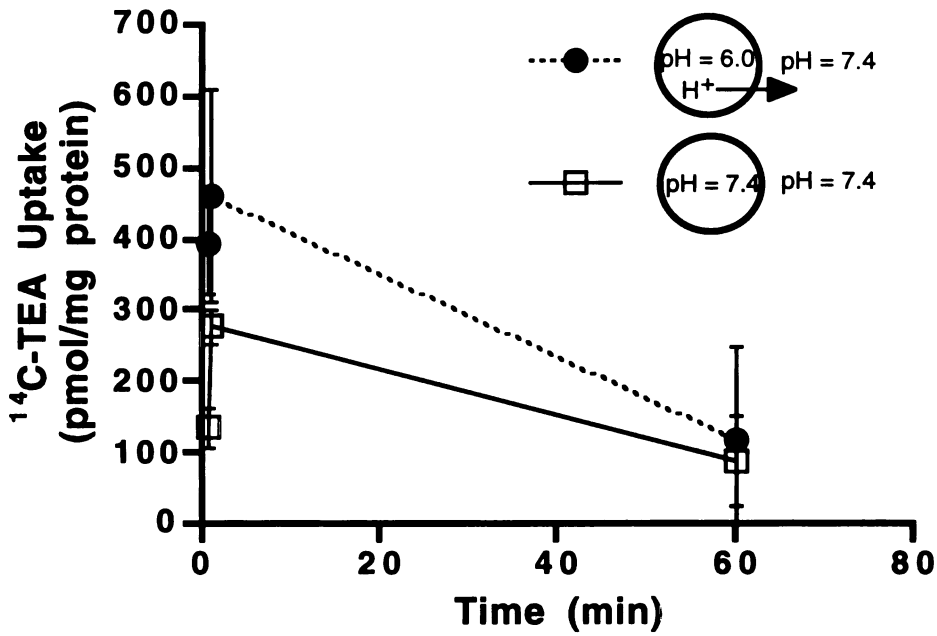

Figure 2.2b Uptake of ^{14}C-TEA (50 μM) in rat kidney BBMV in the presence (pH_{in}:pH_{out} = 6.0:7.4) or absence (pH_{in}:pH_{out} = 7.4:7.4) of an outwardly-directed proton gradient in the K^+-free (replaced with mannitol) buffer. Data are from one representative experiment (mean ± SD), n = 3.

2.3.2 *Effect of Membrane Potential on Guanidine Uptake*

we examined the effect of membrane potential difference on guanidine transport. Imposition of a large inside negative potential (created by an outwardly directed K^+ gradient and valinomycin, a potassium ionophore) generated the largest stimulation in guanidine transport at early time points (78.0 ± 11.7 pmol/mg protein/5 min, mean ± SD). An outwardly directed K^+ gradient alone (K_{in}=150 mM, K_{out}=0 mM, without valinomycin) also stimulated guanidine uptake compared to the voltage-clamped vesicles (K_{in}=K_{out}=150 mM, plus valinomycin) (53.8 ± 3.5 vs. 41.4 ± 7.3 pmol/mg protein/5 min, mean ± SD). Moreover, an inwardly directed K^+ gradient (K_{in}=0 mM, K_{out}=150 mM, plus valinomycin) further decreased the uptake of guanidine (29.6 ± 0.5 pmol/mg protein/5 min, mean ± SD). Collectively, these data suggest that overall guanidine uptake is potential dependent. Inclusion of 20 mM guanidine in the reaction mixture specifically inhibited the uptake of guanidine under all experimental conditions, however, the effect of membrane potential was not altered suggesting that the stimulation of guanidine transport by membrane potential was due to simple diffusion (data not shown).

2.3.3 *Concentration Dependence of Guanidine Uptake*

The rate of guanidine uptake as a function of concentration was determined at 30 sec, a time in which uptake was linear (data not shown). As shown in Table 2.1, the K_m was 3.59 ± 1.12 mM and the V_{max} was 94.4 ± 15.9 pmol/mg protein/sec. In the absence of KCl, the K_m was reduced and the V_{max} was increased ($p < 0.05$, Table 2.1). Both values increased in the presence of an outwardly-directed pH-gradient ($p < 0.05$, Table 2.1).

Table 2.1 Kinetic parameters of guanidine uptake in rat kidney BBMV

	K_m	V_{max}
	mM	*pmol/mg protein/sec*
KCl buffer[a]	3.6 ± 1.1	94 ± 16
(pH_{in} = pH_{out} = 7.4)		
K^+-free Buffer[b]	0.32 ± 0.13	147 ± 20
(pH_{in} = pH_{out} = 7.4)		
K^+-free Buffer[b]	0.61 ± 0.16	345 ± 36
(pH_{in} = 6.0; pH_{out} = 7.4)		

Data are fitted using non-linear regression and are expressed as mean ± SD.

[a] Concentration dependence of ^{14}C-guanidine uptake in rat kidney BBMV in KCl (150 mM) buffer was assayed at 30 sec.

[b] Concentration dependence of ^{14}C-guanidine uptake in rat kidney BBMV in K^+-free buffer was assayed at 15 sec.

Typical organic cations (5 mM) such as guanidine, TEA and cimetidine significantly inhibited both guanidine and TEA uptake (Figure 2.3a and 2.3b). However, rank order differences in potency of inhibition of guanidine and TEA uptake were observed. Namely, for ^{14}C-guanidine uptake, the rank order potency of inhibition was guanidine ≈ cimetidine ≈ procainamide > TEA ≈ choline ≈ NMN. In contrast for ^{14}C-TEA uptake, the rank order potency of inhibition was cimetidine ≈ TEA ≈ procainamide > NMN > guanidine > choline. In addition, PAH, a typical organic anion, inhibited guanidine, but not TEA, uptake (Figures 2.3a and 2.3b). Effects of clinically used drugs on guanidine and TEA uptake were also examined (Table 2.2). All the drugs tested inhibited both guanidine and TEA uptake, however, some drugs such as the antibiotics, cefadoroxil and cephalexin, inhibited guanidine uptake more potently than TEA uptake.

2.3.4 Trans-stimulation Effect on Guanidine and TEA Uptake

To determine whether guanidine and TEA transport could be *trans*-stimulated by either guanidine or TEA, BBMV were preloaded with 5 mM unlabeled guanidine or TEA and uptake of radiolabeled guanidine or TEA was measured. As shown in Figure 2.4a, in the absence of a pH gradient, unlabeled guanidine and TEA (to a less extent) *trans*-stimulated ^{14}C-guanidine uptake at 60 sec. In contrast, the uptake of ^{14}C-TEA (at 60 sec) was *trans*-stimulated significantly by TEA but not by guanidine (Figure 2.4b); however, at 30 sec ^{14}C-TEA uptake in guanidine-preloaded vesicles was significantly different from that in control vesicles (data not shown). In the absence of KCl, strong *trans*-stimulation effects were observed for both guanidine and TEA uptake in vesicles preloaded with either unlabeled guanidine or TEA (Figures 2.5a and 2.5b).

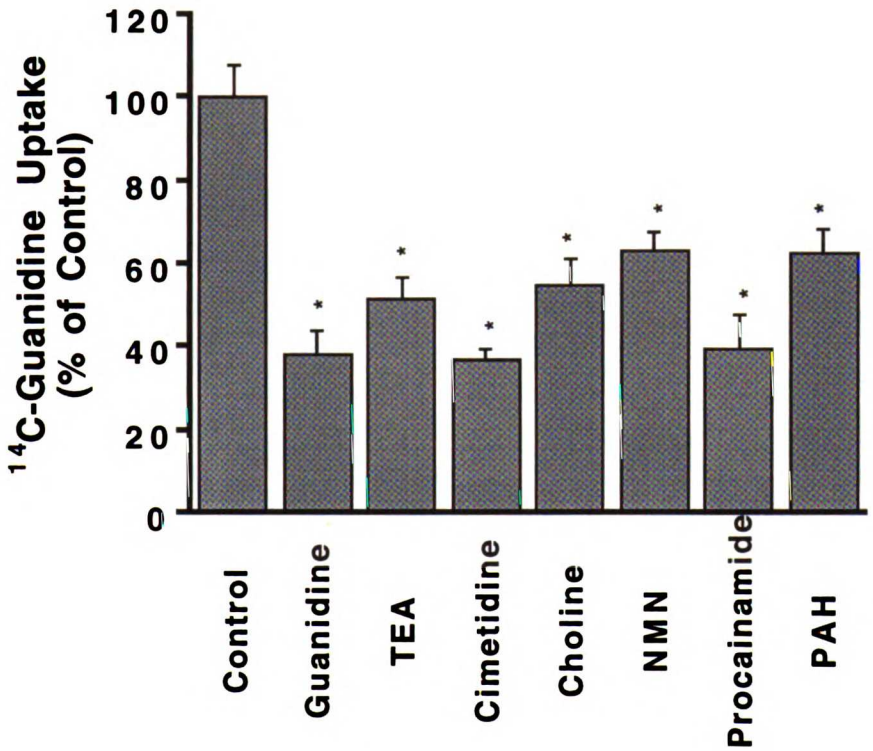

Figure 2.3a pH-gradient stimulated 30 sec uptake of ^{14}C-guanidine (50 μM) in rat kidney BBMV in the presence of various inhibitors (5 mM) in HK buffer. Data are expressed as mean ± SE (n = 6) from two separate experiments of triplicate determinants. * $p < 0.05$.

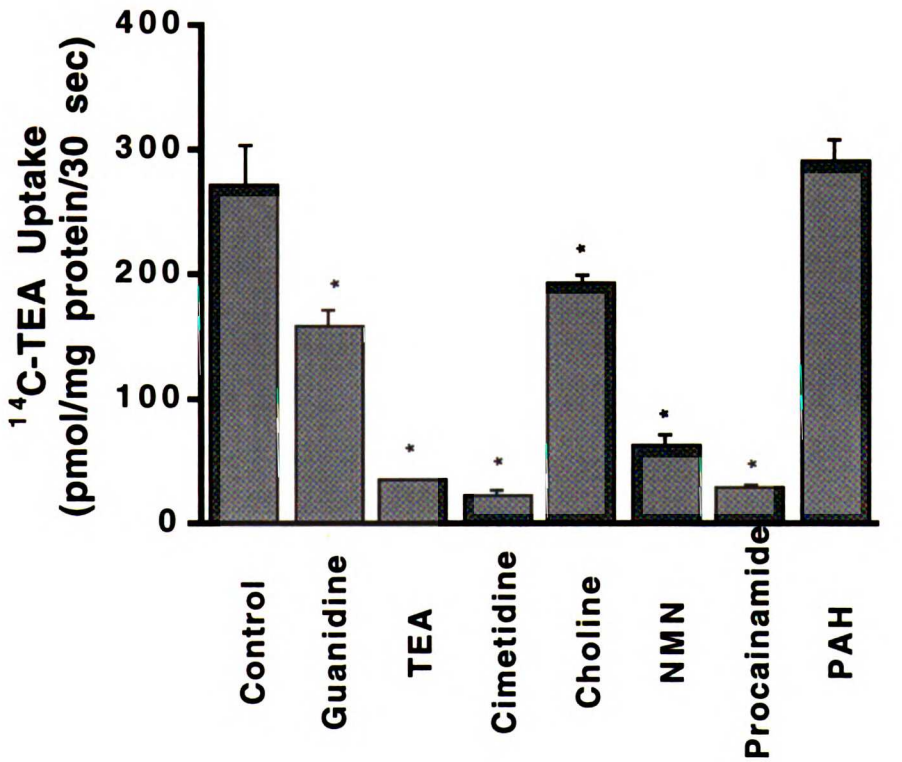

Figure 2.3b pH-gradient stimulated 30 sec uptake of ^{14}C-TEA (50 μM) in rat kidney BBMV with an outwardly directed proton gradient (pH_{in}:pH_{out} = 6.0:7.4) in the presence of various inhibitors (5 mM) in HK buffer. Data are expressed as mean ± SD (n = 3) from one representative experiment. * $p < 0.05$.

Table 2.2 Effect of clinically used drugs on ^{14}C-guanidine and ^{14}C-TEA uptake in rat renal brush border membrane vesicles

	^{14}C-Guanidine uptake	%	^{14}C-TEA uptake	%
	pmol/mg protein/30 sec	*control*	*pmol/mg protein/30 sec*	*control*
Control	31.5 ± 4.07	100	272 ± 32.4	100
Disopyramide[a]	11.3 ± 4.05	35.9	6.86 ± 0.38	2.52
Quinine[b]	6.75 ± 1.52	21.4	4.29 ± 0.69	1.58
(-)Nicotine[b]	13.1 ± 2.14	41.6	54.3 ± 10.7	20.0
AZT[a]	11.1 ± 1.38	35.2	36.3 ± 4.52	13.3
Cefadoroxil[a]	15.2 ± 2.86	48.2	213 ± 15.8	78.3
Cephalexin[a]	11.8 ± 1.74	37.5	143 ± 11.7	52.6

The uptake of ^{14}C-guanidine and ^{14}C-TEA was carried out in the presence of an outwardly-directed proton gradient (pH_{in}:pH_{out} = 6.0:8.0) in the absence (control) and presence of various concentrations of inhibitors. Data are from one representative experiment (mean ± SD) of triplicate determinations. All data were significantly different from their controls ($p < 0.05$).

[a] 5 mM

[b] 1 mM

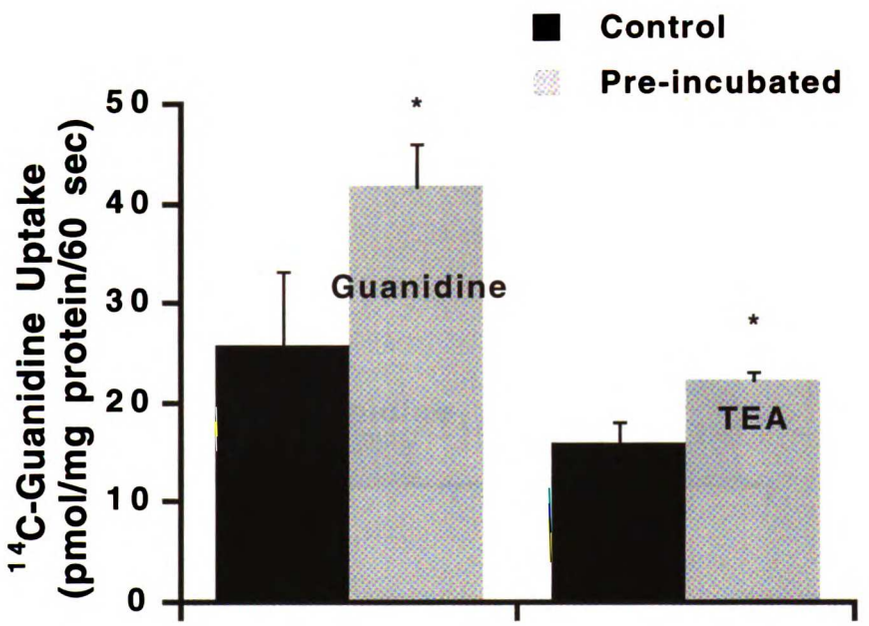

Figure 2.4a Uptake at 60 sec of 50 μM ^{14}C-guanidine in BBMV pre-incubated with 5 mM guanidine or TEA (gray bars) in HK buffer for one hour. Control (dark bars) BBMV were not pre-incubated. Data are expressed as mean ± SD, n = 3. * $p < 0.05$.

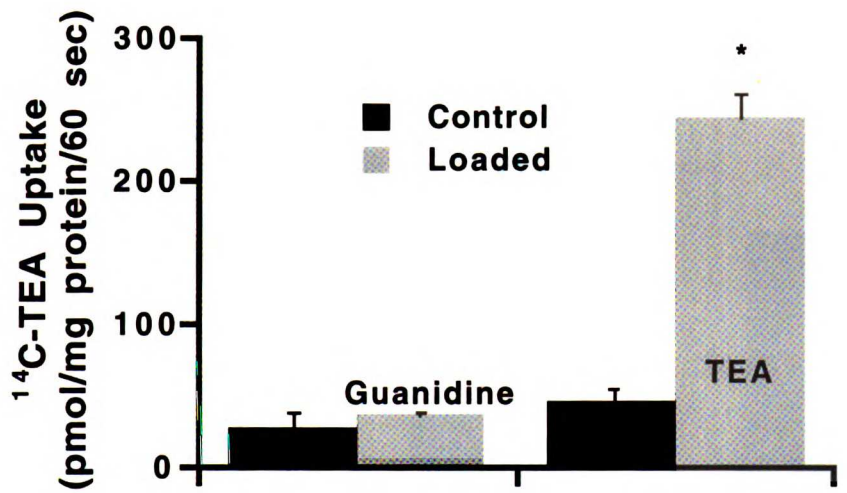

Figure 2.4b Uptake at 60 sec of 50 μM ^{14}C-TEA in BBMV pre-incubated with 5 mM guanidine or TEA (gray bars) in HK buffer for one hour. Control (dark bars) BBMV were not pre-incubated. Data are expressed as mean ± SD, n = 3. * $p < 0.05$.

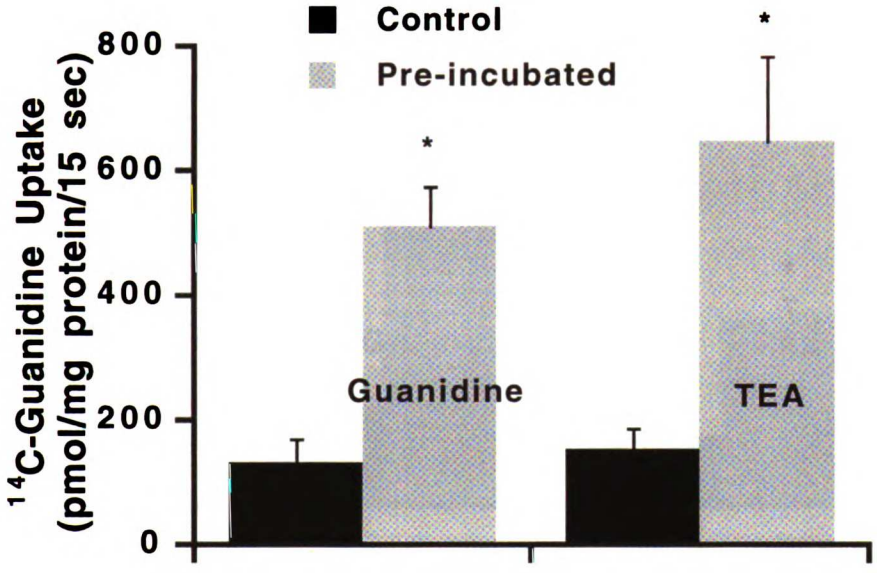

Figure 2.5a Uptake of 50 μM ^{14}C-guanidine (15 sec) in BBMV pre-incubated with 5 mM guanidine or TEA (gray bars) for one hour in K^+-free (replaced with mannitol) buffer. Control (dark bars) BBMV were not pre-incubated. Data are expressed as mean ± SD, n = 3. * $p < 0.05$.

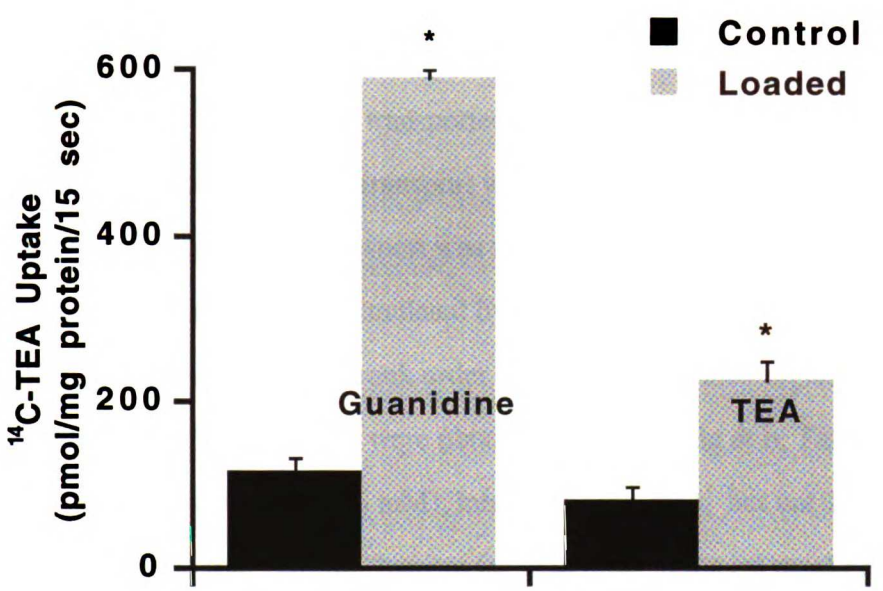

Figure 2.5b Uptake of 50 μM ^{14}C-TEA (15 sec) in BBMV pre-incubated with 5 mM guanidine or TEA (gray bars) for one hour in K^+-free (replaced with mannitol) buffer. Control (dark bars) BBMV were not pre-incubated. Data are expressed as mean ± SD, n = 3. * $p < 0.05$.

2.4 Discussion

In this study, guanidine uptake was characterized in rat kidney BBMV. The uptake of radiolabeled guanidine was saturable, inhibitable by various organic cations and *trans*-stimulated by unlabeled guanidine suggesting a carrier-mediated process. Several lines of evidence suggest that guanidine may be transported by a mechanism distinct from that of TEA. First, a KCl effect for guanidine transport was observed which was not apparent for TEA transport. Namely, guanidine transport was not pH-dependent in the presence of 150 mM KCl whereas TEA transport was stimulated by an outwardly-directed proton-gradient (Figures 2.1 & 2.2). Second, different rank order potencies of various organic cations in inhibiting guanidine and TEA transport were obtained (Figures 2.3a & b, Table 2.2). Furthermore, the organic anion, PAH (5 mM), inhibited guanidine, but not TEA, uptake. These data suggest that the transport mechanism for guanidine in the rat renal brush border membrane differs from that of TEA.

Various clinically used drugs interacted with guanidine transport in rat renal BBMV including the cationic drugs, disopyramide and quinine, the nucleoside analog, AZT, and the β-lactam antibiotics, cefadoroxil and cephalexin (Table 2.2). Interestingly, β-lactam antibiotics did not interact with guanidine transport in rabbit renal BBMV (Miyamoto *et al.*, 1989) suggesting possible species differences in guanidine transport mechanisms.

Since guanidine transport is pH-sensitive in the absence of KCl, the effect of protons on guanidine transport was examined. As shown in Table 2.1, both K_m and V_{max} values changed when introducing the pH-gradient, i.e., K_m was increased from 0.32 ± 0.13 mM to 0.61 ± 0.16 mM and V_{max} was increased from 147 ± 20 pmol/mg protein/sec to 345 ± 36 pmol/mg protein/sec. However, the intrinsic transport rate which can be expressed as V_{max}/K_m did not change (459 pmol/mg protein/sec/mM in the absence of pH gradient vs. 566 pmol/mg protein/sec/mM in the presence of pH gradient).

Our data suggest that there are species differences in the mechanisms of guanidine transport in BBMV prepared from rat, rabbit and human. Unlike guanidine transport in rabbit and human renal BBMV (Chun *et al.*, 1997a; Miyamoto *et al.*, 1989), guanidine transport in rat BBMV was pH-independent in the presence of KCl (Figure 2.1). In addition, TEA both *cis*-inhibited and *trans*-stimulated guanidine transport in rat BBMV (Figures 2.4a and 2.5a); however, in rabbit and human renal BBMV, TEA does not appear to interact with the guanidine transport mechanism (Chun *et al.*, 1997a; Miyamoto *et al.*, 1989). It is also possible that in the rat renal brush border membrane, guanidine is transported by both the TEA transport mechanism and a "guanidine-selective" transport mechanism. However, Michaelis-Menten studies were consistent with only one process (Table 2.1) suggesting that if two mechanisms are involved, guanidine has a similar affinity for both. Recently, two organic cation transporters, rOCT1 and rOCT2, were cloned from rat kidney (Grundemann *et al.*, 1994; Okuda *et al.*, 1996). Both transport TEA. However, only rOCT2 efficiently transports guanidine (Chapter 3) suggesting that rOCT2 may represent the guanidine-selective transporter characterized in this study. However, a recent immunohistochemical study suggested that rOCT2 is located on the basolateral, not the brush border side of the proximal tubule (H Koepsell, unpublished data) indicating that another guanidine-selective transporter is located on the brush border membranes of rat kidney.

In conclusion, guanidine transport in rat kidney BBMV has been characterized. Guanidine is transported by a saturable and inhibitable carrier-mediated mechanism. Guanidine transport is stimulated by an outwardly-directed proton gradient in the absence, but not in the presence, of KCl (150 mM). The data suggest that the mechanism of guanidine transport may be different from the mechanism of TEA transport in rat BBMV. Furthermore, the mechanism of guanidine transport in rat renal BBMV is different from those in rabbit and human.

CHAPTER 3

EXPRESSION OF RAT RENAL GUANIDINE TRANSPORT ACTIVITY IN *XENOPUS LAEVIS* OOCYTES [1]

3.1 Introduction

Organic cation transporters in the kidney play an important role in the elimination of many clinically used drugs including cimetidine, pindolol, procainamide as well as biologically potent amines such as choline, dopamine, and epinephrine. The transport and elimination of organic cations in the proximal tubules of the kidney have been extensively studied using a variety of experimental techniques (McKinney, 1993; Pritchard and Miller, 1993; Roch-Ramel *et al.*, 1992; Zhang *et al.*, 1998a; Chapter 1). In general, organic cation transport in the kidney has been studied using the model organic cations, tetraethylammonium (TEA) or N^1-methylnicotinamide (NMN) (Dantzler *et al.*, 1989; Holohan and Ross, 1981; Hsyu and Giacomini, 1987; Ott *et al.*, 1991; Rafizadeh *et al.*, 1987; Sokol *et al.*, 1985; Takano *et al.*, 1984; Wright, 1985; Wright and Wunz, 1987). However, recent studies have demonstrated that there are organic cation transporters in a number of tissues and species that accept guanidine and 5-(*N*-methyl-*N*-isobutyl)amiloride (MIBA) as substrates, but exclude TEA and NMN (Chun *et al.*, 1997a; Ganapathy *et al.*, 1988; Miyamoto *et al.*, 1988 and 1989; Prasad *et al.*, 1992). These organic cation transporters, collectively termed guanidine organic cation transporters, differ from the classical TEA (or NMN) transporters in terms of their driving forces, substrate selectivity

[1] This study was presented in part at the 9th Annual Meeting of American Association of Pharmaceutical Scientists in November 4-9, 1995 in Miami, FL.

and tissue distribution (Chun *et al.*, 1997a; Ganapathy *et al.*, 1988; Miyamoto *et al.*, 1988 and 1989; Prasad *et al.*, 1992; Zevin *et al.*, 1997).

Molecular cloning is essential to elucidate the characteristics of individual organic cation transporters and to understand the multiple and redundant organic cation transport mechanisms in the kidney and other tissues. Until recently, little information was available about the molecular characteristics of organic cation transporters involved in the handling and elimination of organic cations. In 1994, the first cDNA encoding an organic cation transporter, rOCT1, was cloned (Grundemann *et al.*, 1994). rOCT1 has the functional characteristics of the potential-dependent TEA organic cation transporter found on the basolateral membrane of the renal proximal tubule. More recently, in 1996, a second organic cation transporter, rOCT2, was cloned from a rat kidney cDNA library by homology cloning method (Okuda *et al.*, 1996). rOCT2 is 67% identical to rOCT1. Similar to rOCT1, rOCT2 accepts TEA as its substrate and is located on the basolateral membrane of the proximal tubule (H Koepsell, unpublished data). However, whether rOCT1 or rOCT2 also accepts guanidine as a substrate is not known.

The goals of the present study were to determine whether *Xenopus laevis* oocytes could be used as a functional assay to express and clone a guanidine organic cation transporter from rat kidney and to determine whether the expressed guanidine transport activity results from a transporter distinct from the recently cloned transporters, rOCT1 and rOCT2. The data demonstrate that guanidine transport activity was successfully expressed in *Xenopus laevis* oocytes injected with rat kidney mRNA. The expressed transporter(s) for guanidine appear(s) to be distinct from rOCT1. However, a greatly-enhanced guanidine transport activity was observed in oocytes injected with rOCT2 cRNA suggesting that rOCT2 plays a role in the transport of guanidine in the rat kidney.

3.2 Materials and Methods

3.2.1 Isolation and Size-Fractionation of Poly(A)$^+$ RNA

Renal tissue was isolated from adult male Harlan Sprague-Dawley rats. Total cellular RNA was immediately isolated from the renal tissue by phenol and guanidine isothiocyanate methods using TRIzol® Reagent (Gibco BRL, Gaithersburg, OR) following the protocol provided by the manufacturer. Poly(A)$^+$ RNA (mRNA) was selected by affinity chromatography using an oligo(dT) cellulose spin column (5 Prime —> 3 Prime, Inc., Boulder, CO) and stored in DEPC-treated water (1 μg/μl) at - 80°C until used.

For size-fractionation of mRNA, 80-150 μg of total mRNA was heated at 70°C for 5 min, chilled on ice and then layered on the top of a 6-20% (w/w) continuous sucrose gradient containing 1 mM EDTA and 10 mM Tris, pH 7.4. The sucrose gradient was centrifuged on a Beckman Ultracentrifuge (Beckman SW41T1 rotor; Beckman, Palo Alto, CA) at 100,000 X g (4°C) for 16 hours. Individual mRNA fractions (500-700 μl) were collected in 2 ml Eppendorf tubes and precipitated with 70% ethanol.

The molecular size ranges of the mRNA in different fractions were determined by gel electrophoresis of aliquots (3 μl) of each fraction on a 1% agarose/1.1% formaldehyde gel followed by ethidium bromide staining. RNA molecular weight standards (Gibco BRL) were used as reference to estimate the molecular size range of each mRNA fraction. The amount of mRNA in each fraction was determined by UV spectroscopy (absorbance at 260 nm).

3.2.2 Molecular Cloning

Reverse transcriptase-polymerase chain reaction (RT-PCR) of the rat kidney mRNA with primers specific for the cloned organic cation transporters, rOCT1 and rOCT2, was

performed as previously described (Zhang *et al.*, 1997a). The forward primer for rOCT1, 5'-ATGCCCACCGTGGATGATGTCCTGG-3', was derived from positions 38-62 of rOCT1 cDNA (Genbank accession # X78855, Grundemann *et al.*, 1994) and the reverse primer, 5'-GGTACTTGAGGACTTGCCTGTTTGG-3', was derived from positions 1681-1705. The forward primer for rOCT2, 5'-GGTACCATGTCGACCGTGGATGATATTCTA-3', was derived from positions 92-115 of rOCT2 cDNA (Genbank accession # D83044, Okuda *et al.*, 1996) with Kpn I site (underlined) at the 5'-end and the reverse primer, 5'-CTCGAGTCAGGGGTAAGTGAGGTTGGTTTG-3', was derived from positions 1850-1873 with Xho I site (underlined) at the 5'-end. Following 30 cycles of PCR amplification in a Perkin-Elmer thermal cycler (Perkin-Elmer, Foster City, CA) at an annealing temperature of 55°C, PCR products of expected sizes (1.7 kb and 1.8 kb, respectively) were obtained. The PCR product for rOCT1 was ligated into the pCR™II vector and transformed into INVαF' One Shot™ competent cells using the Original TA cloning® kit (Invitrogen, Carlsbad, CA). The PCR product for rOCT2 was ligated into the pGEM-T vector (Promega, Madison, WI) and then subcloned into a vector containing 5'- and 3'-untranslated regions of *Xenopus* globin, pEXO (Krieg and Melton, 1984; Lesage *et al.*, 1996; Lingueglia *et al.*, 1993). The resulting colonies/transformants were analyzed for proper orientation and size of insert by restriction enzyme digestion and/or sequencing. Plasmid DNA was isolated from the transformants containing the proper insert (Wizard Mini-Prep plasmid DNA isolation kit; Promega) and linearized with BamH I (for both rOCT1 and rOCT2 plasmid DNA) for *in vitro* transcription into cRNA, using T7 RNA polymerase as described previously (Zhang *et al.*, 1997a).

3.2.3 Oocyte Preparation and Functional Assay

The methods and techniques employed in the handling of oocytes have been described previously (Zhang *et al.*, 1997a). Briefly, oocytes were harvested from

Xenopus laevis (Xenopus, Ann Arbor, MI) and defolliculated using collagenase D treatment (Boehringer Mannheim Biochemicals, Indianapolis, IN) in a calcium-free OR II solution (82.5 mM NaCl, 2 mM KCl, 1 mM $MgCl_2$, 10 mM Hepes/Tris, pH 7.4). Oocytes were selected and maintained overnight, at 18°C, in modified Barth's solution (88 mM NaCl, 1 mM KCl, 0.82 mM $MgSO_4$, 0.4 mM $CaCl_2$, 0.33 mM $Ca(NO_3)_2$, 2.4 mM $NaHCO_3$, 10 mM Hepes/Tris, pH 7.4). Oocytes were then injected with 40-50 ng of total mRNA, 30 ng of size-fractionated mRNA, or 30-40 ng of cRNA in a volume of 50 nl using a semi-automatic injector (PL1-188, Nikon, Melville, NY). Control oocytes were injected with water (50 nl). The injected oocytes were maintained for 2-4 days, at 18°C, in modified Barth's solution prior to uptake experiments.

The uptake of ^{14}C-guanidine (56 mCi/mmol, Moravek Biochemicals, Brea, CA) or ^{14}C-TEA (53 mCi/mmol, American Radiolabeled Chemicals, Inc., St. Louis, MO) was carried out as previously described for radiotracer uptake (Zhang *et al.*, 1997b). Briefly, the injected oocytes were washed three times with 3 ml of Na^+-buffer (100 mM NaCl, 2 mM KCl, 1 mM $CaCl_2$, 1 mM $MgCl_2$, 10 mM Hepes/Tris, pH 7.4) and then incubated at 25°C in 200 µl of reaction mixture containing either ^{14}C-guanidine (500 µM) or ^{14}C-TEA (500 µM) in Na^+-buffer. For inhibition studies, unlabeled compounds were also included in the reaction mixture. For studies designed to determine the effect of pH on the uptake of ^{14}C-guanidine, oocytes were incubated for 60 minutes, at 25°C, in 200 µl of reaction mixture containing ^{14}C-guanidine (500 µM) in K^+-buffer (100 mM KCl, 2 mM NaCl, 1 mM $CaCl_2$, 1 mM $MgCl_2$, 10 mM Hepes/Tris) at pH 7.2 (control) or at pH 6.2 and pH 8.2. After incubation, the oocytes were washed 5 times with ice-cold Na^+-buffer (3.5 ml). Each oocyte was placed into a separate scintillation vial and dissolved with 10% SDS (100 µl). The radioactivity was assayed by liquid scintillation counting.

3.2.4 Data Analysis

Uptake values are presented as mean ± standard deviation (SD) of one representative experiment or as mean ± standard error (SE) of at least two replicate experiments. Six to nine oocytes were used in each experiment. For Michaelis-Menten studies, data were fit to the equation $V=V_{max}\bullet S/(S+K_m)+K_{ns}\bullet S$ where V is the uptake of ^{14}C-TEA, S is the substrate concentration, K_{ns} is the rate constant for the linear process. The Kaleidagraph fitting program (Abelbeck Software) was used to fit the data by non-linear regression. Statistical analysis was carried out by comparing the test compounds to the controls using the unpaired Student's *t*-test (Primer of Biostatistics software, Version 3, written by Stanton A. Glantz, McGraw-Hill Companies, 1991). Results were considered statistically different with a probability of $p < 0.05$.

3.2.5 Materials

Molecular biology supplies and radiolabeled compounds were purchased from the indicated manufacturers. Primers were synthesized by the Biomolecular Resource Center at the University of California, San Francisco. All chemicals were purchased from Sigma (St. Louis, MO).

3.3 Results

3.3.1 Initial Characterization of Expression of Guanidine Transport Activity

^{14}C-Guanidine transport activity in oocytes injected with rat kidney mRNA increased over time. Uptake studies were performed on day 3 or 4 when the expression level was high. Four days after injection, an enhanced ^{14}C-guanidine uptake was observed

which was linear with time up to 90 min in mRNA-injected oocytes indicating that guanidine transport activity can be expressed in oocytes (data not shown).

In oocytes injected with total mRNA, a 3-fold enhancement in ^{14}C-guanidine uptake (at 60 min) was obtained in comparison to that obtained in water-injected oocytes (36.7 ± 5.4 and 12.2 ± 3.9 pmol/oocyte/hr, mean ± SD, respectively) (Figure 3.1). The enhanced ^{14}C-guanidine uptake was reduced to values close to that in water-injected oocytes (11.1 ± 5.7 pmol/oocyte/hr) with the addition of 5 mM unlabeled guanidine indicating that the expressed guanidine uptake is specific and carrier-mediated.

Further enhancement of ^{14}C-guanidine uptake was observed in oocytes injected with an enriched size-fraction of mRNA (fraction D) (Figures 3.1 and 3.2). A 9-fold enhancement of ^{14}C-guanidine uptake over water-injected oocytes (110 ± 11 and 12.2 ± 3.9 pmol/oocyte/hr, mean ± SD, respectively) was observed in oocytes injected with fraction D of total mRNA. The size of fraction D mRNA was estimated, by agarose gel electrophoresis, to be approximately 1.4-3.7 kb (average 2.2 kb) in size (Figure 3.2).

3.3.2 Inhibition Studies

We compared the inhibition profile of ^{14}C-guanidine and ^{14}C-TEA uptake in mRNA-injected oocytes. The uptake of ^{14}C-guanidine was significantly inhibited by a number of organic cations including guanidine itself as well as TEA, cimetidine, NMN and choline (Table 3.1). Similarly, ^{14}C-TEA uptake was inhibited by these organic cations, however, the rank order of potency of inhibition differed from that of ^{14}C-guanidine transport. Namely, for ^{14}C-TEA uptake, the rank order of inhibition was cimetidine > TEA > guanidine > choline ≈ NMN, whereas for ^{14}C-guanidine uptake, the rank order of inhibition was choline > guanidine ≈ cimetidine > TEA ≈ NMN.

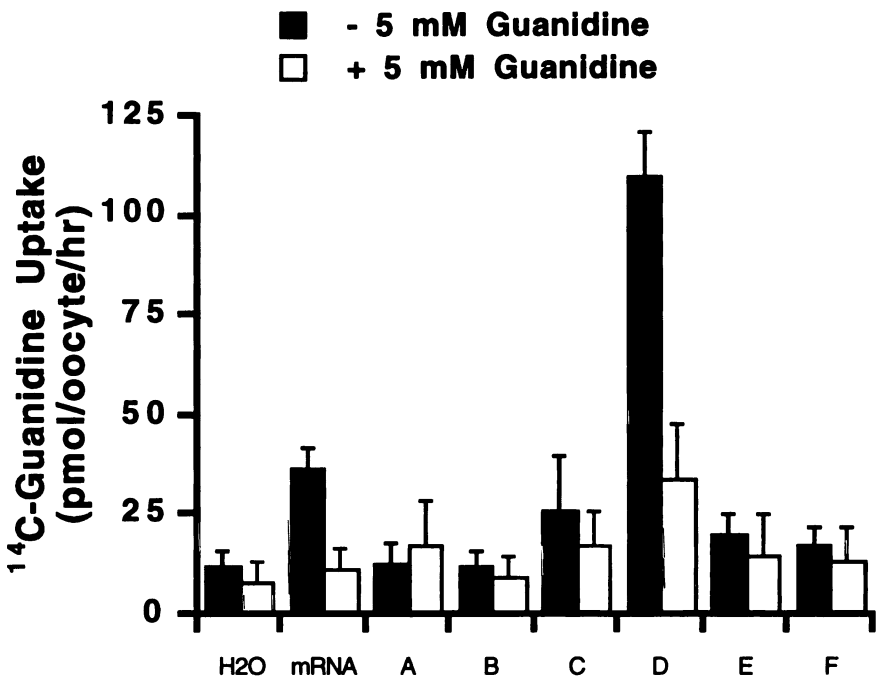

Figure 3.1 Expression of guanidine transport activity *in Xenopus laevis* oocytes injected with rat kidney total mRNA and different size fractions of mRNA. The uptake of 500 μM ^{14}C-guanidine in oocytes (at 25°C) four days after injection with 40-50 ng of total mRNA, 30 ng of size-fracionated mRNA (fractions A-F), or 50 nl of water (control). The uptake values are expressed as mean ± SD obtained from one representative experiment, 6-9 oocytes. Closed bars represent data obtained in the absence of 5 mM unlabeled guanidine and open bars represent data obtained in the presence of 5 mM unlabeled guanidine.

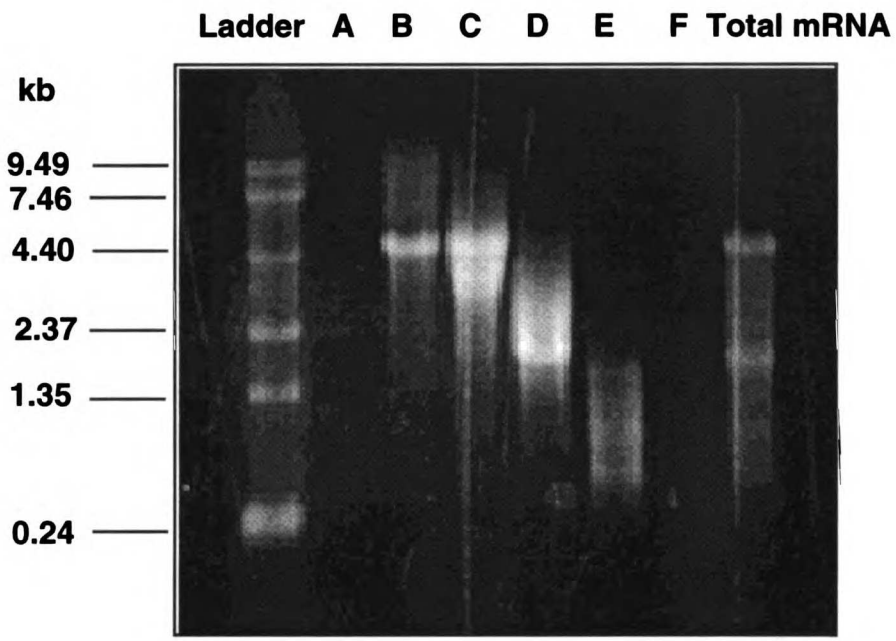

Figure 3.2 1% Agarose/1.1% formaldehyde gel of total and size-fractionated rat kidney mRNA. Aliquots (3 µl) of the mRNA (0.4 µg/µl) were electrophoresed in a denaturing agarose gel with ethidium bromide staining. RNA molecular weight standards (Gibco BRL) are shown on the left. The size range of each mRNA fraction was estimated by reference to the RNA molecular weight standards and the molecular size for fraction D was estimated to range between 1.4 and 3.7 kb.

Table 3.1 Effect of inhibitors on ^{14}C-guanidine and ^{14}C-TEA uptake in rat kidney mRNA-injected oocytes

	^{14}C-Guanidine uptake *pmol/oocyte/hr*	% *control*	^{14}C-TEA uptake *pmol/oocyte/hr*	% *control*
Water-injected				
Control	8.4 ± 2.5		2.4 ± 0.5	
mRNA-injected				
Control	20.6 ± 3.5	100	6.2 ± 1.7	100
Guanidine	10.4 ± 1.9	50.5	3.1 ± 0.8	50
TEA	14.4 ± 2.3	69.9	2.2 ± 0.2	35.5
Cimetidine	10.4 ± 1.8	50.5	1.4 ± 0.03	22.6
NMN	15.1 ± 2.3	73.3	4.1 ± 2.0	66.1
Choline	7.7 ± 0.4	37.4	3.8 ± 1.0	61.3

Each inhibitor was present at 5 mM. Uptake values are expressed as mean ± SE obtained in two to three separate experiments from 6-9 oocytes in each experiment. Data expressed as % control represent percentage of mRNA-injected oocytes/control. All uptake values in mRNA-injected oocytes are significantly lower than control ($p < 0.05$).

3.3.3 *Kinetics of Guanidine Transport*

The initial rate of uptake of ^{14}C-guanidine in rat kidney mRNA-injected oocytes was saturable whereas the initial uptake rate in the water-injected oocytes was linear over the same concentration range (Figure 3.3). The V_{max} and K_m values of guanidine transport were 17.3 ± 1.4 pmol/oocyte/hr and 254 ± 76 μM, respectively and the K_{ns}, the rate constant for the linear process, determined from water-injected oocytes, was 2.50 ± 0.15 fmol/oocyte/hr/μM.

3.3.4 *Effect of pH and Potential on Guanidine Transport in Rat Kidney mRNA-Injected Oocytes*

Studies designed to determine the effect of pH on the uptake of guanidine demonstrated that ^{14}C-guanidine uptake (at 60 min) in mRNA-injected oocytes at pH 6.2 was not significantly different from that at pH 7.2 but was significantly different from that at pH 8.2 ($p = 0.03$). The uptake at pH 7.2 was not significantly different from that at pH 8.2 (Figure 3.4a). These data are consistent with similar studies in rat renal BBMV (Zhang *et al.*, 1997c; Chapter 2) which demonstrated that guanidine uptake was not pH-dependent in the pH range of 6.4-7.4.

The effect of membrane potential on guanidine uptake in mRNA-injected oocytes was examined. Guanidine transport significantly increased under depolarized condition (by replacing Na^+-buffer with K^+-buffer) in both water-injected oocytes and mRNA-injected oocytes (Figure 3.4b). The data may suggest that guanidine uptake induces translocation of a net negative charge. Alternatively, guanidine transport in oocytes may be inhibited by Na^+ or driven by K^+.

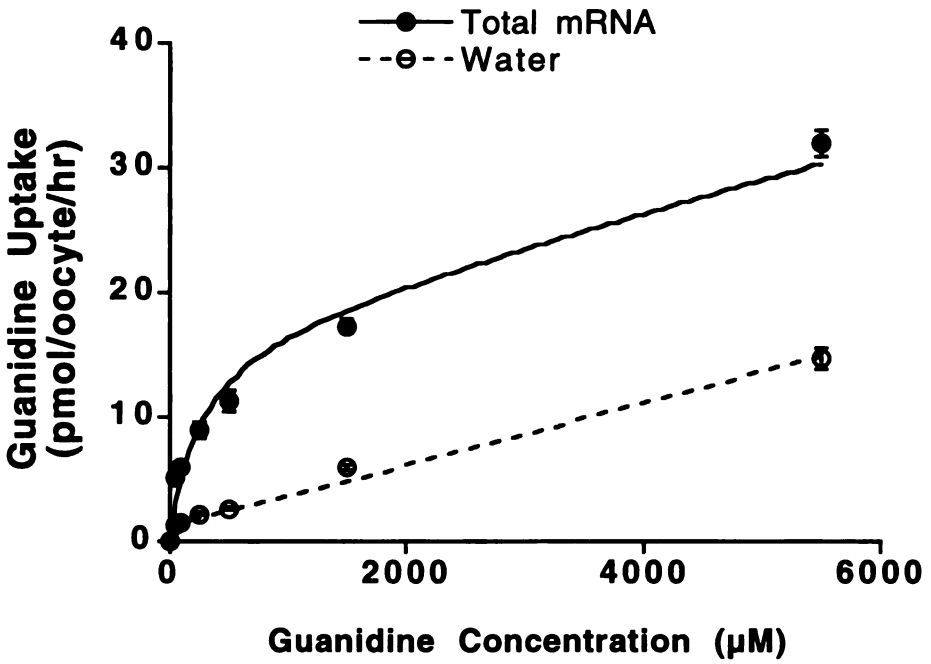

Figure 3.3 Kinetics of guanidine transport in oocytes injected with rat kidney total mRNA (closed circles) or water (open circles). Data were fitted to a Michaelis-Menten equation plus simple diffusion term as described in "Materials and Methods" (K_m = 254 ± 76 μM; V_{max} = 17.3 ± 1.4 pmol/oocyte/hr; K_{ns} = 2.50 ± 0.15 fmol/oocyte/hr/μM). Each point represents mean ± SD from one representative experiments, 6-9 oocytes.

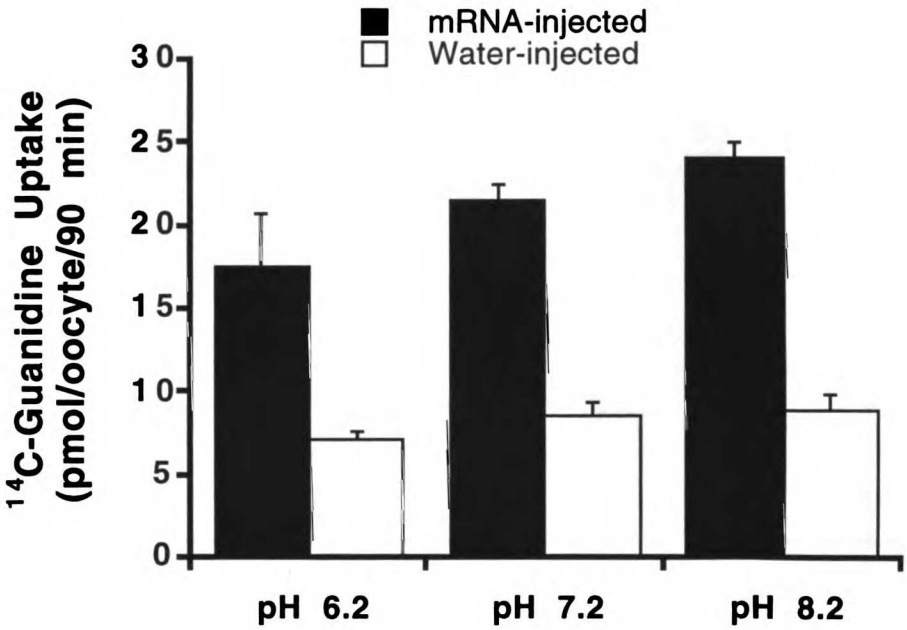

Figure 3.4a Effect of pH on ^{14}C-guanidine (500 μM) uptake in oocytes injected with rat kidney mRNA (closed bars, 50 ng) or water (open bars, 50 nl). Uptake was assayed for 90 min on day 3 after injection. Data are presented as mean ± SD (7-9 oocytes) from one representative experiment.

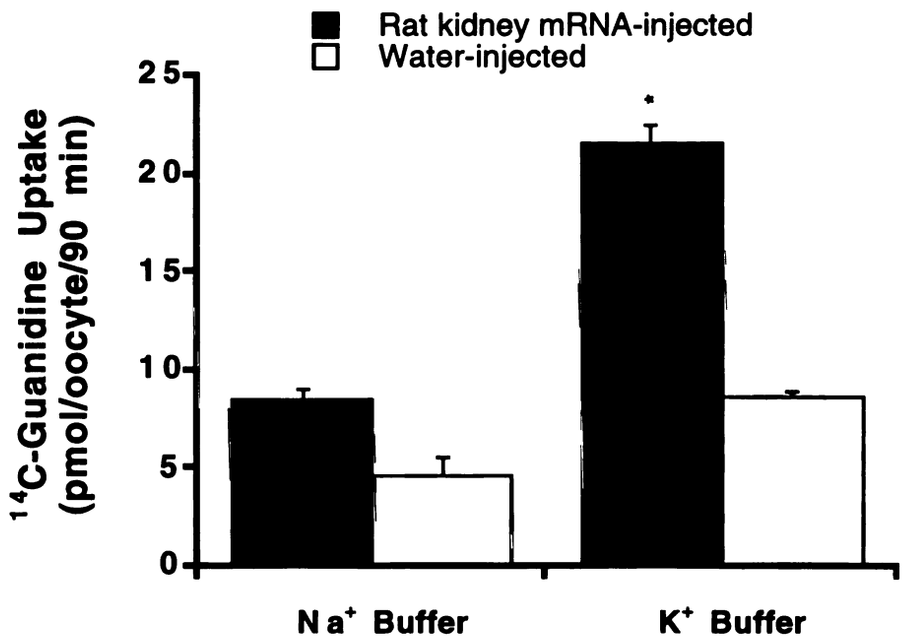

Figure 3.4b Effect of membrane potential on ^{14}C-guanidine (500 μM) uptake in oocytes injected with rat kidney mRNA (closed bars, 50 ng) or water (open bars, 50 nl). Uptake was assayed for 90 min on day 4 after injection. Data are presented as mean ± SD (7-9 oocytes) from one representative experiment. * $p < 0.05$

3.3.5 *Uptake of ^{14}C-Guanidine in Oocytes Expressing rOCT1 and rOCT2*

To determine whether guanidine is translocated by the cloned organic cation transporters, rOCT1 or rOCT2, we examined the uptake of ^{14}C-guanidine (500 μM) in oocytes injected with cRNA encoding rOCT1 or rOCT2. Uptake of ^{14}C-guanidine was less than two-fold enhanced in rOCT1 cRNA-injected oocytes in comparison to uptake in water-injected oocytes. In contrast, uptake of ^{14}C-TEA (500 μM) in rOCT1 cRNA-injected oocytes was approximately 60-fold enhanced over that in water-injected oocytes (Figure 3.5a). Both ^{14}C-guanidine (500 μM) and ^{14}C-TEA (500 μM) uptake in oocytes injected with rOCT2 cRNA were significantly greater than uptakes observed in water-injected oocytes (Figure 3.5b) indicating that both guanidine and TEA are translocated efficiently by rOCT2. These results are consistent with the inhibition data in which guanidine is a weaker inhibitor for rOCT1 than for rOCT2 (data not shown). In comparison to guanidine, TEA has a higher K_m value for rOCT2 (Table 3.2).

3.3.6 *Effects of pH and Potential on Guanidine Transport in rOCT2 cRNA-Injected Oocytes*

^{14}C-Guanidine uptake into rOCT2 cRNA injected-oocytes at pH 6.2 was not significantly different from that at pH 7.2 but was significantly different from that at pH 8.2. Uptake at pH 7.2 was also significantly different from that at pH 8.2 (Figure 3.6a).

Guanidine transport increased under depolarized conditions in water-injected oocytes. However, in contrast to data obtained in mRNA-injected oocytes, guanidine uptake in rOCT2 cRNA-injected oocytes was significantly decreased under depolarizing conditions (Figure 3.6b).

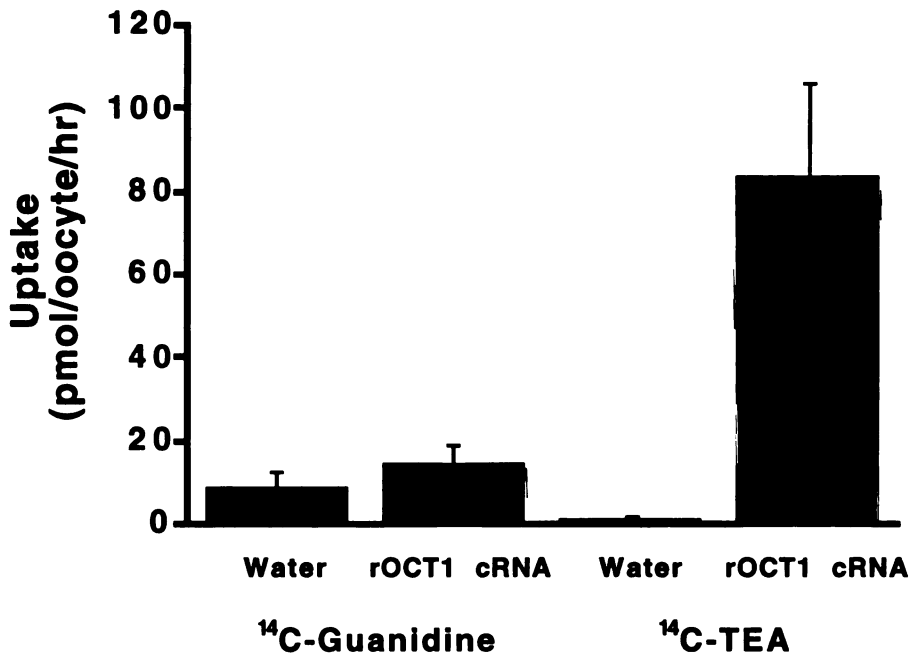

Figure 3.5a ^{14}C-Guanidine (500 μM) and ^{14}C-TEA (500 μM) uptake in oocytes injected with rOCT1 cRNA (40 ng) or water (50 nl). Uptake was assayed for 60 min on day 4 after injection. Data are presented as mean ± SD (7-9 oocytes) from one representative experiment.

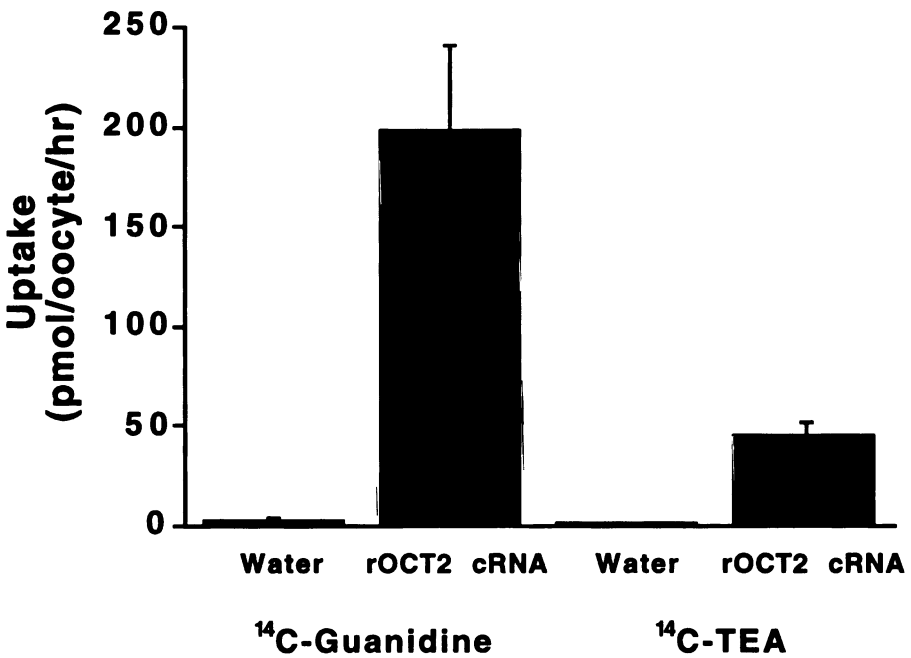

Figure 3.5b ^{14}C-Guanidine (500 μM) and ^{14}C-TEA (500 μM) uptake in oocytes injected with rOCT2 cRNA (40 ng) or water (50 nl). Uptake was assayed for 90 min on day 3 after injection. Data are presented as mean ± SD (7-9 oocytes) from one representative experiment.

Table 3.2 Kinetics of organic cation transport in rOCT2 cRNA-injected oocytes

Substrate	V_{max}	K_m	K_{ns}
	pmol/oocyte/hr	*μM*	*fmol/oocyte/hr/μM*
Guanidine	46.7 ± 1.67	234 ± 34.9	5.40 ± 0.30
TEA	54.8 ± 3.81	357 ± 97.6	2.89 ± 0.38

Data are presented as mean ± SD from fitting to the equation described in "Materials and Methods" (e.g., Figure 3.3).

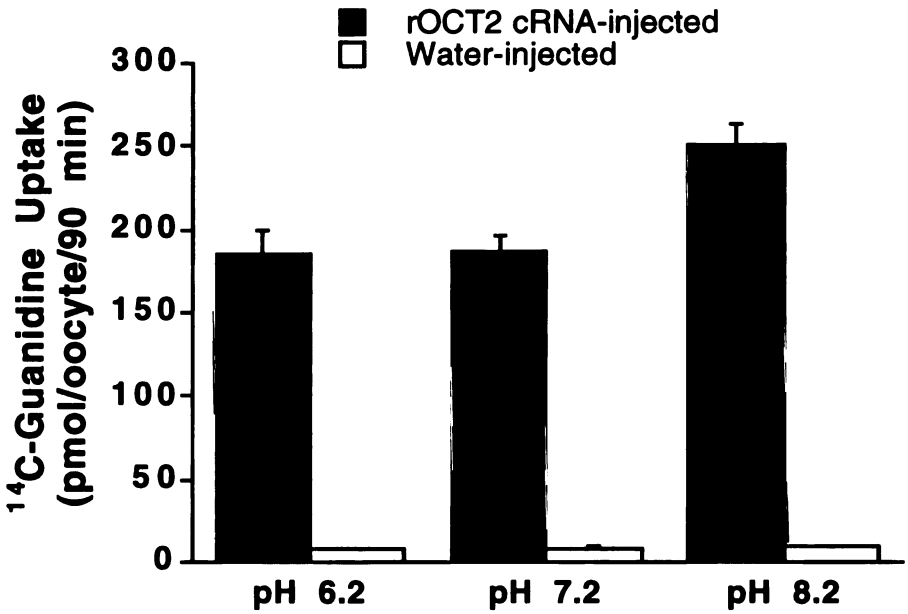

Figure 3.6a Effect of pH on ^{14}C-guanidine (500 μM) uptake in oocytes injected with rOCT2 cRNA (closed bars, 40 ng) or water (open bars, 50 nl). Uptake was assayed for 90 min on day 3 after injection. Data are presented as mean ± SD (7-9 oocytes) from one representative experiment.

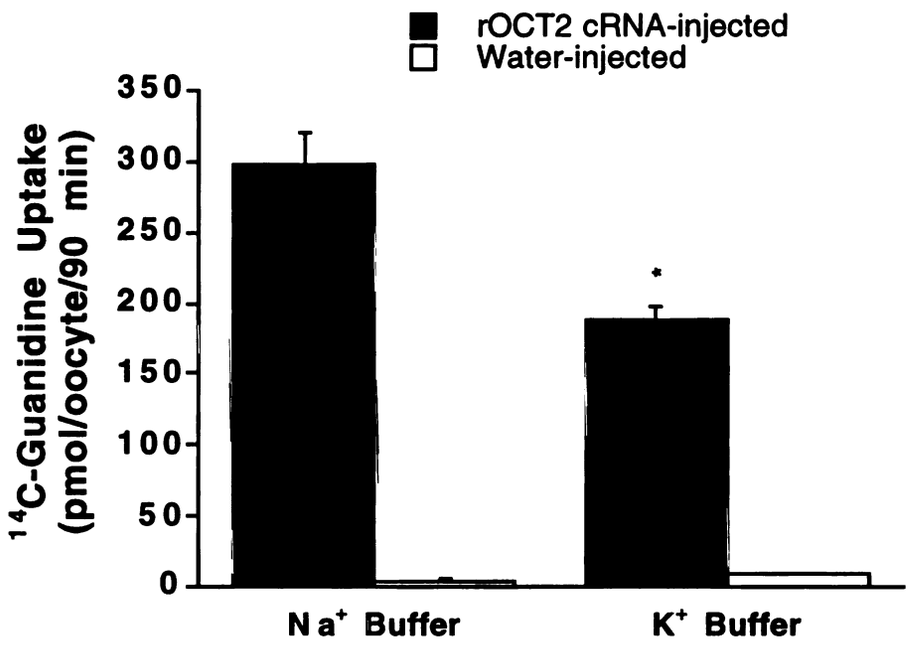

Figure 3.6b Effect of membrane potential on ^{14}C-guanidine (500 μM) uptake in oocytes injected with rOCT2 cRNA (closed bars, 40 ng) or water (open bars, 50 nl). Uptake was assayed for 90 min on day 3 after injection. Data are presented as mean ± SD (7-9 oocytes) from one representative experiment. * $p < 0.05$

3.4 Discussion

Based on studies in isolated membrane vesicles as well as recent molecular studies, multiple transporter families as well as isoforms of organic cation transporters appear to be involved in the transport of organic cations in the kidney (Koepsell, 1998; Zhang *et al.*, 1998a). In the present study, we report the expression of rat renal guanidine transport activity in *Xenopus laevis* oocytes.

Our data demonstrate that rat kidney mRNA contains a transcript or transcripts encoding transporter(s) for guanidine (Figure 3.1). Further enhancement in guanidine uptake in the mRNA-injected oocytes was obtained with injection of the size-enriched fraction D of mRNA (1.4-3.7 kb, average size of 2.2 kb) (Figures 3.1 and 3.2) suggesting that the size of mRNA transcripts encoding guanidine transporter(s) is approximately 2.2 kb.

The expressed uptake of guanidine in the oocytes was saturable (K_m = 254 μM, Figure 3.3) and inhibited by various organic cations (5 mM) including TEA, cimetidine, NMN and choline (Table 3.1). The data are consistent with data obtained in rat kidney brush border membrane vesicles demonstrating that these organic cations inhibit guanidine transport (Zhang *et al.*, 1997c; Chapter 2). Interestingly, the rank order potency of compounds in inhibiting the expressed guanidine transport differed from that of the compounds in inhibiting the expressed TEA transport suggesting that different transporters are involved in mediating the uptake of guanidine and TEA in the mRNA-injected oocytes (Table 3.1). The expressed uptake of guanidine in the oocytes was not significantly affected by a pH gradient (6.2-7.2) which is similar to data obtained in studies in rat renal BBMV (Zhang *et al.*, 1997c; Chapter 2).

Recently, two organic cation transporters, rOCT1 and rOCT2, were cloned from rat kidney (Grundemann *et al.*, 1994; Okuda *et al.*, 1996). TEA was a substrate for both

rOCT1 and rOCT2. The cDNA sizes of rOCT1 (1.9 kb) and rOCT2 (2.5 kb) are within the size range of mRNA (fraction D) responsible for guanidine transport. Accordingly, we examined whether rOCT1 or rOCT2 may play a role in the observed guanidine transport activity in the mRNA-injected oocytes.

Our studies suggest that the mRNA transcript encoding the guanidine transporter is not the same as that encoding rOCT1 (Figure 3.5a). Namely, the uptake of TEA was greatly enhanced (60-fold) in rOCT1 cRNA-injected oocytes whereas the uptake of guanidine in the same batch of oocytes was less than two-fold enhanced over that in water-injected oocytes (Figure 3.5a). In addition, the uptake of guanidine in the cRNA-injected oocytes was less than that in oocytes injected with the same amount of total mRNA from rat kidney suggesting that transporters other than rOCT1 are more important in the uptake of guanidine in mRNA-injected oocytes (data not shown).

Our data suggest that rOCT2 may play a role in the transport of guanidine in the kidney. Namely, the uptake of guanidine in rOCT2 cRNA-injected oocytes was 6 to 60 fold enhanced over that in water-injected oocytes (Figure 3.5b). The K_m value of guanidine transport in rOCT2 cRNA-injected oocytes is comparable to that obtained in oocytes injected with mRNA (254 μM vs. 234 μM). Guanidine uptake in both mRNA- and rOCT2 cRNA-injected oocytes was not pH-dependent (pH ranges 6.2 to 7.2) (Figures 3.4a and 3.6a).

Studies examining the effect of membrane potential on guanidine transport suggest that rOCT2 may not be the only transporter responsible for guanidine uptake. Namely, guanidine uptake was decreased in rOCT2 cRNA-injected oocytes incubated in a K^+-depolarizing buffer (Figure 3.6b). These data suggest that guanidine uptake via rOCT2 is sensitive to membrane potential. The data are also consistent with an inhibitory effect of K^+ on guanidine uptake -- similar to that observed in renal BBMV (Miyamoto *et al.*, 1989). In contrast, guanidine uptake was increased in mRNA-injected oocytes incubated in a K^+-depolarizing buffer (Figure 3.6a). The explanation for this is unknown, but may be related

to the co-transport of a net negative charge. Collectively, the data indicate that other transporters which utilize different driving forces are involved in the expressed guanidine transport activity.

In summary, functional expression of guanidine transport activity in *Xenopus laevis* oocytes injected with mRNA isolated from rat kidney was demonstrated. Our data indicate that the cloned renal organic cation transporter, rOCT2, transports guanidine and may contribute to the expressed guanidine transport observed in oocytes injected with total mRNA. The data are also consistent with the involvement of transporters in addition to rOCT2 in the transport of guanidine in rat kidney. Functional expression of guanidine transport activity in the oocytes will provide a useful functional assay for expression cloning of guanidine transporters.

CHAPTER 4

CLONING AND FUNCTIONAL CHARACTERIZATION OF A RAT RENAL ORGANIC CATION TRANSPORTER ISOFORM (rOCT1A) [1]

4.1 Introduction

Polyspecific organic cation transporters in the renal proximal tubule mediate the secretion of many endogenous compounds as well as various classes of clinically used drugs including β-adrenergic blocking agents, antiarrhythmics, antihistamines, opiates, and various sedatives (Gisclon *et al.*, 1987; McKinney and Kunnemann, 1987; Pritchard and Miller, 1993; Roch-Ramel *et al.*, 1992; Sokol *et al.*, 1985; Ullrich, 1994). The presence of polyspecific organic cation transporters asymmetrically distributed to the brush border and basolateral membrane of the renal epithelium promotes the vectorial movement of molecules in the secretory direction. The mechanisms of organic cation transport across each of these membranes have been studied in isolated renal plasma membrane vesicles from a number of species using the model compound, tetraethylammonium (TEA) (Holohan and Ross, 1980; Holohan and Ross, 1981; Katsura *et al.*, 1993; Ott *et al.*, 1991; Takano *et al.*, 1984; Wright and Wunz, 1987). In general, the studies have shown that TEA is transported from the blood into the cell across the basolateral membrane via a facilitative, but passive, electrogenic carrier-mediated system (Takano *et al.*, 1985; Takano *et al.*, 1984; Wright and

[1] Most of this work was published in *The Journal of Biological Chemistry* 272:16548-16554, 1997. Permission from the publisher is included in "Acknowledgments".

Wunz, 1987). The driving force is the inside negative membrane potential. Subsequently, TEA is transported into the tubule lumen across the brush border membrane via a secondarily active organic cation proton antiporter (Dantzler *et al.*, 1989; Holohan and Ross, 1981; Hsyu and Giacomini, 1987; Ott *et al.*, 1991; Sokol *et al.*, 1985; Takano *et al.*, 1984). The inwardly directed proton gradient, which serves as the major driving force, is generated mostly by the Na^+-H^+ exchanger on the brush border membrane (Aronson, 1985; Roch-Ramel *et al.*, 1992).

Until recently little was known about the molecular characteristics of organic cation transporters at either the basolateral or brush border membrane of the renal proximal tubule. However, in 1994, Grundemann *et al.* (1994), using expression cloning in *Xenopus laevis* oocytes, cloned a polyspecific organic cation transport protein, rOCT1, from a cDNA library derived from rat kidney. rOCT1 is encoded by a 1.8-kb cDNA and has the properties of a basolateral membrane organic cation transporter, *i.e.,* it is sensitive to membrane potential and insensitive to pH. Recently, a second organic cation transporter, rOCT2, from a rat kidney cDNA library was cloned using homology cloning with degenerate oligonucleotide probes to rOCT1 (Okuda *et al.*, 1996).

Isoforms of proteins may represent the translation products of mRNA transcripts from multiple genes or the products of alternatively spliced mRNA transcripts from a single gene. The process of alternative RNA splicing may result in increased genetic flexibility. For example, alternatively spliced mRNA transcripts may be translated into proteins with distinct functional characteristics. On the other hand, the protein products may have identical functional properties but differ in terms of regulation mechanisms that are critical in the tissue-specific role of the protein or in the course of cell differentiation. It is increasingly clear that alternative RNA splicing plays a critical role in increasing the diversity of membrane transporters such as the Ca^{2+} pump (Carafoli, 1994; Hilfiker *et al.*, 1994; Preiano *et al.*, 1996; Shull and Greeb, 1988; Stauffer *et al.*, 1993; Strehler *et al.*, 1989). To understand the biological role of organic cation transporters in renal and other

epithelia, it is essential to identify relevant, functional organic cation transporter isoforms. Although isoforms of organic cation transporters encoded by different genes have been identified (Grundemann *et al.*, 1994; Okuda *et al.*, 1996; Zhang *et al.*, 1997b; Chapter 5), it is not known whether there are isoforms of organic cation transporters resulting from alternative RNA splicing.

By RT-PCR, we identified and cloned a novel isoform of rOCT1, rOCT1A, from the rat kidney. Sequence analysis, molecular modeling and studies with synthetic constructs suggest that a functional organic cation transporter(s) is encoded by the mRNA of rOCT1A after initiation of protein synthesis at an internal start codon. This is the first evidence of a functional, alternatively spliced variant of a polyspecific organic cation transporter.

4.2 Materials and Methods

4.2.1 cDNA Cloning

Total RNA was isolated from male Harlan Sprague Dawley rat kidneys and other tissues using TRIzol® Reagent (Gibco BRL, Gaithersburg, MD). Poly(A)$^+$ RNA (mRNA) was selected by affinity chromatography using oligo(dT) cellulose spin columns (5 Prime → 3 Prime, Inc., Boulder, CO). Total RNA or mRNA was primed with oligo(dT) primer to synthesize the first strand cDNA using the SuperScript™ preamplification system for first strand cDNA synthesis (Gibco BRL). The synthesized cDNA and primers (10 μM) (see Table 4.1 and Figure 4.1) specific for the rat kidney organic cation transporter (rOCT1) cDNA (Grundemann *et al.*, 1994) were used in the subsequent PCR under the following conditions: 94°C for 0.5 min, 55°C for 1.5 min, 72°C for 2 min, 35 cycles. The PCR products were electrophoresed through 1% agarose gels, and size-selected DNA fragments were extracted and subcloned into the pCR™II vector (original TA® Cloning®

Kit, Invitrogen, San Diego, CA) or the pGEM-T vector (Promega, Madison, WI) using T4 DNA ligase followed by transformation into INVαF' One Shot™ (original TA Cloning® Kit, Invitrogen) or DH5α (Gibco BRL) competent cells. Plasmid DNA was isolated using the Wizard™ minipreps DNA purification system (Promega) and was analyzed by restriction enzyme analysis and/or sequencing.

Table 4.1 Sequences of primers and their positions in the rOCT1 cDNA

	Sequence	Position
		bp
Primer 1 (sense)	5'-GCAGGCCTGGCTAAACTGGTGAG-3'	1-23
Primer 2 (antisense)	5'-TTGCGGCCGCTCAGGTACTTGAGGACTT-3'	1691-1708
Primer 3 (antisense)	5'-AGTGCGGAACAGGTC-3'	1046-1060
Primer 4 (sense)	5'-CCAGAATCCCCCCGGTGG-3'	877-904
Primer 5 (sense)	5'-AGCGGTGTGGCTGGAGCCAGGCAGAG-3'	216-241
Primer 6 (sense)	5'-ATTGGGCCCCTGCGAGCATGGCTG-3'	391-414
Primer 7 (antisense)	5'-ACACCCAGCTGCCCTTGCTGACCAT-3'	695-671
Primer 8 (antisense)	5'-AACATGGATGTATAGTCTGGG-3'	648-628
Primer 9 (sense)	5'-ATCGTCACTGA*GTT*TGGCCGTAAGCTC-3'	start at 440
Primer 10 (antisense)	5'-GAGCTTACGGCCA*AAC*TCAGTGACGAT-3'	start at 671
Primer 11 (sense)	5'-GCTCTAGAGCCTGAGTTTAACCTGGTGTGT-3' (*Xba*I site)	447-466
Primer 12 (antisense)	5'-GGAATTCCTGGAATGGCATAGGCCA-3' (*Eco*RI site)	801-817

Sequences added that are not related to the rOCT1 cDNA, including restriction enzyme sites, are underlined, and mutation sites are indicated in italics.

4.2.2 Genomic DNA Cloning

To obtain the genomic DNA sequence flanking the spliced region (exon/intron junctions), we used a novel method for walking upstream or downstream in genomic DNA from the cDNA sequence (Siebert *et al.*, 1995) with the Rat GenomeWalker™ kit (Clontech, Palo Alto, CA) according to the manufacturer instructions. Primers were designed from the cDNA sequence upstream or downstream of the splice site (primers 5 to

8) (see Table 4.1). PCR reactions were performed with the Advantage™ genomic PCR kit (Clontech) and used cycle parameters suggested by the manufacturer. The PCR products were subcloned as described above.

4.2.3 Mutagenesis of rOCT1A

To generate the in-frame deletion (105 bp) variant of rOCT1, the QuickChange™ site-directed mutagenesis kit (Stratagene, La Jolla, CA) was used according to the manufacturer protocol. Briefly, two primers (sense and antisense to each other) flanking the mutagenesis site (primers 9 and 10, see Table 4.1) were used in PCR with plasmid DNA containing the rOCT1A inserts as the template and *Pfu* DNA polymerase (Stratagene). The PCR product was then digested with *Dpn* I restriction enzyme (Gibco BRL) followed by transformation and subcloning as described above.

4.2.4 Sequence Analysis

Subcloned cDNA inserts isolated from multiple reverse transcription and/or PCR reactions were sequenced using universal and gene specific primers by the Biomolecular Resource Center DNA Sequencing Facility at the University of California, San Francisco with an automated sequencer (Applied Biosystems, model 373A). Sequence alignments of rat rOCT1 and rOCT1A were produced using the Gap and Bestfit programs in the Genetics Computer Group (Wisconsin Package, version 8) software package. The Motifs program in the Genetics Computer Group package was used to determine potential protein kinase C phosphorylation sites and *N*-glycosylation sites. The transmembrane domains of rOCT1A were predicted based on hydropathy analysis using the Kyte-Doolittle algorithm (Kyte and Doolittle, 1982) in the Genetics Computer Group Pepplot program as well as the hydropathy analysis program in DNA Strider 1.2, a C program for DNA and protein analysis designed and written by Christian Marck (Service de Biochimie et de Genetique Molecularie, Gif-Sur-Yvette, France).

4.2.5 Xenopus Laevis Oocytes and ^{14}C-TEA Transport Measurements

Healthy stage V and VI oocytes were defolliculated and then injected with 50 nl of water, mRNA or capped cRNA (1 μg/μl in water) transcribed *in vitro* using T7 or SP6 RNA polymerase (mCAP™ RNA capping kit, Stratagene) from linearized plasmid DNA (Giacomini *et al.*, 1994). The uptake of ^{14}C-TEA (53 mCi/mmol, American Radiolabeled Chemicals, Inc., St. Louis, MO) was measured in oocytes 3 days after injection using the methods previously described (Giacomini *et al.*, 1994). Briefly, groups of 9-10 oocytes were incubated in the reaction mixture (100 mM NaCl, 2 mM KCl, 1 mM $CaCl_2$, 1 mM $MgCl_2$, 10 mM Hepes/Tris, pH 7.4) containing 500 μM ^{14}C-TEA with or without 5 mM cimetidine for 60-120 minutes at 25°C. For inhibition studies, 5 mM concentrations of various unlabeled compounds were also included in the reaction mixture. For the Michaelis-Menten kinetic study, 30-100 μM ^{14}C-TEA plus various amounts of unlabeled TEA were included in the reaction mixture. After incubation, oocytes were washed and each oocyte was lysed individually with 100 μl of 10% SDS. The radioactivity was determined by liquid scintillation counting.

4.2.6 In Vitro Translation and SDS-Polyacrylamide Gel Electrophoresis Analysis

The TNT®-coupled transcription/translation reticulocyte lysate system (Promega) and L-^{35}S-methionine (1000 Ci/mmol, 10 mCi/ml, DuPont NEN, Boston, MA) were used for eukaryotic *in vitro* translations following the manufacturer protocol. Five microliters of translation product was denatured in 20 μl of Laemmli sample buffer plus 5% (v/v) 2-mercaptoethanol at 75°C for 10 min and then loaded onto 4-20% gradient gels (Tris/glycine ready gels, Bio-Rad, Hercules, CA). To increase the sensitivity of detection of ^{35}S-labeled protein, gels were soaked in Amplify™ (Amersham Life Science, Inc., Arlington Height,

IL) after the fixing step. Gels were dried and exposed to Hyperfilm-MP film (Amersham Life Science, Inc.).

4.2.7 RNase Protection Assay

A 370-nucleotide *Eco*R I-*Xba* I fragment of rat rOCT1 cDNA was amplified with primers 11 and 12 (see Table 4.1 and Figure 4.7a) by PCR. After double digestion with *Eco*R I and *Xba* I, the PCR product was ligated into the pGEM®-11Zf(-) vector (Promega). A 416-nucleotide biotin labeled antisense RNA probe was synthesized from the linearized plasmid (cut by *Xba* I) by *in vitro* transcription with T7 RNA polymerase (BrightStar™ BIOTINscript™ T7 kit, Ambion, Austin, TX). The RNase protection assay (RPA) was performed using a HybSpeed™ RPA kit (Ambion) according to manufacturer protocol. rOCT1 and rOCT1A cRNA (600 pg) were also included in the RPA as controls and size indicators. After RNase digestion, the protected RNA fragments were precipitated, separated on a 5% polyacrylamide, 8 M urea gel, blotted onto a positively charged nylon membrane (BrightStar®-Plus™ positively charged nylon membrane, Ambion) and then fixed by cross linking. The protected fragments corresponding to rOCT1 and rOCT1A were detected using the BrightStar™ nonisotopic RNA detection system (Ambion) followed by membrane exposure to film.

4.2.8 Data Analysis

Uptake values are expressed as pmol/oocyte/hr and presented as mean ± standard error (SE) or as specified in the figure legends. A minimum of 6-9 oocytes was used in each experiment. Statistical analysis was carried out by the unpaired Student's *t* test.

4.2.9 Materials

All chemicals were purchased from Sigma or Fisher. Molecular biology supplies and radiolabeled compounds were purchased from the indicated manufacturers. Primers

were synthesized by the Biomolecular Resource Center at the University of California, San Francisco.

4.3 Results and Discussion

4.3.1 Detection of a Novel Isoform of the mRNA Transcript of rOCT1 in the Rat Kidney

Using first strand cDNA from mRNA isolated from several rat kidneys and primers 1 and 2 (Table 4.1, Figure 4.1a) derived from the published cDNA sequence of rOCT1 (Grundemann *et al.*, 1994), we obtained two PCR products of approximately 1.5 and 1.6 kb in size (Figure 4.1b, lane 2). The PCR product at 1.6 kb matched the predicted size of the rOCT1 cDNA, whereas the 1.5-kb PCR product was of unknown origin. These two products were also detected after PCR using plasmid DNA isolated from a rat kidney cDNA library and the same primers (Figure 4.1b, lane 3). Furthermore, both bands were detected from RT-PCR starting with total RNA isolated from the kidney of a single rat (data not shown). In order to confirm that the 1.5-kb PCR product was not generated from the mRNA transcript of the 1.6-kb PCR product due to either a PCR error or an error in reverse transcription, cRNA transcribed from the subcloned 1.6-kb PCR product was used in RT-PCR. This reaction resulted in a single detectable band on the gel (data not shown). Collectively, these data suggest that there are two RNA species in the rat kidney that can be amplified by RT-PCR using rOCT1-specific primers derived from the beginning and the end of the open reading frame (ORF) of the rOCT1 cDNA sequence. Furthermore, the resulting PCR product of primers 1 and 3 produced double bands (Figure 4.1b, lane 5), whereas the product resulting from primers 4 and 2 produced a single band on the gel (Figure 4.1b, lane 7), suggesting that the difference in size is near the 5'-end of the cDNA.

(a)

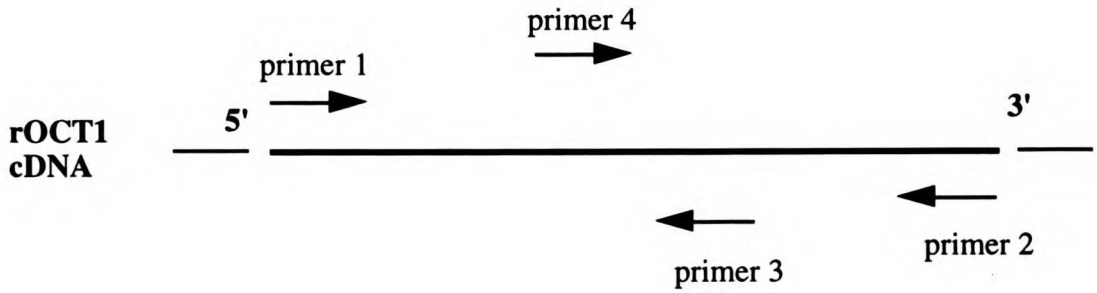

(b)

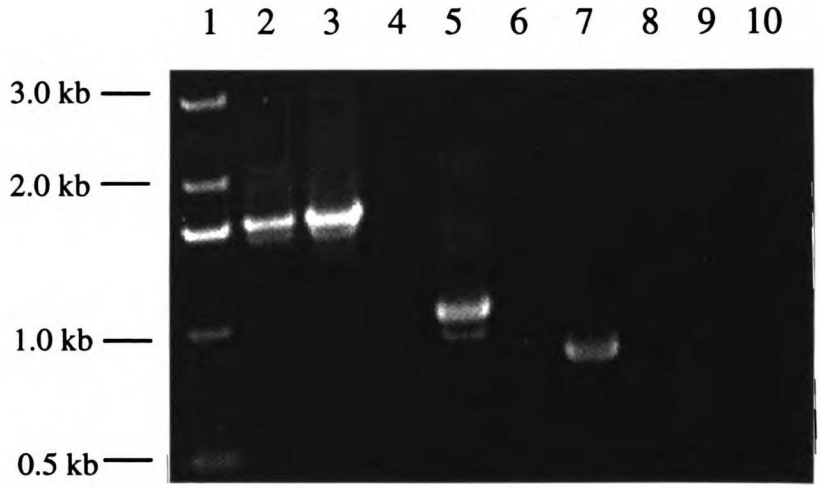

Figure 4.1 Results of RT-PCR. ***(a)*** Diagram showing the regions being amplified by RT-PCR with designated primers. ***(b)*** Gel picture of RT-PCR. 1% agarose gel showing that two bands were detected from the RT-PCR products using rOCT1-specific primers derived from the beginning (*primer 1*) and the end (*primer 2*) of the open reading frame (ORF) (*lane 2*), and the beginning (*primer 1*) and the middle (*primer 3*) of the ORF (first half) (*lane 5*), but a single band was detected when using primers from the middle (*primer 4*) and the end (*primer 2*) of the ORF (*lane 7*). Double bands also were detected when using plasmid DNA from a rat kidney cDNA library as a template and primers 1 and 2 (*lane 3*). *Lane 1,* 1 kb DNA ladder (from Gibco BRL); *lane 4, 6* and *8*, no cDNA control; *lane 9*, no RT control; *lane 10*, blank.

Sequence analysis demonstrated that the sequence of the 1.6-kb cDNA was identical to the published rOCT1 cDNA sequence (data not shown) (Grundemann *et al.*, 1994).

4.3.2 Functional Expression in Xenopus Laevis Oocytes

To determine whether the 1.5-kb cDNA encodes a functional organic cation transporter, recombinant plasmids containing the cDNA insert oriented for sense transcription under the control of a T7 or SP6 promoter were used as templates for cRNA synthesis before injection into *Xenopus laevis* oocytes. A significant increase in the cimetidine-inhibitable ^{14}C-TEA uptake was observed in cRNA-injected oocytes. ^{14}C-TEA uptake in the cRNA injected oocytes was increased 16-fold over that in the water-injected oocytes and 11-fold over that in the rat kidney total mRNA-injected oocytes (Figure 4.2a). However, the relative enhancement in ^{14}C-TEA uptake varied depending on the batch of oocytes (range approximately 2-20-fold).

To determine the specificity of transport, we studied the effect of various compounds on ^{14}C-TEA uptake in the cRNA-injected oocytes. Consistent with the characteristics of polyspecific renal organic cation transporters, the organic cations (5 mM) TEA, guanidine, cimetidine, choline, N^1-methylnicotinamide (NMN), and procainamide all significantly inhibited the uptake of ^{14}C-TEA (Figure 4.2b, $p < 0.05$). Similar functional characteristics of both rOCT1 and rOCT2 have been observed (Grundemann *et al.*, 1994; Okuda *et al.*, 1996). In addition, *p*-aminohippuric acid (PAH, 5 mM), a model organic anion, weakly inhibited ^{14}C-TEA uptake (Figure 4.2b, $p < 0.05$). Organic anions at high concentrations (e.g., 5 mM) have been shown previously to inhibit renal organic cation transporters (Cacini *et al.*, 1982; Gisclon *et al.*, 1987; Hsyu *et al.*, 1988). These data suggest that the 1.5-kb cDNA encodes a functional organic cation transporter having similar characteristics as rOCT1. Quantitative studies are under way to determine whether rOCT1 and rOCT1A differ in the potency of interaction with various substrates.

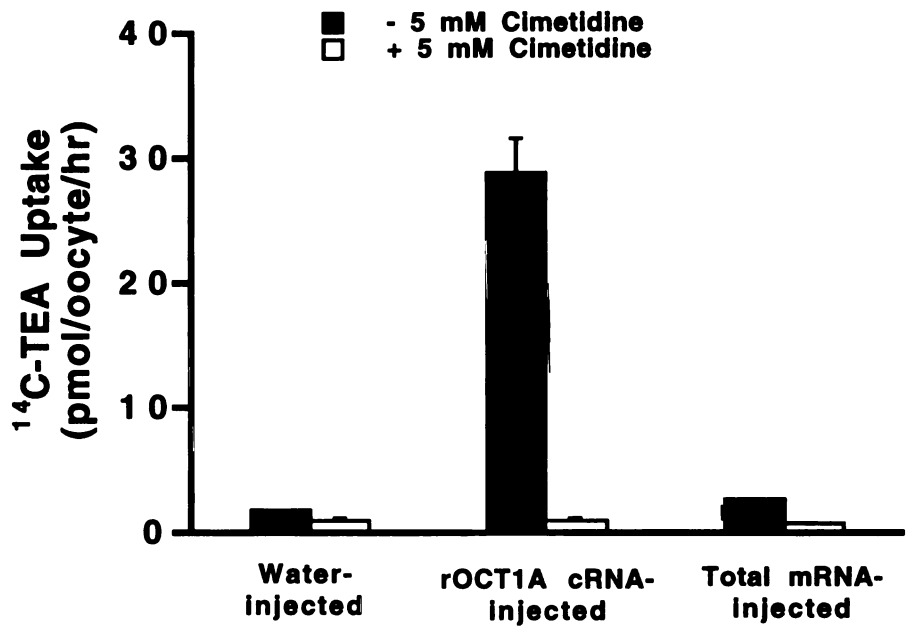

Figure 4.2a Functional expression of rOCT1A in *Xenopus laevis* oocytes. ^{14}C-TEA uptake in rOCT1A cRNA-injected oocytes compared to water-injected and mRNA-injected oocytes. ^{14}C-TEA (500 μM) uptake by oocytes was assayed for 90 min at 25°C 3 days after injection of 50 nl of water, rOCT1A cRNA or rat total mRNA. Each *column* represents the mean ± SE of one representative experiment. 7-9 oocytes were used for each *column*. *Dark bars* represent the uptake in the absence of 5 mM cimetidine and *open bars* represent uptake in the presence of 5 mM cimetidine.

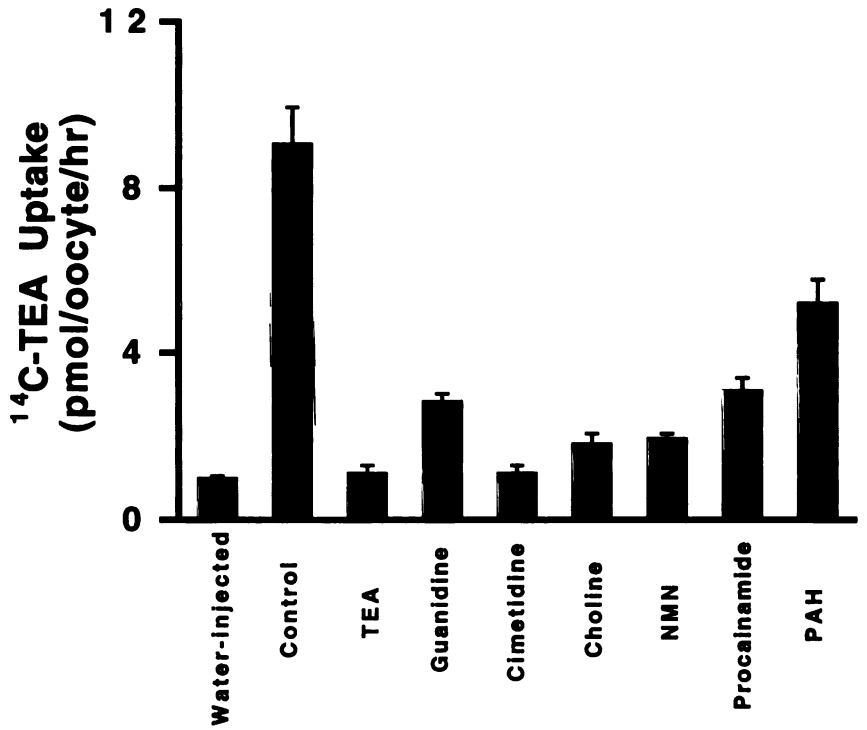

Figure 4.2b Effect of various organic cations and the organic anion (*p*-aminohippuric acid) on ^{14}C-TEA (500 μM) uptake by oocytes injected with water or rOCT1A cRNA. Each *column* represents the mean ± SE of one representative experiment. 7-9 oocytes were used for each column. *NMN*, N^1-methylnicotinamide; *PAH*, *p*-aminohippuric acid. All data were significantly different from the control, $p<0.05$. Control represents uptake in oocytes in the absence of unlabeled compounds.

To determine the kinetic characteristics of TEA transport in oocytes injected with the cRNA of the 1.5-kb PCR product, we measured TEA uptake over a range of concentrations (30-500 μM). Figure 4.2c shows the data together with the computer generated nonlinear regression fit curve for the Michaelis-Menten equation. The V_{max} and K_m of TEA in this experiment were 5.4 ± 0.4 pmol/oocyte/hr and 42 ± 11 μM, respectively. The K_m of TEA uptake (42 μM, Figure 4.2c) is somewhat lower than the value of 95 μM obtained previously for rOCT1 (Grundemann *et al.*, 1994). The V_{max} is considerably lower (5.4 *versus* 81 pmol/oocyte/hr (Grundemann *et al.*, 1994)) suggesting that there may be fewer functional rOCT1A transporters present; however, V_{max} values are difficult to compare due to differences in experimental conditions between laboratories.

4.3.3 DNA Sequencing and Primary Amino Acid Sequence

After ascertaining the function of the transporter, we carried out sequence analysis to deduce the primary sequence of the functional protein from the cDNA sequence. Because PCR may result in fidelity errors in amplification of DNA, we performed sequence analyses of cDNAs isolated from multiple reverse transcription and PCR reactions. A consistent sequence was obtained (Figure 4.3a). DNA sequence alignment between the 1.5- and 1.6-kb clone (rOCT1) demonstrates that the 1.5-kb cDNA sequence is identical to that of the 1.6-kb cDNA with a deletion between bp 451 and 556 of the rOCT1 cDNA. This is consistent with the PCR results (Figure 4.1b). The deletion results in a stop codon at bp 460 in reading frame 2 (RF2, the same reading frame encoding the ORF of rOCT1), and a large ORF is present from the ATG at bp 312 to the stop codon at bp 1602 in RF3 (Figure 4.3a). This large open reading frame in RF3 encodes a protein (rOCT1A) of 430 amino acids that, after sequence alignment, is 92% identical to that of rOCT1 (the reading frame of rOCT1 is restored in the RF3 of rOCT1A cDNA after the deletion junction and the only different region lies at the amino terminus) and 57% identical to that of rOCT2.

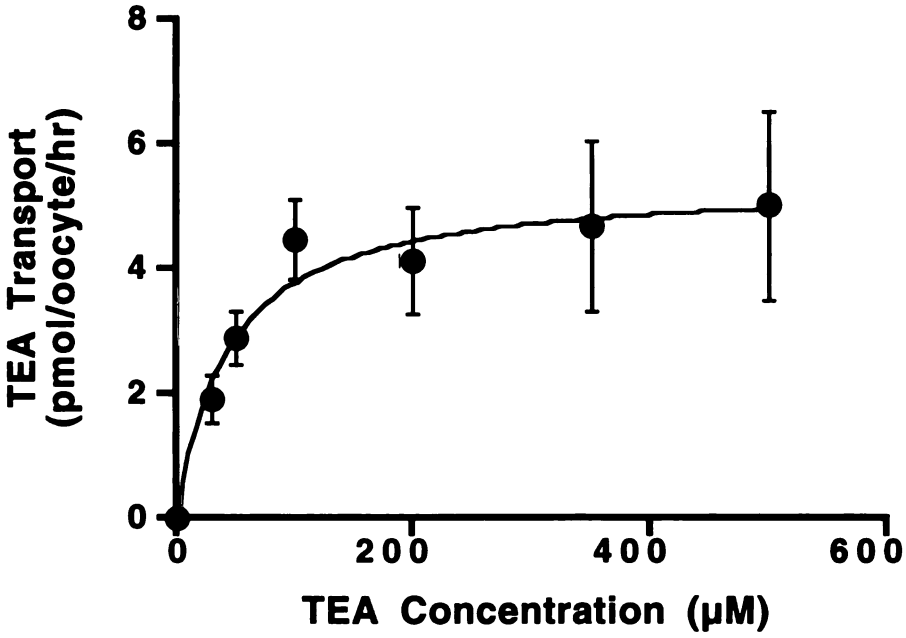

Figure 4.2c Kinetics of TEA transport in rOCT1A cRNA-injected oocytes. Data were fit to a Michaelis-Menten equation (K_m = 42 ± 11 μM; V_{max} = 5. 4 ± 0.4 pmol/oocyte/hr). Each point represents mean ± SE from seven oocytes.

(a)

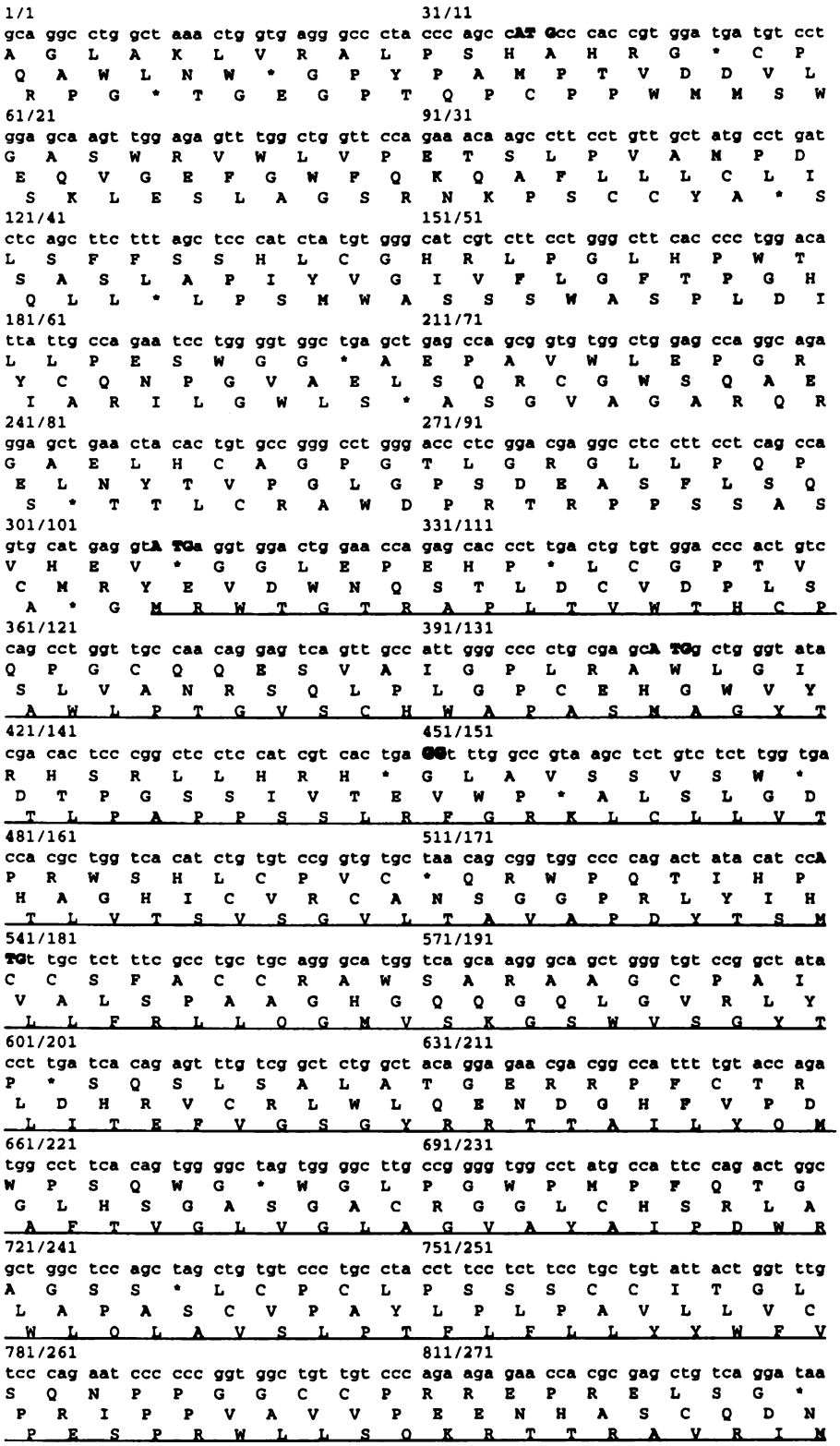
1/1
gca ggc ctg gct aaa ctg gtg agg gcc cta
A G L A K L V R A L
Q A W L N W * G P Y
R P G * T G E G P T
61/21
gga gca agt tgg aga gtt tgg ctg gtt cca
G A S W R V W L V P
E Q V G E F G W F Q
S K L E S L A G S R
121/41
ctc agc ttc ttt agc tcc cat cta tgt ggg
L S F F S S H L C G
S A S L A P I Y V G
Q L L * L P S M W A
181/61
tta ttg cca gaa tcc tgg ggt ggc tga gct
L L P E S W G G * A
Y C Q N P G V A E L
I A R I L G W L S *
241/81
gga gct gaa cta cac tgt gcc ggg cct ggg
G A E L H C A G P G
E L N Y T V P G L G
S * T T L C R A W D
301/101
gtg cat gag gtA TGa ggt gga ctg gaa cca
V H E V * G G L E P
C M R Y E V D W N Q
A * G M R W T G T R
361/121
cag cct ggt tgc caa cag gag tca gtt gcc
Q P G C Q Q E S V A
S L V A N R S Q L P
A W L P T G V S C H
421/141
cga cac tcc cgg ctc ctc cat cgt cac tga
R H S R L L H R H *
D T P G S S I V T E
T L P A P P S S L R
481/161
cca cgc tgg tca cat ctg tgt ccg gtg tgc
P R W S H L C P V C
H A G H I C V R C A
T L V T S V S G V L
541/181
TGt tgc tct ttc gcc tgc tgc agg gca tgg
C C S F A C C R A W
V A L S P A A G H G
L L F R L L Q G M V
601/201
cct tga tca cag agt ttg tcg gct ctg gct
P * S Q S L S A L A
L D H R V C R L W L
L I T E F V G S G Y
661/221
tgg cct tca cag tgg ggc tag tgg ggc ttg
W P S Q W G * W G L
G L H S G A S G A C
A F T V G L V G L A
721/241
gct ggc tcc agc tag ctg tgt ccc tgc cta
A G S S * L C P C L
L A P A S C V P A Y
W L Q L A V S L P T
781/261
tcc cag aat ccc ccc ggt ggc tgt tgt ccc
S Q N P P G G C C P
P R I P P V A V V P
P E S P R W L L S Q
31/11
cAT Gcc cac cgt gga tga tgt cct
H A H R G * C P
M P T V D D V L
M M S W
91/31
gaa aca agc ctt cct gtt gct atg cct gat
E T S L P V A M P D
K Q A F L L L C L I
P S C C Y A * S
151/51
cgt ctt cct ggg ctt cac ccc tgg aca
R L P G L H P W T
I V F L G F T P G H
S S W A S P L D I
211/71
gag cca gcg gtg tgg ctg gag cca ggc aga
E P A V W L E P G R
S Q R C G W S Q A E
A S G V A G A R Q R
271/91
acc ctc gga cga ggc ctc ctt cct cag cca
T L G R G L L P Q P
D E A S F L S Q
P R T R P P S S A S
331/111
gag cac cct tga ctg tgt gga ccc act gtc
E H P * L C G P T V
L D C V D P L S
L T V W T H C P
391/131
ggg ccc ctg cga gcA TGg ctg ggt ata
G P L R A W L G I
P C E H G W V Y
P A S M A G Y T
451/151
GGt ttg gcc gta agc tct gtc tct tgg tga
G L A V S S V S W *
V W P * A L S L G D
F G R K L C L L V T
511/171
taa cag cgg tgg ccc cag act ata cat ccA
* Q R W P Q T I H P
N S G G P R L Y I H
T A V A P D Y T S M
571/191
tca gca agg gca gct ggg tgt ccg gct ata
S A R A A G C P A I
Q Q G Q L G V R L Y
S K G S W V S G Y T
631/211
cga cgg cca ttt tgt acc aga
R P F C T R
N D G H F V P D
R R T T A I L Y Q M
691/231
cct atg cca ttc cag act ggc
P M P F Q T G
G L C H S R L A
A Y A I P D W R
751/251
tct tcc tct tcc tgc tgt att act ggt ttg
S S S C C I T G L
P L P A V L L V C
F L L Y Y W F V
811/271
aga aga gaa cca cgc gag ctg tca gga taa
R R E P R E L S G *
E E N H A S C Q D N
R T T R A V R I M

841/281 871/291

tgg agc aaa ttg cac aga aga acg gga agg tgc ctc ctg ctg acc tga aga tgc tct gcc

W S K L H R R T G R C L L L T * R C S A

G A N C T E E R E G A S C * P E D A L P

E Q I A Q K N G K V P P A D L K M L C L

901/301 931/311

ttg agg agg atg cct cag aaa agc gaa gtc ctt cgt ttg ccg acc tgt tcc gca ctc cca

L R R M P Q K S E V L R L P T C S A L P

* G G C L R K A K S F V C R P V P H S Q

E E D A S E K R S P S F A D L F R T P N

961/321 991/331

acc tga gga agc aca ccg tca tcc tga tgt atc tat ggt tct ctt gtg ctg tgc tgt acc

T * G S T P S S * C I Y G S L V L C C T

P E E A H R H P D V S M V L L C C A V P

L R K H T V I L M Y L W F S C A V L Y Q

1021/341 1051/351

agg gtc tca tca tgc acg tgg gag cca cag ggg cca acc tct acc tgg act tct ttt att

R V S S C T W E P Q G P T S T W T S F I

G S H H A R G S H R G Q P L P G L L L F

G L I M H V G A T G A N L Y L D F F Y S

1081/361 1111/371

ctt ctc tgg tgg aat tcc ccg cgg cct tca tca tcc tgg tca cca ttg acc gca ttg gcc

L L W W N S P R P S S S W S P L T A L A

F S G G I P R G L H H P G H H * P H W P

S L V E F P A A F I I L V T I D R I G R

1141/381 1171/391

gca tct acc caa tag cgg cct cga atc tgg tga cgg ggg cag cct gcc tcc tca tga tct

A S T Q * R P R I W * R G Q P A S S * S

H L P N S G L E S G D G G S L P P H D L

I Y P I A A S N L V T G A A C L L M I F

1201/401 1231/411

tta tcc cgc atg agc tgc act ggt tga acg tta ccc tcg cct gtc ttg gcc gta tgg ggg

L S R M S C T G * T L P S P V L A V W G

Y P A * A A L V E R Y P R L S W P Y G G

I P H E L H W L N V T L A C L G R M G A

1261/421 1291/431

cca cca ttg tgc tgc aga tgg tct gcc tgg tga acg ctg agc tgt acc cta cat tca tca

P P L C C R W S A W * T L S C T L H S S

H H C A A D G L P G E R * A V P Y I H Q

T I V L Q M V C L V N A E L Y P T F I R

1321/441 1351/451

gga atc ttg gga tga tgg tat gct ctg ccc tgt gtg acc tgg gtg gga tct tca ccc cct

G I L G * W Y A L P C V T W V G S S P P

E S W D D G M L C P V * P G W D L H P L

N L G M M V C S A L C D L G G I F T P F

1381/461 1411/471

tca tgg tgt tca ggc tga tgg aag ttt ggc aag ccc tgc ccc tca ttt tgt ttg ggg ttt

S W C S G * W K F G K P C P S F C L G F

H G V Q A D G S L A S P A P H F V W G F

M V F R L M E V W Q A L P L I L F G V L

1441/481 1471/491

tgg gcc tga ctg ctg ggg cca tga ctc ttc ttc tcc cag aga cca agg gtg tgg ctt tgc

W A * L L G P * L F F S Q R P R V W L C

G P D C W G H D S S S P R D Q G C G F A

G L T A G A M T L L L P E T K G V A L P

1501/501 1531/511

ctg aga cta ttg aag aag cag aga acc tgg gga gga gga aat caa agg cca aag aaa aca

L R L L K K Q R T W G G G N Q R P K K T

* D Y * R S R E P G E E E I K G Q R K H

E T I E E A E N L G R R K S K A K E N T

1561/521 1591/531

cga ttt acc ttc agg tcc aaa cag gca agt cct caa gta cct ga

R F T F R S K Q A S P Q V

D L P S G P N R Q V L K Y

I Y L Q V Q T G K S S S T *

(b)

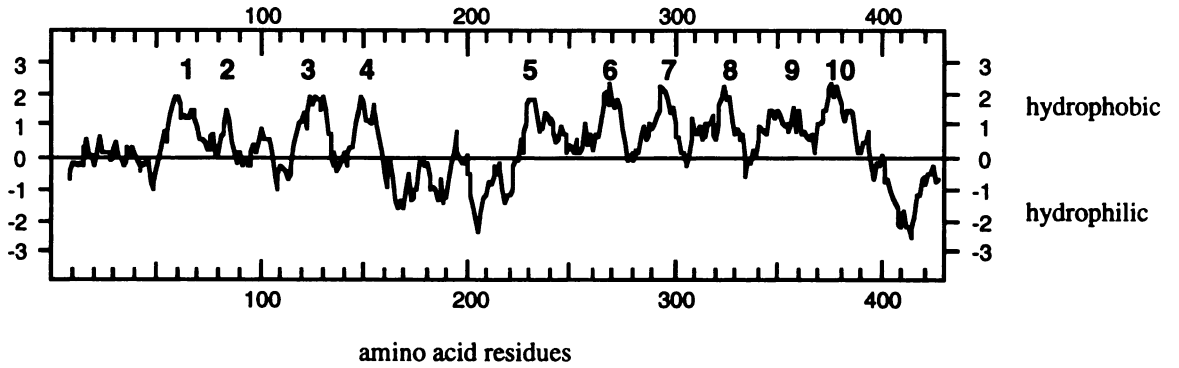

Figure 4.3 *(a)* cDNA sequence of the 1.5-kb (rOCT1A) clone and the corresponding three possible translational reading frames. The positions of the four putative initiation sites are indicated in *bold.* Nucleotides flanking the splice sites are indicated by *outlines.* The putative amino acid sequence of rOCT1A is *underlined.* Stop codons are indicated by *asterisks.* *(b)* Kyte-Doolittle hydropathy analysis of rOCT1A (the protein encoded from bp 312 to bp 1601) using a window of 11 amino acids; putative transmembrane domains are *numbered (1-10).*

(Alternative ATG sites at bp 408 or 540 of RF3 are other possible initiation sites and would encode truncated versions of rOCT1A.) Based upon hydropathy analysis using the Kyte-Doolittle algorithm and application of the positive inside rule (Kyte and Doolittle, 1982; von Heijne, 1992), rOCT1A is predicted to have 10 transmembrane domains with both amino and carboxy termini intracellular (Figure 4.3b). In comparison, both rOCT1 and rOCT2 are predicted to have 12 transmembrane domains (Grundemann *et al.*, 1994; Okuda *et al.*, 1996). As a result of the deletion, rOCT1A lacks the first two transmembrane domains as well as the three potential glycosylation sites in the first extracellular loop of rOCT1. Nevertheless rOCT1A exhibits similar functional characteristics to those of rOCT1, which implies that the first two transmembrane domains and these three putative glycosylation sites are not essential for the transport function. However, other properties of the transporter such as synthesis, targeting and sorting may be different between the two isoforms. Five potential protein kinase C phosphorylation sites at serine residues 160, 166, and 202 and threonine residues 170 and 424 were identified in the intracellular loops of rOCT1A. (The positions correspond to the deduced amino acid sequence of rOCT1A beginning at the internal ATG at bp 312.) Additionally, one potential *N*-glycosylation site was identified in the extracellular loop between helices 7 and 8. These sites are conserved in both rOCT1 and rOCT1A (Grundemann *et al.*, 1994).

4.3.4 Genomic DNA Cloning

To determine the genomic nature of rOCT1A, genomic DNA fragments of rOCT1 flanking the splice sites were cloned and sequenced. As shown in Figure 4.4, there is an intron of at least 6 kb in length between bp 451 and 452 of the rOCT1 cDNA followed by a short exon of 104 bp in length, which matches the deleted sequence. There is another intron of 439 bp in length between bp 555 and 556 of the rOCT1 cDNA. Based on the genomic sequence of rOCT1 in this region and the fact that rOCT1 and rOCT1A are 100% identical at the cDNA level (except for the 104 bp deletion in rOCT1A), rOCT1A represents

(a)

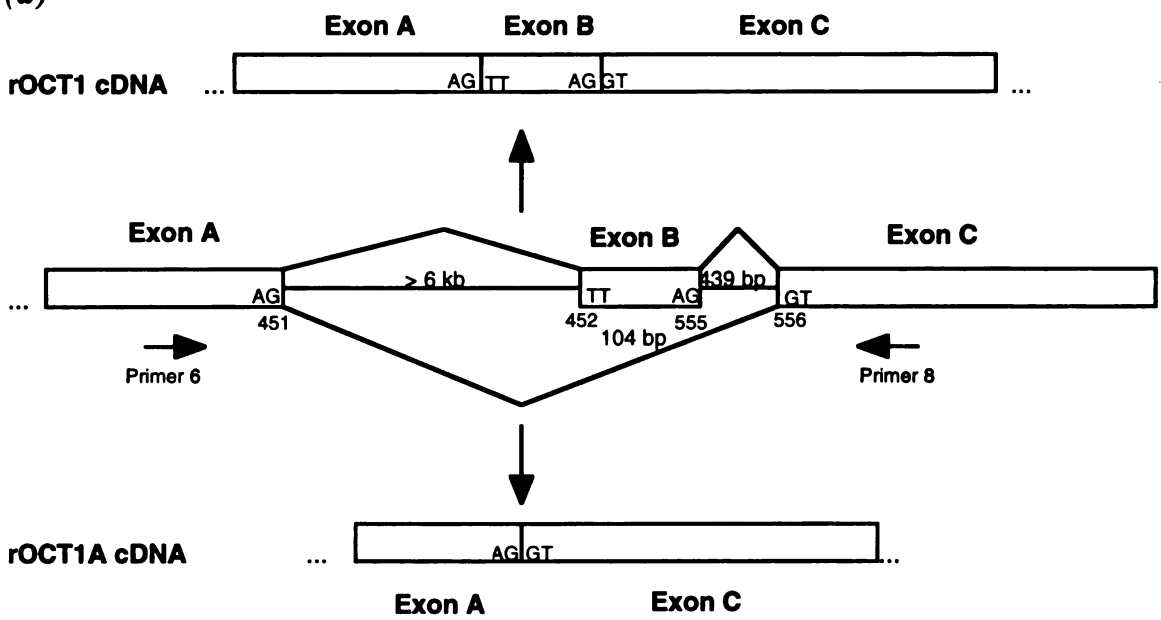

(b)

Exon	Splice donor	Splice acceptor	Exon
A	...ATCGTCACTGAGgtactaatgggt.....ccactgcttcagTTTAACCTGGTG...		B
B	...CATTGCAGACAGgtaggtgaaagc.....ttgtctctgcagGTTTGGCCGTAA...		C

Figure 4.4 *(a)* Diagram of rOCT1 gene (*middle panel*) showing the alternative splicing sites. The positions of the introns (*lines*) and exons (*boxes*) are indicated, including the 104 bp exon (Exon B) that is included in the nucleotide sequence of rOCT1 (*top panel*) but not rOCT1A (*bottom panel*). Nucleotides flanking the splicing sites are indicated in the appropriate positions in the *boxes*. Primers on the cDNA that are used for the genome walking are indicated by *horizontal arrows*. *(b)* Partial nucleotide sequences flanking the splicing sites. Good splicing donor and acceptor sequences at splicing junction are present.

an alternatively spliced isoform from a common precursor mRNA transcript. In addition, a recent chromosomal localization study of *Roct1* excludes the possibility of multiple *Roct1* genes or pseudogenes (Koehler *et al.*, 1996).

The 104 bp (exon B) in rOCT1 include part of the loop between transmembrane domain 1 and 2 and the whole transmembrane domain 2. This deletion interrupts a codon (AGG) between 555 and 556 that results in a frameshift and leads to an earlier stop codon in RF2. Frame shift in splice variants of membrane proteins in higher organisms (*i.e.*, humans and other mammals) has been reported (Canton *et al.*, 1996; Shire *et al.*, 1995; Strehler *et al.*, 1989). In addition, the large intron of at least 6 kb between exon A and B presents the possibility of further alternative splicing. It will be of interest to ascertain whether other subtypes or isoforms of rOCT1 exist and to determine their functional significance.

4.3.5 In Vitro Translation

In vitro translation experiments in the rabbit reticulocyte lysate system were performed to synthesize proteins from the cRNAs of rOCT1A and rOCT1 (as a comparison). Translation products were analyzed by SDS-polyacrylamide gel electrophoresis. Figure 4.5 shows that translation of the cRNA of rOCT1 produced a single band with an apparent molecular size of 47 kDa (Figure 4.5, lane 2). In contrast, translation of the mRNA encoding rOCT1A resulted in several bands with one major band of about 16 kDa in size and a major band(s) of about 37 kDa (Figure 4.5, lane 3). The multiple bands at 37 kDa may be a result of translation beginning at multiple internal ATG sites as discussed previously and suggested by the sequence. The 16-kDa band may be encoded by the short open reading frame in RF2 (bp 38-460, 141 amino acids). Alternatively, it can be a result of proteolysis. The protein products produced in the *in vitro* translation experiments have apparent molecular masses smaller than predicted based upon the deduced sequences. However, anomalous migration of membrane proteins is not

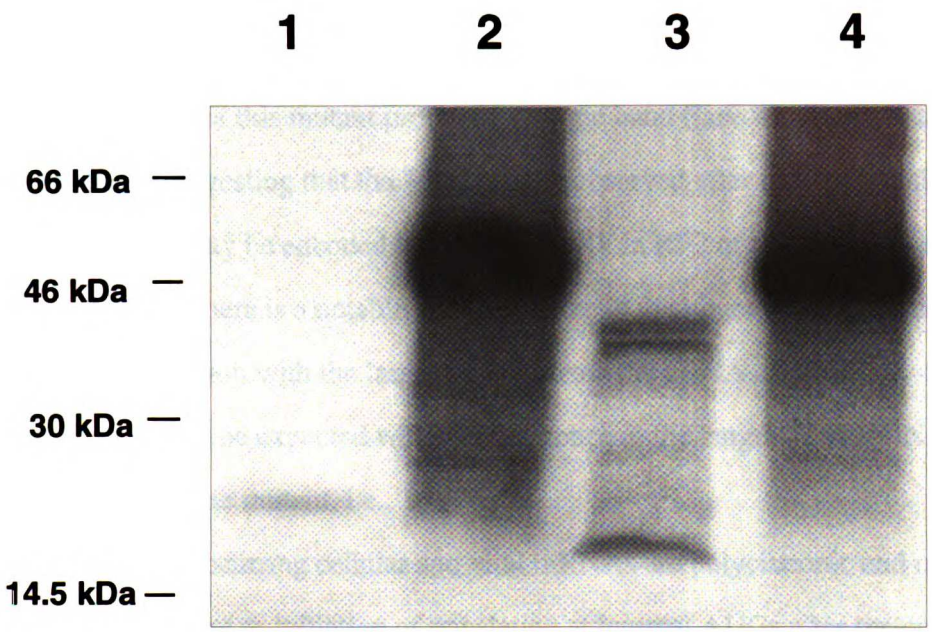

Figure 4.5 Autoradiograph of an SDS-polyacrylamide gel electrophoresis (gradient, 4-20%) showing *in vitro* translation products of rOCT1 and rOCT1A cDNA. TNT® coupled transcription/translation rabbit reticulocyte lysate system and ^{35}S-methionine were used to synthesize proteins from plasmid DNAs of rOCT1 (*lane 2*), rOCT1A (*lane 3*) and rOCT1A mutant (*lane 4*). *Lane 1* displays the blank control in which nuclease-free water was used instead of DNA. *kDa*, kilodaltons.

unusual (Hediger *et al.*, 1987; James *et al.*, 1989).

In order to determine whether the smaller band of about 16 kDa was due to the early stop codon at 460 bp in RF2, a mutant of rOCT1A was generated. This mutant contained a 105 bp in-frame deletion in the rOCT1 cDNA, thus eliminating the early stop codon and restoring the RF2 as in rOCT1 of the spliced RNA. As shown in Figure 4.5, *in vitro* translation of the cRNA of this mutant produced a single band (lane 4). These data provide the indirect evidence suggesting that the 16-kDa band observed after *in vitro* translation of the cRNA of rOCT1A may be encoded by the short ORF in RF2 of rOCT1A. In addition, after *in vitro* translation there is a notable size difference in the larger band from the cRNA of the mutant in comparison with the larger band(s) from the cRNA of rOCT1A. Such a size difference would not be expected with the difference in the length of the cDNA's encoding rOCT1A and the mutant, i.e., 1 bp.

Many naturally occurring cellular and viral mRNAs are polycistronic and multiple proteins are synthesized by re-initiation of translation at internal AUGs after meeting the terminator codon of the upstream ORF. Examples of polycistronic mRNA transcripts in eukaryotes are rare and have never been reported in mammalian mRNA (Kozak, 1992; Merrick, 1992; Peabody and Berg, 1986). Further studies are needed to determine whether the multiple bands observed in *in vitro* translation studies are a result of a polycistronic mRNA transcript of rOCT1A or proteolysis. Future studies utilizing antibodies recognizing different ORFs will provide the definitive evidence to determine whether multiple proteins from different ORFs were encoded. Mutagenesis studies will be important in determining the internal initiation site(s) of translation for rOCT1A.

4.3.6 Functional Expression of Synthetic Constructs

Based upon comparative sequence analysis with rOCT1 and the general structure of membrane transporters that normally have multiple membrane spanning regions (von Heijne, 1995), we hypothesized that the larger protein is the functional transporter.

Accordingly, we constructed a synthetic cDNA that would encode for the 16 kDa product (Pro 1) and two synthetic cDNAs which would encode for two possible functional transport proteins (Pro 2 and Pro 3) (Figure 4.6a). The function of the synthetic proteins was tested by injecting oocytes with cRNA transcribed from the cDNA encoding Pro 1, 2 and 3. ^{14}C-TEA uptake was enhanced significantly in oocytes injected with the cRNA of Pro 2 or 3 in comparison to water-injected oocytes (Figure 4.6b, $p<0.05$). In contrast, ^{14}C-TEA uptake was not enhanced in oocytes injected with the cRNA of Pro 1 (2.35 ± 0.13 pmol/oocyte/hr in cRNA injected oocytes vs 2.51 ± 0.31 pmol/oocyte/hr in water-injected oocytes, mean ± SE). The reasons why Pro 3 had a higher expressed activity than either Pro 2, rOCT1 or rOCT1A are unknown. Differences in efficiency of the *in vivo* translation or protein processing may explain the data. Alternatively, Pro 3 may have a higher intrinsic activity. These data suggest that Pro 2 and 3, representing possible proteins encoded by the cRNA of rOCT1A, can mediate the transport of TEA whereas Pro 1 cannot. In *in vitro* translation experiments, Pro 2 migrated at a similar rate as the 37 kDa translation product of the cRNA of rOCT1A (data not shown) suggesting that Pro 2 might be the functional organic cation transporter. These data have implications to the function of rOCT1 since rOCT1A is 92% identical in sequence to rOCT1.

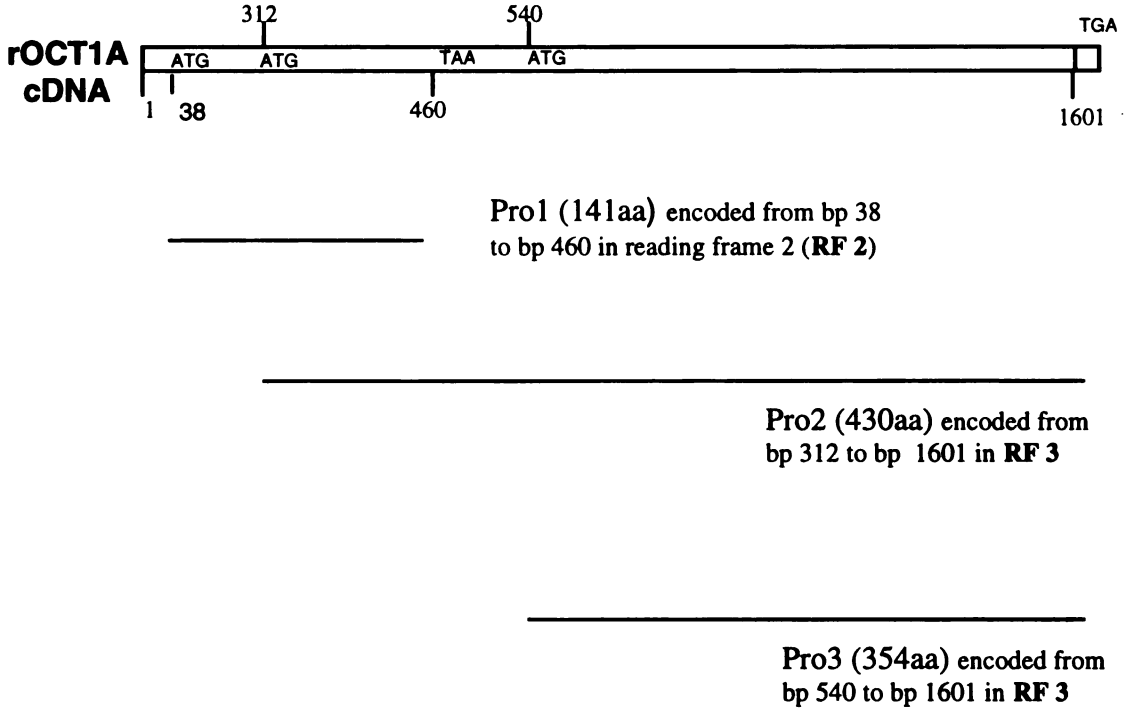

Figure 4.6a Schematic diagram showing the construction of Pro 1, 2 and 3. *aa*, amino acids.

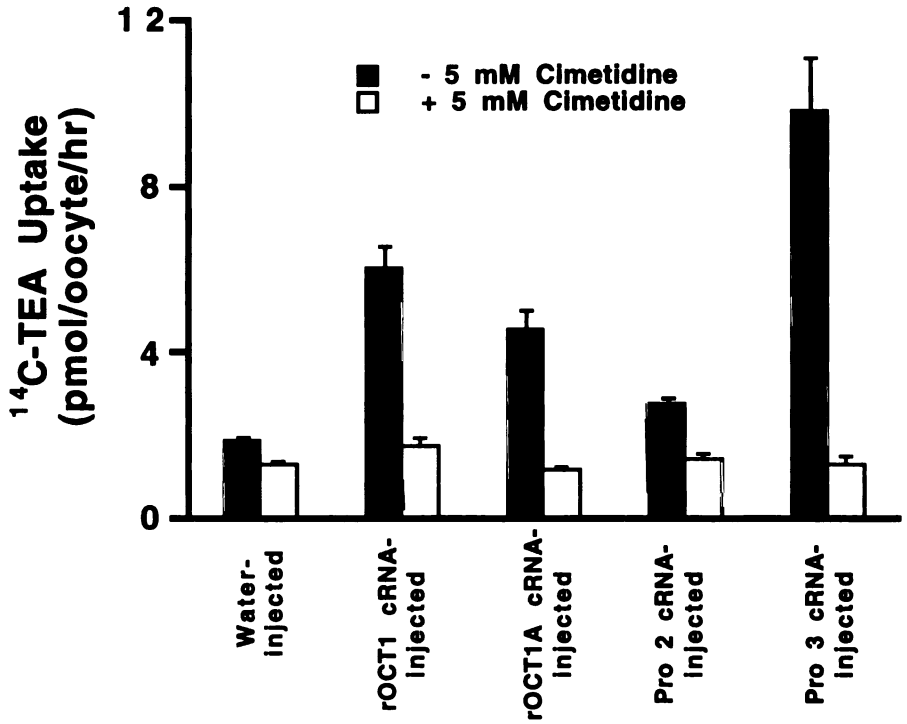

Figure 4.6b ^{14}C-TEA uptake in Pro 1, 2 and 3 cRNA-injected oocytes compared to water and rOCT1 and rOCT1A cRNA-injected oocytes. Uptake was conducted 3 days after injection for 90 min at 25°C. Each *column* represents the mean ± SE of 1-3 experiments. 7-18 oocytes were used for each *column*. *Dark bars* represent the uptake in the absence of 5 mM cimetidine and *open bars* represent the uptake in the presence of 5 mM cimetidine. TEA uptake in each (rOCT1, rOCT1A, Pro 2, and Pro 3) of cRNA-injected oocytes was significantly different from the uptake in water-injected oocytes, $p < 0.05$.

4.3.7 RNA Expression of rOCT1A and Its Tissue Distribution

To characterize the rOCT1A RNA expression in the kidney, RNase protection assays (RPAs) were performed. A 416-nucleotide biotin labeled antisense RNA probe was synthesized to specifically detect rOCT1 and rOCT1A RNA fragments differing by approximately 110 nucleotides (Figure 4.7a). As shown in Figure 4.7b, two RNase-protected fragments of expected size for rOCT1 and rOCT1A (370 and 263 nucleotides, respectively) were detected in the RNA of total kidney, kidney cortex, and kidney medulla. In addition, from the intensities of the protected fragments, it appears that the rOCT1 RNA transcript is present at a higher level than that of rOCT1A in the kidney. Additional RPAs using this probe detected rOCT1 and rOCT1A RNA transcripts in the intestine but not in the heart or spleen (data not shown).

Tissue distribution of rOCT1A transcript was also determined by RT-PCR using primers 1 and 3 (Table 4.1). Figure 4.8a shows that, consistent with the RPA results, transcripts of rOCT1 and rOCT1A (double bands at about 1.0 kb) are present in the rat kidney (total), kidney cortex, kidney medulla, intestine, liver and colon, but not in the stomach, brain, spleen, lung and heart. Localization of rOCT1 and rOCT1A in the intestine was further determined by RT-PCR using primers 1 and 3 (see Table 4.1). Figure 4.8b demonstrates that mRNA transcripts of both rOCT1 and rOCT1A are expressed in all regions of the intestine, *i.e.*, duodenum, jejunum, ileum and colon. These data suggest that the tissue distribution of the mRNA transcripts of rOCT1A and rOCT1 is similar, but differs from that of rOCT2, which is confined to the kidney (Okuda *et al.*, 1996). We also noticed that although the mRNA transcript of rOCT1A and rOCT1 coexpress in the same tissues, their relative levels appear different in results from both RPA and RT-PCR. Whether the expression level of the RNA of rOCT1A and rOCT1 reflects the protein expression level and relates to their physiological roles in different tissues or whether the alternative splicing represents a regulatory mechanism will be further investigated.

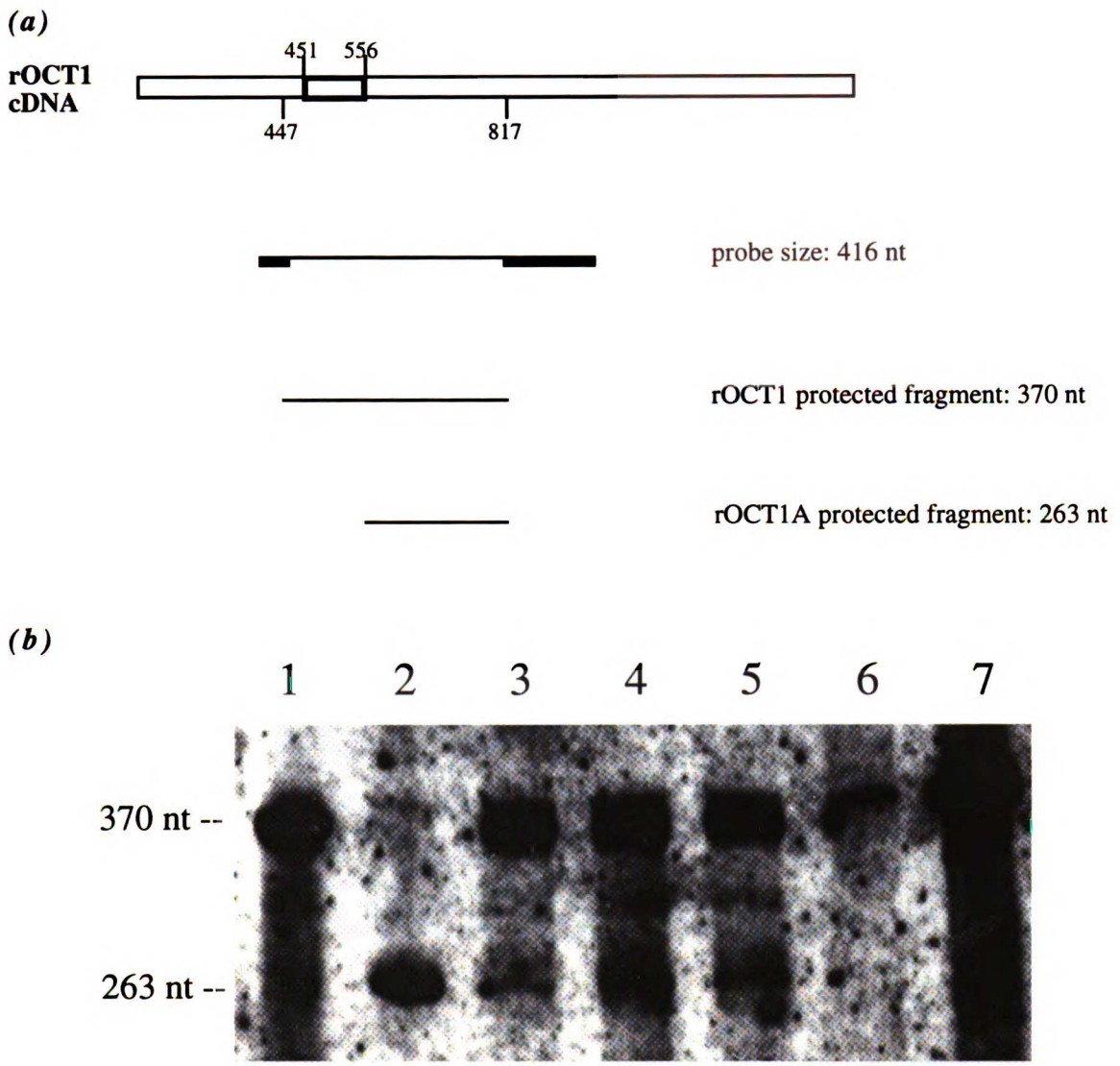

Figure 4.7 Expression of rOCT1 and rOCT1A transcripts detected by RPA. ***(a)*** Schematic representation of protected fragments of rOCT1 and rOCT1A transcripts by the RNase protection assay. The expected lengths of the protected fragments are indicated. The *thick bars* represent the vector sequences. ***(b)*** Results of RPA. Total RNA of rat total kidney (5 mg, *lane 3*), kidney cortex (15 mg, *lane 4*), kidney medulla (15 mg, *lane 5*), yeast (negative control, *lane 6*), and cRNA of rOCT1 and rOCT1A (600 pg, *lanes 1* and *2*, respectively) were protected with 100 pg of the antisense cRNA probe and digested with RNase T1 before precipitation and loading on the polyacrylamide gel as described under "Experimental Procedures". *Lane 7*, yeast RNA plus probe without Rnase T1 digestion (probe size). *nt*, nucleotides.

(a)

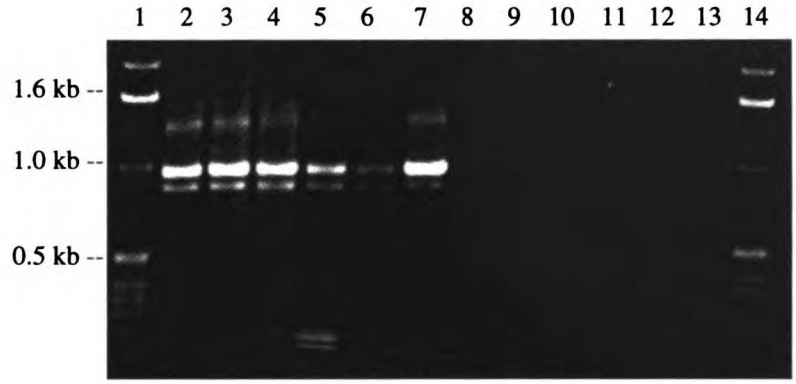

(b)

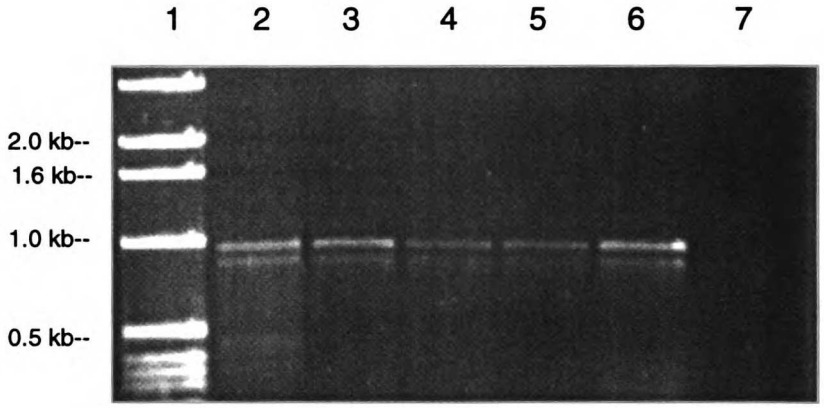

Figure 4.8 Expression of rOCT1 and rOCT1A transcripts detected by RT-PCR using *primers 1* and *3* (see Table 4.1). RT-PCR products were separated by electrophoresis through 1% agarose and stained with ethidium bromide. ***(a)*** Expression of rOCT1 and rOCT1A mRNA in different tissues. *Lanes 1 & 14*, 1-kb DNA ladder (Gibco BRL); *lane 2*, kidney total; *lane 3*, kidney cortex; *lane 4*, kidney medulla; *lane 5*, intestine; *lane 6*, colon; *lane 7*, liver; *lane 8*, stomach; *lane 9*, brain; *lane 10*, heart; *lane 11*, lung; *lane 12*, spleen; *lane 13,* no cDNA control. ***(b)*** Expression of rOCT1 and rOCT1A mRNA in different segments of rat intestinal tract. *Lanes 1*, 1-kb DNA ladder (Gibco BRL); *lane 2*, colon; *lane 3*, duodenum; *lane 4*, jejunum; *lane 5*, ileum; *lane 6*, colon; *lane 7*, no cDNA control.

In summary, a polyspecific organic cation transporter, rOCT1A, from rat kidney has been cloned and expressed. rOCT1A is an alternatively spliced variant of rOCT1 and is similar in function to rOCT1 and rOCT2. RT-PCR indicates that rOCT1A mRNA transcripts are also present in the intestine and liver, and RNase protection assays indicate that the RNA transcript of rOCT1A is present in detectable quantities in the rat kidney. Future studies will be performed to determine the underlying structural requirements for the function of organic cation transporters, the physiologic role of rOCT1A in the intact tissue and the mechanisms involved in the translation of the rOCT1A mRNA transcript.

CHAPTER 5

MOLECULAR CLONING AND FUNCTIONAL EXPRESSION OF A HUMAN LIVER ORGANIC CATION TRANSPORTER [1]

5.1 Introduction

Polyspecific organic cation transporters in the liver are critical in the systemic and pre-systemic elimination of many endogenous amines as well as a wide array of drugs and environmental toxins (Groothuis and Meijer, 1996; McKinney and Hosford, 1992; Meijer *et al.*, 1990; Moseley *et al.*, 1992; Oude Elferink *et al.*, 1995; Sandker *et al.*, 1994; Steen *et al.*, 1992). To mediate elimination (or excretion), transporters on the sinusoidal membrane of the hepatocyte function in the uptake of organic cations from the blood into the intracellular space. Once in the hepatocyte, organic cations may be sequestered, metabolized or transported across the canalicular membrane into the biliary tract.

At least five organic cation transporters on the sinusoidal membrane of the rat hepatocyte have been described (Oude Elferink *et al.*, 1995). Of these, two organic cation-selective transporters seem to mediate the uptake of exogenous organic cations (type I and type II). The type I carrier accepts small monovalent organic cations such as tributylmethylammonium (TBuMA), TEA and MPP^+ whereas the type II carrier accepts larger organic cations which are mostly bivalent. In addition, a multispecific, non-charge-

[1] This work was published in *Molecular Pharmacology* 51:913-922, 1997. Permission from the publisher is included in "Acknowledgements".

selective transporter appears to mediate the uptake of a number of compounds including various organic cations across the sinusoidal membrane (Steen *et al.*, 1992).

Recently, a polyspecific transporter for organic cations (rOCT1) was cloned from a rat kidney cDNA library (Grundemann *et al.*, 1994). Northern analysis revealed that rOCT1 was also found in rat liver. Subsequent studies suggest that in the liver, rOCT1 represents a transporter for organic cations on the sinusoidal membrane which mediates the uptake of type I substances (Busch *et al.*, 1996b; Nagel *et al.*, 1997).

Despite the critical role that hepatic transporters play in drug absorption and elimination as well as in detoxification, there have been few studies of hepatic transport of organic cations in humans (Sandker *et al.*, 1994; Steen and Meijer, 1991) and no study has elucidated the molecular structure or function of human polyspecific organic cation transporters in any tissue. In a recent study, notable species differences were observed in the rate of transport of the organic cation, vecuronium, in human hepatocytes in comparison to rat hepatocytes. Namely, the influx rate constant (k_{in}) of vecuronium in isolated rat hepatocytes was 10-fold greater than in human hepatocytes (Sandker *et al.*, 1994). Importantly, these interspecies differences in the rate of uptake of organic cations were also observed in the intact organ (Sohn *et al.*, 1986; Waser *et al.*, 1987).

In this study, we cloned and functionally characterized the first human organic cation transporter from liver (hOCT1). The sequence of hOCT1, its functional expression in *Xenopus laevis* oocytes, and its tissue distribution are presented. Differences in the functional activity and tissue distribution of hOCT1 in comparison to rOCT1 were observed. Further studies of the function and regulation of hOCT1 will enhance our understanding of the mechanisms involved in organic cation transport in the human liver and the factors responsible for the observed interspecies differences.

5.2 Materials and Methods

5.2.1 Isolation and Subcloning of OCT1-Like Homologous PCR Fragments From Human Liver cDNA

The cDNA template for PCR amplification was synthesized from human liver mRNA (Clontech, Palo Alto, CA) with the oligo (dT) primer using the SuperScript™ Preamplification System (Gibco BRL, Gaithersburg, MD) according to the manufacturer's protocol. The primers 1 and 2 (Table 5.1) used in reverse transcriptase (RT)-PCR were designed from the conserved regions after alignment of several homologous genes including rOCT1 (Grundemann *et al.*, 1994) and OCT2, a rat kidney specific organic cation transporter (designated rOCT2) (Okuda *et al.*, 1996). The PCR was performed in a thermal cycler (Perkin Elmer, Foster City, CA) set to the following parameters: 94°C for 1 min, 48°C for 2 min, 72°C for 2 min, and 40 cycles followed by a final 15 min incubation at 72°C. *Pfu* DNA polymerase (Stratagene, La Jolla, CA) was mixed with Ex*Taq* DNA polymerase (TaKaRa, Japan) (v/v 1:15) in the reaction mixture in order to increase the fidelity of the PCR reactions.

The PCR products were electrophoresed through 1% agarose gel, and size-selected DNA fragments were extracted and ligated (subcloned) into the pGEM-T vector (Promega, Madison, WI) using T4 DNA ligase according to the T-A cloning method followed by transformation into DH5α competent cells (Gibco BRL). Plasmid DNA was isolated using the Wizard™ Miniprep DNA Purification System (Promega) and was analyzed by restriction enzyme analysis and/or sequencing.

5.2.2 *DNA Amplification of the cDNA 5'- and 3'-Ends and the Full-Length cDNA*

To obtain the remaining 5' portion of human liver OCT1 cDNA, a PCR-based method, 5'-RACE (rapid amplification of cDNA ends), was utilized. Three gene specific antisense primers, designated 5'-RACE-1, 5'-RACE-2 and 5'-RACE-3 (see Table 5.1), were designed from the partial human liver OCT1 sequence (the sequenced PCR fragment). First-strand cDNA synthesis for 5'-RACE was primed with 5'-RACE-1 using the 5' RACE System for Rapid Amplification of cDNA Ends (Gibco-BRL) from human liver mRNA (Clontech). Homopolymeric tails were added to the 3'-end of the cDNA which was then amplified by PCR using the anchor primer 1 (see Table 5.1) and nested 5'-RACE-2 primer. A nested PCR was performed with the anchor primer 2 and the nested 5'-RACE-3 primer with a different annealing temperature (50°C) to assess the specificity of the PCR product. The amplified products from the nested PCR were then subcloned as previously described.

3'-RACE protocol was used to obtain the remaining 3' portion of human liver OCT1 cDNA. Two gene specific sense primers, designated 3'-RACE-1 and 3'-RACE-2 (see Table 5.1), were designed from the partial human liver OCT1 sequence (the sequenced PCR fragment). First strand cDNA synthesis was initiated at the poly(A)$^+$ tail of human liver mRNA (Clontech) using the adapter primer provided with the 3' RACE System for Rapid Amplification of cDNA Ends (Gibco BRL) following the manufacturer's protocol. PCR was performed on this first-strand cDNA using 3'-RACE-1 primer and the nested amplification primer. The resulting amplified products from the nested PCR with 3'-RACE-2 primer and the amplification primer were then subcloned as described above.

The entire human liver OCT1 cDNA coding region was obtained by RT-PCR with the 5'-end primer and 3'-end primer (see Table 5.1) which were designed from the beginning and the end regions of the open reading frame according to the following

protocol: 94°C for 1 min, 55°C for 2 min, 72°C for 2 min, and 35 cycles followed by a final 30 min incubation at 72°C.

Table 5.1 Primers used for PCR cloning of hOCT1 cDNA

Primer designation	Primer sequence
Primer 1	5'-ATGCCCACCGTGGATGATGTCCTGG-3'
Primer 2	5'-AGTGCGGAACAGGTC-3'
5'-RACE-1	5'-AGCCGGGCGTGTCATACACCCA-3'
5'-RACE-2	5'-AGCGGCAGGTGGCTCCTGTTGG-3'
5'-RACE-3	5'-CACTGTATAGTTCAGCTCCTCC-3'
Anchor primer 1 [a] (5'-RACE)	5'-CUACUACUACUAGGCCACGCG TCGACTAGTACGGGIIGGGIIGGGIIG-3'
Anchor primer 2 [a] (5'-RACE)	5'-CUACUACUACUAGGCCACGCG TCGACTAGTAC-3'
3'-RACE-1	5'-TACTACTGGTGTGTGCCGGAG-3'
3'-RACE-2	5'-ATCGCTCAAAAGAATGGGAAG-3'
Adapter primer [a] (3'-RACE)	5'-GGCCACGCGTCGACTAGTACTTTT TTTTTTTTTTTT-3'
Amplification primer [a] (3'-RACE)	5'-GGCCACGCGTCGACTAGTAC-3'
5'-end primer	5'-GGAATTCCATCATGCCCACCGTGGA-3' *Eco*R I site
3'-end primer	5'-GCTCTAGAGCAAAACATCTCTCTCA-3' *Xba* I site

Restriction enzyme recognition sites incorporated into primer sequences are indicated by lines beneath appropriate sequences. [a] These primers were provided with the 5'- and 3'-RACE system (Gibco BRL).

5.2.3 Sequence Analysis

cDNA isolated from multiple reverse-transcription and PCR reactions were sequenced using universal and gene specific primers by the Biomolecular Resource Center DNA Sequencing Facility at the University of California, San Francisco with an automated sequencer (Model 373A ; Applied Biosystems, Foster City, CA).

Multiple sequence alignments were produced using the Gap and Pileup programs in the Genetics Computer Group (Wisconsin Package, Version 8) software package. The Motifs program in the Genetics Computer Group package was used to determine potential protein kinase C phosphorylation sites and N-glycosylation sites. The transmembrane domains of hOCT1 were predicted on the basis of hydropathy analysis using the Kyte-Doolittle algorithm (Kyte and Doolittle, 1982) in the Genetics Computer Group Pepplot program as well as the hydropathy analysis program in DNA Strider 1.2, a C program for DNA and protein analysis designed and written by Christian Marck (Service de Biochemie et de Genetique Moleculaire, Gif-sur-Yvette, France).

5.2.4 Expression of hOCT1 in Xenopus Laevis Oocytes and ^{3}H-MPP^{+} and ^{14}C-TEA Transport Measurements

Oocytes were harvested from *Xenopus laevis* (Xenopus I, Ann Arbor, MI and Nasco, Fort Atkinson, WI) and defolliculated with collagenase D (Boehringer-Mannheim Biochemicals, Indianapolis, IN) in a calcium-free OR II solution as previously described (Giacomini *et al.*, 1994). Healthy stage V and VI oocytes were injected with 50 nl diethylpyrocarbonate-treated water, mRNA or 5-100 ng of capped cRNA transcribed *in vitro* with T7 RNA polymerase (mCAP RNA Capping Kit; Stratagene) from linearized plasmid DNA. The injected oocytes were maintained in modified Barth's solution at 18°C before uptake experiments.

The uptake of ^{3}H-MPP^{+} (79.9 Ci/mmol, DuPont-New England Nuclear, Boston, MA) or ^{14}C-TEA (55 mCi/mmol, American Radiolabeled Chemicals, St. Louis, MO) in oocytes was measured as previously described (Giacomini *et al.*, 1994). Briefly, groups of six to nine oocytes were incubated in a Na^{+}-uptake buffer (100 mM NaCl, 2 mM KCl, 1 mM $CaCl_2$, 1 mM $MgCl_2$, 10 mM HEPES/Tris, pH 7.4) containing ^{3}H-MPP^{+} (0.15 μM ^{3}H-MPP^{+} and 0.7 μM of unlabeled MPP^{+}) or ^{14}C-TEA (100 μM) at 25°C. For inhibition studies, various unlabeled compounds (concentrations are specified in the figure legends)

were included in the reaction mixture. For the Michaelis-Menten kinetics study, 0.15 μM ^{3}H-MPP$^+$ plus various amounts of unlabeled MPP$^+$ were included in the reaction mixture. The K^+-uptake buffer (2 mM NaCl, 100 mM KCl, 1 mM $CaCl_2$, 1 mM $MgCl_2$, 10 mM HEPES/Tris, pH 7.4) was used to test the potential-dependency. The resting membrane potentials of water and hOCT1 cRNA injected-oocytes incubated in the specified Na^+- and K^+-buffer were measured with the use of standard microelectrode techniques (Quick and Lester, 1994). In the pH-dependency studies, the K^+-buffers were used at various pH values (6.4, 7.4 and 8.4 in HEPES/Tris buffer). The radioactivity associated with each oocyte was assayed by liquid scintillation counting.

5.2.5 In Vitro Translation and Sodium Dodecyl Sulfate-Polyacrylamide Gel Electrophoresis (SDS-PAGE) Gel Analysis

The TNT® T7 Quick Coupled Transcription/Translation System (Promega) and L-^{35}S-methionine (1000 Ci/mmol, 10 mCi/ml, DuPont-New England Nuclear) was used for eukaryotic *in vitro* translation according to the manufacturer's protocol. Five microliters of translation products was denatured in 20 μl Laemmli sample buffer plus 5% (v/v) 2-mercaptoethanol at 75°C for 10 min and loaded onto the 4-20% gradient gel (Tris-Glycine Ready Gels; Bio-Rad, Hercules, CA). To increase the sensitivity of detection of ^{35}S-labeled proteins, the gel was soaked in Amplify™ (Amersham Life Science, Arlington Heights, IL) for 15-30 min after the fixing step. The gel was then dried and exposed to Hyperfilm-MP film (Amersham Life Science) overnight at -70°C before development.

5.2.6 Northern Blot Analysis

A commercially available hybridization-ready blot containing poly(A)$^+$ mRNA from different human tissues (Multiple Tissue Northern Blot; Clontech) was used in Northern blot analysis. The blot is from an agarose gel of 2 μg of poly (A)$^+$ RNA from various human tissues. The blot was probed at 65°C overnight with a full-length antisense cRNA

probe. The probe was synthesized using BrightStar™ BIOTINscript™ nonisotopic *in vitro* transcription kit (Ambion, Austin, TX) according to the manufacturer's protocol. After hybridization and stringent washings, the signals were detected using the BrightStar™ Nonisotopic Detection System (Ambion) followed by membrane exposure to Hyperfilm-ECL film (Amersham Life Science).

To check the quality and quantity of the poly $(A)^+$ RNA of each tissue loaded on the blot, the membrane was stripped and reprobed with a human β-actin cDNA probe. A prominent β-actin signal was observed in each lane of the blot (data not shown).

5.2.7 Data Analysis

Uptake values are expressed as fmol/oocyte/hr or pmol/oocyte/hr and presented as mean ± standard error (SE) or as specified in the figure legends. A minimum of six to nine oocytes were used in each experiment. Statistical analysis was carried out by unpaired Student's *t*-test, and a $p < 0.05$ was considered significant.

5.2.8 Materials

All chemicals were purchased from Sigma Chemical (St. Louis, MO) and Fisher Scientific (Pittsburgh, PA)or as indicated. Molecular biology enzymes, reagents, and kits and radiolabeled compounds were purchased from specific manufacturers as indicated. Primers were synthesized by Biomolecular Resource Center (University of California, San Francisco) and Gibco BRL.

5.3 Results

5.3.1 Molecular Cloning of the Full-Length hOCT1 cDNA

An amplification product of ~1 kb in length was obtained when the PCR was performed with primers 1 and 2 and with human liver first-strand cDNA as template. DNA sequencing revealed that the PCR product was 1024 bp in length and was 82% identical to the rOCT1 cDNA, suggesting that a partial cDNA encoding a human organic cation transporter had been obtained. To clone the full-length cDNA a PCR-based cloning strategy involving 5'- and 3'- RACE protocols was pursued (Frohman *et al.*, 1988; Schaefer, 1995). The resulting 5'- (~280 bp) and 3'- (~900 bp) RACE products were derived from the partial human cDNA as indicated by sequence analysis and the full-length cDNA was obtained by RT-PCR using primers flanking the 5'- and 3'-ends and human liver mRNA as the initial template. The resultant product (~1.7 kb) was subcloned into a TA-based vector; this human clone is designated hOCT1.

5.3.2 DNA Sequencing and Primary Amino Acid Sequence

The nucleotide sequence and the deduced primary amino acid sequence of the hOCT1 cDNA are shown in Figure 5.1a. The cDNA is 1870 bp in length, including the poly(A)$^+$ tail. The open reading frame (ORF) is 1662 bp long and encodes a protein of 554 amino acids with a calculated molecular mass of 61 kDa. The predicted initiation codon is preceded by a Kozak consensus sequence (A/GXXAUG) (Kozak, 1989). The putative 12 transmembrane domains (TMDs) were predicted by a combination of Kyte-Doolittle hydropathy analysis (Kyte and Doolittle, 1982) (Figure 5.1b), application of the positive-inside rule (von Heijne, 1992) and multiple sequence alignment analysis of hOCT1 and its related rat and mouse sequences (i.e. rOCT1, rOCT2, Lx1 (Schweifer and Barlow, 1996)). The protein sequence contains three potential N-linked glycosylation sites (N-X-T/S) at

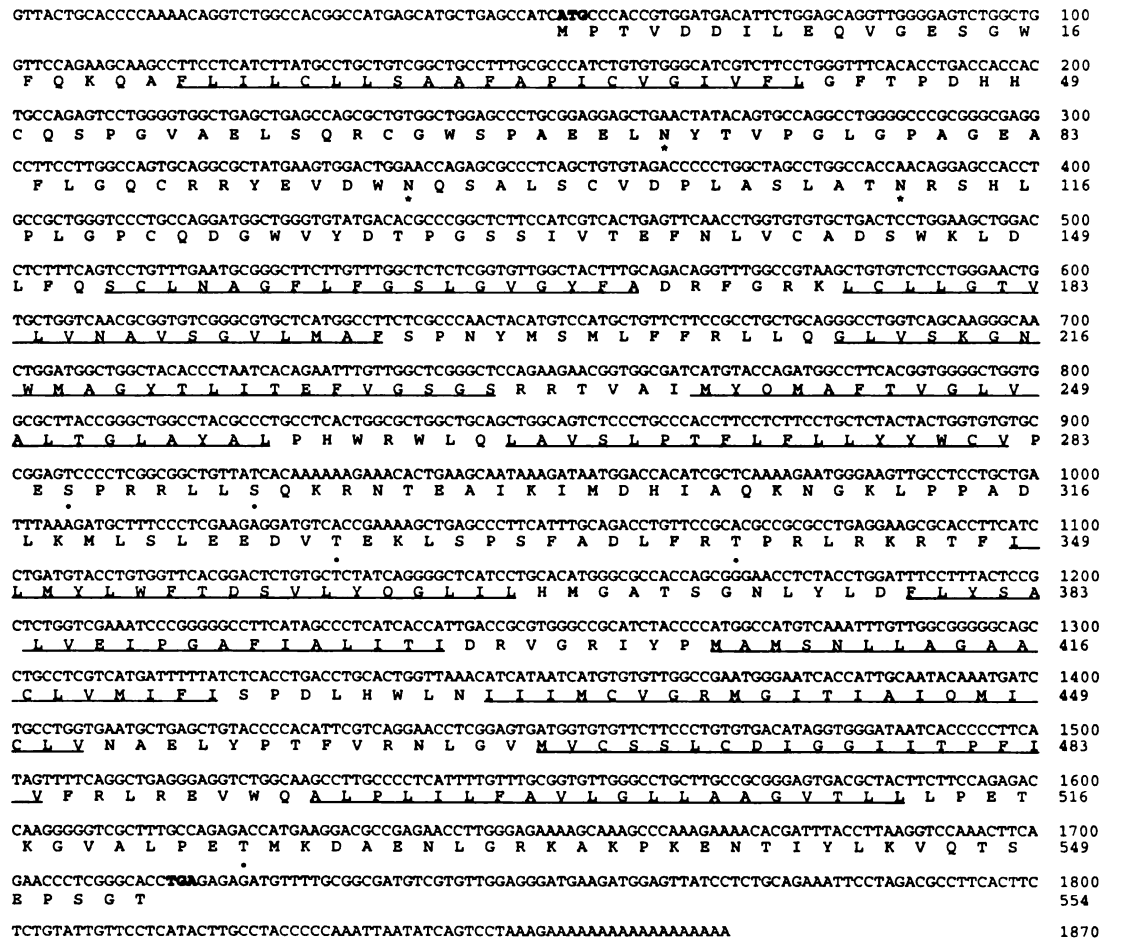

Figure 5.1a Nucleotide and deduced amino acid sequences of hOCT1 cDNA. *Bold*, the start (ATG) and stop (TGA) codons. *Underlined*, 12 putative transmembrane domains; *, potential N-glycosylation sites of the type N-X-T/S; *points*, five potential protein kinase C phosphorylation sites.

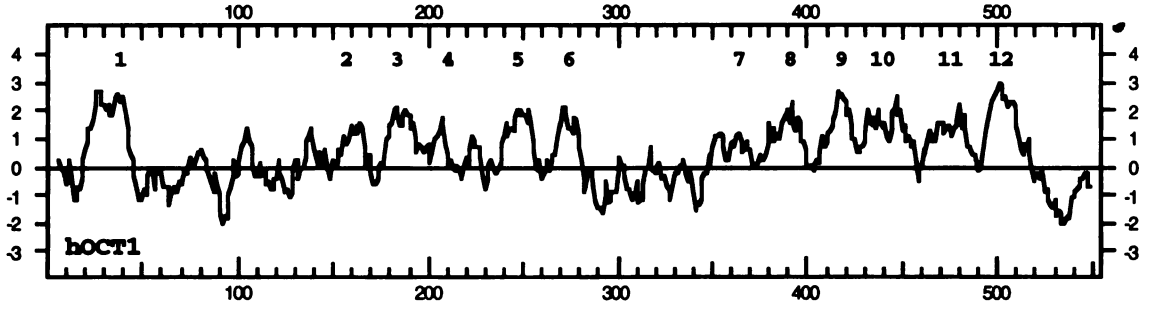

Figure 5.1b Kyte-Doolittle hydropathy analysis of hOCT1 using a window of 11. Putative transmembrane-spanning domains are numbered.

positions 71, 96 and 112. In addition, five potential protein kinase C phosphorylation sites were identified at residues 285, 291, 327, 340, and 524.

5.3.3 Functional Expression and Characterization in Xenopus Laevis Oocytes

A significant increase in the cimetidine-inhibitable ^{3}H-MPP^{+} uptake was observed in cRNA-injected oocytes (429 ± 36.8 fmol/oocyte/hr in the absence of 5 mM cimetidine vs. 11.6 ± 0.933 fmol/oocyte/hr in the presence of 5 mM cimetidine, mean ± SE, $p < 0.01$) three days following injection (Figure 5.2a). (A 3-fold increase in the specific uptake (TEA-inhibitable) of ^{14}C-TEA (100 μM) over that in water-injected oocytes (3.83 ± 0.777 vs. 1.29 ± 0.163 pmol/oocyte/hr, mean ± S.D.) was observed indicating that TEA is also a substrate of the transporter.) ^{3}H-MPP^{+} uptake in the cRNA-injected oocytes increased 8-fold over that in the water-injected oocytes (53.0 ± 6.40 fmol/oocyte/hr, mean ± SE, $p <$ 0.01) and approximately 3-fold over that in oocytes injected with poly(A)$^{+}$ RNA (mRNA) from human liver (data not shown). The uptake of ^{3}H-MPP^{+} in the oocytes was significantly higher than water-injected oocytes on day one and further enhanced on days two and three following injection of the cRNA (Figure 5.2a). Subsequent uptake studies were carried out after at least two days incubation following cRNA injection as indicated in the figure legends.

The uptake of ^{3}H-MPP^{+} was dependent on the injected dose of cRNA. In oocytes injected with 5, 10, 25, 50, and 100 ng hOCT1 cRNA, the uptake of ^{3}H-MPP^{+} was 107 ± 10.4 , 183 ± 14.7, 376 ± 29.3, 429 ± 36.8, and 848 ± 108 fmol/oocyte/hr (means ± SE eight to nine oocytes), respectively. However, the relative enhancement in ^{3}H-MPP^{+} uptake varied depending on the batch of oocytes and the cRNA integrity. ^{3}H-MPP^{+} uptake was linear up to 120 min (data not shown); therefore, subsequent kinetic studies were carried out between 60 and 90 min.

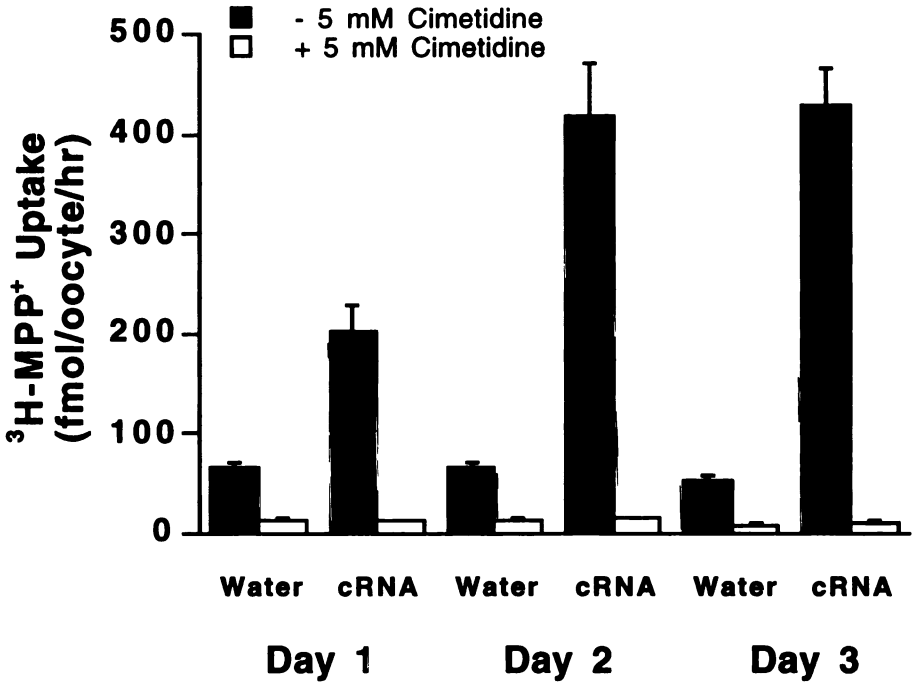

Figure 5.2a Functional expression of hOCT1 in *X. laevis* oocytes. ^{3}H-MPP$^+$ uptake in hOCT1 cRNA (25 ng)-injected oocytes with comparison to water (50 ng)-injected oocytes on days 1, 2 and 3 after injection. ^{3}H-MPP$^+$ (0.15 μM) uptake by oocytes was assayed for 90 min at 25 °C. Each column represents the mean ± SE (seven to nine oocytes) of one representative experiment. Closed bars represent uptake in the absence of 5 mM cimetidine and open bars represent uptake in the presence of 5 mM cimetidine.

The rate of MPP^+ uptake (at 90 min) was saturable (Figure 5.2b). The data were found to fit best to a model incorporating a saturable process plus a simple diffusion term. The V_{max} and K_m of MPP^+ transport were 3.69 ± 0.409 pmol/oocyte/hr and 14.6 ± 4.39 μM, respectively.

Small organic cations significantly reduced the uptake of ^3H-MPP^+ (Figure 5.3a and 5.3b, $p < 0.01$). The endogenous organic cation, guanidine (5 mM), is a weaker inhibitor ($p < 0.05$). Bulkier organic cations, including the bivalent organic cations, vecuronium and pancuronium, significantly inhibited ^3H-MPP^+ uptake (Figure 5.3b, $p < 0.01$). Further studies were performed to determine the IC_{50} values of decynium-22, vecuronium and TEA (Figure 5.3c). Decynium-22 (IC_{50} = 4.70 ± 1.28 μM) was the most potent inhibitor of ^3H-MPP^+ followed by vecuronium (IC_{50} = 127 ± 41.2 μM) and TEA (IC_{50} = 173 ± 8.76 μM). The bile acid, taurocholate (5 mM and 100 μM), and the nucleosides, thymidine and inosine, also significantly inhibited the uptake of ^3H-MPP^+ ($p < 0.01$, Table 5.2). In contrast, D-glucose (5 mM) and the classic organic anion, *p*-aminohippurate (PAH) (5 mM), showed no inhibition (Table 5.2).

The effect of pH and membrane potential on ^3H-MPP^+ uptake in oocytes injected with hOCT1 cRNA were studied. When the pH of the medium was varied from 6.4 to 7.4, there was a significant change in ^3H-MPP^+ uptake in cRNA-injected oocytes after subtraction of ^3H-MPP^+ uptake in water-injected oocytes (pH 6.4, 100 ± 28.0 fmol/oocyte/hr; pH 7.4, 145 ± 51.3 fmol/oocyte/hr; pH 8.4, 120 ± 9.85 fmol/oocyte/hr, means ± standard deviation). The effect of membrane potential on ^3H-MPP^+ uptake in cRNA-injected oocytes was determined. The membrane potential of oocytes in the Na^+ buffer was -32 ± 2 mV (mean ± SE, five oocytes), and the potential of oocytes was reduced to -13 ± 2 mV (mean ± SE, five oocytes) in the K^+ medium. ^3H-MPP^+ uptake in cRNA-injected oocytes was significantly lower in K^+ medium in comparison to that in Na^+ medium ($p < 0.01$, Figure 5.3d) suggesting that the transport of MPP^+ by hOCT1 is sensitive to membrane potential.

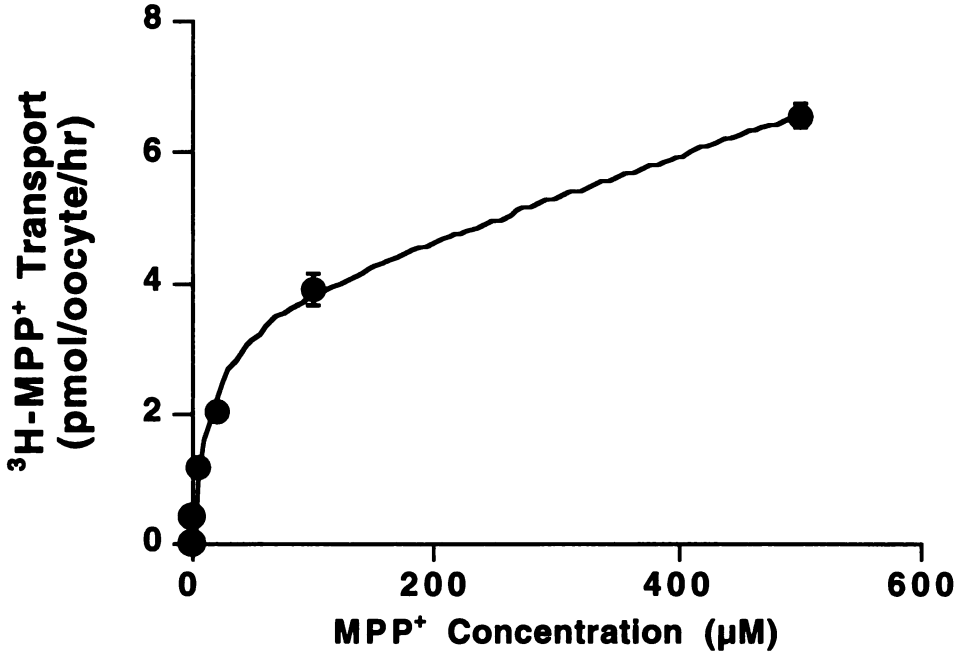

Figure 5.2b Kinetics of MPP^+ transport in hOCT1 cRNA (25 ng)-injected oocytes. Data were fitted to the Michaelis-Menten equation. (K_m=14.6 ± 4.39 μM, V_{max}=3.69 ± 0.409 pmol/oocyte/hr). Each point represents mean ± SE (seven to nine oocytes) from one representative experiment.

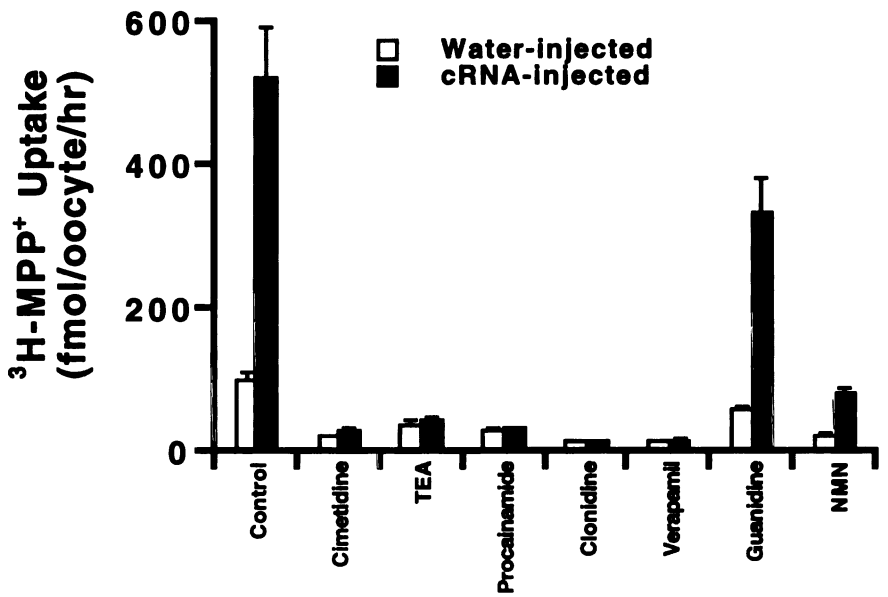

Figure 5.3a Specificity of hOCT1 expressed in *X. laevis* oocytes. Effect of various organic cations (5 mM) on ^{3}H-MPP$^+$ uptake in oocytes injected with hOCT1 cRNA (25 ng, closed bars) and water (open bars). Uptake was assayed for 90 min on day 2 following injection. Each column represents the mean ± SE (seven to nine oocytes) of one representative experiment. Controls represent uptake in oocytes in the absence of inhibitors.

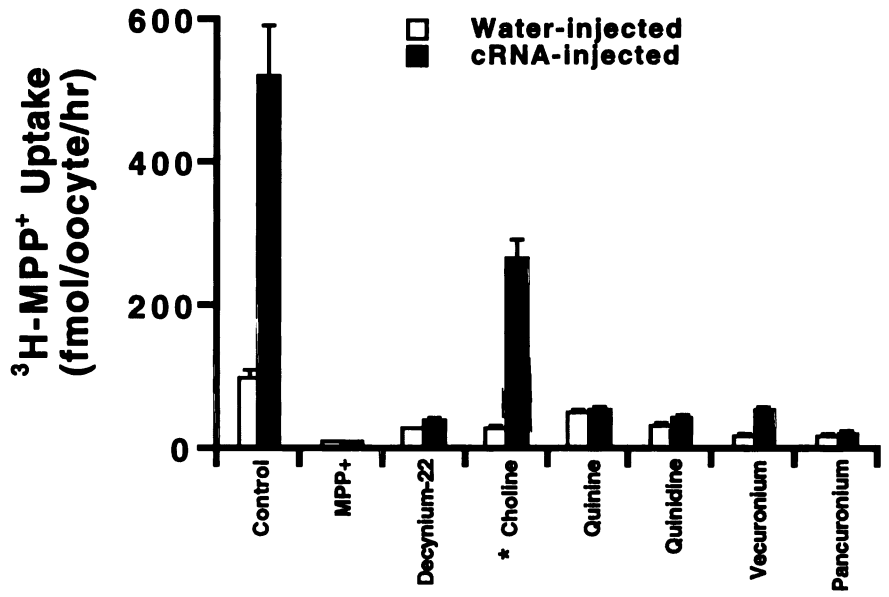

Figure 5.3b Specificity of hOCT1 expressed in *X. laevis* oocytes. Effect of various organic cations (1 mM) on ^{3}H-MPP$^+$ uptake in oocytes injected with hOCT1 cRNA (25 ng, closed bars) and water (50 ng, open bars). Uptake was assayed for 90 min on day 2 post-injection. *, control values for choline (1 mM) inhibition was 37.6 ± 2.65 fmol/oocyte/hr (water-injected) and 424 ± 46.8 fmol/oocyte/hr (hOCT1 cRNA-injected). Uptake was assayed for 60 min on day 4 post-injection. Each column represents the mean ± SE (seven to nine oocytes) of one representative experiment. Controls represent uptake in oocytes in the absence of inhibitors.

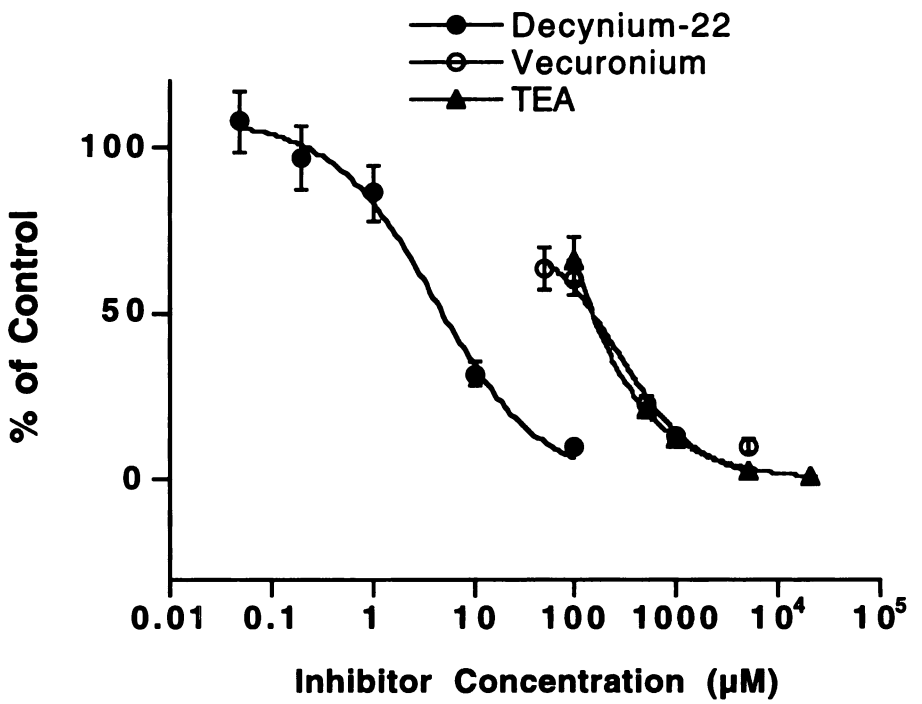

Figure 5.3c Study of the effects of the organic cations, decynium-22 (filled circles), vecuronium (open circles), and TEA (closed triangles) on ^{3}H-MPP^{+} uptake. ^{3}H-MPP^{+} uptake was assayed for 90 min on day 3 post-injection in oocytes injected with hOCT1 cRNA (25 ng) or water (50 ng). Percent of control was calculated after subtraction of MPP^{+} uptake in water-injected oocytes. The data were fit to a logistic equation. Each point represents mean ± SE (seven to nine oocytes) from one representative experiment.

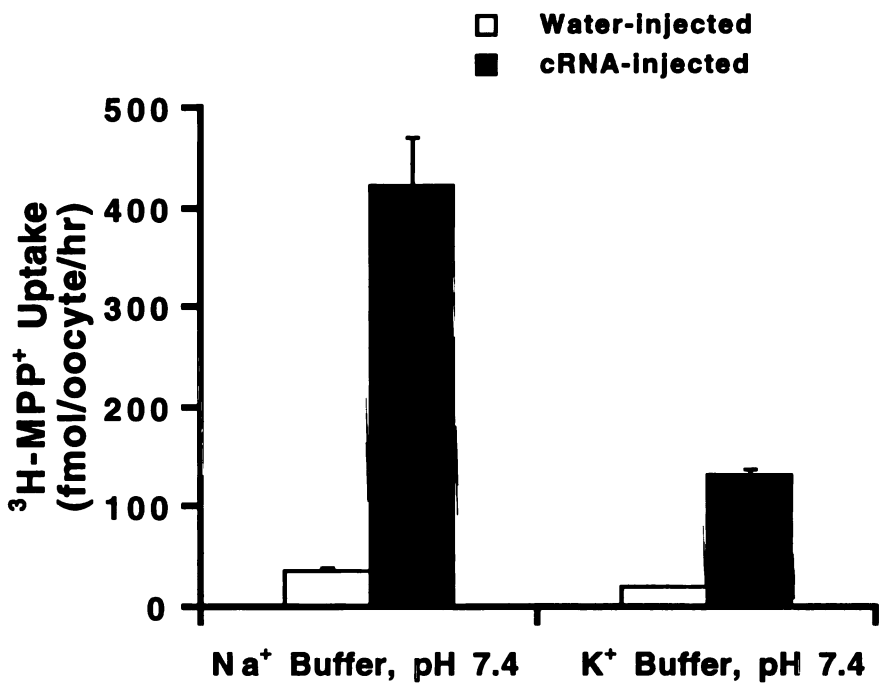

Figure 5.3d Effect of membrane potential on ^{3}H-MPP$^+$ uptake in oocytes injected with hOCT1 cRNA (25 ng, closed bars) and water (50 ng, open bars). Uptake was assayed for 60 min on day 4 after injection. Each point represents mean ± SE (seven to nine oocytes) from one representative experiment.

Table 5.2 Uptake of ^{3}H-MPP^{+} in the presence of non-classic organic cation transport inhibitors

	Uptake of ^{3}H-MPP^{+} in water-injected oocytes	Uptake of ^{3}H-MPP^{+} in cRNA-injected oocytes
	fmol/oocyte/hr	
Day 3, 90 min		
Control	102 ± 7.79	523 ± 68.4
Taurocholate (5 mM)	78.4 ± 5.44	184 ± 4.78
PAH (5 mM)	349 ± 98.9	738 ± 86.1
D-glucose (5 mM)	133 ± 14.6	679 ± 46.2
Thymidine (5 mM)	142 ± 15.9	292 ± 9.00
Day 4, 60 min		
Control	37.6 ± 2.65	424 ± 46.8
Thymidine (1 mM)	28.3 ± 5.41	299 ± 23.7
Inosine (1 mM)	25.9 ± 3.26	178 ± 20.9
Taurocholate (100 μM)	44.6 ± 2.68	284 ± 28.1
Vecuronium (100 μM)	25.0 ± 1.22	232 ± 17.6

The uptake of ^{3}H-MPP^{+} (0.15 μM) at 60 or 90 min in water- and hOCT1 cRNA- injected oocytes in the absence (control) and presence of various organic compounds was measured on day 3 or day 4 after injection as described in Materials and Methods. The data represent means ± SE from seven to nine oocytes. All uptake values in cRNA-injected oocytes are significantly lower than control ($p < 0.05$) except those for PAH and D-glucose. Controls represent uptakes in the oocytes in the absence of inhibitors.

5.3.4 In Vitro Translation of hOCT1 mRNA

The translation product, analyzed with the use of SDS-PAGE gel, resulted in a single band with an apparent molecular size of approximately 47 kDa (Figure 5.4). This apparent molecular mass is smaller than that predicted value based on the deduced sequence (approximately 61 kDa); however, anomalous migration (smaller than predicted sizes) for membrane proteins is not unusual.

5.3.5 Tissue Distribution and Expression of hOCT1 mRNA

The tissue distribution of hOCT1 mRNA transcripts was examined by Northern blot analysis (Figure 5.5). A strong 2.0-kb hybridizing signal (the approximate molecular size of the mRNA transcript of hOCT1) as well as a weaker band at 4.3-kb (data not shown) were detected only from liver mRNA . A weak 2.5-kb signal was detected in heart, skeletal muscle, kidney, and a very weak signal was detected in brain and placenta. No signal was detected in lung, pancreas or intestine (data not shown). These data suggest that hOCT1 mRNA transcript is expressed primarily in the human liver. (A full length cDNA of hOCT1 was detected following RT-PCR from human kidney and intestine mRNA suggesting that low copy numbers of the mRNA transcripts of hOCT1 may be present in these tissues.)

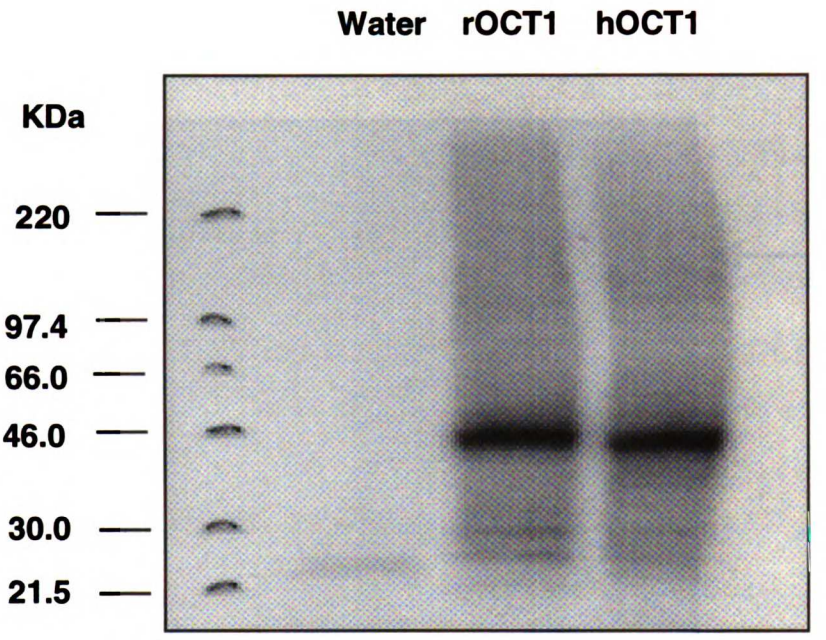

Figure 5.4 Autoradiograph of an SDS-polyacrylamide gel electrophoresis (gradient, 4-20%) showing *in vitro* translation products of rOCT1 and hOCT1 cDNA. TNT® coupled transcription/translation rabbit reticulocyte lysate system and ^{35}S-methionine were used to synthesize proteins from plasmid DNAs of rOCT1, hOCT1. Nuclease-free water was used instead of DNA as blank control. *kDa*, kilodaltons.

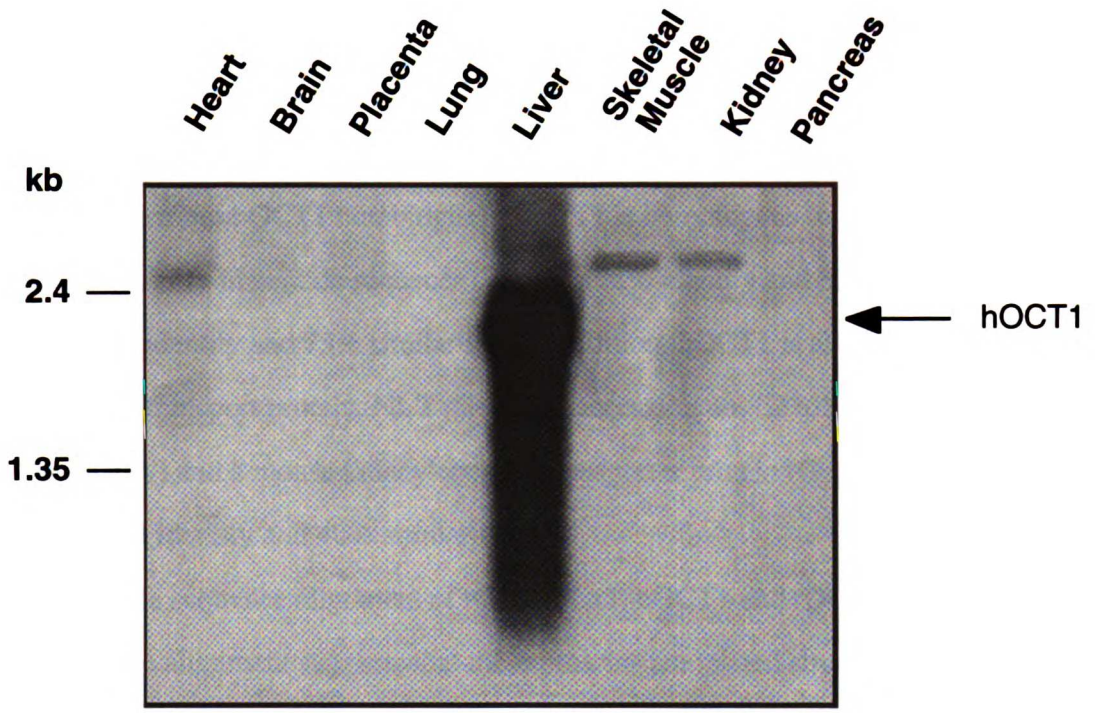

Figure 5.5 Northern blot analysis of hOCT1 mRNA in various human tissues. A commercially available hybridization-ready blot composed of poly(A)$^+$ mRNA from different human tissues (Multiple Tissue Northern Blot; Clontech) was hybridized with a full length antisense cRNA probe representing the entire coding region of hOCT1. Lanes represent mRNA samples (2 μg/lane) from heart, brain, placenta, lung, liver, skeletal muscle, kidney, and pancreas.

5.3.6 Homology of hOCT1 to Other Organic Cation Transporters

A computer-based homology search of GenBank, EMBL, and SwissProt 23 data bases indicated that the cloned hOCT1 cDNA has not been described previously. The hOCT1 cDNA clone shares the greatest homology with a group of organic cation transport proteins including rOCT1, rOCT2 from rat kidney, and the recently cloned murine Lx1 gene (putative mouse OCT1 homologue). hOCT1 is homologous to rOCT1 (78% identity and 82% similarity in peptide sequence), to Lx1 (78% identity and 82% similarity), and to rOCT2 (64% identity and 73% similarity). In addition, hOCT1 is also homologous to a rat liver-specific transport protein, NLT (Genbank accession no. L27651, 31% identity and 52% similarity) and a mouse kidney-specific transporter protein (Genbank accession no. U52842, 32% identity and 40% similarity).

Peptide sequence alignment of rOCT1, Lx1, hOCT1 and rOCT2 is shown in Figure 5.6. Sequence alignment suggests that these proteins are related structurally and functionally. Notably, each is predicted to have 12 transmembrane domains. In addition, rOCT1, rOCT2 and hOCT1 all transport TEA. However, the function of Lx1 has not been ascertained. Among the four proteins, rOCT1 and Lx1 are most homologous (95% identity). The alignment demonstrates that the sequence at the N-terminus and the first extracellular loop between transmembrane domains (TMDs) 1 and 2 are most conserved among the three species. Three putative N-glycosylation sites for rOCT1, Lx1, and hOCT1 are conserved in the extracellular loop between TMDs 1 and 2 whereas only two are conserved in rOCT2. The N-glycosylation site in rOCT1 and Lx1 in the loop between TMDs 9 and 10 is lacking in both hOCT1 and rOCT2. Only one potential protein kinase C phosphorylation site is conserved in all four proteins, at the amino acid residue 285 of hOCT1 between TMDs 6 and 7 whereas two potential protein kinase C sites at 291 and 327 of hOCT1 are conserved in rOCT1, Lx1 and hOCT1. Other protein kinase C phosphorylation sites on hOCT1 (i.e., at positions 340 and 534) do not align. In addition,

Figure 5.6 Alignment of amino acid sequence of rOCT1, Lx1, hOCT1, and rOCT2 using Pileup program. *Periods*, gaps introduced to generate this alignment; *bold*, putative N-glycosylation sites; *outlined letters*, potential protein kinase C phosphorylation sites. Amino acid motifs characteristics for a number of family I transmembrane transporters found within sequences are labeled with open rectangles.

several conserved regions for the members of the transport proteins of family I which include glucose transporters (Griffith *et al.*, 1992) were also observed. The first is a G-$(X)_3$- D-R/K-X-G-R-R/K (or D-R/K-X-G-R) (motif 1, Figure 5.6) which is conserved in the intracellular loop between TMDs 2 and 3, and TMDs 8 and 9. The second motif is EXXXXXXR (motif 2, Figure 5.6) which is conserved between TMDs 4 and 5, and between TMDs 10 and 11. The third set of conserved motifs includes the sequences of P-E-S-P-R-X-L and P-E-T-K (motif 3, Figure 5.6) located after the predicted TMDs 6 and 12, respectively. These data indicate that hOCT1 along with rOCT1, Lx1 and rOCT2 belong to the transporter family I.

5.4 Discussion

Studies in which a variety of tissue preparations are used, including isolated hepatocytes, perfused liver, and isolated plasma membrane vesicles, as well as functional studies of the recently cloned polyspecific organic cation transporter (rOCT1) have greatly advanced our understanding of the mechanisms of organic cation transport in the rat liver (Busch *et al.*, 1996a and 1996b; Groothuis and Meijer, 1996; Grundemann *et al.*, 1994; Martel *et al.*, 1996; McKinney and Hosford, 1992; Meijer *et al.*, 1990; Moseley *et al.*, 1992; Nagel *et al.*, 1997; Oude Elferink *et al.*, 1995; Steen *et al.*, 1992). In contrast, there have been few studies examining the mechanisms of organic cation transport in the human liver (Sandker *et al.*, 1994; Steen and Meijer, 1991) and no study elucidating the molecular structure or function of polyspecific organic cation transporters in human liver or other human tissue. Limited data suggest that there are large differences in the rate of uptake of organic cations in human and in rat hepatocytes (Sandker *et al.*, 1994).

In this study, we used information from the published sequences of recently cloned polyspecific organic cation transporters from rat to clone a human liver polyspecific organic

cation transporter (hOCT1). hOCT1 is 78% identical and 82% similar to both rOCT1 and Lx1 (Figures 5.1 and 5.5). We observed that the small organic cation, MPP^+, was a permeant of hOCT1 (Figure 5.2). The uptake of MPP^+ was inhibited by small organic cations (Figure 5.3a & b) as well as by bulky organic cations, pancuronium and vecuronium. These data are consistent with functional studies of rOCT1 (Busch *et al.*, 1996b; Martel *et al.*, 1996; Nagel *et al.*, 1997) and with the characteristics of the type I transporter in the rat hepatocyte which accepts small monovalent organic cations, but can be inhibited by larger type II molecules (Oude Elferink *et al.*, 1995). These characteristics are also consistent with the multi-specific non-charge-selective transporter which accepts both large and small organic cations as well as other compounds (Steen *et al.*, 1992). Similar to the type I carrier and to rOCT1, hOCT1 appears to be sensitive to membrane potential (Figure 5.3d).

In contrast to previous studies documenting no effect of the organic anion, taurocholate, on the transport of organic cations by the type I carrier in rat liver (Vonk *et al.*, 1978a and 1978b), taurocholate (100 μM and 5 mM) significantly inhibited the uptake of MPP^+ in oocytes expressing hOCT1 (Table 5.2). These data suggest that hOCT1 is not charge selective with respect to bulky organic compounds and are consistent with the characteristics of the multispecific non-charge-selective transporter (Steen *et al.*, 1992). It is possible that the interaction of taurocholate with hOCT1 represents a species difference in the selectivity of the two transporters. However, because no data are available, it is unclear if taurocholate also interacts with rOCT1.

To determine whether there are interspecies differences in the kinetics of interaction of organic cations with the human (hOCT1) and rat (rOCT1) transporters, we determined the K_m value (or K_i, assuming a competitive inhibition model) of several organic cations. The K_m value (14.6 μM) of the small organic cation, MPP^+, for hOCT1 is similar to that reported previously for rOCT1 (13 μM) (Grundemann *et al.*, 1994). In contrast, the K_i value of TEA (163 μM) in inhibiting MPP^+ uptake in oocytes expressing hOCT1 is

somewhat higher than the reported K_m value of TEA (95 μM) uptake in oocytes expressing rOCT1. Notably, the K_i value (4.4 μM) of the large organic cation, decynium-22, in oocytes expressing hOCT1 is considerably higher than that observed previously (0.36 μM) for rOCT1 (Grundemann *et al.*, 1994). These data indicate that there are important interspecies differences in the affinity of organic cations for hepatic organic cation transporters. A detailed characterization of the structure activity relationships of each of the transporters (i.e., hOCT1 and rOCT1) is important to understand the interspecies differences in the uptake of organic cations in the human and rat liver.

Previous data suggest that the organic cation, vecuronium, is transported at a considerably slower rate in human hepatocytes in comparison to rat hepatocytes (Sandker *et al.*, 1994). Notably, the functional rate of uptake of vecuronium in cultured human hepatocytes is one-10th that in rat hepatocytes suggesting that the relevant transporter or transporters in the human hepatocyte have a lower activity than that in the rat. The data suggest that the functional activity of organic cation transporter or transporters in the human liver involved in the transport of vecuronium may be lower than that in the rat liver.

A lower functional activity may be a result of a higher K_m or a lower V_{max} value. The K_i value of vecuronium obtained in this study (120 μM) is ~10-fold the K_m value of vecuronium in the intact rat hepatocyte (Mol *et al.*, 1988) and 3-fold the IC_{50} of vecuronium in interacting with the rat type I organic cation transporter (Steen *et al.*, 1992). Thus, the lower affinity of vecuronium for hOCT1 may explain, in part, its lower rate of transport in the human hepatocyte. However, a compound may inhibit transport without being translocated and further studies are needed to determine whether vecuronium is an actual permeant of hOCT1.

In this study the V_{max} value of MPP^+ transport in oocytes injected with the cRNA of hOCT1 (25 ng) was 3.7 pmol/oocyte/hr (Figure 5.2b) whereas in a previous study of oocytes injected with the cRNA of rOCT1 (8 ng) (Grundemann *et al.*, 1994), the V_{max} value was 97 pmol/oocyte/hr. In addition, the uptake of TEA (100 μM) was markedly

lower in oocytes expressing hOCT1 in comparison to oocytes expressing rOCT1 (< 3-fold enhanced for hOCT1 in comparison to ~100-fold enhanced for rOCT1) (Grundemann *et al.*, 1994). (Because of the low uptake values of TEA, we were unable to obtain a value for V_{max}). Collectively, the results suggest that the V_{max} values of small organic cations are substantially lower in oocytes expressing hOCT1 than in oocytes expressing rOCT1. These data are consistent with previous studies suggesting that transporters in human hepatocytes have a much lower functional activity compared with those in rat hepatocytes (Sandker *et al.*, 1994). However, V_{max} values may differ between laboratories because of differences in experimental conditions and batches of oocytes. The availability of the cloned transporters (hOCT1 and rOCT1) will allow the development of antibodies to investigate, in detail, the mechanisms (e.g., differences in turnover rate or differences in the number of functional transporters) responsible for the observed interspecies differences in the activity of the transporters.

Organic cations are taken up by epithelial cells of the liver, kidney and intestine (Gramatte *et al.*, 1996; Ott *et al.*, 1991; Pritchard and Miller, 1993; Turnheim and Lauterbach, 1977a and 1977b; Wright and Wunz, 1987) . In agreement with its functional role in the various epithelia, the mRNA transcripts of rOCT1 and its mouse homologue, Lx1, were found in the kidney, liver, intestine, and colon (Grundemann *et al.*, 1994; Schweifer and Barlow, 1996). In striking contrast, the mRNA transcript of hOCT1 is predominant in human liver (Figure 5.5), with minor bands detected at 2.5 kb (a putative hOCT1 homologue) in heart, kidney and skeletal muscle. It will be important to determine the transcription (or other) factors that are involved in the tissue specific distribution of hOCT1 compared with the rat and mouse homologous proteins. In addition, these data have important implications for the understanding of the differences in the mechanisms of organic cation transport in the various epithelia. For example, it is well-known that the characteristics of organic cation transport differ between liver and kidney (Pritchard and Miller, 1993); in fact, it has been found that certain organic cations are eliminated

exclusively in the liver and not the kidney and vice versa. Because hOCT1 is liver-specific, our data strongly suggest that other transporters are responsible for the secretion of organic cations in nonhepatic epithelia. Alternatively, hOCT1 is expressed in a confined region of the kidney. With the availability of the cloned transporters, we can begin to understand the organ specific elimination of drugs.

In conclusion, we cloned hOCT1, a polyspecific organic cation transporter from human liver. This transporter represents the first polyspecific organic cation transporter cloned from human tissue. The transporter is similar in sequence to rOCT1, but notable differences in the kinetics of interaction of some organic cations were observed. Moreover, in contrast to rOCT1 and Lx1, Northern blot analysis suggests that the mRNA transcript of hOCT1 is preferentially expressed in human liver. The cloning of hOCT1 provides the opportunity to define the pharmacological profiles of this gene product, and to determine its functional role in the disposition of many clinically used drugs and other xenobiotics.

CHAPTER 6

FUNCTIONAL CHARACTERIZATION OF AN ORGANIC CATION TRANSPORTER (hOCT1) IN A TRANSIENTLY TRANSFECTED HUMAN CELL LINE (HeLa) [1]

6.1 Introduction

Organic cations are positively-charged amines under physiological pH. Drugs from a wide array of clinical classes including H_2-receptor antagonist (e.g., cimetidine), antiarrhythmics (e.g., procainamide), skeletal muscle relaxants (e.g., vecuronium) and beta-adrenoceptor blocking agents (e.g., acebutolol) as well as endogenous bioactive amines such as dopamine, N^1-methylnicotinamide (NMN), and choline are organic cations. These polar molecules are transported across epithelia by carrier-mediated processes. Based upon previous studies in isolated plasma membrane vesicles and intact tissue preparations, a three-step model for the secretory flux of organic cations across various epithelia has been proposed: an electrogenic, facilitated diffusion step at the basolateral membrane, intracellular sequestration, and a proton or an organic cation exchange mechanism at the apical side (Pritchard and Miller, 1993; Zhang *et al.*, 1998a; Chapter 1).

The first organic cation transporter, rOCT1, was cloned in 1994 from rat kidney (Grundemann *et al.*, 1994). Since then several organic cation transporters have been cloned from various species and tissues (Gorboulev *et al.*, 1997; Grundemann *et al.*, 1997; Tamai *et al.*, 1997, Okuda *et al.*, 1996; Terashita *et al.*, 1998; Zhang *et al.*, 1997a and

[1] This work is currently in press in *The Journal of Pharmacology and Experimental Therapeutics*. Permission from the publisher is included in "Acknowledgments".

1997b; Chapters 4 and 5). Recently, using homology cloning methods, we and others cloned a human organic cation transporter, hOCT1, from liver (Gorboulev *et al.*, 1997; Zhang *et al.*, 1997b; Chapter 5). Initial functional expression studies, carried out in *Xenopus laevis* oocytes (Zhang *et al.*, 1997b; Chapter 5) demonstrated that hOCT1, similar to rOCT1, is polyspecific with respect to substrate selectivity. Namely, the prototype organic cations, TEA and MPP^+, are its permeants (substrates). In addition, both small and bulkier organic cations as well as other compounds such as nucleosides and bile acids inhibit the transport of MPP^+ mediated by hOCT1 (Zhang *et al.*, 1997b; Chapter 5). Northern blot analysis indicates that the mRNA transcripts of hOCT1 are expressed primarily in the liver, however, RT-PCR analysis demonstrates that hOCT1 mRNA transcripts are also expressed in lower abundance in the human kidney and intestine as well as in other tissues (Gorboulev *et al.*, 1997; Zhang *et al.*, 1997b; Chapter 5).

Xenopus laevis oocytes have been used extensively in elucidating the functional characteristics of transport proteins (Giacomini *et al.*, 1994; Gorboulev *et al.*, 1997; Grundemann *et al.*, 1994; Murer and Biber, 1997; Okuda *et al.*, 1996; Sigel, 1990; Terashita *et al.*, 1998; Zhang *et al.*, 1997a and 1997b; Chapters 3, 4 and 5). Although the oocyte expression system has important advantages for studying transporters, the expression system also has major disadvantages which limit its use particularly for routine studies of drug transport and in high throughput screening of drugs. Notably, oocytes are subject to seasonal variability in their viability as well as in their protein translation function. mRNA, which is very unstable, needs to be transcribed *in vitro* before being injected into oocytes. Moreover, injecting mRNA into oocytes requires tedious micro-injection techniques and specialized equipment. In contrast, mammalian expression systems do not require the *in vitro* handling of mRNA and are more readily adapted to routine use in drug screening processes. Recently, mammalian expression systems have been developed and used in expressing a number of transport proteins (Boyer *et al.*, 1994; Cardarelli *et al.*, 1995; Clark and Amara, 1994; Martel *et al.*, 1996a; Risso *et al.*, 1996;

Schaner *et al.*, 1997; Varoqui *et al.*, 1996). For organic cation transporters, the human embryonic kidney (HEK) 293 cell line has been used to study the function of rOCT1 (Martel *et al.*, 1996a), OCT2p, a second member of the OCT family cloned from $LLCPK_1$ cells (Grundemann *et al.*, 1997) and OCTN1, another new member of the OCT family cloned from human fetal liver cDNA library (Tamai *et al.*, 1997).

The goal of the present study was to develop a mammalian cell expression system for hOCT1 and to elucidate the functional characteristics of the transporter in this cell line. Specifically, we determined the potency of various organic cations and other compounds in interacting with hOCT1. In addition, we examined the stereoselectivity of hOCT1 using the enantiomers of disopyramide and the diastereomers, quinine and quinidine. Finally, we determined whether the transporter can operate bidirectionally as an organic cation/organic cation exchanger. Our data represent the first demonstration of functional expression of a human organic cation transporter in a mammalian cell line (HeLa). A comparison of the data obtained in this study with data in the literature suggests that there are notable differences in the intrinsic function of hOCT1 and its rat homologue, rOCT1. Furthermore there are differences in the transport function of hOCT1 and a second human organic cation transporter, hOCT2 (Gorboulev *et al.*, 1997). Transiently transfected HeLa cells represent a useful tool for the elucidation of the molecular mechanisms involved in the function of hOCT1.

6.2 Materials and Methods

6.2.1 Construction and Isolation of Plasmid DNA for Transfection

hOCT1 cDNA was obtained by RT-PCR as previously described (Zhang *et al.*, 1997b; Chapter 5). After gel purification, the PCR products were ligated to the mammalian expression vector pTargeT (Promega, Madison, WI) using T4 DNA ligase followed by

transformation into DH5α competent cells (Gibco BRL, Gaithersburg, MD). The construct with the cDNA under the CMV promoter (sense orientation), pTargeT-hOCT1, was identified by restriction enzyme analysis and the sequence was confirmed by DNA sequencing (Biomolecular Resource Center, UCSF, CA). Empty vector of pTargeT was constructed by cutting the hOCT1 insert out of pTargeT-hOCT1 with *Eco*R I followed by gel purification and ligation. The construct of empty vector was confirmed by restriction enzyme analysis.

DNA for transfection was isolated with the QIAGEN Endo-free DNA isolation kit (QIAGEN Inc., Santa Clarita, CA). Several different DNA preparations were carried out for the study. DNA concentration ranged from 1.7 to 4.0 μg/μl as determined by UV spectroscopy. The DNA was stored in endotoxin-free TE buffer (QIAGEN) at -20°C until use.

6.2.2 HeLa Cell Culture and Transfection

HeLa cells were obtained from the UCSF Cell Culture Facility. Original stocks were from American Type Culture Collection (ATCC, Rockville, MD). Passages from 3 to 18 were used in the studies. The cells were grown at 37°C in a 5% CO_2/95% air humidified atmosphere. The medium was Eagle's minimum essential medium with Earle's balanced salt supplemented with 2 mM glutamine, 100 IU/ml penicillin, 100 μg/ml streptomycin, 0.25 μg/ml fungizone , and 10% (vol/vol) fetal bovine serum. The cells were maintained in Nunc cell culture flasks (Nalge Nunc International, Naperville, IL). The cells were seeded at a density of 1.8 X 10^5 cells/well in 12-well tissue culture plates (Corning Costar Corp, Cambridge, MA) 24 hours prior to transfection. The cells were transfected with a cationic liposome technique using LIPOFECTAMINE (2 mg/ml, Gibco, BRL) following a modified protocol from Gibco, BRL. For each well, 100 μl Opti-MEM media (Gibco, BRL) was incubated with 2 μg DNA and another 100 μl Opti-MEM media with the lipid (4-8 μl, and 7 μl for most of the experiments). The two solution were then

mixed together and incubated for 30 minutes at room temperature. After incubation, 800 µl Opti-MEM media was added to the previous mixture. The final mixture (1 ml) was applied to each well after rinsing the cells with the Opti-MEM media once. The cells were exposed to the lipid-DNA complex for 18 hours prior to replacing the transfection media by the fresh standard culture media.

6.2.3 Uptake Measurements

The uptake studies were carried out between 24-72 hours post transfection. Cells were incubated and washed with phosphate buffered saline (PBS) once before the uptake studies. Subsequently, the cells were incubated at room temperature or 4°C (for temperature-dependence study) with 5 µM ^{14}C-TEA (55 mCi/mmol, American Radiolabeled Chemicals, St. Louis, MO) in 0.5 ml of PBS. For Michaelis-Menten studies, various amounts of unlabeled TEA were also included in the reaction mixture. For inhibition and IC_{50} studies, various amounts of the tested compounds were included in the reaction mixture. Incubation was stopped by rinsing the cells once with 2 ml of ice-cold PBS and twice with 1 ml of ice-cold PBS buffer. After solubilizing the cells with 1 ml of 0.5% Triton-X 100, 0.5 ml of sample was assayed using liquid scintillation counting (Beckman, Palo Alto, CA).

In *trans*-stimulation studies, each well of cells was preincubated with either 0.5 ml PBS (control) or 0.5 ml PBS plus the indicated concentration of unlabeled compounds at 37°C for one hour. Cells were then rinsed with 1 ml of ice-cold PBS twice before the uptake studies.

6.2.4 Protein Assay

For each plate used in the uptake study, 2 wells were saved for protein analysis. Cells were washed with PBS buffer and then solubilized with 0.5 ml of 1N NaOH. After 2 hours, the solution was neutralized with 0.5 ml of 1N HCl. 100 µl of solubilized cells

were used for the protein assay using the Bio-Rad reagent (Bio-Rad, Hercules, CA). Absorbance was read at 595 nm and the amount of protein was calculated from the standard curve generated by using the known amounts of bovine serum albumin as standard.

6.2.5 Data Analysis

Uptake values are presented as mean ± standard deviation (SD) or mean ± standard error (SE) as indicated in "Figure Legends". In each experiment, a minimum of two wells was used to generate each data point and each experiment was repeated at least once. For Michaelis-Menten studies, data were fit to the equation $V=V_{max}[S]/(K_m+[S])+K_{ns}[S]$ by non-linear regression using Kaleidagraph™ Version 3.0 (Abelbeck Software). V is the transport rate, [S] is the substrate concentration, and K_{ns} is rate constant of non-specific uptake. K_{ns} was calculated from the rate constant of uptake in cells transfected with empty vector. The IC_{50} was estimated by a sigmoidal inhibition model and was fit to the equation $V=V_0/(1+(I/IC_{50})^n)$ by nonlinear regression. V is the uptake of TEA in the presence of the inhibitor, V_0 is the uptake of TEA in the absence of inhibitor, I is the inhibitor concentration and n is the slope constant. Data from nonlinear regression are presented as mean ± SD. For each compound, the K_i was calculated from the corresponding IC_{50} assuming a competitive inhibition; however, since the ratio of ^{14}C-TEA (5 μM) concentration used in the inhibition studies to the K_m of TEA (230 μM) was less than 5%, K_i is virtually identical to IC_{50} regardless of the inhibition model (e.g., competitive *versus* non-competitive) (Cheng and Prusoff, 1973). Statistical analysis was carried out by comparing the treated to the controls from the same experiments using an unpaired Student's *t*-test (Primer of Biostatistics software, Version 3, written by Stanton A. Glantz, McGraw-Hill Companies, 1991), and a value of $p < 0.05$ was considered significant.

6.2.6 Materials

All the media and buffers used to maintain the cells were obtained from the UCSF Cell Culture Facility unless otherwise indicated. All chemicals were obtained from Sigma (St. Louis, MO) and Fisher (Pittsburgh, PA) or as indicated. R-(-)-disopyramide and S-(+)-disopyramide were resolved as previously described to greater than 98% purity (Valdivieso *et al.*, 1988). ^{14}C-TEA (55 mCi/mmol) was purchased from American Radiolabeled Chemicals (St. Louis, MO). ^{3}H-MPP^{+} (79.9 Ci/mmol) was purchased from DuPont NEN Research Products (Boston, MA) and ^{3}H-cimetidine (23.0 Ci/mmol) was purchased from Amersham (Arlington Heights, IL).

6.3 Results

6.3.1 Initial Characterization of hOCT1 Expression in Transiently-Transfected HeLa Cells

The lipid to DNA ratio has been shown previously to be important in the transient expression of the DNA products in transfected cells (Hawley-Nelson *et al.*, 1993). Initial titration studies with 1 to 3 μg lipid per μg DNA resulted in no significant ^{14}C-TEA uptake in the cells transfected with pTargeT-hOCT1 versus untransfected cells (data not shown). Significant uptake was observed in the transfected cells when the lipid to DNA ratio ranged between 4:1 and 8:1 (the highest lipid to DNA ratio tested). A lipid to DNA ratio of 7:1, 6.5:1 or 6:1 which resulted in the highest activity was used in subsequent studies. Because the ^{14}C-TEA uptake in mock-transfected cells (cells transfected with the empty vector) was not significantly different from that in the untransfected cells, in some experiments, untransfected cells were used as controls (see figure legends).

^{14}C-TEA influx into HeLa cells transfected with hOCT1 plasmid DNA increased with time and reached an apparent plateau (at 90 min) that was approximately 5-fold that in

HeLa cells transfected with empty vector. At 1, 5, 10, 30, 60 and 90 min, the respective uptake values in the hOCT1 plasmid DNA transfected cells were 8.45 ± 1.04, 20.9 ± 5.8, 24.2 ± 6.3, 56.3 ± 4.4, 77.6 ± 20.4, and 93.3 ± 30.3 pmol/mg protein. Uptake in the empty vector transfected cells also increased with time (data not shown). A plot of uptake versus time was linear to 30 minutes with a positive intercept (which was apparent even in plots over the first 5 min). Therefore, further studies were carried out between 25 and 30 min.

The transient expression of hOCT1-mediated ^{14}C-TEA uptake in the HeLa cells was determined at various hours post-transfection (24-72 hr). At 24 hours, ^{14}C-TEA uptake was significantly greater (around 3-fold) in the pTargeT-hOCT1-transfected cells than that in the cells transfected with the empty vector. At 41 hours post-transfection, ^{14}C-TEA uptake was approximately 5-fold enhanced over that in empty vector-transfected cells (Figure 6.1). At 65 hours post-transfection, ^{14}C-TEA uptake in the pTargeT-hOCT1-transfected cells declined to 2-fold over that in the mock-transfected cells (Figure 6.1). For further studies, uptake was measured between 24 and 48 hours after transfection.

To determine whether ^{14}C-TEA uptake in pTargeT-hOCT1 transfected HeLa cells is temperature dependent, an important characteristic of carrier-mediated processes, ^{14}C-TEA uptake at various time-points was measured at 22°C and 4°C in HeLa cells transfected with pTargeT-hOCT1 and empty vector. Figure 6.2 showed that ^{14}C-TEA uptake in pTargeT-hOCT1 transfected cells was significantly higher at 22°C than at 4°C.

6.3.2 Permeant Studies

The rate of ^{14}C-TEA uptake in the pTargeT-hOCT1-transfected cells was saturable whereas the uptake rate in the empty vector-transfected cells was linear over the same concentration range (Figure 6.3). The V_{max} and K_m of TEA transport were 2.89 ± 0.45 nmol/mg protein/30 min and 229 ± 78 μM, respectively and the K_{ns}, the rate constant for

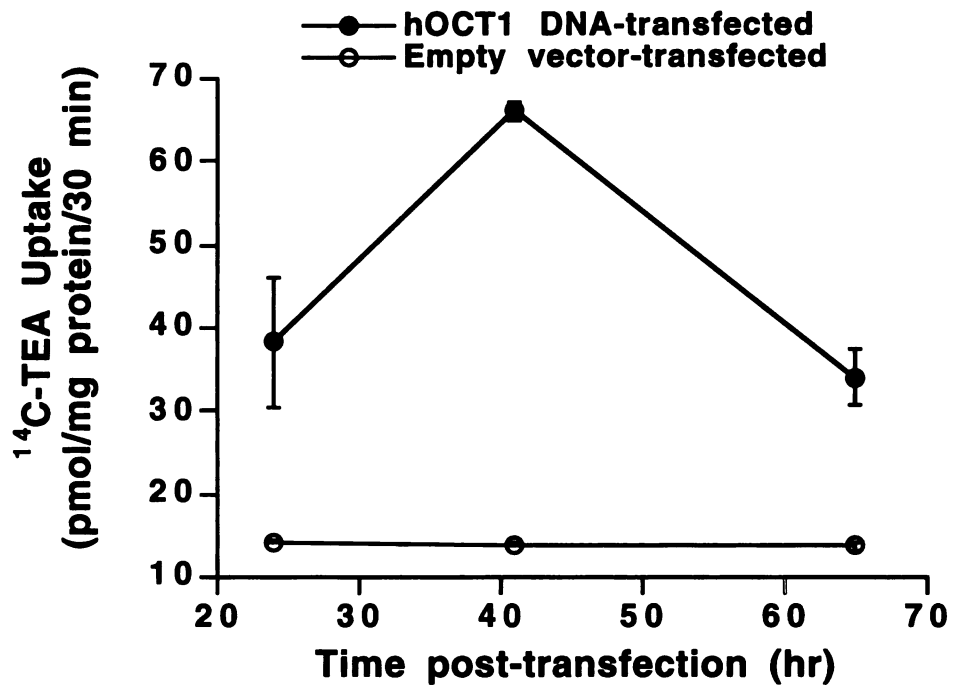

Figure 6.1 Transient expression of transfected hOCT1 plasmid DNA in HeLa cells over time. Following transfection of pTargeT-hOCT1 (closed circles) and empty vector (open circles) in HeLa cells, the 30 min uptake of ^{14}C-TEA was measured at 24, 41, and 65 hours post-transfection. Data represent mean ± SD of duplicate determinations from one representative experiment.

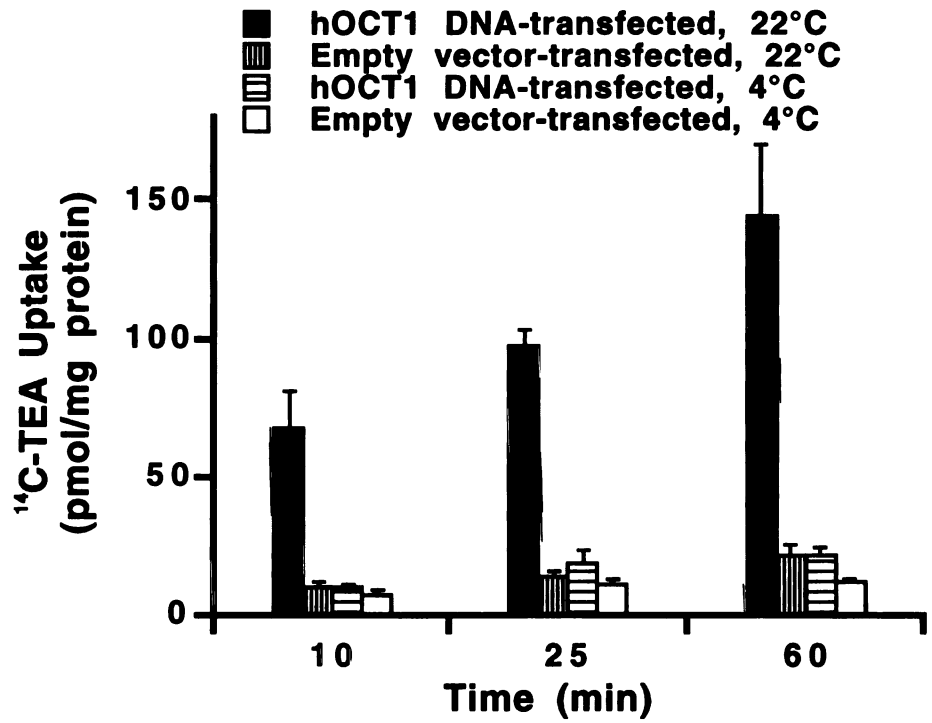

Figure 6.2 Temperature dependence of ^{14}C-TEA transport in pTargeT-hOCT1 (dark solid bars and horizontal hatched bars) and empty vector (vertical hatched bars and open bars)-transfected HeLa cells. Uptake of ^{14}C-TEA (5 μM) was measured at various time-points at 22°C (dark bars and vertical hatched bars) and 4°C (horizontal bars and open bars) 42 hours post-transfection. Data represent mean ± SD of duplicate determinations from one representative experiment.

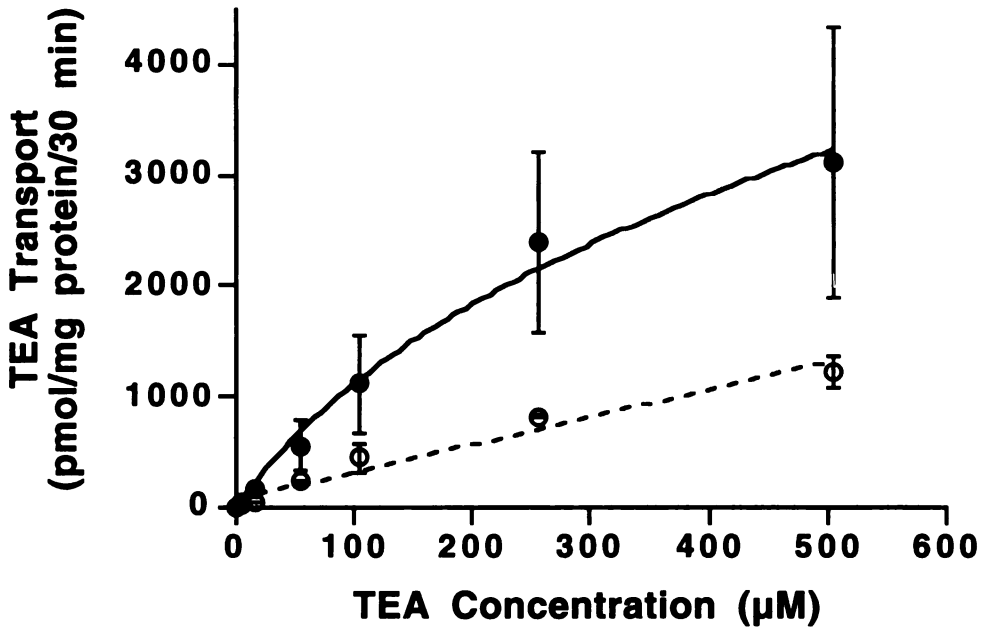

Figure 6.3 Concentration dependence of ^{14}C-TEA transport in pTargeT-hOCT1 (closed circles) and empty vector (open circles)-transfected HeLa cells. ^{14}C-TEA transport (at 30 min) was measured over increasing concentrations of TEA. The solid and dotted lines represent the estimated overall and nonsaturable transport, respectively. Data represent mean ± SD of duplicate determinations from one representative experiment.

the linear process, determined from TEA uptake in the empty vector-transfected cells, was 2.46 pmol/mg protein/30 min/μM.

^{3}H-MPP$^+$ (35 nM labeled and 1 μM unlabeled) uptake in the hOCT1-transfected cells was high but not significantly different from that in the mock-transfected cells (34.0 ± 1.5 vs. 26.2 ± 2.2 pmol/mg protein at 5 min and 50.3 ± 4.0 vs. 44.0 ± 3.5 pmol/mg protein at 30 min). In comparison to the endogenous uptake of TEA, there was a high endogenous uptake of MPP$^+$ in HeLa cells (42.6 pmol/mg protein/μM for MPP$^+$ uptake versus 2.12 pmol/mg protein/μM for TEA uptake at 30 min). This high endogenous uptake may have obscured detection of the expressed transporter when MPP$^+$ was used as the radiolabeled ligand.

Cimetidine, an H_2-receptor antagonist, has been used as a model compound for organic cation transport in some studies. During a 60-min period, ^{3}H-cimetidine (24 nM labeled plus 5 μM unlabeled) uptake in HeLa cells expressing hOCT1 was only slightly enhanced over that in the mock-transfected cells suggesting that under the experimental conditions, cimetidine is not translocated appreciably by hOCT1 (Figure 6.4). The endogenous uptake of cimetidine was moderate (6.84 versus 2.12 pmol/mg protein/μM for cimetidine versus TEA uptake at 30 min).

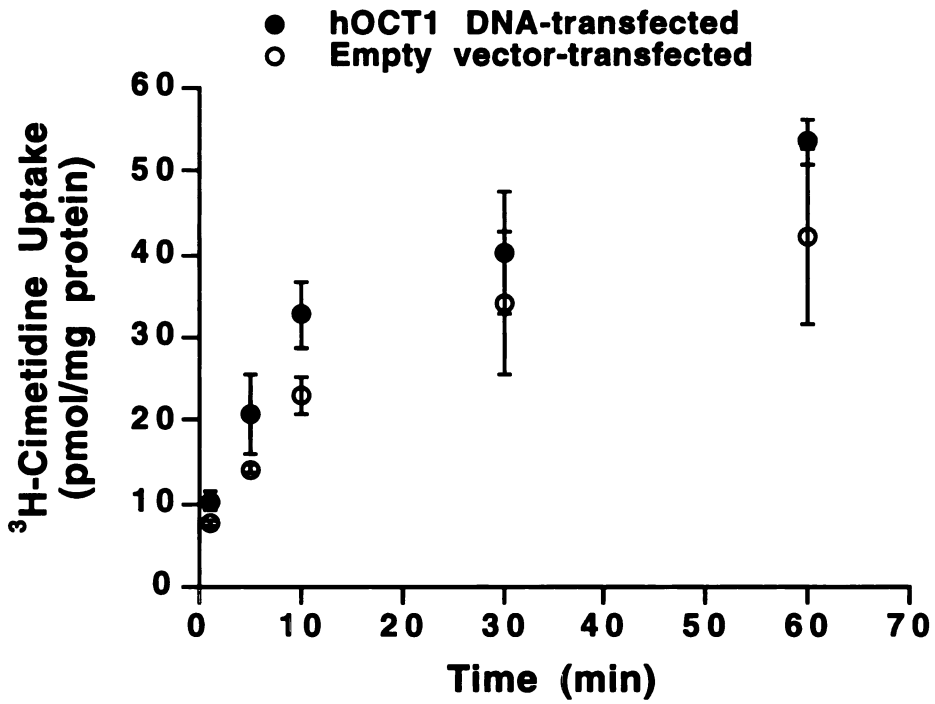

Figure 6.4 Time course of ^{3}H-cimetidine (5 μM) uptake in the pTargeT-hOCT1-transfected (closed circles) and empty vector-transfected (open circles) HeLa cells. Data represent mean ± SD of duplicate determinations from one representative experiment.

6.3.3 Inhibition Studies

To further characterize the function of hOCT1, we studied ^{14}C-TEA uptake in the presence of various compounds at concentrations of 0.1 mM, 0.5 mM or 5 mM (Figure 6.5 a-d). At 0.1 mM, the organic cations, amantadine, clonidine, verapamil, quinine, quinidine, S-(+)-disopyramide and R-(-)-disopyramide significantly inhibited ^{14}C-TEA uptake (Figure 6.5a, $p < 0.05$). In contrast, paraquat, dopamine and its precursors (L-dopa and D-dopa) (not shown) did not significantly affect the uptake of ^{14}C-TEA. At 0.5 mM, cimetidine, choline, NMN, amantadine, dopamine, acebutolol, (+)-nicotine, (-)-nicotine, and midazolam significantly inhibited ^{14}C-TEA uptake (Figure 6.5b & c, $p < 0.05$), whereas spermidine (polyamine), creatinine (zwitterion), and the organic anion, *p*-aminohippuric acid (PAH) did not produce any inhibition (Figure 6.5c). At high concentrations (5 mM), paraquat, spermidine, L-dopa, D-dopa and PAH (data not shown) did not produce significant inhibition whereas creatinine did (Figure 6.5d, $p < 0.05$). These data indicate that hOCT1 is broadly-selective for organic cations and some other compounds, but not the organic anion, PAH nor the multivalent cations, paraquat and spermidine.

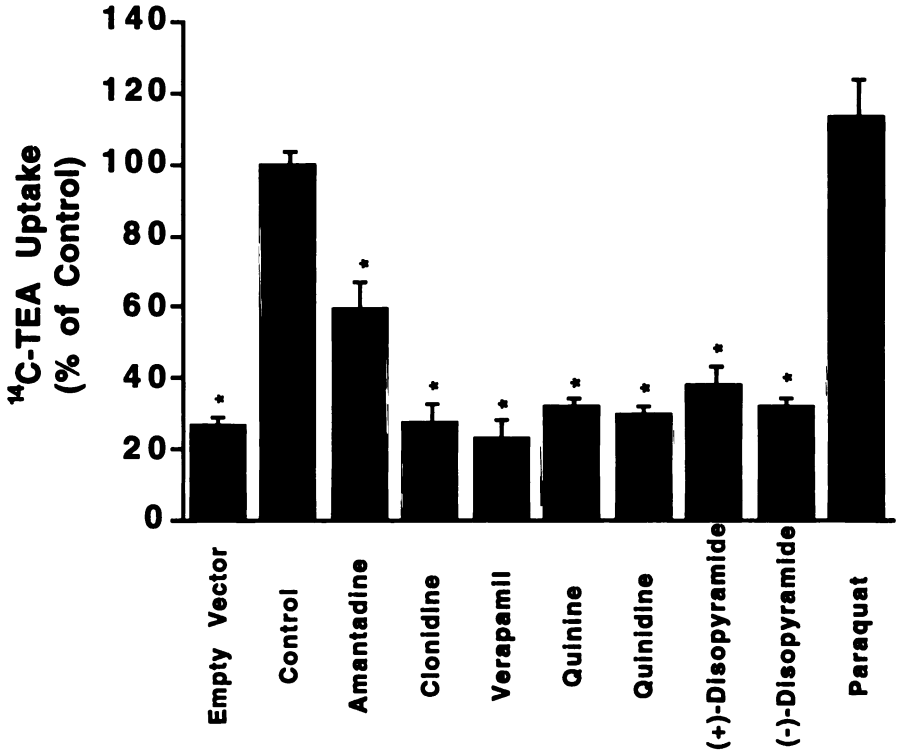

Figure 6.5a Inhibition of ^{14}C-TEA uptake. The uptake of 5 μM ^{14}C-TEA (at 25 min) was measured in the presence of 0.1 mM of the given compounds in pTargeT-hOCT1-transfected HeLa cells. Controls represent uptake of ^{14}C-TEA in the HeLa cells transfected with pTargeT-hOCT1 in the absence of inhibitors. Uptake of ^{14}C-TEA in the empty vector-transfected cells in the absence of inhibitors is shown as well (indicated as Empty Vector). Data represent mean ± SE (n = 4-22) obtained from two to ten separate experiments.
* $p < 0.05$.

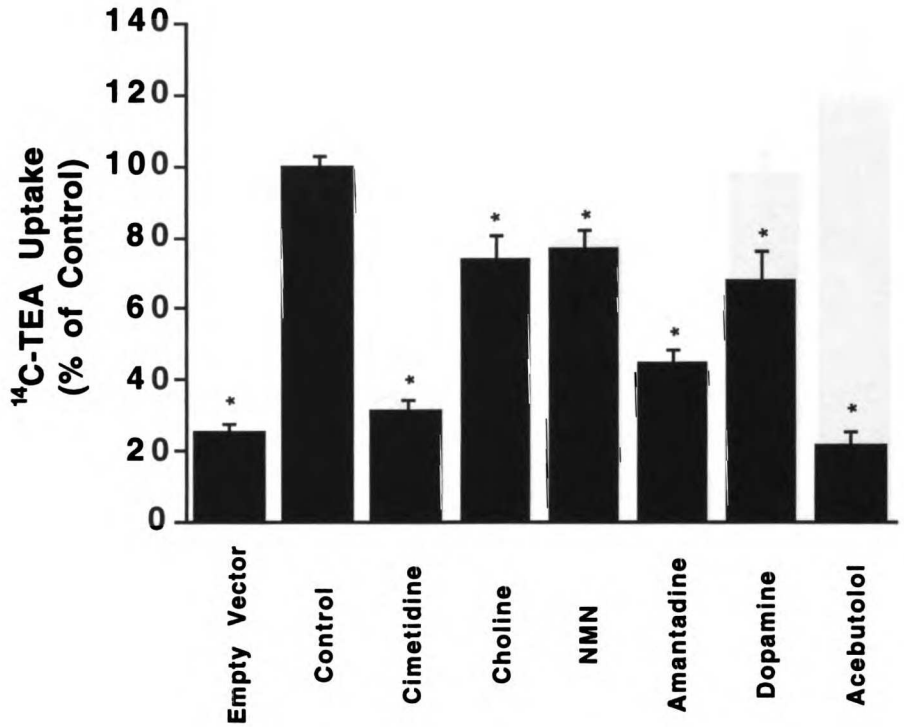

Figure 6.5b Inhibition of ^{14}C-TEA uptake. The uptake of 5 μM ^{14}C-TEA (at 25 min) was measured in the presence of 0.5 mM of the given compounds in pTargeT-hOCT1-transfected HeLa cells. Controls represent uptake of ^{14}C-TEA in the HeLa cells transfected with pTargeT-hOCT1 in the absence of inhibitors. Uptake of ^{14}C-TEA in the empty vector-transfected cells in the absence of inhibitors is shown as well (indicated as Empty Vector). Data represent mean ± SE (n = 4-22) obtained from two to ten separate experiments.

* $p < 0.05$.

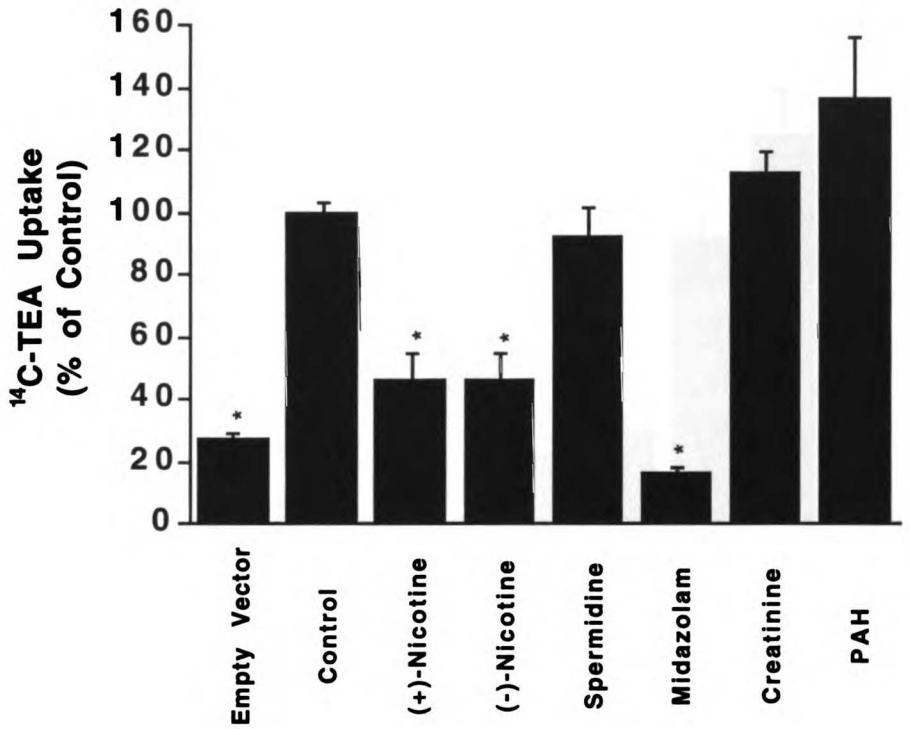

Figure 6.5c Inhibition of ^{14}C-TEA uptake. The uptake of 5 μM ^{14}C-TEA (at 25 min) was measured in the presence of 0.5 mM of the given compounds in pTargeT-hOCT1-transfected HeLa cells. Controls represent uptake of ^{14}C-TEA in the HeLa cells transfected with pTargeT-hOCT1 in the absence of inhibitors. Uptake of ^{14}C-TEA in the empty vector-transfected cells in the absence of inhibitors is shown as well (indicated as Empty Vector). Data represent mean ± SE (n = 4-22) obtained from two to ten separate experiments.

* $p < 0.05$.

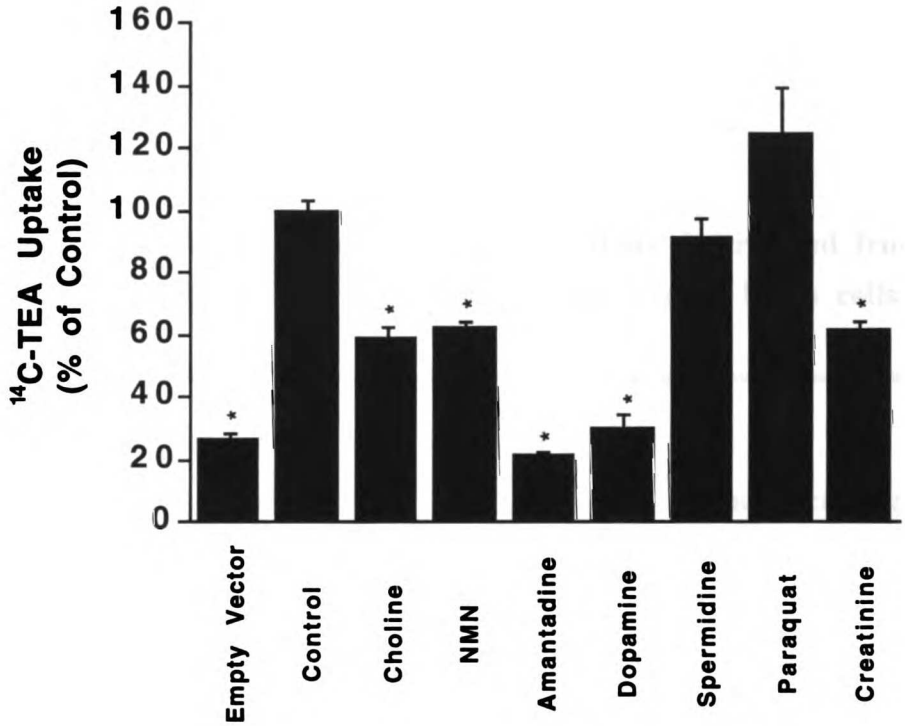

Figure 6.5d Inhibition of ^{14}C-TEA uptake. The uptake of 5 μM ^{14}C-TEA (at 25 min) was measured in the presence of 5 mM of the given compounds in pTargeT-hOCT1-transfected HeLa cells. Controls represent uptake of ^{14}C-TEA in the HeLa cells transfected with pTargeT-hOCT1 in the absence of inhibitors. Uptake of ^{14}C-TEA in the empty vector-transfected cells in the absence of inhibitors is shown as well (indicated as Empty Vector). Data represent mean ± SE (n = 4-22) obtained from two to ten separate experiments.
* $p < 0.05$.

To elucidate the functional properties of hOCT1 expressed in different expression systems, K_i values of the organic cations TEA, decynium-22 and vecuronium were compared to those obtained previously in the oocyte expression system (Table 6.1) (Zhang *et al.*, 1997b; Chapter 5). In the transfected cells, vecuronium had a somewhat higher K_i (232 μM *versus* 120 μM) whereas decynium-22 had a slightly lower K_i (2.7 μM *versus* 4.4 μM).

Table 6.1 Comparison of K_i values of organic cations determined from experiments conducted in *X. laevis* oocytes or transfected HeLa cells

	K_i	
	Oocytes [a]	**Transfected cells**
	μM	
Compounds		
TEA	163 (± 8)	161 (± 109)
Decynium-22	4.44 (±1.21)	2.73 (± 1.24)
Vecuronium	120 (± 39)	232 (± 8)

Values in the parentheses are SD values determined from the SD of the IC_{50} of each individual compound assuming K_m is a constant without an error.

[a] Data obtained from the Chapter 5 as published in Zhang *et al.*, 1997b.

IC_{50} values of selected compounds in inhibiting ^{14}C-TEA uptake mediated by hOCT1 were determined by non-linear regression analysis. K_i values were calculated from the IC_{50} values assuming a competitive model; however, since substrate concentration used

in the experiment is low compared to the K_m (i.e., 5 μM vs. 229 μM), K_i values will be virtually identical to the IC_{50} values despite the mechanism of inhibition (e.g., competitive or noncompetitive) (Cheng and Prusoff, 1973). K_i values were compared to those determined previously for rOCT1 and hOCT2 (see Table 6.2) (Gorboulev *et al.*, 1997; Grundemann *et al.*, 1994; Grundemann *et al.*, 1997). Notable differences were observed in the K_i values of some compounds in interacting with hOCT1 and rOCT1 suggesting that there may be important interspecies differences in the intrinsic function of the transporters. Furthermore, with the exception of desipramine, K_i values were generally lower for hOCT2 than for hOCT1.

To test whether there are stereoselective interactions of organic cations with hOCT1, the IC_{50} values of pairs of isomers were determined and compared. The IC_{50} for quinine was 23.4 ± 6.9 μM, and 17.9 ± 4.7 μM for quinidine (Figure 6.6a). The IC_{50} of S-(+)-disopyramide was 29.9 ± 8.5 μM and 15.4 ± 11.0 μM for R-(-)-disopyramide (Figure 6.6b) ($p < 0.05$).

6.3.4 Trans-Stimulation Studies

To determine whether hOCT1 can transport organic cations in both directions, *trans*-stimulation studies were performed. As shown in Figure 6.7, after preincubation of the pTargeT-hOCT1-transfected HeLa cells with TEA (2 mM) or MPP^+ (0.5 mM) for one hour at 37°C, ^{14}C-TEA uptake was significantly enhanced ($p < 0.05$). The *trans*-stimulation could also be *cis*-inhibited more than 50% with 0.5 mM unlabeled TEA in the reaction media (data not shown). In contrast, preincubation of cells with 2 mM cimetidine did not result in a significant change in ^{14}C-TEA uptake and preincubation of cells with 50 μM decynium-22 resulted in a significant decrease (apparent "*trans*-inhibition") of ^{14}C-TEA uptake ($p < 0.05$).

Table 6.2 K_i values of various compounds in inhibiting TEA uptake mediated by hOCT1

Compounds	K_i		
	hOCT1[a]	rOCT1[b]	hOCT2[c]
		μM	
TEA	161	95[d]	76[d]
MPP^+	12.3	13[d]	2.4
Decynium-22	2.73	0.36	0.1
Tetrapentylammonium	7.46	0.43	1.5
Procainamide	73.9	13	50
Desipramine	5.36	2.8	16
NMN	7,715	1,000	266
Quinine	22.9	4.3	3.4
Quinidine	17.5	6.0	—
Corticosterone	7.02	72	—
Clonidine	0.551	1.4	—
Vecuronium	232	4.3[e]	—
Cimetidine	166	—	—
Midazolam	3.70	—	—
(±)-Verapamil	2.90	—	—
Acebutolol	95.8	—	—

[a] Data obtained from the present study in transfected HeLa cells. The coefficient of variation values ranged from 3.29% for vecuronium to 83.3% for midazolam.

[b] Data obtained from Grundemann *et al.*, 1994, 1997 and Martel *et al.*, 1996a. Studies were conducted in either oocytes or transfected HEK-293 cells.

[c] Data from Gorboulev *et al.*, 1997. Studies were conducted in oocytes.

[d] K_m values.

[e] Unpublished data from this laboratory.

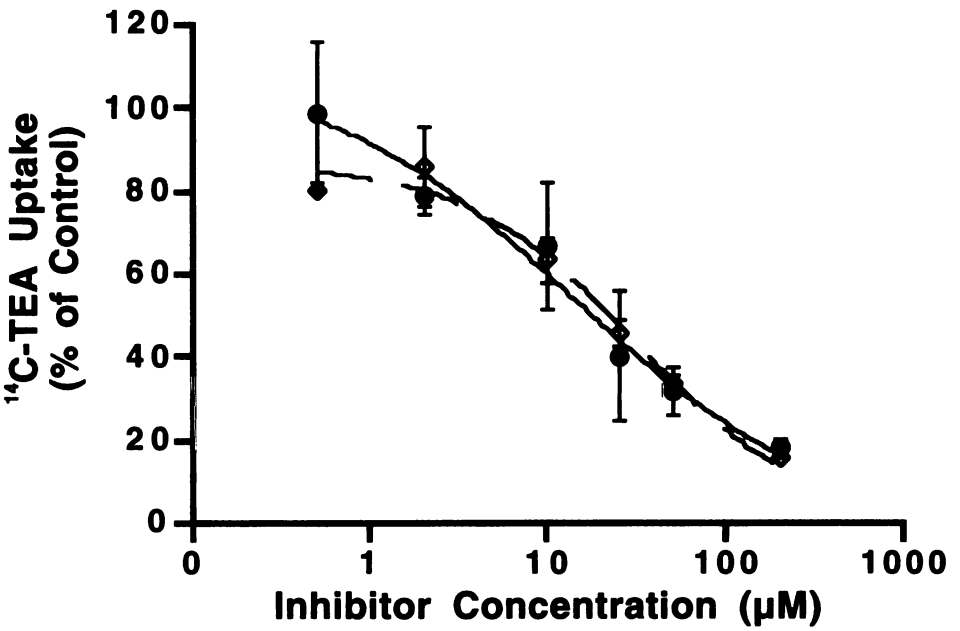

Figure 6.6a Concentration-dependent inhibition of ^{14}C-TEA uptake by stereoisomers in HeLa cells transfected with pTargeT-hOCT1. Initial rates of transport were determined in the presence of quinidine (closed circles), quinine (open diamonds). Data represent mean ± SD of duplicate determinations from one representative experiment.

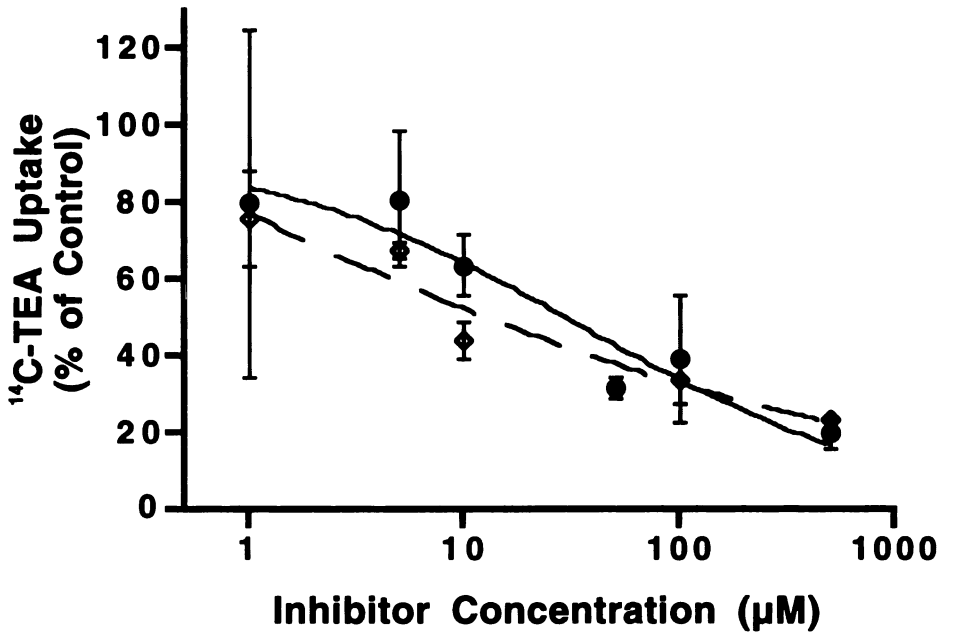

Figure 6.6b Concentration-dependent inhibition of ^{14}C-TEA uptake by stereoisomers in HeLa cells transfected with pTargeT-hOCT1. Initial rates of transport were determined in the presence of S-(+)-disopyramide (closed circles) and R-(-)-disopyramide (open diamonds). Data represent mean ± SD of duplicate determinations from one representative experiment.

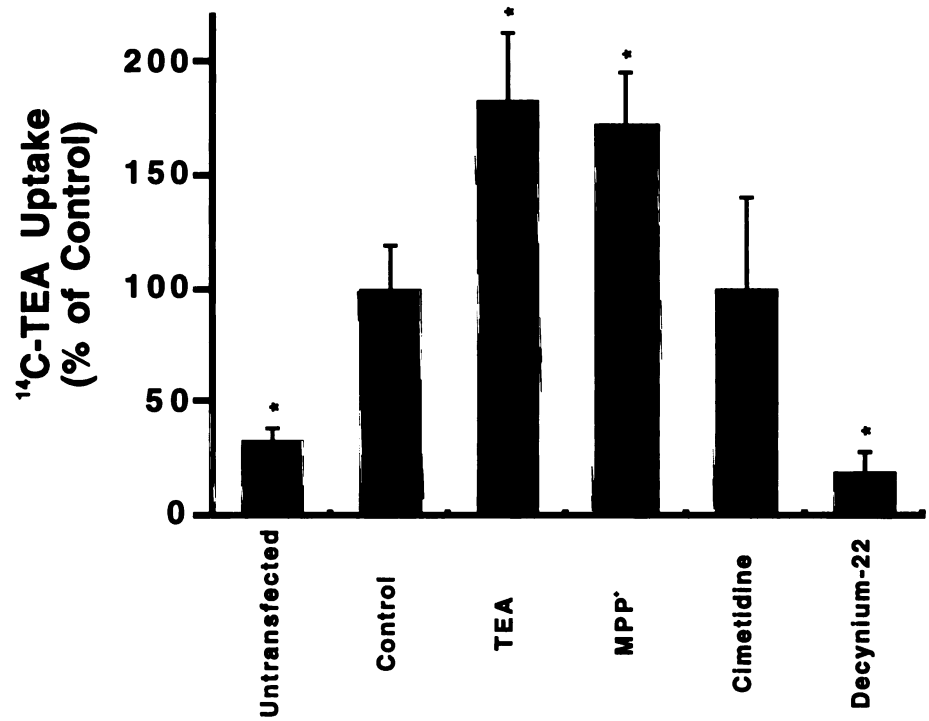

Figure 6.7 *Trans*-stimulation of ^{14}C-TEA uptake in pTargeT-hOCT1 transfected HeLa cells. The uptake (at 25 min) of ^{14}C-TEA (5 μM) was measured after 60 min incubation of the untransfected cells with PBS, and pTargeT-hOCT1-transfected cells with PBS (control) or PBS containing 2 mM TEA, 0.5 mM MPP^+, 2 mM cimetidine, or 50 μM decynium-22, respectively at 37°C. Data represent the mean ± SE (n = 4) obtained from two separate experiments. * $p < 0.05$.

6.4 Discussion

The present study demonstrates that hOCT1 can be functionally expressed in a transiently transfected mammalian cell expression system (HeLa cells) using a lipofection method. Maximal TEA transport activity occurred between 36 and 48 hours (Figure 6.1) after transfection and was observed when the lipid to DNA ratio was between 6:1 and 8:1 (data not shown). In this system, TEA transport was temperature dependent and was saturable with kinetic values comparable to those obtained in *X. laevis* oocytes injected with the cRNA of hOCT1 (Zhang *et al.*, 1997b; Chapter 5) (K_i = 161 μM in HeLa cells versus 163 μM in oocytes). In addition, less than two-fold differences in the K_i values of decynium-22 and vecuronium were observed in cRNA-injected oocytes (Zhang *et al.*, 1997b; Chapter 5) and transfected HeLa cells (Table 6.1) suggesting that hOCT1 has similar functional characteristics in the two expression systems.

A major goal of this study was to determine the functional characteristics of hOCT1. In particular, the substrate selectivity of the transporter was examined. Paraquat and spermidine are multivalent organic cations. Our data demonstrated that neither compound interacted with hOCT1 at 5 mM suggesting that the transporter does not play a role in the uptake of these compounds in human epithelia. These data are consistent with data in the literature demonstrating that paraquat has a distinct transport pathway from TEA in the peritubular membrane of the rabbit kidney (Groves *et al.*, 1995). The data also suggest that the polyamine, spermidine, is not a substrate of hOCT1, consistent with data in the literature demonstrating unique transporters for polyamines (Sokol and Gates, 1990). Interestingly, spermidine was shown previously to induce inward currents in oocytes expressing the rat homolog, rOCT1 (Busch *et al.*, 1996b) indicating that spermidine may be translocated by rOCT1. The data suggest that there are interspecies differences in the function of the OCT1 transporters. However, recent studies demonstrated that a compound

(e.g., quinine) could induce large inward currents without being translocated (Nagel *et al.*, 1997). Further studies are needed to determine if spermidine is a substrate for rOCT1. Although spermidine and paraquat did not interact with hOCT1, the multivalent organic cation, vecuronium interacts in micromolar concentrations (K_i = 232 μM) suggesting that the nature of the hydrophobic moiety may play a role in the potency of interaction of multivalent organic cations with hOCT1.

We determined the effect of the neutral molecules, corticosterone and midazolam, on the transport of ^{14}C-TEA via hOCT1. Previously, corticosterone was thought to enter the cell via simple diffusion to gain access to its sites of action. However it is becoming increasingly clear that transporters may be involved in the entry of corticosterone into cells. For example, corticosterone has been shown to interact with both organic cation and organic anion transport in the microperfused kidney (Ullrich *et al.*, 1993) and recently, has been shown to interact specifically with the rat liver organic anion transporter (oatp) (Bossuyt *et al.*, 1996; Kanai *et al.*, 1996), and the rat organic cation transporter, rOCT1 (Grundemann *et al.*, 1994 and 1997). The present study demonstrated that corticosterone is a potent inhibitor of TEA uptake mediated by hOCT1. Further studies are needed to determine if corticosterone is an actual substrate or whether, it inhibits, but is not translocated by hOCT1.

The neutral compound, midazolam, is a cytochrome P450 3A (CYP3A) substrate with a K_m of approximately 10 μM for 1'-hydroxy midazolam formation (Wrighton and Ring, 1994). The K_i of midazolam in inhibiting TEA transport by hOCT1 is in the same range of its K_m of metabolism by CYP3A. Because hOCT1 is expressed primarily in the liver which is the major site for the metabolism of midazolam, it is possible that the transport rate-limits the metabolism of midazolam. In addition, potential drug-drug interactions between organic cations and midazolam may not only occur at the metabolism level but also occur at the transport level. Collectively, these data indicate that hOCT1 is polyspecific not only for organic cations but also for various neutral compounds. The

positive charge(s) of a molecule may not be the only structural requirement for interaction with hOCT1 as previously hypothesized for OCT transporters. The hydrophobic moiety may also play a role in the potency of interaction of a chemical entity with hOCT1. Further structure function relationship studies are needed to clarify this.

A considerable number of xenobiotics are chiral and contain one or more asymmetric carbon atoms, resulting in two or more enantiomeric forms. There are many examples of differences in pharmacological activity between enantiomeric compounds (Blaschke and Giacomini, 1987; Drayer, 1986; Levy and Boddy, 1991). Stereoselective metabolism of xenobiotics has been well studied and documented (Drayer, 1986; Levy and Boddy, 1991). In this study, we examined the potency of the interaction of various isomers in inhibiting TEA uptake in hOCT1-transfected cells. Within the two pairs tested, the diastereoisomers, quinine and quinidine had no significant differences in IC_{50} values (23.4 ± 6.9 μM *versus* 17.9 ± 4.7 μM) whereas S-(+)-disopyramide was approximately two-fold less potent than R-(-)-disopyramide (29.9 ± 8.5 μM *versus* 15.4 ± 11.0 μM). These data suggest that hOCT1 is not highly stereoselective, which is consistent with the polyspecificity of the transporter.

K_i values of various compounds in inhibiting TEA or MPP^+ uptake mediated by hOCT1 (Gorboulev *et al.* 1997; Zhang *et al.*, 1997b; Chapter 5) and rOCT1 (Grundemann *et al.*, 1994 and 1997; Martel *et al.*, 1996a) (i.e., between species) are listed in Table 6.2. K_i values of TEA, MPP^+, desipramine and clonidine in interacting with hOCT1 and rOCT1 are similar (within 3-fold). In contrast, most of the other organic cations studied including decynium-22, procainamide, NMN, quinine, and vecuronium have much higher K_i values (more than 3-fold) for hOCT1 than for rOCT1. These data indicate that in comparison to the rat, the human possesses an organic cation transporter with a lower affinity for most compounds suggesting that in human epithelial cells organic cations translocated primarily by OCT1 transporters will be eliminated more slowly than in the rat. For example, it has been shown previously that the organic cation vecuronium is transported at a considerably

slower rate in human hepatocyte in comparison to rat hepatocyte (Sandker *et al.*, 1994). Higher K_i values of vecuronium for hOCT1 than for rOCT1 may explain in part its slower transport rate in human. The steroid, corticosterone, however, has a higher affinity for hOCT1 than for rOCT1, which may suggest that cholesterol compounds will exhibit a more potent interaction with organic cation transport in humans than in rats. However, further studies are needed to determine whether the interacting compounds are actual substrates of OCT1 transporters and not simply inhibitors. Moreover, it will be essential to study the site-specific localization of the OCT1 and the relative amounts of the transporters expressed in various tissues.

Comparisons were made between K_i values of various compounds in interacting with the organ-specific transporters in humans, hOCT1 (expressed primarily in liver) (Gorboulev *et al.*, 1997; Zhang *et al.*, 1997b; Chapter 5) and hOCT2 (expressed primarily in kidney) (Gorboulev *et al.*, 1997) (Table 6.2). hOCT2 appears to have a higher affinity for most of the organic cations studied except for desipramine which appears to have lower affinity for hOCT2 than for hOCT1. Thus, it appears that the kidney-specific organic cation transporter, hOCT2 more potently interacts with potential substrates than the liver-specific transporter, hOCT1.

Studies described in Chapter 5 demonstrated that the transport of organic cations via hOCT1 can be driven by a favorable (inside negative) electrical potential difference (Zhang *et al.*, 1997b; Chapter 5). However, it is not known whether transport of organic cations may also be driven by the exchange or countertransport of other organic cations. Our data demonstrate that ^{14}C-TEA transport can be driven by the countertransport of unlabeled TEA (Figure 6.7) suggesting that hOCT1 may operate as an organic cation/organic cation exchanger. In addition, the ability of a compound to *trans*-stimulate the transport of ^{14}C-TEA mediated by hOCT1 indicates that the compound is also translocated by the transporter. The finding that MPP^+ *trans*-stimulated ^{14}C-TEA transport is consistent with studies in Chapter 5 demonstrating that MPP^+ is a substrate of hOCT1 (Zhang *et al.*,

1997b; Chapter 5). However, because of the high background uptake of ^{3}H-MPP$^+$ in the empty vector-transfected cells, an enhanced uptake of ^{3}H-MPP$^+$ was not observed in the hOCT1-transfected cells. The finding that cimetidine did not *trans*-stimulate TEA uptake is consistent with results from permeant studies indicating that cimetidine is not a good permeant of hOCT1 under the experimental conditions (Figure 6.4). In contrast, decynium-22 was shown to "*trans*-inhibit" TEA uptake which suggests that decynium-22 binds tightly to the transporter and is not washed off during the experimental procedures. Alternatively, hOCT1 loaded with decynium-22 cycles more slowly than the unloaded transporter. Collectively, these data suggest that hOCT1 is a uniporter which can translocate organic cations in both directions. When radiolabeled compounds are not available, *trans*-stimulation studies provide an alternative way of determining whether a chemical entity is a substrate for the transporter.

In summary, hOCT1 has been transiently expressed in a mammalian cell line, HeLa. The fundamental properties of TEA transport in this system are similar to those previously described in *Xenopus laevis* oocytes. Using this expression system, studies were conducted which demonstrated the selectivity of the transporter for a variety of substrates. Differences in the K_i values of certain compounds in interacting with the rat and the human organic cation transporters, and the human liver-specific versus kidney-specific organic cation transporters were observed. This study provides the first information about the molecular basis for the differences in organic cation transport observed among species and organs. The development of this mammalian expression system will facilitate the study of drug interactions and transport *in vitro* and the development of drugs that specifically target cells which express hOCT1.

CHAPTER 7

INTERACTIONS OF HIV PROTEASE INHIBITORS WITH A HUMAN ORGANIC CATION TRANSPORTER IN A MAMMALIAN EXPRESSION SYSTEM

7.1 Introduction

HIV protease is a virally encoded enzyme that is essential in the production of mature, infectious HIV virion particles. As soon as the HIV protease enzyme was recognized as a unique target for the treatment of AIDS, HIV protease inhibitors were developed and they represent a new classes of therapeutically important drugs (Deeks and Volberding, 1997; Kakuda *et al.*, 1998; McDonald and Kuritzkes, 1997; Pakyz and Israel, 1997). HIV protease inhibitors are peptidomimetics that competitively bind to the HIV protease active site and inhibit its proteolytic function, which leads to the production of immature, non-infectious HIV particles. They are quite specific for the viral enzyme versus distantly-related cellular enzymes, such as pepsin, renin, and cathepsin D, and able to discriminate among them by several orders of magnitude (Deeks and Volberding, 1997; Kakuda *et al.*, 1998; McDonald and Kuritzkes, 1997). Currently, four HIV protease inhibitors have been approved by the FDA for the treatment of AIDS: saquinavir, ritonavir, indinavir and nelfinavir (Figure 7.1). These protease inhibitors have high potency in inhibiting HIV protease activity with IC_{95} (or EC_{95}) values in the nanomolar ranges (saquinavir, 5-80 nM (EC_{90}); ritonavir, 3.8-153 nM (EC_{50}); indinavir, 25-100 nM; nelfinavir, 7-196 nM) (Drug package inserts).

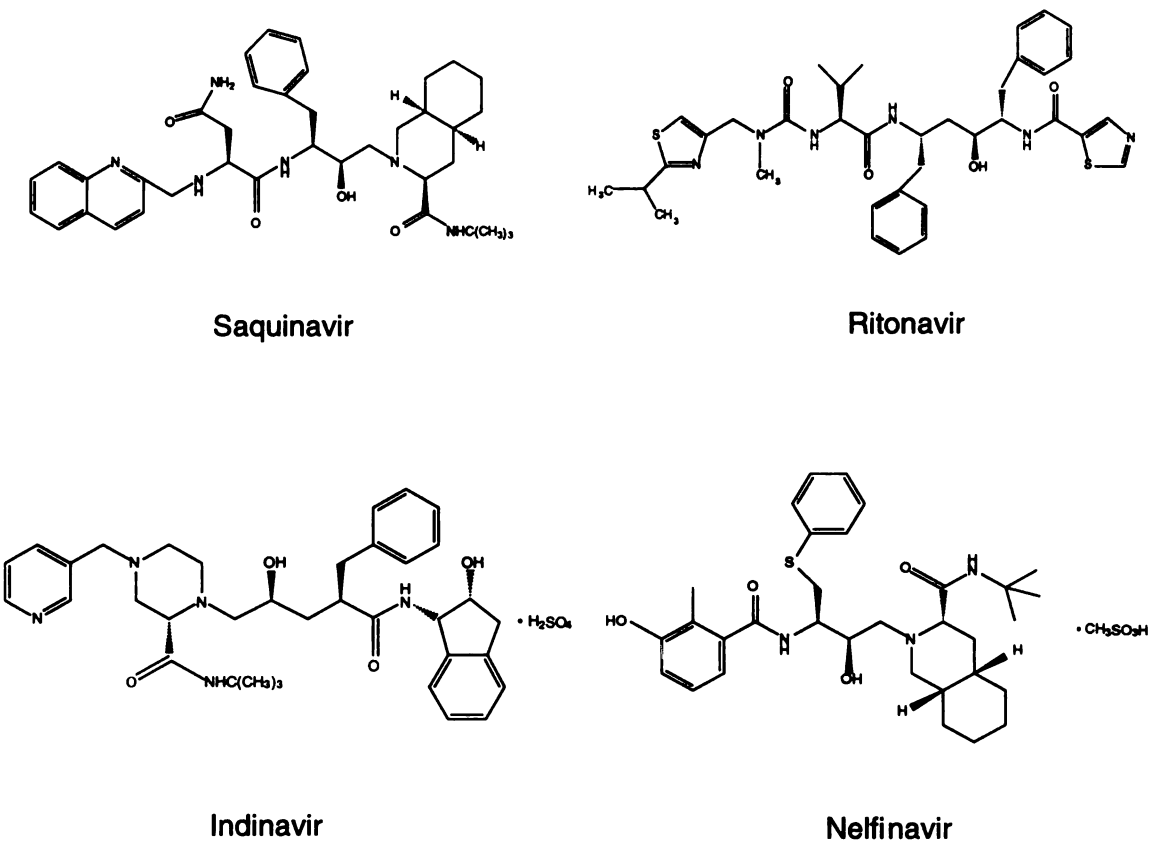

Figure 7.1 Chemical structures of HIV protease inhibitors.

Generally, both metabolizing enzymes and xenobiotic transporters play a role in the elimination and detoxification of drugs. It is critical to understand which enzymes and transporters may interact with a drug to understand its pharmacokinetics and to predict potential drug-drug interactions. Saquinavir, ritonavir and indinavir are primarily metabolized by cytochrome P450 3A4 (CYP3A4) forming oxidative metabolites (Balani *et al.*, 1996; Deeks and Volberding, 1997; Denissen *et al.*, 1997; Lin *et al.*, 1996; Merry *et al.*, 1997 and 1998). Nelfinavir is metabolized by multiple P450 isoforms (Deeks and Volberding, 1997; Kaldor *et al.*, 1997). Recent data demonstrated that saquinavir, indinavir and nelfinavir are substrates for the drug efflux pump, P-glycoprotein (P-gp), which may play an important detoxification role via countertransport of these agents (Kim *et al.*, 1998). It is not clear whether other xenobiotic transporters also play a role in the elimination of HIV protease inhibitors.

Organic cation transporters, often termed as polyspecific organic cation transporters because of their broad substrate-selectivity, are xenobiotic transporters which play a critical role in the disposition of various organic cations (Koepsell, 1998; Pritchard and Miller, 1993; Zhang *et al.*, 1998a). Recently, we cloned a human organic cation transporter, hOCT1, which is expressed primarily in the liver (Zhang *et al.*, 1997b; Chapter 5). Functional studies in heterologous expression systems have demonstrated that various organic cations as well as other hydrophobic compounds interact with hOCT1 (Zhang *et al.*, 1997b and 1998b; Chapters 5 and 6). Further investigation of this uptake process is relevant in view of the major role of the liver in the distribution and elimination of cationic drugs and endogenous amines. Since HIV protease inhibitors carry positive charged amine moieties (Figure 7.1), they may interact with organic cation transporters. In the present study, we investigated the interaction of these therapeutically important agents with hOCT1 in the transiently-transfected HeLa cells. We carried out both *cis*-inhibition and *trans*-

stimulation studies to determine both the interaction kinetics and substrate selectivity of hOCT1 for HIV protease inhibitors.

7.2 Materials and Methods

7.2.1 DNA Isolation

hOCT1 DNA subcloned into the mammalian expression vector pTargeT (Promega, Madison, WI) was used for transfection studies. Plasmid DNA was purified using the Qiagen Endo-free DNA isolation kit (Qiagen, Santa Clarita, CA). The DNA was stored in endotoxin-free TE buffer (10 mM Tris•Cl, 1 mM EDTA, pH 8.0) and its concentration was determination by UV spectroscopy. The yield from each isolation was approximately 400-900 μg with the DNA concentration ranging from 2.1-5.0 μg/μl in TE buffer.

7.2.2 HeLa Cell Culture and Transfection

HeLa cells were maintained in the growth medium in 175 ml cell culture flasks (Nalge Nunc International, Naperville, IL) at 37°C in a humidified 5% CO_2/95% air atmosphere as previously described (Zhang *et al.*, 1998b; Chapter 6). All studies were performed in cells between passages 2 and 20. Prior to transfection, cells were seeded at a density of 1.6 X 10^5 cells/well in 12-well tissue culture plates (Corning Costar Corp, Cambridge, MA). Following a modified protocol from Gibco/BRL, LIPOFECTAMINE™ (2mg/ml, Gibco, BRL) was used to deliver DNA to the cells (Zhang *et al.*, 1998b; Chapter 6). Briefly, for each well 100 μl of Opti-MEM (Gibco, BRL) was mixed with 1 μg of DNA, and another 100 μl of media was mixed with 3.25 μl of lipid. The two solutions were then mixed and incubated for 30 minutes at room temperature. After incubation, 800 μl of Opti-MEM was added to the 200 μl mixture. After rinsing the cells with 1 ml of the Opti-MEM, the final volume of 1 ml

DNA/lipid complex mixture was applied to each well. The cells were incubated for 18 hours before the transfection mixture was replaced with standard complete growth medium.

7.2.3 Uptake Measurements

Uptake studies were carried out 24 to 44 hours post transfection as previously described (Zhang *et al.*, 1998b; Chapter 6). Briefly, the growth medium was gently removed, and each monolayer was rinsed with 1 ml of phosphate-buffered saline (PBS) buffer. To initiate uptake, 0.5 ml of PBS containing ^{14}C-TEA (10 μM) was added to each well and incubated at room temperature for 20 minutes. In inhibition and IC_{50} studies, various concentrations of unlabeled compounds were included in the reaction mixture. The uptake was stopped by aspiration of the medium, and then each well of cells was immediately washed with ice-cold PBS buffer. The cells were solubilized with 1 ml of 0.5% Triton-X 100 and 0.5 ml of sample was assayed by liquid scintillation counting (LS 1801, Beckman, Palo Alto, CA).

In *trans*-stimulation studies, each well of cells was preincubated with either 0.5 ml of PBS buffer (control) or 0.5 ml of PBS buffer plus the indicated amount of an unlabeled test compound at 37°C for one hour. Cells were then rinsed with ice-cold PBS buffer before the uptake studies was performed as described above.

The protein concentration was determined by the Bio-Rad Protein Assay Kit (Bio-Rad, Hercules, CA) with bovine serum albumin as the standard as previously described (Zhang *et al.*, 1998b; Chapter 6).

7.2.4 RT-PCR

The first strand cDNA of MOLT-4 cells for PCR amplification was purchased from Clontech (Palo Alto, CA). The primers used in PCR were designed from the cDNA of hOCT1 (5'- and 3'-end primers in Zhang *et al.*, 1997b and Chapter 5), MDR1 (sense and antisense primers were designed to amplify from positions 2419 to 2683 bp of the MDR1

gene (Genbank accession #M14758) (Chen *et al.*, 1986; Ueda *et al.*, 1987) and MRP1 (sense and antisense primers were designed to amplify from 273 to 615 bp of the MRP1 gene (Genbank accession #L05628) (Cole *et al.*, 1992). PCR was performed in a thermal cycler (GennAmp PCR system 2400, Perkin-Elmer, Foster City, CA) using the cycle as previously described (Zhang *et al.*, 1997b; Chapter 5). The PCR products were electrophoresed through 1% agarose gel and stained with ethidium bromide.

7.2.5 Data Analysis

In general, uptake values are expressed as mean ± standard deviation (SD). A minimum of two wells were used to generate a data point in each experiment. All experiments were repeated at least once on a different day using a different cell passage. Statistical analysis was carried out by an unpaired Student's *t*-test (Primer of Biostatistics software, Version 3, written by Stanton A. Glantz, McGraw-Hill Companies, 1991). Results were considered statistically different with a probability (p) < 0.05.

For IC_{50} studies, data were fit to the equation $V=V_0/[1+(I/IC_{50})^n]$ where V is the uptake of ^{14}C-TEA (20 min) in the presence of inhibitor, V_0 is the uptake of ^{14}C-TEA in the absence of inhibitor, I is the inhibitor concentration and n is the Hill coefficient. The Kaleidagraph fitting program (Abelbeck Software) was used to fit the data by non-linear regression.

7.2.6 Materials

HeLa cells and the media and buffers used to maintain the cells were purchased from the UCSF Cell Culture Facility. Original stocks of HeLa cells were obtained from American Type Culture Collection (ATCC, Rockville, MD). ^{14}C-TEA (55 mCi/mmol) was purchased from American Radiolabeled Chemicals (St. Louis, MO). Indinavir sulfate and nelfinavir were purchased from the hospital pharmacy. Saquinavir mesylate was purchased from the hospital pharmacy and obtained in powdered form from Roche and ^{14}C-saquinavir (3.30

mCi/mmol) was provided by Roche (Nutley, NJ). Ritonavir was purchased from the hospital pharmacy and obtained in powdered form from Abbott (Abbott Park, IL). All other chemicals were obtained from Sigma (St. Louis, MO) and Fisher (Pittsburgh, PA) or as indicated.

7.3 Results

7.3.1 Cis-Inhibition Studies

The concentration dependence of the HIV protease inhibitors in inhibiting ^{14}C-TEA uptake was determined. All HIV protease inhibitors significantly inhibited ^{14}C-TEA uptake in HeLa cells expressing hOCT1. Data from multiple experiments were fit to the equation as described in the data analysis by nonlinear regression to obtain IC_{50} values. Figure 7.2 demonstrates a representative IC_{50} curve for ritonavir. IC_{50} values for these protease inhibitors ranged from 5.2 μM for ritonavir to 62 μM for indinavir. n values ranged from 0.59 for indinavir to 0.95 for ritonavir (Table 7.1).

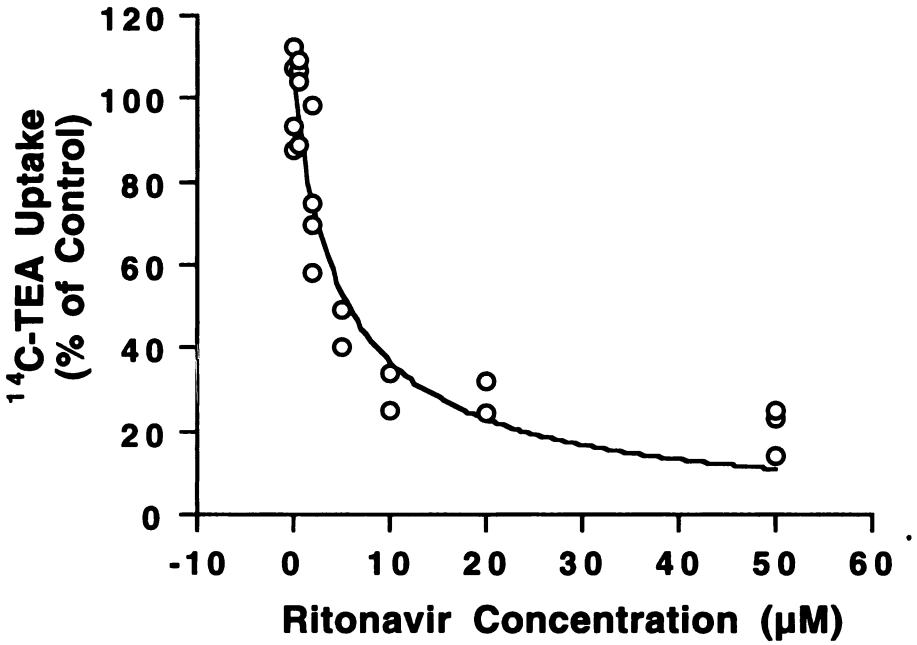

Figure 7.2 Concentration-dependent inhibition of ^{14}C-TEA uptake by ritonavir in HeLa cells transfected with pTargeT-hOCT1. Initial rates of transport were determined in the presence of various concentrations of ritonavir. Data represent determinations from three experiments and were fitted with non-linear regression as described in "Materials and Methods". The IC_{50} value of ritonavir obtained from the fit was 5.18 ± 1.21 μM.

Table 7.1 IC_{50} values of HIV protease inhibitors inhibiting ^{14}C-TEA uptake in hOCT1 DNA-transfected HeLa cells

Compounds	IC_{50} μM	n
Indinavir	61.7 ± 18.4	0.59 ± 0.10
Nelfinavir	21.8 ± 5.4	0.68 ± 0.12
Ritonavir	5.18 ± 1.21	0.95 ± 0.17
Saquinavir	8.26 ± 1.64	0.70 ± 0.09

IC_{50} and n values were obtained by fitting data from two to four separate experiments (e.g., Figure 7.2) as described in "Materials and Methods" and are presented as means ± SD.

7.3.2 Trans-Stimulation Studies

Trans-stimulation studies were used to determine whether the HIV protease inhibitor were substrates of hOCT1, i.e., translocated by hOCT1. In previous studies, we determined that *trans*-stimulation is concentration dependent, i.e., the *trans*-stimulation effect increased with increasing *trans*-TEA concentrations and it was saturable at high concentrations (concentrations ≥ 10 times the K_m or K_i values) (Zhang *et al.*, 1998c; Chapter 8). Therefore, we assumed that at high concentrations, the maximum *trans*-stimulation effect for ^{14}C-TEA uptake will be produced for any compound. After preincubating hOCT1 DNA-transfected HeLa cells with 2 mM TEA (positive control) for one hour at 37°C, ^{14}C-TEA uptake was significantly enhanced ($p < 0.05$) in hOCT1 DNA transfected-cells preincubated with TEA (Figure 7.3). Preincubation of hOCT1 DNA-transfected cells with 200 μM indinavir did not result in a significant change in TEA uptake, whereas preincubation of cells with 200 μM nelfinavir, ritonavir, or saquinavir resulted in a significant decrease (apparent "*trans*-inhibition") in ^{14}C-TEA uptake ($p < 0.05$) (Figure 7.3). Similar results were obtained after incubation of the hOCT1 DNA-transfected cells with a lower concentration (50 μM) of unlabeled compounds (data not shown) suggesting that the apparent "*trans*-inhibition" was due to a decrease in the turnover rate of the transporter.

Indinavir is the weakest inhibitor among the four HIV protease inhibitors. *Trans*-stimulation studies were carried out after preincubating the cells with 1 mM indinavir (i.e., > 10 times of its K_i value). Uptake studies were carried out at two different time points. As shown in Figure 7.4, no *trans*-stimulation effect was observed in cells preincubated with 1 mM indinavir.

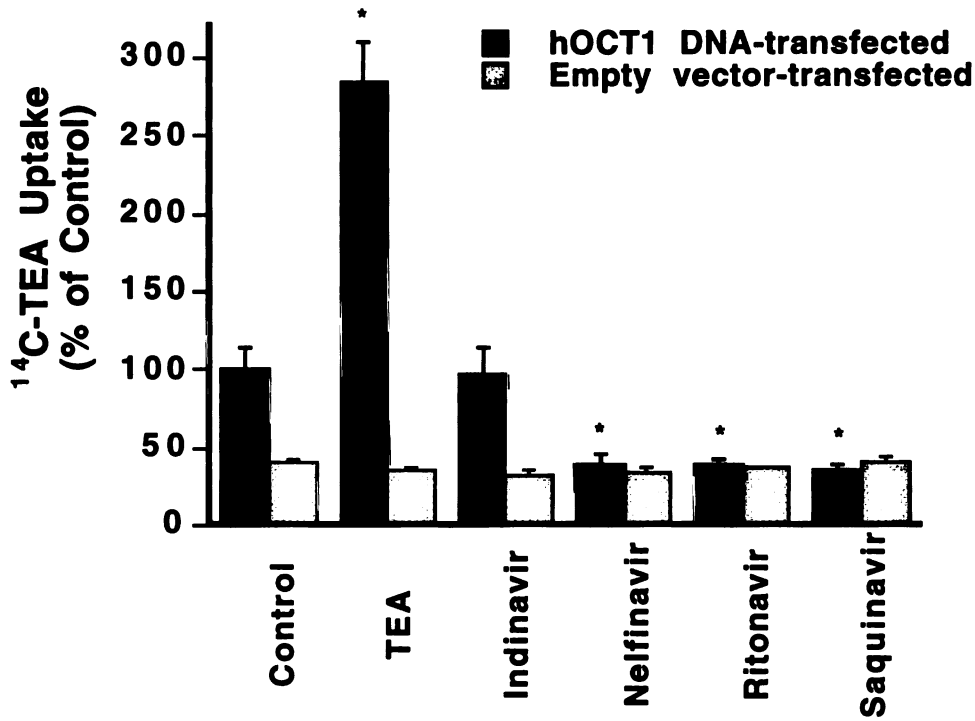

Figure 7.3 *Trans*-stimulation of ^{14}C-TEA uptake in pTargeT-hOCT1 transfected HeLa cells. The uptake (at 20 min) of ^{14}C-TEA (10 μM) was measured after a 60 min pre-incubation (followed by washing) of the hOCT1 DNA-transfected cells (dark bars) and empty vector-transfected cells (gray bars) with PBS (control) or PBS containing 2 mM TEA or 200 μM of indinavir, nelfinavir, ritonavir, or saquinavir, respectively at 37°C. Data represent the mean ± SD of duplicate determinations obtained from one representative experiment. * $p < 0.05$.

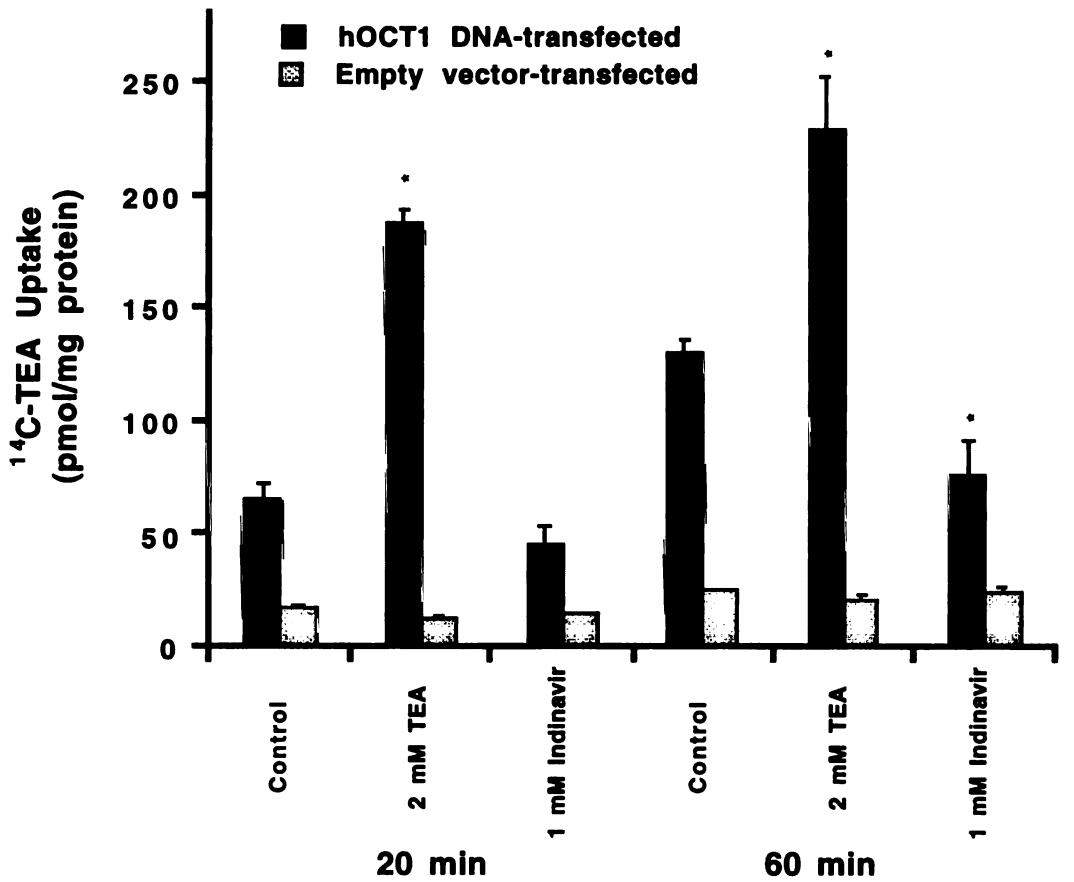

Figure 7.4 *Trans*-stimulation of ^{14}C-TEA uptake in pTargeT-hOCT1 transfected HeLa cells. The uptake (at 20 and 60 min) of ^{14}C-TEA (10 μM) was measured after a 60 min pre-incubation (followed by washing) of the hOCT1 DNA-transfected cells (dark bars) and empty vector-transfected cells (gray bars) with PBS (control) or PBS containing 2 mM TEA or 1 mM indinavir, respectively at 37°C. Data represent the mean ± SD of duplicate determinations obtained from one representative experiment. * $p < 0.05$.

7.3.3 Permeant (Substrate) Studies

^{14}C-Radiolabeled saquinavir uptake (26 μM) was directly measured in the hOCT1 DNA-transfected HeLa cells. As shown in Figure 7.5, ^{14}C-saquinavir uptake in hOCT1 DNA-transfected cells was not significantly different from that in empty vector-transfected cells indicating that saquinavir was not translocated by hOCT1. As a positive control, ^{14}C-TEA uptake (20 min) in the same experiment demonstrated a 3-fold enhanced uptake over that in empty vector-transfected cells at 20 min (data not shown).

The endogenous saquinavir uptake in empty vector-transfected cells (496 pmol/mg protein/μM at 20 min) was high in comparison to endogenous TEA uptake (3.64 pmol/mg protein/ μM at 20 min), thus an enhanced uptake of saquinavir might be masked by its high endogenous uptake. Accordingly, we determined the uptake of ^{14}C-saquinavir (20 μM) in hOCT1 cRNA-injected oocytes which have a low endogenous saquinavir uptake. We found that ^{14}C-saquinavir uptake was not enhanced in hOCT1 cRNA-injected oocytes in comparison to water-injected oocytes (7.14 ± 1.13 vs. 8.20 ± 2.34 pmol/oocyte/90 min, mean ± SD) three days post-injection.

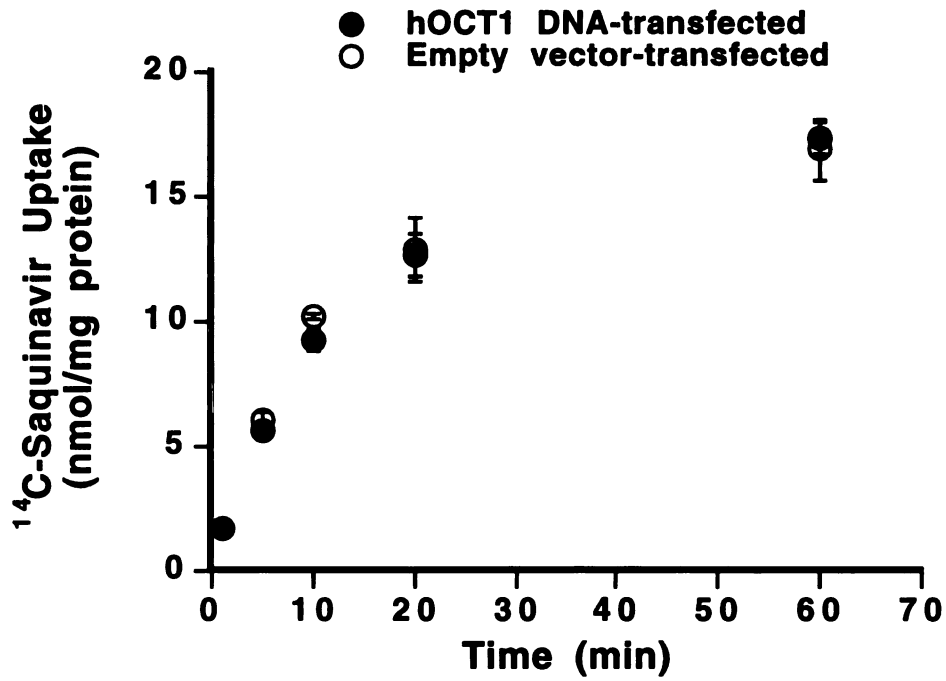

Figure 7.5 Uptake of ^{14}C-saquinavir (26 μM) in the pTargeT-hOCT1-transfected (closed circles) and empty vector-transfected (open circles) HeLa cells. Data represent mean ± SD of duplicate determinants from one representative experiment.

7.3.4 Expression of hOCT1, MDR1, MRP1 in MOLT-4 Cells

The expression of the mRNA transcripts of the human xenobiotic transporters, hOCT1, MDR1 and MRP1 in MOLT-4 cells was determined. As shown in Figures 7.6a and 7.6b, the mRNA transcripts of these transporters are expressed in MOLT-4 cells. However, RT-PCR using primers designed from hOCT1 cDNA resulted in amplifying an apparent splice variant of hOCT1. Further PCR using primers designed to amplify the first half (5'-end) of hOCT1 and second half (3'-end) of hOCT1 DNA demonstrated that the deleted sequence was at the 3'-end of cDNA (data not shown).

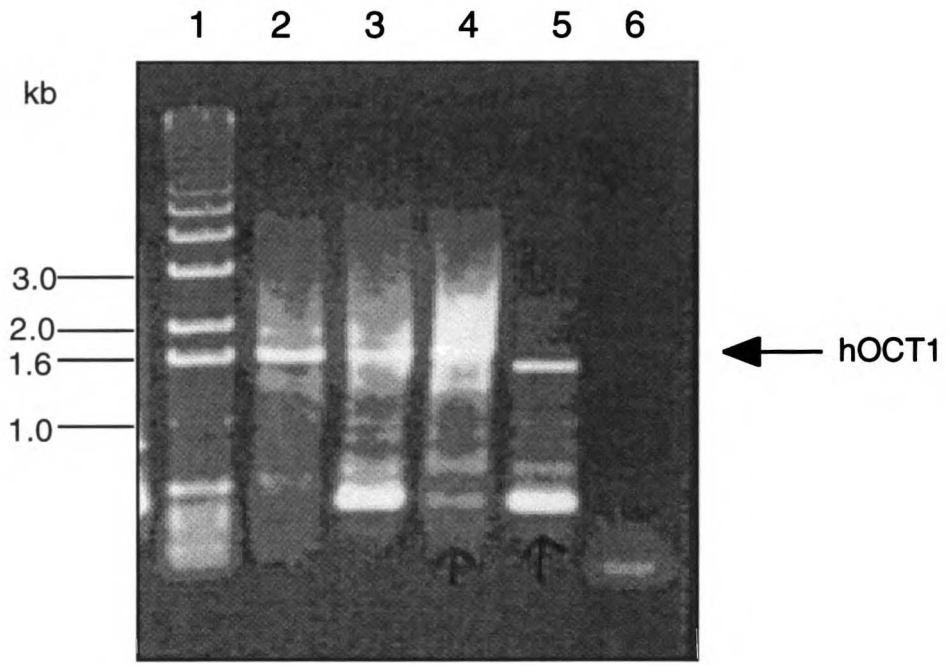

Figure 7.6a RT-PCR analysis of hOCT1 mRNA transcript expression in various tissues and cells. mRNA from human liver (*lane 2*), Caco-2 cells (*lane 3*), human small intestine (*lane 4*) or MOLT-4 cells (*lane 5*) was subjected to RT-PCR using primers designed to obtain a full-length DNA of the hOCT1 open reading frame (~1.6 kb) as described in "Materials and Methods". Water (*lane 6*) was used as control in PCR reactions. The PCR products were analyzed by 1% agarose gel and stained with ethidium bromide. A 1-kb DNA ladder (Gibco BRL) was used to determine the band size (*lane 1*).

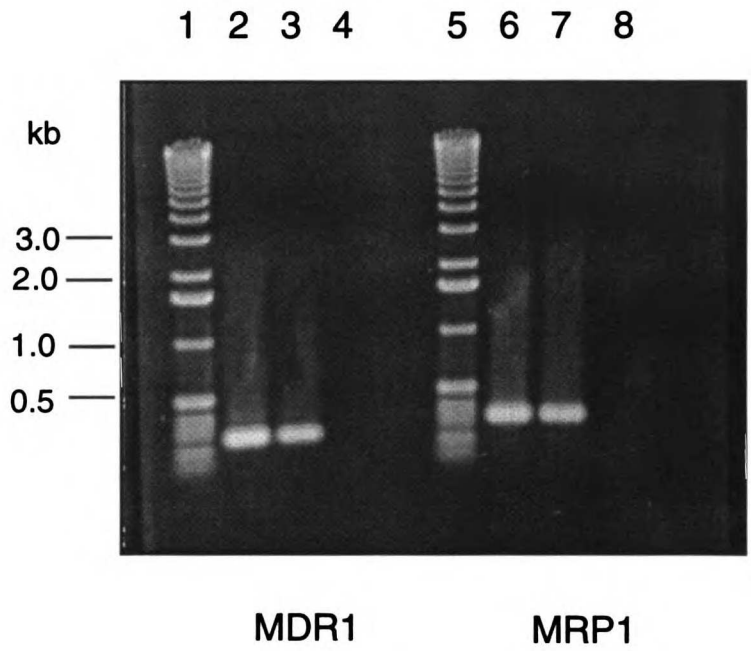

Figure 7.6b RT-PCR analysis of MDR1 and MRP1 mRNA transcript expression in MOLT-4 cells. Plasmid DNA containing MDR1 gene (*lane 2*, as positive control) or MRP1 gene (*lane 6*, as positive control) or mRNA from MOLT-4 cells (*lanes 3 and 7*) was subjected to RT-PCR as described in "Materials and Methods). Water (*lanes 4 and 8*) was used as negative control in PCR reactions. The PCR products were analyzed by 1% agarose gel and stained with ethidium bromide. A 1-kb DNA ladder (Gibco BRL) was used to determine the band size (*lanes 1 and 5*).

7.4 Discussion

HIV protease inhibitors are a new class of therapeutic agents for the treatment of AIDS. Although these drugs represent a clear advance in the management of HIV disease, drug resistance, side effects and drug interactions are common. Both metabolizing enzymes and xenobiotic transporters play an important role in the elimination of these compounds and drug interactions can occur at both the metabolism and transport level. Furthermore, increasing evidence suggests that there is considerable overlapping in the substrate selectivities of P450 3A4 (CYP 3A4) and P-gp indicating an increased potential for numerous drug interactions (Benet *et al.*, 1996; Schinkel *et al.*, 1997; Schuetz *et al.*, 1996a and 1996b; van Asperen *et al.*, 1997; Wacher *et al.*, 1995; Zhang *et al.*, 1998d). Previous studies have demonstrated that HIV protease inhibitors are inhibitors/substrates for CYP3A4 and P-gp (Balani *et al.*, 1996; Deeks and Volberding, 1997; Denissen *et al.*, 1997; Kaldor *et al.*, 1997; Kim *et al.*, 1998; Lin *et al.*, 1996; Merry *et al.*, 1997 and 1998). Coadministration of protease inhibitors and drugs primarily metabolized by CY3A4 and/or substrates for P-gp will result in altered plasma level of other drugs leading to adverse effects. For example, co-administration of rifampin, a known inducer of CYP3A4 and P-gp, with saquinavir decreased the steady state AUC and C_{max} of saquinavir by approximately 80% (saquinavir (Invirase®) package insert).

To understand and predict pharmacokinetics and drug interactions, it is essential to determine the interaction of these agents with xenobiotic transporters. In the current study, interactions of HIV protease inhibitors with hOCT1 was investigated in hOCT1 DNA-transfected HeLa cells. We found that all four currently approved HIV protease inhibitors are potent inhibitors of hOCT1 with IC_{50} values ranging from 5.18 μM for saquinavir to 61.7 μM for indinavir (Table 7.1). These data suggest that HIV protease inhibitors will potently interact with organic cation transport mediated by hOCT1.

We further determined whether HIV protease inhibitors are transported by hOCT1. Both *trans*-stimulation studies and permeant studies with ^{14}C-saquinavir indicated that these compounds are not substrates of hOCT1 (Figures 7.3 and 7.5). Because HIV protease inhibitors are bulky molecules with molecular weights greater than 600, these data are consistent with our other findings that hydrophobic and bulky molecules are potent inhibitors but poor substrates of hOCT1 (Zhang *et al.*, 1998c; Chapter 8).

Since HIV protease inhibitors are poorly translocated by hOCT1, it is likely that hOCT1 does not play a role in the elimination of these agents. However, these protease inhibitors will potently inhibit the transport of cationic drugs which are substrates of hOCT1 and lead to potential drug-drug interactions. For example, HIV protease inhibitors may inhibit the uptake and elimination of cardiovascular drugs by the hepatocyte. Inhibition of uptake will lead to a poorer access of these drugs to metabolizing enzymes that are located inside the cells. Notably, the AUC and C_{max} of the antihistamine, terfenadine, were increased 358% and 253%, respectively, when co-administered with saquinavir (fortovase®) (package insert).

It is of considerable interest to determine the expression of xenobiotic transporters which may control the intracellular concentrations of a number of therapeutic agents including HIV protease inhibitors in HIV-target cells. CD4, the target for HIV virion infection, is expressed in MOLT-4 cells, a human lymphoblast leukemia cell line derived from the peripheral blood. Accordingly, we studied the expression of the xenobiotic transporters, hOCT1, MDR1, and MRP1, in MOLT-4 cells to determine their possible roles in HIV-target cells. By RT-PCR analysis, we found that the multidrug resistant proteins, MDR1 (P-gp) and MRP1, are expressed in MOLT-4 cells (Figure 7.6b). In addition, a putative spliced variant of hOCT1 is also expressed in this cell line (Figure 7.6a). Since HIV protease inhibitors are substrates of P-gp, these data suggest that P-gp may function in limiting the access of HIV protease inhibitors to the target (Kim *et al.*,

CHAPTER 8

THE INTERACTION OF n-TETRAALKYLAMMONIUM COMPOUNDS WITH A HUMAN ORGANIC CATION TRANSPORTER, hOCT1

8.1 Introduction

It is widely recognized that an array of organic cations with diverse chemical structures undergo hepatobiliary secretion (Groothuis and Meijer, 1996; Meijer *et al.*, 1990; Oude Elferink *et al.*, 1995). Distinct transporters for small molecular weight, hydrophilic (type I) and large molecular weight, bulkier (type II) organic cations appear to be involved in the uptake across the sinusoidal membrane of the hepatocyte (Meijer *et al.*, 1990; Mol *et al.*, 1988; Moseley *et al.*, 1992 and 1996a; Oude Elferink *et al.*, 1995; Steen *et al.*, 1991). Previous studies demonstrated that lipophilicity was a major determinant for the hepatobiliary transport of a series of small molecular weight monoquaternary compounds (<200 daltons; type I compounds) in the rat. That is, increasing lipophilicity was associated with increasing hepatic clearances of these compounds (Neef and Meijer, 1984). However, because the studies were carried out *in vivo*, the specific transporters involved in the hepatic clearance of these compounds were not identified. Furthermore, the structure activity relationships established in these studies were limited to hepatobiliary secretion in the rat. It is not known whether such relationships also describe the hepatobiliary transport of organic cations in the human.

Recently, the first human organic cation transporter, hOCT1, was cloned (Gorboulev *et al.*, 1997; Zhang *et al.*, 1997b; Chapter 5). Northern blot analysis demonstrated that hOCT1 is expressed primarily in human liver. Functional studies carried out in *Xenopus laevis* oocytes suggest that hOCT1 represents an organic cation transporter located on the sinusoidal side of the hepatocyte (Zhang *et al.*, 1997b; Chapter 5). To study the functional properties of hOCT1, we developed a transiently transfected cell line, HeLa (Zhang *et al.*, 1998b; Chapter 6). We determined the effect of various organic cations and other compounds on the transport of the model organic cation, TEA. Our data suggest that a number of organic cations with diverse structures inhibited TEA uptake in the hOCT1 DNA-transfected HeLa cells (Zhang *et al.*, 1998b; Chapter 6). In addition, we observed that TEA and MPP^+, known substrates of hOCT1, *trans*-stimulated the uptake of ^{14}C-TEA. Namely, a high concentration of unlabeled TEA or MPP^+ inside the cells stimulated the uptake of ^{14}C-TEA (Zhang *et al.*, 1998b; Chapter 6). These data suggest that *trans*-stimulation studies may be used to assess whether a compound is actually translocated by hOCT1 in the HeLa cell expression system.

Although our previous study demonstrated that structurally diverse organic cations interact with hOCT1, systematic studies ascertaining structure activity relationships were not performed. To obtain insight into the relationship between physicochemical properties, particularly molecular weight and hydrophobicity, and transport by hOCT1, we studied a series of n-tetra-alkylammonium (n-TAA) compounds in transfected HeLa cells. By performing both *trans* -stimulation and *cis*-inhibition studies we determined the effect of hydrophobicity on inhibition potency and translocation by hOCT1. For n-TAA compounds with molecular sizes greater than or equal to 130, we observed a reverse correlation between IC_{50} and partition coefficient (octanol/water). A reverse correlation was also observed between transport rate and partition coefficient indicating that factors other than binding affinity contribute to the overall transport rate of these compounds by hOCT1.

These data indicate that a balance between hydrophobic and hydrophilic properties is required for interaction and subsequent translocation by hOCT1.

8.2 Materials and Methods

8.2.1 DNA Isolation

hOCT1 DNA was subcloned into the mammalian expression vector pTargeT (Promega, Madison, WI) as previously described in Chapter 6 (Zhang *et al.*, 1998b). DNA for transfection studies was isolated with the Qiagen Endo-free DNA isolation kit (Qiagen, Santa Clarita, CA). The DNA was resuspended in endotoxin free TE buffer and its concentration was determination by UV spectroscopy. The yield from each isolation was approximately 400-900 μg with a DNA concentration ranging from 2.1-5.0 μg/μl in TE buffer.

8.2.2 RT-PCR

The first strand cDNA for PCR amplification was synthesized from mRNA generated from various tissues or Caco-2 cells with oligo-(dT) primers using the SuperScript preamplification system (Gibco BRL, Gaithersburg, MD) (Zhang *et al.*, 1997a; Chapter 4). The primers used in PCR were designed from hOCT1 cDNA (5'- and 3'-end primers in Zhang *et al.*, 1997b; Chapter 5). PCR was performed in a thermal cycler (Perkin-Elmer, Foster City, CA) using the cycle as previously described in Chapter 5 (Zhang *et al.*, 1997b). The PCR products were electrophoresed through 1% agarose gel and stained with ethidium bromide.

8.2.3 Maintenance of Cell Culture and Transfection

HeLa cells were maintained in the growth medium in 175 ml cell culture flasks (Nalge Nunc International, Naperville, IL) at 37°C in a humidified 5% CO_2/95% air atmosphere as previously described in Chapter 6 (Zhang *et al.*, 1998b). All studies were performed in cells of passages 3-19. Cells were seeded at a density of 1.6 X 10^5 cells/well in 12-well tissue culture plates (Corning Costar Corp, Cambridge, MA) 24 hours prior to transfection. LIPOFECTAMINE™ (Gibco BRL) was used to deliver DNA to the cells following a modified protocol from Gibco/BRL (Zhang *et al.*, 1998b; Chapter 6). Briefly, for each well 1 μg of the purified plasmid DNA was added to 100 μl of Opti-MEM (Gibco BRL) and 3.25 μl lipid (2 mg/ml) was added to another 100 μl of media. The two solutions were then mixed and incubated for 30 minutes at room temperature. After incubation, 800 μl of Opti-MEM was added to the 200 μl mixture. The final volume of 1 ml mixture was applied to each well after rinsing the cells with 1 ml of the Opti-MEM. The cells were incubated for 18 hours before the transfection mixture was removed by aspiration and replaced with standard complete growth medium.

8.2.4 Uptake Measurements

In general, uptake studies were carried out 24-44 hours post transfection as previously described in Chapter 6 (Zhang *et al.*, 1998b). Briefly, the growth medium was gently aspirated and each well was rinsed with 1 ml of phosphate-buffered saline (PBS). To initiate uptake, 0.5 ml of PBS containing 10 μM ^{14}C-TEA was added to each well. Inhibition and IC_{50} studies were carried out by adding various concentrations of unlabeled compounds to the reaction mixture. The uptake was carried out at room temperature for 20 minutes and stopped by aspiration of the uptake medium. The cell monolayers of each well were immediately washed with 2 ml of ice-cold PBS buffer once and 1 ml of the buffer twice. The cells were then solubilized with 1 ml 0.5% Triton-X 100 and 0.5 ml of sample was assayed using liquid scintillation counting (Beckman, Palo Alto, CA).

In *trans*-stimulation studies, each well of cells was preincubated with either 0.5 ml of PBS buffer (control) or 0.5 ml of PBS buffer plus the indicated amount of unlabeled compound at 37°C for one hour. Cells were then rinsed once with 2 ml of ice-cold PBS buffer and once with 1 ml of the buffer before the uptake studies were performed as described above.

The protein concentration was determined by the Bio-Rad protein assay kit (Bio-Rad, Hercules, CA), with bovine serum albumin as the standard as previously described in Chapter 6 (Zhang *et al.*, 1998b).

8.2.5 Partition Coefficient Determinations

Octanol-water partition coefficient was determined from an n-octanol and water system (Neef and Meijer, 1984). Briefly, 5 ml of 4 mM procainamide, quinine and quinidine water solution was prepared. Then each water solution was mixed with 5 ml of n-octanol by vortexing. The mixture was rotated for 2 hr at room temperature. The layers were separated by centrifugation at 2,500 rpm for 15 min. Aliquots (100 µl) from each layer were diluted to 5 ml of water or octanol. The concentration ratio of octanol to water was determined as the ratio of UV absorbance from octanol to water solutions at λ_{max}. The λ_{max} value for procainamide is 278 nm; for quinine and quinidine, the value is 330 nm.

8.2.6 Data Analysis

In general, uptake values are expressed as mean ± standard error (SE) or mean ± standard deviation (SD) as indicated in the figure legends. A minimum of two wells were used to generate a data point in each experiment. All experiments were repeated at least once on a different day using a different cell passage.

For IC_{50} studies, data were fit to the equation $V = V_0/[1+(I/IC_{50})^n]$ where V is the uptake of ^{14}C-TEA in the presence of inhibitor, V_0 is the uptake of ^{14}C-TEA in the absence

of inhibitor, I is the inhibitor concentration and n is the Hill coefficient. The Kaleidagraph fitting program (Abelbeck Software) was used to fit the data by non-linear regression.

Statistical analysis was carried out by comparing the tested compounds to the controls from the same experiments using the unpaired Student's *t*-test (Primer of Biostatistics software, Version 3, written by Stanton A. Glantz, McGraw-Hill Companies, 1991). Results were considered statistically different with a probability of $p < 0.05$.

8.2.7 Materials

HeLa cells and all the media and buffers used to maintain the cells were obtained from the UCSF Cell Culture Facility. Original stocks of HeLa cells were from American Type Culture Collection (ATCC, Rockville, MD). LIPOFECTAMINE™ and Opti-MEM™ were purchased from Gibco/BRL (Gaithersburg, MD). All chemicals were obtained from Sigma (St. Louis, MO) and Fisher (Pittsburgh, PA) or as indicated. ^{14}C-TEA (55 mCi/mmol) was purchased from American Radiolabeled Chemicals (St. Louis, MO). The n-tetraalkylammonium (n-TAA) compounds (i.e., M-methyl, E-ethyl, Pr-propyl, Bu-butyl, Pe-pentyl, and H-hexyl) and n-octanol were purchased from Aldrich Chemicals (Milwaukee, WI) and tributylmethylammonium (TBuMA) was purchased from Fluka Chemicals (Rokonkoma, NY).

8.3 Results

8.3.1 Tissue Distribution of hOCT1

The tissue distribution of hOCT1 was determined by RT-PCR using primers derived from hOCT1 cDNA (Zhang *et al.*, 1997b; Chapter 5). Although no detectable signals were observed from Northern blot analysis, bands corresponding to the full-length hOCT1 cDNA were detected in cDNA isolated from human liver, kidney and small

intestine (data not shown) as well as in cDNA isolated from human Caco-2 cells (Figure 8.1). However, the band from hOCT1 mRNA was strongest in the liver (Figure 8.1) indicating that hOCT1 mRNA transcripts are expressed in abundance in human liver.

8.3.2 Expression of hOCT1 in HeLa Cells

Previous studies in this laboratory demonstrated that hOCT1 can be transiently expressed in HeLa cells (Zhang *et al.*, 1998b; Chapter 6). In this study, we halved the amount of DNA (i.e., 1 μg DNA per well) used in transfection. With this modification, we used less lipid while maintaining a lipid to DNA ratio of 6.5:1. Under these conditions, we observed an enhancement in TEA uptake (data not shown) similar in magnitude to that observed in our previous studies (Zhang *et al.*, 1998b; Chapter 6).

8.3.3 Inhibition Studies

Cis-inhibition studies were carried out to determine whether n-TAA compounds inhibit the uptake of ^{14}C-TEA in hOCT1 DNA-transfected HeLa cells. TMA (50 μM or 10 mM) did not inhibit ^{14}C-TEA uptake (data not shown), whereas (50 μM) unlabeled TPrA, TBA, TPeA and THA significantly inhibited ^{14}C-TEA uptake with various degrees of inhibition (Figure 8.2).

The concentration dependence of the various n-TAA compounds (e.g., TEA, TPrA, TBA, TPeA, and THA) in inhibiting ^{14}C-TEA uptake was determined. To obtain IC_{50} values, data from multiple experiments were fit to an equation as described in "Materials and Methods". Figure 8.3 depicts a representative inhibition curve for TPeA. As shown in Table 8.1, IC_{50} values decreased with increasing alkyl chain lengths (or molecular weights) from 260 ± 61 μM for TEA to 3.0 ± 1.6 μM for THA.

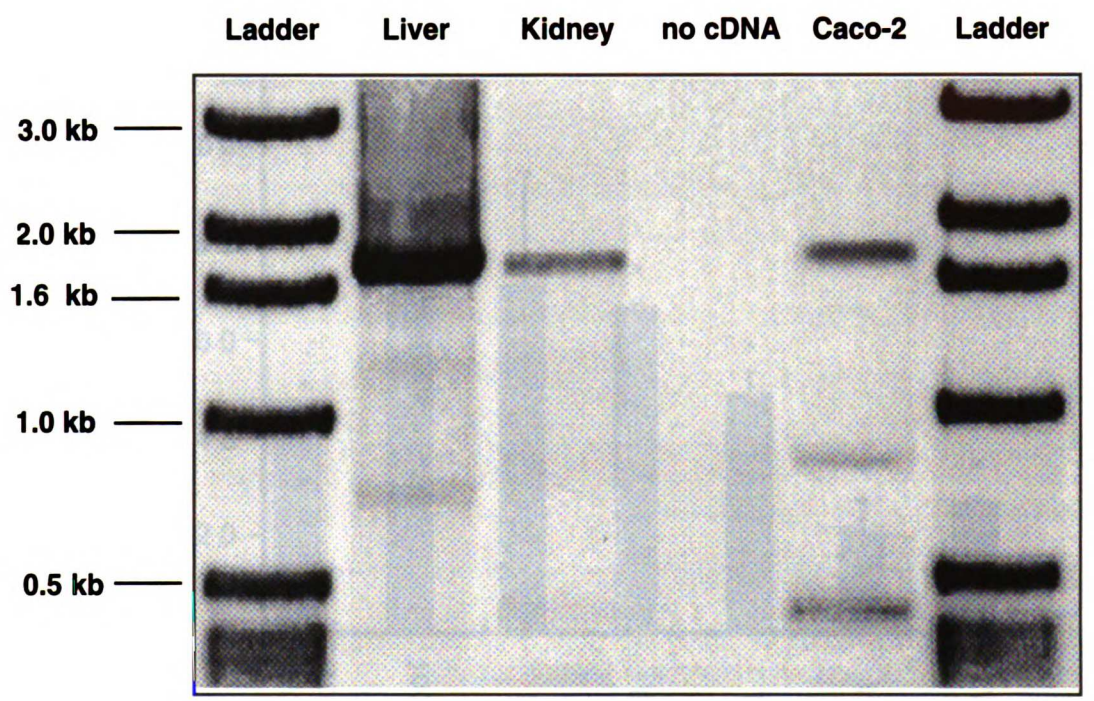

Figure 8.1 RT-PCR analysis of hOCT1 mRNA transcript expression in various tissues. mRNA from human liver, kidney and Caco-2 cells was subjected to RT-PCR using 5'-end primer and 3'-end primer (see Zhang *et al.*, 1997b and Chapter 5) to obtain a full-length DNA of the hOCT1 open reading frame. Water was used as the "no cDNA" control in PCR reactions. The PCR products were analyzed by 1% agarose gel and stained with ethidium bromide. The gel is shown as a negative version. A 1-kb DNA ladder (Gibco BRL) was used to determine the band size.

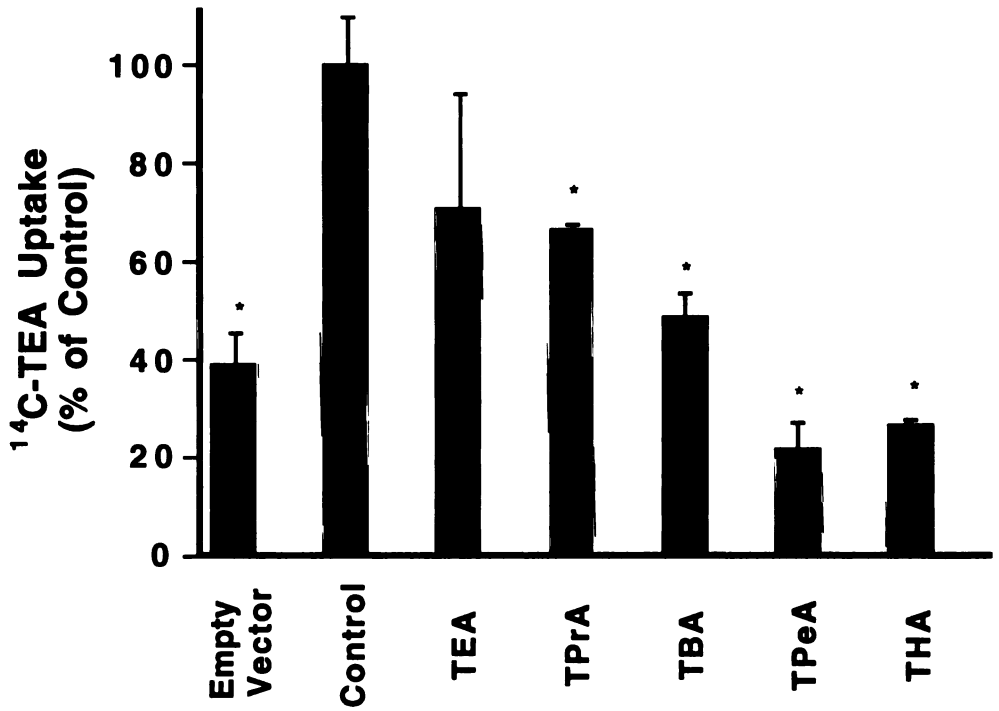

Figure 8.2 Inhibition of ^{14}C-TEA uptake by n-TAA compounds. The uptake of 10 mM ^{14}C-TEA (at 20 min) was measured in pTargeT-hOCT1-transfected HeLa cells in the presence of 50 μM of the given compounds. Controls represent uptake of ^{14}C-TEA in the pTargeT-hOCT1-transfected HeLa cells in the absence of inhibitors. Uptake of ^{14}C-TEA in the empty vector-transfected cells in the absence of inhibitors is shown as well (indicated as Empty Vector). Data represent mean ± SE (n = 6-8) obtained from three to four separate experiments. * $p < 0.05$.

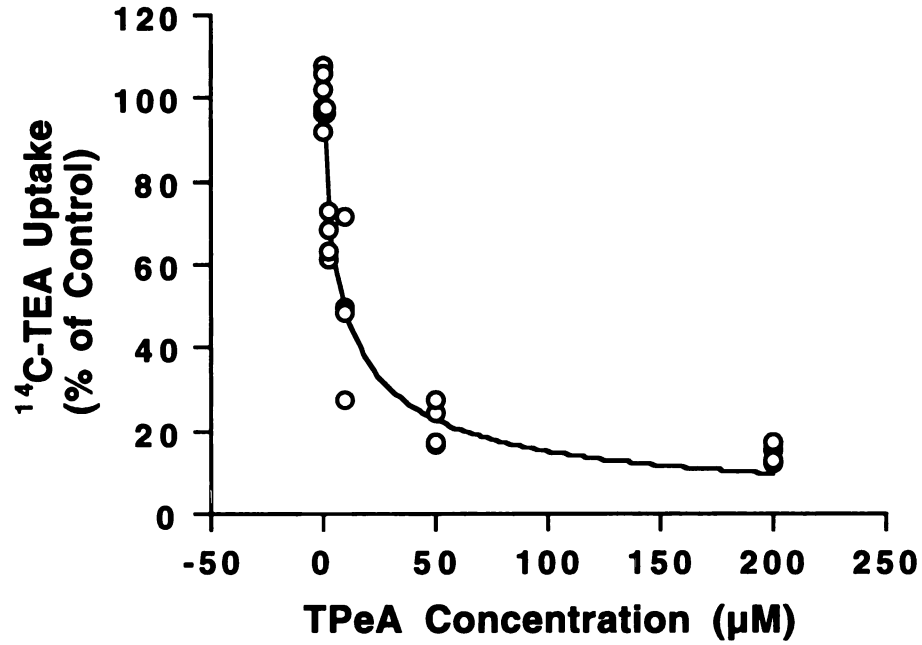

Figure 8.3 Concentration-dependent inhibition of ^{14}C-TEA uptake by TPeA in HeLa cells transfected with pTargeT-hOCT1. Initial rates of transport were determined in the presence of various concentrations of TPeA. Data represent determinations from two experiments and were fitted by non-linear regression as described in "Materials and Methods". The IC_{50} value of TPeA obtained from the fit was 8.6 ± 2.2 μM.

Table 8.1 Partition coefficients and IC_{50} values of n-tetraakylammonium compounds

Compound	MW of OC	P* (octanol/water)	LogP	IC_{50} μM
TMA	74	0.0002	-3.699	> 10,000
TEA	130	0.0027	-2.568	260 ± 61
TPrA	186	0.0457	-1.340	90 ± 28
TBuMA	200	0.0744	-1.128	66 ± 24
TBA	242	0.773	-0.112	52 ± 19
TPeA	298	13.06	1.116	8.6 ± 2.2
THA	354	220.8	2.344	3.0 ± 1.6

OC: organic cations.

* Partition coefficients derived from Neef and Meijer, 1984.

IC_{50} values were obtained by fitting data from two to four separate experiments (e.g., Figure 8.3) as described in "Materials and Methods" and are presented as means ± SD.

A semi-logrithmic plot of IC_{50} values versus alkyl chain length (N) resulted in a straight line (i.e., log (IC_{50}) = -0.490 • N + 3.46, where N = alkyl chain length, r^2 = 0.990) (Figure 8.4) suggesting that there is a good correlation between IC_{50} values and alkyl chain length (or alternatively molecular weight). Since alkyl chain length is related to the hydrophobicity of these compounds, we further determined whether there was a correlation between IC_{50} and partition coefficient (P) because hydrophobicity (or lipophilicity) can be expressed as the partition coefficient between octanol and an aqueous solution.

Previous studies have demonstrated that the molecular weights (MW) and partition coefficients (P, octanol/water) of "homologous" monoquaternary ammonium compounds are highly correlated (Neef and Meijer, 1984). Based on data in the literature (Neef and Meijer, 1984), we plotted MW versus log(P) (Figure 8.5), and obtained a linear relationship, i.e., MW = 45.6 • log (P) + 247, r^2 = 0.935. Using this equation, we derived P for the various n-TAA compounds used in this study (Table 8.1). As a consequence, a linear relationship was observed from a double-logrithmic plot of IC_{50} versus P, i.e., log (IC_{50}) = -0.395 • log (P) + 1.44, r^2 = 0.988 (Figure 8.6).

To determine whether such a trend is also apparent for other quaternary n-alkylammonium compounds with different side-chain lengths, we determined the IC_{50} value of tributylmethylammonium (TBuMA) in inhibiting TEA uptake in HeLa cells expressing hOCT1. The IC_{50} for TBuMA (66 ± 24 μM) was plotted against P of TBuMA (0.0744). As shown in Figure 8.6, TBuMA also fit to the straight line.

Many organic cations, especially cationic drugs, are non-aliphatic. Accordingly, we also examined the relationship of IC_{50} values and partition coefficients for nonaliphatic organic cations, e.g., procainamide (type I), quinine (type II), quinidine (type II), and vecuronium (type II). Octanol-water partition coefficient values of procainamide, quinine and quinidine were determined. As listed in Table 8.2, P for procainamide is 0.00261, for quinine is 0.434, and for quinidine is 0.413.

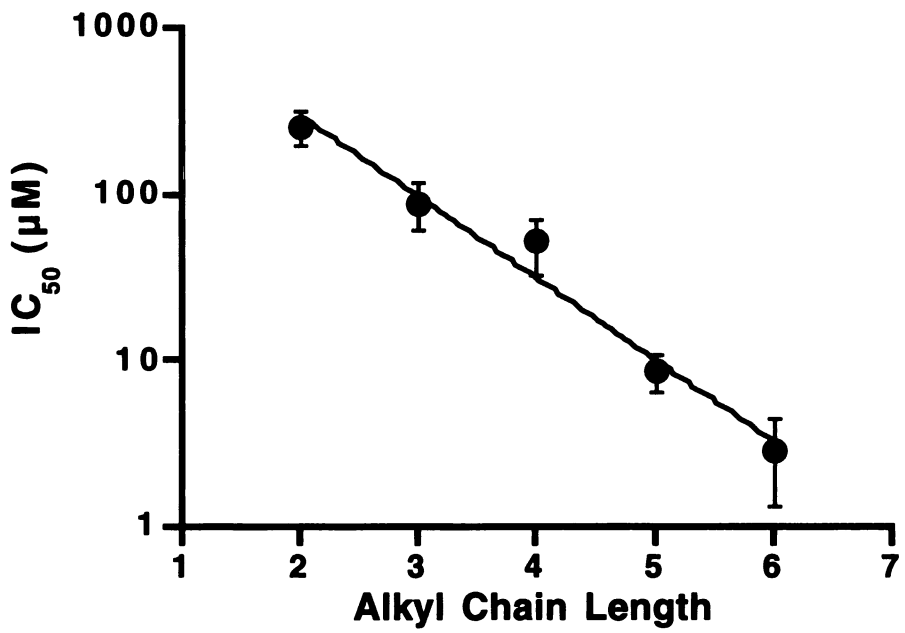

Figure 8.4 Relationship between IC_{50} values in inhibiting ^{14}C-TEA uptake in HeLa cells expressing hOCT1 and alkyl chain length (N) of n-TAA compounds. Each IC_{50} value represents the mean ± SE fitted with data from two to four separate experiments by non-linear regression as described in "Materials and Methods". The fitted equation is $\log (IC_{50}) = -0.490 \bullet N + 3.46$, $r^2 = 0.990$.

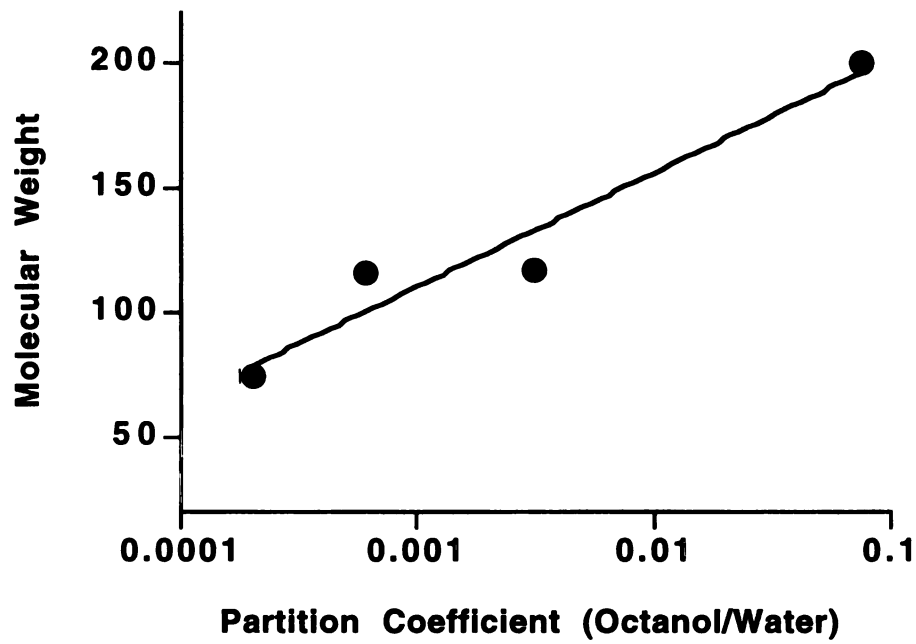

Figure 8.5 Relationship between molecular weight (MW) of quaternary ammonium compounds and partition coefficient (P) determined from octanol/water solution (data cited from Neef and Meijer, 1984). The fitted equation is MW = 45.6 • log (P) + 247, $r^2 = 0.935$.

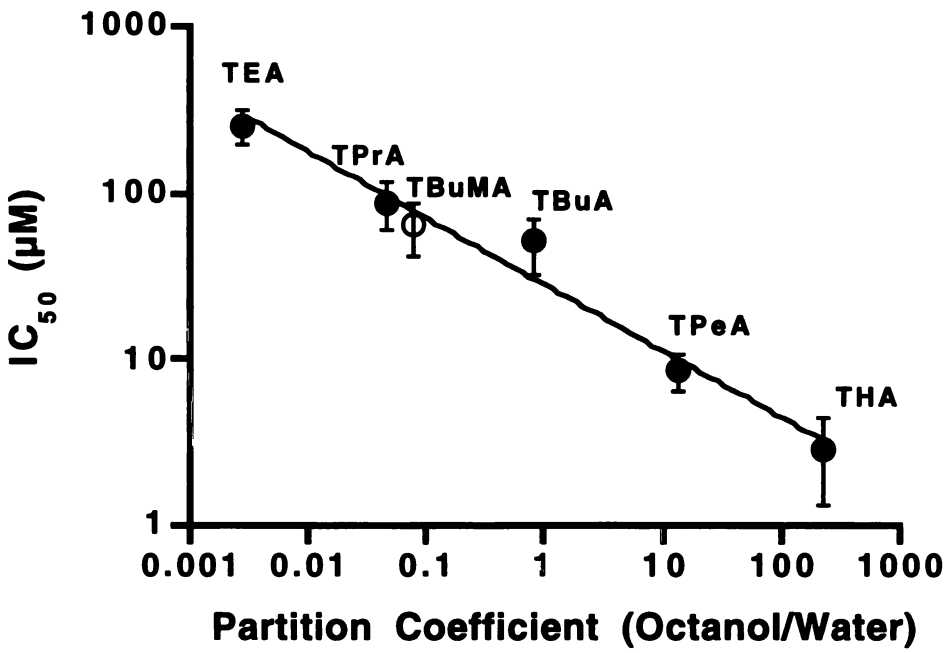

Figure 8.6 Relationship between IC_{50} values in inhibiting ^{14}C-TEA uptake in HeLa cells expressing hOCT1 and partition coefficient (P) values of n-TAA compounds estimated from Figure 8.5. The fitted equation is log (IC_{50}) = -0. 395 • log (P) + 1.44, r^2 = 0.988. Data for TBuMA (open circle) was fitted into the correlation curve.

Table 8.2 Partition coefficients and IC_{50} values of non-aliphatic organic cations

Compound	MW of OC	P (octanol/water)	LogP	IC_{50} μM
Procainamide	235	0.00261	-2.583	107 ± 46
Vecuronium	558	0.165*	-0.782	237 ± 8
Quinine	324	0.434	-0.362	22.6 ± 5.5
Quinidine	324	0.413	-0.384	23.4 ± 6.4

OC: organic cations.

* Partition coefficient cited from Proost *et al.*, 1997.

IC_{50} values were obtained by fitting data from two to four separate experiments as described in "Materials and Methods" and are presented as means ± SD.

8.3.4 Trans-Stimulation Studies

Trans-stimulation studies have been used previously in determining whether an inhibitor is also a substrate of hOCT1, i.e., translocated by hOCT1 (Zhang *et al.*, 1998b; Chapter 6). We preincubated hOCT1 plasmid DNA-transfected HeLa cells with various concentrations of unlabeled TEA. We observed that the magnitude of the *trans*-stimulation effect increased with increasing *trans*-TEA concentrations, and it was saturable at high concentrations. When we incubated the cells with a concentration representing 10 times the K_m or K_i value, i.e., 2 mM of TEA, the *trans*-stimulation effect was maximum (data not shown). Therefore, we preincubated cells with concentrations approximately 10 times the K_m or K_i value of unlabeled test compounds under the assumption that this condition would produce a maximum *trans*-stimulation effect. As shown in Figure 8.7, after preincubating hOCT1 plasmid DNA-transfected HeLa cells with TEA (2 mM), TPrA (1 mM), TBuMA (1 mM), TBA (0.5 mM) for one hour at 37°C, ^{14}C-TEA uptake was significantly enhanced ($p < 0.05$) and the enhanced effect decreased with increasing alkyl chain length. This *trans*-stimulation effect was not observed in empty-vector transfected HeLa cells. Preincubating hOCT1 DNA-transfected cells with TMA (10 mM), or TPeA (0.2 mM) did not result in a significant change in ^{14}C-TEA uptake, whereas preincubation of cells with 0.1 mM THA resulted in a significant decrease (apparent "*trans*-inhibition") of ^{14}C-TEA uptake ($p < 0.05$).

Trans-stimulation studies were also performed with nonaliphatic organic cations, i.e., procainamide, vecuronium, quinine and quinidine, which were previously shown to inhibit ^{14}C-TEA uptake via hOCT1 (Zhang *et al.*, 1998b; Chapter 6) to determine whether they are translocated by hOCT1. Figure 8.8 demonstrates that preincubating hOCT1 DNA-transfected cells with procainamide (1 mM) *trans*-stimulated TEA uptake, whereas preincubating cells with vecuronium (2 mM), quinine (0.2 mM) and quinidine (0.2 mM) did not.

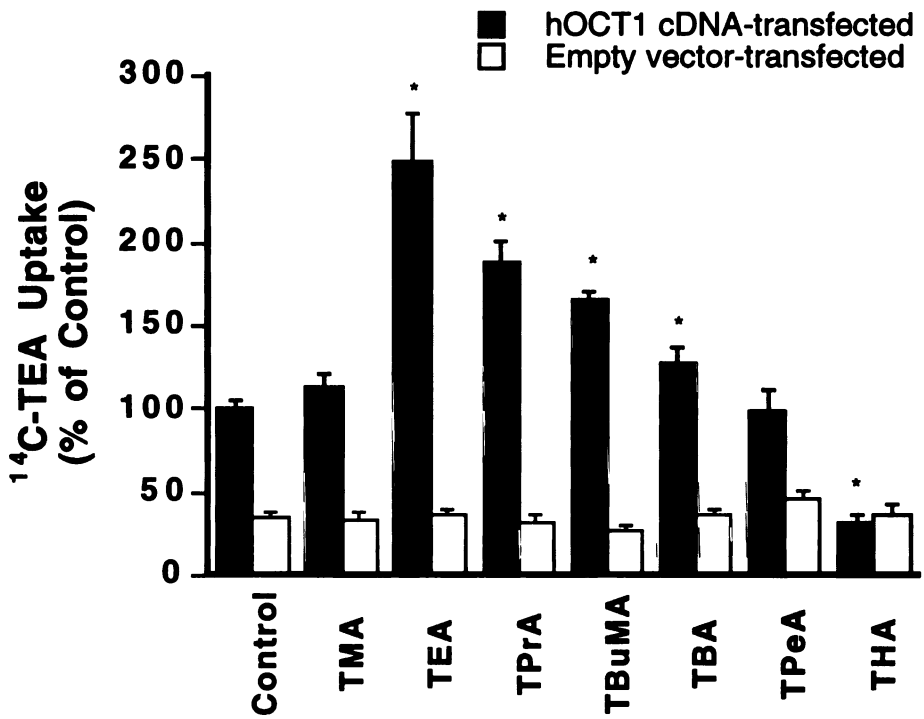

Figure 8.7 *Trans*-stimulation of ^{14}C-TEA uptake in pTargeT-hOCT1 transfected HeLa cells. The uptake (at 20 min) of ^{14}C-TEA (10 μM) was measured after a 60 min pre-incubation (followed by washing) of the hOCT1 DNA-transfected cells (dark bars) and empty vector-transfected cells (open bars) with PBS (control) or PBS containing 10 mM TMA, 2 mM TEA, 1 mM TPrA, 1 mM TBuMA, 0.5 mM TBA, 0.2 mM TPeA, or 0.1 mM THA, respectively at 37°C. Data represent the mean ± SE (n = 4-10) obtained from two to five separate experiments. * $p < 0.05$ as compared to the uptake value in hOCT1 DNA-transfected cells preincubated with PBS buffer.

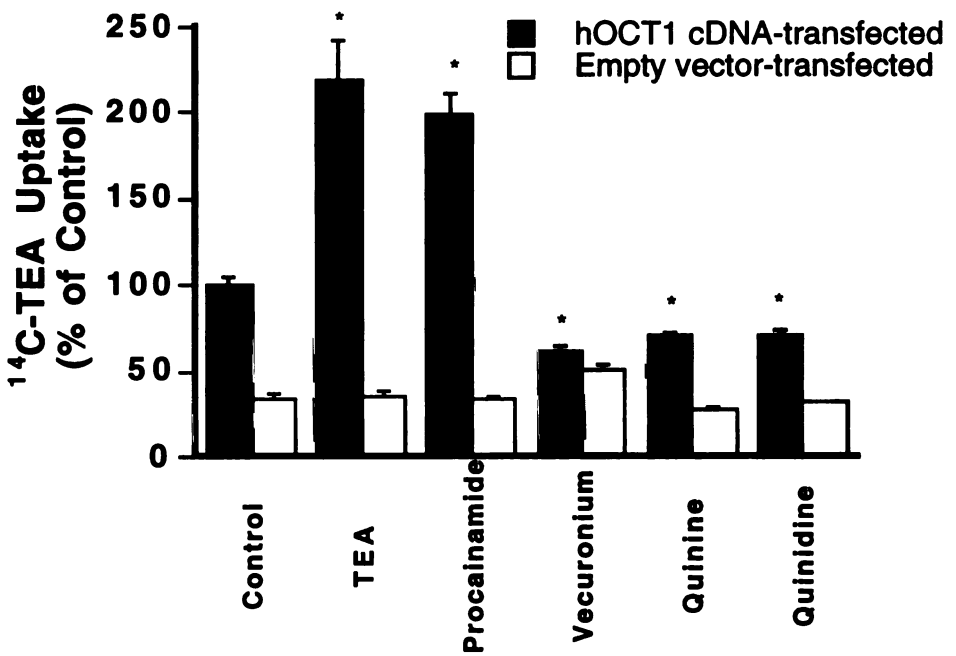

Figure 8.8 *Trans*-stimulation of ^{14}C-TEA uptake in pTargeT-hOCT1 transfected HeLa cells. The uptake (at 20 min) of ^{14}C-TEA (10 μM) was measured after a 60 min pre-incubation of the hOCT1 DNA-transfected cells (dark bars) and empty vector-transfected cells (open bars) with PBS (control) or PBS containing 2 mM TEA, 1 mM procainamide, 2 mM vecuronium, 0.2 mM quinine, or 0.2 mM quinidine, respectively at 37°C. Data represent the mean ± SE (n = 4-8) obtained from two to four separate experiments. * $p < 0.05$ as compared to the uptake value in hOCT1 DNA-transfected cells preincubated with PBS buffer.

8.4 Discussion

Secretory transporters in the liver, kidney and intestine play a role in the elimination of organic cations from the body (Miyamoto *et al.*, 1988; Oude Elferink *et al.*, 1995; Pritchard and Miller, 1993; Tomita *et al.*, 1997; Turnheim and Lauterbach, 1977a and 1977b; Zhang *et al.*, 1998a; Chapter 1). hOCT1 appears to be predominantly involved in the uptake of organic cations in the liver. However, data obtained in this study as well as in our previous study as in Chapter 5 (Zhang *et al.*, 1997b) suggest that hOCT1 may also play a role in the renal and intestinal secretion of organic cations. Namely, RT-PCR studies demonstrated that hOCT1 mRNA transcripts were present, although in much lower abundance, in kidney and Caco-2 cells, a human colon carcinoma cell line (Figure 8.1).

Functional studies of hOCT1 utilizing heterologous expression systems (e.g., *Xenopus laevis* oocytes and transfected HeLa cells) have demonstrated that various organic cations as well as some neutral and anionic compounds inhibit the transport of model organic cations by hOCT1 (Zhang *et al.*, 1997b and 1998b; Chapters 5 and 6). The goal of the current study was to use a series of n-TAA compounds to systematically determine the effect of hydrophobicity on inhibition potencies of compounds in interacting with the human organic cation transporter, hOCT1. Furthermore, the effect of hydrophobicity on the rate of transport by hOCT1 was determined.

Initially, a good correlation between IC_{50} values and alkyl chain length (or molecular weight) was found. Namely, we observed that n-TAA compounds with the longer alkyl chain lengths were the more potent inhibitors of hOCT1. This observation is consistent with what is generally found for these compounds in inhibiting organic cation transport (Dantzler *et al.*, 1991; Groves *et al.*, 1994; Ullrich *et al.*, 1991; Wright *et al.*, 1995). In the literature, a linear relationship between partition coefficient (P) values of the quaternary ammonium cations (including n-TAAs) and molecular weights has been

reported (Neef and Meijer, 1984). We used this relationship to estimate the P values of several n-TAAs (Table 8.1). A good correlation between IC_{50} and P in a double-logrithmic plot was generated (i.e., $\log(IC_{50}) = -0.395 \bullet \log(P) + 1.44$, $r^2 = 0.988$) (Figure 8.6). The data indicate that for inhibition, binding affinity is increased with increasing free energy to transfer a substance from octanol to water. This correlation also applies to TBuMA for which the four alkyl chains are not of equal length (Figures 8.4 & 8.6). However, such correlation does not apply to non-aliphatic organic cations, i.e., the correlation coefficient (r^2) was reduced from 0.988 to 0.403 when data for non-aliphatic compounds were included in the same plot as Figure 8.6. These data suggest that for the nonaliphatic compounds factors other than hydrophobicity such as steric effect and three-dimensional fold of the compound also affect the potency of interaction (Table 8.2).

Inhibition does not necessarily imply that a compound is also translocated by a transporter. Since radiolabeled n-TAA compounds are not available except for TEA, we used *trans*-stimulation studies to determine whether the n-TAA compounds are also substrates of hOCT1. *Trans*-stimulation is a frequently-used method to test whether two molecules share a common transport pathway (Dantzler *et al.*, 1991; Holohan and Ross, 1980; Miyamoto *et al.*, 1988). If the presence of the test compound on the opposite side (*trans*) of the membrane results in an enhanced flux of the radiolabeled probe, the test compound is considered to be a substrate for the same transporter as the probe, and vice versa. *Trans*-stimulation has been used previously in the hOCT1 DNA-transfected cell line to determine whether an inhibitor is also a substrate (Zhang *et al.*, 1998b; Chapter 6).

TMA did not *trans*-stimulate TEA uptake which is consistent with our inhibition study suggesting that TMA does not interact with hOCT1. For all other n-TAA compounds, we observed that the compounds with the shorter alkyl chain lengths (or smaller P, i.e., less lipophilic), TEA, TPrA, TBuMA and TBA, demonstrated *trans*-stimulation effects. However, the magnitude of the effect decreased with increasing alkyl chain length suggesting that the transport rate was decreased. In contrast, compounds with

a longer alkyl chain length (or larger P, i.e., more lipophilic), TPeA and THA, did not demonstrate a *trans*-stimulation effect. Moreover, THA demonstrated an apparent "*trans*-inhibition" effect suggesting that the transporter loaded with THA has a slower turnover rate than that of the unloaded transporter. The same situation may also occur when preincubating the cells with quinine, quinidine and vecuronium.

Previously, it was shown that lipophilicity is a determinant factor for hepatobiliary transport of a series of monoquaternary ammonium compounds (type I) and neuromuscular blocking agents (NMBA) (type II) in rat, resulting in an increase in hepatic clearance with increasing lipophilicity (Neef and Meijer, 1984; Proost *et al.*, 1997). These results are in contrast to our data suggesting that with increasing lipophilicity, the transport rate of these compounds by hOCT1 decreases. The discrepancies between our data and the previous studies in the intact liver may be explained in several ways. First, multiple transporters on both the canalicular and sinusoidal membrane contribute to hepatobiliary secretion in the intact organ or animal. These transporters may be rate limiting in the hepatic clearance of various organic cations in the intact animal. Second, hOCT1 is a transporter cloned from human liver; species differences between the structure activity relationships between rat and human transporters may be present. Previously, Wright and coworkers observed notable species differences in the effect of hydrophobicity on transport of organic cations in rat and rabbit kidney preparations (Groves *et al.*, 1994; Ullrich *et al.*, 1991).

Consistent with our data demonstrating that the less hydrophobic, smaller molecular weight n-TAA compounds were substrates of hOCT1, we observed that the smaller molecular weight non-aliphatic compound (type I), i.e., procainamide, was also a substrate (Figure 8.8). These data suggest that hOCT1, like rOCT1, may represent a "type I" organic cation transporter. It contains a non-specific hydrophobic interaction site, however, it does not translocate (or poorly translocates) larger molecules. Further studies are needed to determine whether hOCT1 is a "type I" organic cation transporter.

In summary, our observations suggest that the longer the alkyl chain length (i.e., the more hydrophobic and bulkier), the higher the affinity of the tetraalkylammonium compounds for hOCT1, but the slower the rate of transport (i.e., poorer substrate) by hOCT1. hOCT1 may represent a "type I" organic cation transporter in human liver which accepts smaller organic cations as its substrates. The correlation observed between IC_{50} values and partition coefficients can be used to predict the IC_{50} values of various n-alkylammonium compounds in interacting with hOCT1. A balance between hydrophobic and hydrophilic properties is required for efficient transport of an organic cation by hOCT1.

CHAPTER 9

SUMMARY/CONCLUSIONS AND FUTURE PERSPECTIVES [1]

9.1 Introduction

Detoxification mechanisms including enzymes involved in metabolism (e.g., cytochrome P450) and secretory transporters (e.g., P-gp, MRP) in the kidney, liver and intestine are critical in the body's defense against deleterious xenobiotics (Barrand *et al.*, 1997; Borst, 1997; Ernest and Bello-Reuss, 1998; Evers *et al.*, 1998; Ferry, 1998; Leveque and Jehl, 1995; Ling, 1997; Loe *et al.*, 1996; Meijer *et al.*, 1997; Yamazaki *et al.*, 1996). Organic cation transporters play a key role in the elimination of many endogenous amines and xenobiotics including a variety of clinically used drugs. For years, our knowledge of the mechanisms of organic cation transport has been based primarily on studies in isolated tissue preparations including cell culture and purified brush border and basolateral membrane vesicles. From these studies, multiple mechanisms for organic cation transport have been proposed (Pritchard and Miller, 1993; Zhang *et al.*, 1998a; Chapter 1).

Since I started my dissertation research, great progress has been made in the cloning of organic cation transporters both in our and other laboratories. These studies have paved the way to an enhanced understanding of the multiple mechanisms involved in the transport of organic cations (Gorboulev *et al.*, 1997; Grundemann *et al.*, 1994 and

[1] Part of this chapter was published in *Annual Review of Pharmacology and Toxicology* 38: 431-460, 1998. Permission from the publisher is included in "Acknowledgments".

1997; Kekuda *et al.*, 1998; Okuda *et al.*, 1996; Tamai *et al.*, 1997; Terashita *et al.*, 1998; Wu *et al.*, 1998a and 1998b; Zhang *et al.*, 1997a and 1997b). With the availability of cloned transporters, it is now possible to delineate the functional roles and mechanisms involved in the regulation of the various transporters. Furthermore, structure function relationships can be established and antibodies can be developed to localize the transporters to various tissues in the body to understand their physiological roles. From these studies a more complete understanding of the mechanisms of organic cation transport in the body can be established.

In this conclusion chapter, I will focus largely on the dramatic progress made in both this and other laboratories in understanding the molecular and functional characteristics of cloned organic cation transporters. Future directions in the field of organic cation transport will be discussed.

9.2 Molecular and Functional Characteristics of Cloned Organic Cation Transporters (OCT)

Several transport proteins including organic cation and organic anion transporters that have been identified by molecular cloning seem to be members of a superfamily, the major facilitator superfamily (MSF), as proposed by Marger and Saier (1993). Sequence alignments and hydropathy analysis suggest that these organic cation and anion transporters exhibit greater homology to each other than to other members of the MSF family in terms of both the sequence (> 25% identity) and the predicted secondary structure. They comprise a distinct facilitated transporter superfamily which has been tentatively termed as the amphiphilic solute facilitator (ASF) family (Schomig *et al.*, 1998). This family includes the organic cation transporter (OCT) family, OCT1 (Grundemann *et al.*, 1994; Terashita *et*

al., 1998; Zhang *et al.*, 1997a and 1997b), OCT2 (Gorboulev *et al.*, 1997; Grundemann *et al.*, 1997; Okuda *et al.*, 1996), OCT3 (Kekuda *et al.*, 1998; Wu *et al.*, 1998a), OCTN1 (Tamai *et al.*, 1997), OCTN2 (Wu *et al.*, 1998b), and organic anion/dicarboxylate exchanger, OAT1 (organic anion transporter 1) (Sekine *et al.*, 1997; Sweet *et al.*, 1997), plus putative transport proteins of unknown function, NLT (Simonson and Iwanij, 1995), NKT (Lopez-Nieto *et al.*, 1997), UST1 and UST2 (Schoemig *et al.*, 1998). I will focus on the OCT family: OCT1, OCT2, OCT3, OCTN1 and OCTN2 (Table 9.1), especially OCT1.

Table 9.1 Pairwise comparison of amino acid sequences of selected members of the OCT family

	rOCT1	rbOCT1	hOCT1	rOCT2	pOCT2	hOCT2	rOCT3	OCTN1	OCTN2
rOCT1	—	**82**[a]	**78**	**67**	**67**	**68**	**48**	**33**	**34**
rbOCT1	85[b]	—	**80**	**65**	**69**	**68**	**48**	**32**	**33**
hOCT1	82	83	—	**64**	**69**	**70**	**48**	**32**	**34**
rOCT2	74	72	73	—	**81**	**81**	**49**	**32**	**33**
pOCT2	73	75	75	90	—	**85**	**50**	**32**	**32**
hOCT2	74	76	76	84	89	—	**49**	**33**	**33**
rOCT3	57	57	57	59	60	60	—	**30**	**31**
OCTN1	40	40	39	40	41	41	38	—	**77**
OCTN2	41	40	42	41	42	42	40	82	—

[a] Percentage identity (expressed in *bold*) and [b] percentage similarity were computed from sequence alignments using the Gap program in the Genetics Computer Group (Wisconsin Package, Version 9; Madison, WI) software package.

9.2.1 OCT Family: OCT1

9.2.1.1 rOCT1

Because of technical difficulties in isolating membrane proteins, the molecular structure of organic cation transporters was not elucidated until recently. Following initial studies in *Xenopus laevis* oocytes demonstrating the feasibility of expression cloning of organic cation transporters (Chan *et al.*, 1995; Chun *et al.*, 1997b; Hori *et al.*, 1992; Takeda *et al.*, 1994; Zhang *et al.*, 1995; Chapter 3), the first organic cation transporter (rOCT1) was cloned from a rat kidney cDNA library (Tables 9.1, 9.2, and 9.3) (Grundemann *et al.*, 1994). The cDNA of rOCT1 is 1,882 bp in length, including its poly-A tail. A protein of 556 amino acids with 11 or 12 putative transmembrane domains is encoded by the rOCT1 cDNA. The gene of rOCT1, *Roct1*, was mapped to chromosome 1q11-12 (Koehler *et al.*, 1996).

Functional studies in *Xenopus laevis* oocytes (Grundemann *et al.*, 1994) and in transiently transfected human embryonic kidney (HEK) 293 cells (Martel *et al.*, 1996a) demonstrated that rOCT1 is polyspecific, transporting small organic cations such as TEA and MPP^+. Electrophysiologic studies in oocytes injected with rOCT1 cRNA indicated that bulkier organic cations such as pancuronium, quinine, and D-tubocurarine, monoamine neurotransmitters (e.g., dopamine, serotonin), and polyamines such as spermine and spermidine may also be transported by rOCT1 since they induced inward currents in oocytes (Busch *et al.*, 1996a and 1996b). However, recent studies demonstrated that a compound (e.g., quinidine) could induce large inward currents without being translocated (Nagel *el al.*, 1997). Therefore, electrophysiology techniques do not represent a reliable way to determine whether or not a compound is a bona fide substrate of a cloned transporter. rOCT1 is potential sensitive and may represent the electrogenic organic cation transporter located on the basolateral membrane of the kidney (or liver) (Grundemann *et al.*, 1994). Direct evidence for its location on the basolateral side will require further study

(e.g., antibody studies). Northern blot analysis as well as *in situ* hybridization indicated that the mRNA transcripts of rOCT1 are not only expressed in the kidney (proximal tubules), but also in the liver (hepatocytes), small intestine (enterocytes of villi and crypts), and colon (Table 9.2) (Grundemann *et al.*, 1994).

9.2.1.2 rOCT1A

Recently, our laboratory cloned a novel splice variant of rOCT1, termed rOCT1A, from rat kidney (Table 9.2) (Zhang *et al.*, 1997a; Chapter 4). Initial studies demonstrated that rOCT1A is encoded by a unique mRNA transcript spliced from the same gene that encodes rOCT1. rOCT1A has functional characteristics similar to those of rOCT1. Although the tissue distribution of the mRNA transcripts of rOCT1A is qualitatively similar to that of rOCT1, there are apparent quantitative differences in the relative amounts of the mRNA transcript of each isoform in the different tissues. For example, the ratio of rOCT1 to rOCT1A mRNA transcripts is higher in the liver in comparison to the kidney and intestine. Both rOCT1 and rOCT1A mRNA transcripts are located in all of the regions of rat small intestine (i.e., duodenum, jejunum, ileum) and colon (Zhang *et al.*, 1996; Chapter 4). However, further studies are needed to determine if there are quantitative differences in the expressed levels of the isoforms.

Mutagenesis and *in vitro* translation studies demonstrated that there are at least two open reading frames of rOCT1A mRNA, i.e., at least two corresponding proteins were translated (Chapter 4; data not shown). Furthermore, the stop codon of the first reading frame is not required for the second reading frame to be translated (data not shown). These data strongly suggest that rOCT1A mRNA is polycistronic.

Table 9.2 General characteristics of cloned organic cation transporters

	Species	Protein (a.a.)	Tissue Distribution	Known Substrates
OCT1				
rOCT1	rat	556	kidney, liver intestine, etc.	TEA, MPP^+, NMN, choline, dopamine
rOCT1A	rat	430	kidney, liver intestine, etc.	TEA
rbOCT1	rabbit	554	liver (predominant), kidney, intestine, etc.	MPP^+
hOCT1	human	553/554	liver (predominant), kidney, intestine, etc.	TEA, MPP^+, NMN
OCT2				
rOCT2	rat	593	kidney (predominant), brain	TEA, MPP^+, guanidine, cimetidine
pOCT2	pig	554	—	TEA
hOCT2	human	555	kidney, brain, placenta, etc.	TEA, MPP^+, NMN, choline
OCT3				
rOCT3	rat	551	placenta (abundant), intestine, heart, etc.	TEA, MPP^+, guanidine
OCTN1				
OCTN1	human	551	fetal liver, kidney, etc. adult kidney, trachea, cancer cell lines, etc.	TEA
OCTN2				
OCTN2	human	557	placenta, kidney, heart, pancreas, brain, etc.	TEA

Table 9.3 Interactions of various compounds with rOCT1, hOCT1, rOCT2 and hOCT2

	K_m or K_i μM			
	OCT1		**OCT2**	
	rOCT1 [a]	hOCT1 [b]	rOCT2 [c]	hOCT2 [d]
TEA [e]	95	229	500 (357)	76
MPP^+ [e]	9.6	12.3	17 (4.4)	19
NMN	340 [e]	7,715 [f]	800 [e]	266 [f]
Desipramine [f]	2.8	5.36	10	16
Procainamide [f]	13	73.9	1,500	50
Tetramethylammonium [f]	1,000	> 10,000	770	180
Tetrapentylammonium [f]	0.43	7.46	—	1.5
Quinine [f]	0.9	22.9	14	3.4
3-*O*-methylisoprenaline [f]	43	—	2100	570
Decynium-22 [f]	0.36	2.73	0.45	0.1
Corticosterone [f]	72	7.02	5	—

All functional studies are carried out in *X. laevis* oocytes, transfected HEK 293 cells or transfected HeLa cells (see individual references).

[a] Data cited from Grundemann *et al.*, 1994.

[b] Data cited from Zhang *et al.*, 1998b, Chapters 6 and 8.

[c] Data cited from Koepsell, 1998. Data obtained in this laboratory are in parentheses (Chapter 3 and L Zhang, unpublished data).

[d] Data cited from Gorboulev *et al.*, 1997.

[e] K_m values.

[f] K_i values.

9.2.1.3 hOCT1

Recently, a human organic cation transporter (hOCT1) was cloned from liver (Tables 9.1, 9.2 and 9.3) (Gorboulev *et al.*, 1997; Zhang *et al.*, 1997b; Chapter 5). hOCT1 cDNA is approximately 1,870 bp in length and encodes a protein of 553 or 554 amino acids. hOCT1 is 78% identical to rOCT1 and 64% identical to rOCT2.

The initial functional characterization of hOCT1 was carried out using the *X. laevis* oocyte expression system (Zhang *et al.*, 1997b; Chapter 5). An eight-fold enhanced uptake of ^{3}H-MPP^{+} was observed in hOCT1 cRNA-injected oocytes in comparison to that in water-injected oocytes. ^{3}H-MPP^{+} uptake was saturable (K_m of 14.6 μM) and was sensitive to membrane potential. MPP^{+} uptake via hOCT1 was inhibited by structurally diverse organic cations. Both smaller and bulkier organic cations such as TEA, choline, procainamide, verapamil, decynium-22 and quinine potently inhibited ^{3}H-MPP^{+} uptake mediated by hOCT1 in oocytes. TEA was also a permeant of hOCT1 with a K_m value of 163 μM. Besides organic cations, other compounds such as taurocholate (bile acid), inosine and thymidine (nucleosides) at 1 mM also significantly inhibited ^{3}H-MPP^{+} uptake whereas D-glucose and PAH did not (at 5 mM).

Recently, a mammalian expression system, HeLa cells transiently transfected with the cDNA of hOCT1, was developed in this laboratory to study the interactions of various compounds with hOCT1 (Zhang *et al.*, 1998b; Chapter 6). In this system, transient expression of hOCT1 activity was observed between 24 and 72 hours post-transfection, with maximal expression at approximately 40 hours. TEA transport was temperature-dependent and saturable with a K_m of 229 μM. Organic cations including clonidine (K_i of 0.55 μM), acebutolol (K_i of 96 μM), quinine (K_i of 23 μM), quinidine (K_i of 18 μM) and verapamil (K_i of 2.9 μM) potently inhibited ^{14}C-TEA uptake. In addition, the neutral compounds, corticosterone (K_i of 7.0 μM) and midazolam (K_i of 3.7 μM), also potently

inhibited ^{14}C-TEA uptake. Collectively, these data indicate that TEA transport via hOCT1 can be inhibited not only by organic cations but also by various other compounds. However, inhibitors may not be substrates of the transporter. For example, cimetidine, an H_2-receptor antagonist, has been used as a model compound for renal organic cation transport. Although it inhibits ^{14}C-TEA uptake in hOCT1 cDNA transfected HeLa cells (K_i of 166 μM), no significant ^{3}H-cimetidine uptake was observed in the cDNA transfected cells versus cells transfected with "empty" vector, i.e. vector not containing the cDNA of hOCT1. These data suggest that cimetidine is not translocated appreciably by hOCT1 under these experimental conditions. Further studies are needed to determine whether the compounds found to inhibit the transport of the model organic cations are also substrates of hOCT1 and the role that hOCT1 plays in the elimination and disposition of these compounds.

To determine whether a compound is a substrate for the transporter, radiolabeled compound is needed to directly demonstrate its translocation. However, radiolabeled compounds are not always available. As an alternative, *trans*-stimulation studies can be carried out for those transporters which can operate in both directions. For example, as described in Chapter 6 we demonstrated that hOCT1 can operate as an exchanger (Zhang *et al.*, 1998b). Preincubating hOCT1 cDNA transfected HeLa cells with saturating concentrations of unlabeled TEA *trans*-stimulated TEA uptake (influx). However, if a compound (e.g., cimetidine) is not translocated by the transporter, such a *trans*-stimulation phenomenon is not observed. If a compound (e.g., decynium-22) binds tightly to the transporter, we observed an apparent *trans*-"inhibition" effect. We subsequently used *trans*-stimulation studies to determine whether an inhibitor is also translocated by hOCT1 (Chapters 7 and 8).

Using HeLa cell expression system, we carried out drug interaction studies to determine the role of hOCT1 in the elimination of organic cations, especially therapeutically important drugs. We found that cationic compounds with large molecular weights, e.g.,

azole compounds, ketoconazole; HIV protease inhibitors, indinavir, nelfinavir, ritonavir, and saquinavir, potently inhibited TEA transport by hOCT1 (Chapter 7; Appendix). However, *trans*-stimulation studies demonstrated that these compounds are poorly translocated by hOCT1. Thus, larger, hydrophobic compounds will interact with cationic drug transport mediated by hOCT1 leading to potential drug-drug interactions.

To study the details of substrate selectivity of hOCT1, we used a series of n-TAA compounds as probes (Chapter 8). We found that with increasing alkyl chain length, n-TAA compounds were more potent inhibitors but poorer substrates. These data also indicate that hOCT1 may represent a liver transporter which accepts smaller, more hydrophilic organic cations as substrates. Furthermore, hOCT1 does not exhibit stereoselectivity which is consistent with its polyspecificity (Zhang *et al.*, 1998b; Chapter 6; Appendix).

hOCT1 is 78% identical to rOCT1, however, it shows significant differences in tissue distribution and functional characteristics from those of rOCT1 (Zhang *et al.*, 1997b; Chapter 5). Namely, hOCT1 mRNA transcripts are expressed primarily in the human liver, whereas rOCT1 mRNA transcripts are expressed in the rat kidney, liver, small intestine, and colon (Table 9.2) (Gorboulev *et al.*, 1997; Grundemann *et al.*, 1994; Zhang *et al.*, 1997b; Chapter 5). Bulkier organic cations such as decynium-22 and vecuronium are less potent in inhibiting organic cation transport in oocytes expressing hOCT1 than those expressing rOCT1 (Table 9.3) (Grundemann *et al.*, 1994; Zhang *et al.*, 1997b; Zhang *et al.*, 1998b; Chapters 5 and 6). The cloning of hOCT1 provides the opportunity to define the pharmacological profile of this gene product, and to elucidate its functional roles in the hepatic disposition of many clinically-relevant drugs and other xenobiotics.

Splice variants of hOCT1 were identified by PCR cloning. Sequencing of splice variants which was confirmed by genomic DNA sequencing suggests that there are at least three splice variants of hOCT1, termed hOCT1A(Δ100), hOCT1B(Δ113), and hOCT1C

(Δ213) (data not shown). Unlike rOCT1A which is the splice variant of rOCT1 with a deletion at 5'-end, these splice variants of hOCT1 have sequence deletions at the 3'-end (data not shown). Expression of the individual splice variants differed among tissues (Figure 9.1) . For example, multiple splice variants were expressed in the kidney, however, only hOCT1C mRNA transcripts were expressed in MOLT-4 cells, a human lymphoblast leukemia cell line derived from the peripheral blood (Figure 9.1) (Chapter 7). Whether these splice variants are functional and their physiological roles need further investigation.

9.2.1.4 rbOCT1

An organic cation transporter (rbOCT1) was cloned in this laboratory from rabbit kidney using homology cloning (Tables 9.1 and 9.2) (Terashita *et al.*, 1998) . rbOCT1 (554 amino acids) is 81% identical to rOCT1 and 65% identical to rOCT2. Similar to both transporters, rbOCT1 is a polyspecific organic cation transporter; however, its mRNA transcripts are highly expressed in the liver with low levels of expression detected in the kidney and intestine.

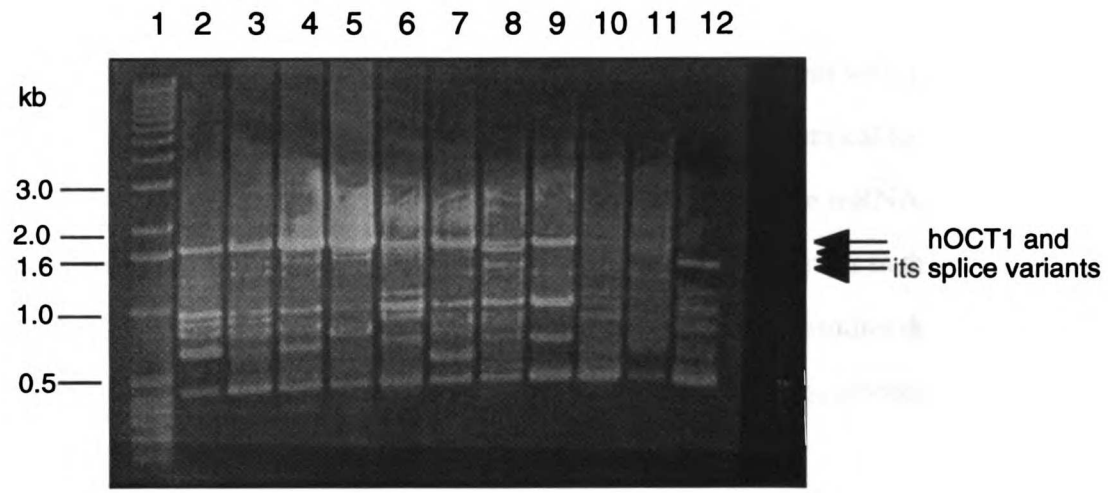

Figure 9.1 Expression of hOCT1 and its splice variants in different human tissues and cells detected by PCR. First strand cDNA were either purchased from Clontech, Palo Alto, CA or synthesized as described in Chapters 7 and 8. PCR products were separated by electrophoresis through 1% agarose gel and stained with ethidium bromide. *Lane 1*, 1-kb DNA ladder (Gibco BRL); *lane 2*, brain; *lane 3*, heart; *lane 4*, kidney; *lane 5*, liver; *lane 6*, lung; *lane 7*, pancreas; *lane 8*, placenta; *lane 9*, skeletal muscle; *lane 10*, Caco-2; *lane 11*, small intestine; *lane 12*, MOLT-4.

9.2.2 OCT Family: OCT2

9.2.2.1 rOCT2

Another member of the OCT family (rOCT2) has been cloned from rat kidney by homology cloning methods (Tables 9.1, 9.2 and 9.3) (Okuda *et al.*, 1996; Walsh *et al.*, 1996). rOCT2 cDNA (2,205 bp) encodes a 593-amino acid protein with 12 putative transmembrane domains (Okuda *et al.*, 1996). rOCT2 is 67% identical to rOCT1. Unlike rOCT1, Northern blot analysis and RT-PCR demonstrated that the mRNA transcripts of rOCT2 are expressed predominantly in the kidney and at higher levels in the medulla than in the cortex (Okuda *et al.*, 1996). Recent immunohistochemical studies demonstrated that rOCT2 is localized to the basolateral membrane of the S2 and S3 segments of the proximal tubule (H Koepsell, unpublished data).

Initial functional characterization studies in oocytes demonstrated that TEA is a substrate for rOCT2. The K_m of TEA transport is 357 μM (Chapter 3). I determined that MPP^+ (K_m of 4.4 μM), cimetidine and the endogenous organic cation, guanidine (K_m of 234 μM) (Chapter 3) are also substrates of rOCT2 (Tables 9.2 and 9.3).

9.2.2.2 pOCT2

A pig homolog, pOCT2 (original manuscript named it as OCT2p), was cloned from LLC-PK_1 cells (Grundemann *et al.*, 1997) suggesting that OCT2 family members may represent transporters important in the renal disposition of organic cations (Tables 9.1 and 9.2). However, unlike rOCT2, pOCT2 may be localized to the apical membrane as suggested by functional studies conducted in wild-type $LLCPK_1$ in comparison to studies in pOCT2 transfected HEK-293 cells. MPP^+ was shown to be a substrate (K_m of 19 μM).

9.2.2.3 hOCT2

Recently, a human homolog of rOCT2, hOCT2, was cloned from kidney (Tables 9.1, 9.2 and 9.3) (Gorboulev *et al.*, 1997). The cDNA of hOCT2 encodes a protein of 555 a.a. which is 70% identical to hOCT1. hOCT2 is localized to chromosome 6q25-26 (H Koepsell, unpublished data). This transporter also appears to be highly localized to the kidney. Immunohistochemical studies demonstrated that hOCT2 is localized to the apical membrane of the distal tubule which may suggest that this transporter functions in the reabsorption of organic cations (Gorboulev *et al.*, 1997).

Functional studies of hOCT2 were carried out in *X. laevis* oocytes injected with the cRNA of hOCT2 (Gorboulev *et al.*, 1997). In radiolabel tracer flux experiments it was determined that TEA (K_m of 76 μM), MPP^+ (K_m of 19 μM), NMN (K_m of 300 μM), and choline (K_m of 210 μM) are permeants (substrates) of hOCT2 (Table 9.2). Therefore, hOCT2 is a polyspecific organic cation transporter. Concentration-dependent inhibition of TEA uptake by different organic cations was measured and K_i values were estimated (Table 9.3). The K_i values of several compounds for hOCT2 differs substantially from those for hOCT1 (Zhang *et al.*, 1998b; Chapter 6). In general, most compounds have a higher affinity for hOCT2 than for hOCT1 (Table 9.3). These data together with information about the tissue distribution of hOCT1 and hOCT2, may aid in the prediction of the whole body disposition of organic cations.

9.2.3 OCT Family: OCT3

9.2.3.1 rOCT3 and mOCT3

Recently, a new member of the OCT family, OCT3, was cloned from rat placenta (Kekuda *et al.*, 1998) and mouse kidney cDNA libraries (Wu *et al.*, 1998a) (Tables 9.1 and 9.2). In general, OCT3 shares approximately 30-51% identity with other members of the OCT family and the greatest homology is seen with OCT1 and OCT2 (~50% identity). Tissue distribution of rOCT3 determined by Northern blot analysis suggests that rOCT3 mRNA transcripts are abundantly expressed in the placenta, moderately in the intestine, heart, and brain. The expression is comparatively low in the kidney and is undetectable in the liver (Table 9.2) (Kekuda *et al.*, 1998).

OCT3 is polyspecific, TEA, MPP^+ and guanidine are its substrates (Table 9.2). The K_m for TEA transport by rOCT3 is relatively high, 2.5 ± 0.2 mM. Like rOCT1 and rOCT2, rOCT3 is also potential-sensitive (Kekuda *et al.*, 1998).

9.2.4 OCT Family: OCTN1

9.2.4.1 OCTN1

Another new member of the OCT family termed OCTN1 was cloned from a human fetal liver cDNA library (Tables 9.1 and 9.2) (Tamai *et al.*, 1997). OCTN1 (551 amino acids) is quite different from the other members of the organic cation transporter family; OCTN1 is only 31% identical to hOCT1 and 33% identical to hOCT2. In addition, unlike hOCT1 or hOCT2, OCTN1 has a nucleotide binding site sequence motif, which suggests that it might operate as an ATP-dependent transporter. There has been one report in the literature of an ATP-dependent organic cation transport mechanism for tetraethylammonium (TEA) in the renal brush border membrane (McKinney and Hosford, 1993). The tissue

distribution of OCTN1 was determined by Northern blot analysis. It appears to have a broad tissue distribution. It was strongly expressed in the fetal kidney, liver and lung. In adult tissue, it was expressed most abundantly in the kidney, trachea, bone marrow and pancreas. In addition, OCTN1 mRNA transcripts were detected in several human cancer cell lines including lung carcinoma A459, colorectal adenocarcinoma SW480, myelogenous leukemia K-562 and HeLa cells S3 (Tamai *et al.*, 1997).

Initial functional studies were carried out using transiently-transfected HEK-293 cells. ^{14}C-TEA uptake in OCTN1 cDNA-transfected cells was saturable with a K_m of 0.436 mM. pH-dependency of TEA transport was observed in acidic to neutral medium (pH 6.0 to 7.5), whereas no pH-dependency was observed in neutral to alkaline medium (pH 7.5 to 8.5). Based on these data, Tamai and coworkers proposed that this transporter may represent the pH-sensitive organic cation transporter located on the apical side of the cell and function in the secretion of organic cations from cell into the lumen. However, further studies are clearly needed to support this proposal. Analysis alone of driving force is not conclusive, since several of the cloned OCT1 and OCT2 transporters are also sensitive to pH (Grundemann *et al.*, 1997; Zhang *et al.*, 1997b). Immunological studies as well as detailed functional studies are needed to determine the functional and physiological roles of OCTN1.

9.2.5 OCT Family: OCTN2

9.2.5.1 OCTN2

Very recently, one more new member of the OCT family, OCTN2, which is more close to OCTN1 than other members of the OCT family, was cloned from a cDNA library derived from a human placental trophoblast cell line, JAR (Tables 9.1 and 9.2) (Wu *et al.*, 1998b). The cDNA of OCTN2 is 3,252 bp in length which encodes a 557 a.a. protein. OCTN2 is 77% identical to OCTN1, 37% identical to hOCT1 and 33% identical to hOCT2

(Table 9.1). It has twelve putative TMDs with conserved motifs such as N-glycosylation and PKC sites similar to other members of the OCT family. Like OCTN1, it also has an ATP/GTP binding motif (GTEILGKS) in the intracellular loop between the 4th and 5th TMDs. OCTN2 mRNA is widely expressed including heart, placenta, skeletal muscle, pancreas, brain, lung, liver and kidney (Table 9.2). It is also expressed in various human cell lines including placental (JAR and BeWo), intestinal (Caco2 and HT-29), cervical carcinoma (HeLa), breast cancer (MCF-7), and kidney proximal tubule (HKPT) cell lines.

^{14}C-TEA was used as a model compound to determinine the function of OCTN2 in transfected HeLa cells. pH-dependency was also observed (Wu *et al.*, 1998b).

In summary, functional studies of the cloned organic cation transporters have begun to provide information about the mechanisms of organic cation transport. The information on the kinetic characteristics of the cloned organic cation transporters, rOCT1, hOCT1, rOCT2, and hOCT2 is summarized in Table 9.3. With the availability of cloned human organic cation transporters along with various *in vitro* functional assays, it is now possible to develop *in vitro* systems (especially in high-throughput screening) to understand drug interactions with these transporters individually. Ultimately, *in vitro* systems can be used for the prediction of drug disposition and targeting in the organism.

9.2.6 Other Members of the OCT Family

Other genes related to organic cation transporters have been described. A mouse homolog of rOCT1, Lx1, was mapped to chromosome 17 (Schweifer and Barlow, 1996). Its cDNA is 95% identical to that of rOCT1. The mouse homolog of rOCT2 has also been recently cloned (Genbank accession number AJ006036). In the GenBank database, homologous genes of rOCT1 have also been reported from non-mammalian species such as *Caenorhabditis elegans* (GenBank accession number Z83228) and *Drosophila*

melanogaster (GenBank Accession number Y12399 and Y12400) which may suggest gene evolution of the organic cation transporters. However, functions and/or tissue distributions of these possible members of organic cation transporters have not been determined.

9.3 Future Directions

Defining the mechanisms by which organic cations are transported will contribute significantly to our knowledge of the processes involved in drug absorption, elimination and disposition. In particular, the molecular cloning of the organic cation transporters has set the stage for a comprehensive understanding of these mechanisms. Comparative studies can now be performed to link the functional characteristics of the individual clones with the multiple mechanisms that have been described in epithelial tissues. For example, does rOCT1 represent the well-described hepatic sinusoidal type I organic cation transporter? Structure function studies are now possible to elucidate the molecular events that occur during a translocation cycle and to identify the domains of the cloned transporters that are responsible for substrate recognition, binding, translocation and release. In addition, functional studies with the cloned transporters can be performed to predict the absorption, disposition as well as targeting of potential drug candidates. Organic cation transporters are polyspecific and therefore, have overlapping substrate specificities. It will be interesting to identify and characterize the various organic cation transporters that are involved in the elimination of a wide array of xenobiotics and endogenous metabolites.

High-throughput screening (HTS)-based pharmacological testing has recently been developed as a useful *in vitro* assay to study drug interactions with cloned human metabolizing enzyme and drug receptor targets in a fast and large-scale way. By this method, clinically relevant data can be obtained in early drug discovery. It is a safe, time- and cost-saving method. Similarly, development of HTS for transporters, important

determinants for drug absorption, elimination and disposition, will be in demand. Major factors for such systems are: cloned transporters, sensitive analytical methods and automation systems for handling larger numbers of compounds. Several organic cation transporters have been cloned and transfected into mammalian cell lines. The development of sensitive analytical methods such as LC-MS, LC-NMR are still needed for detection of organic cation transport. As noted in Chapter 1, some organic cations, such as 4-Di-1-ASP$^+$, are fluorescent, which may be used to develop a fluorescent detection method in microplates. We demonstrated that 4-Di-1-ASP$^+$ is a substrate of hOCT1 (Figure 9.2) in HeLa cells transfected with hOCT1 DNA by fluorescent microscopy. With the use of heterologous expression systems, it is possible to carry out high through-put screening of potential therapeutic agents that may interact with the multiple organic cation transporters. This information may be important in design and development of drugs targeted to or away from a specific organ.

Major questions about the localization of the cloned transporters, as well as the events involved in the targeting of the transporters to specific membranes, i.e., basolateral or apical, have not been addressed. For example, it is not clear whether OCT1 is a basolateral membrane transporter as has been suggested by functional studies and if so, if it remains a basolateral membrane transporter in all tissues or species. Structural differences between apical and basolateral organic cation transporters need further investigation and in particular, the molecular elements responsible for their sorting need to be identified. Information gained from these studies will update our current models of organic cation transport and will provide the basis for protein engineering to develop membrane specific targeted transporters.

No ASP+

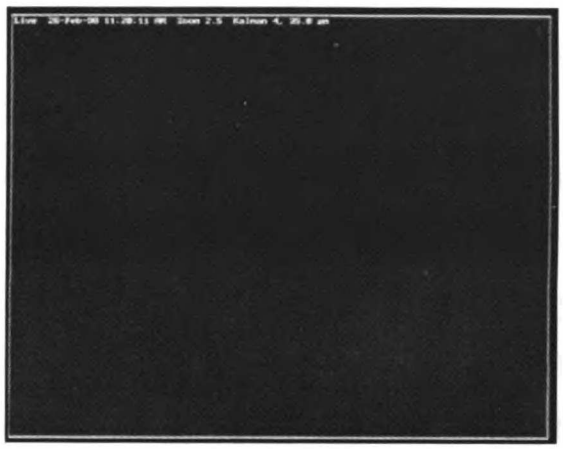

10 µM ASP+

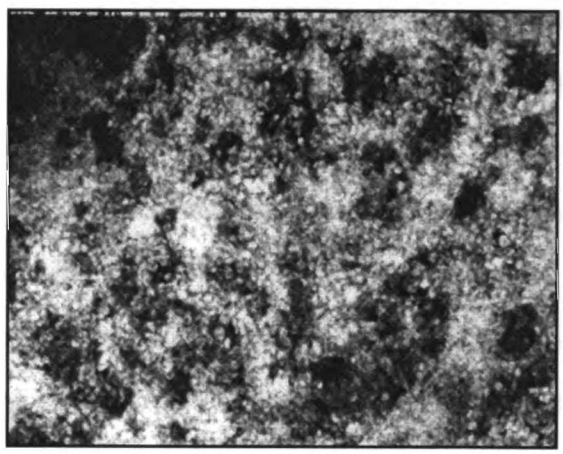

10 µM ASP+
+
2 mM TEA

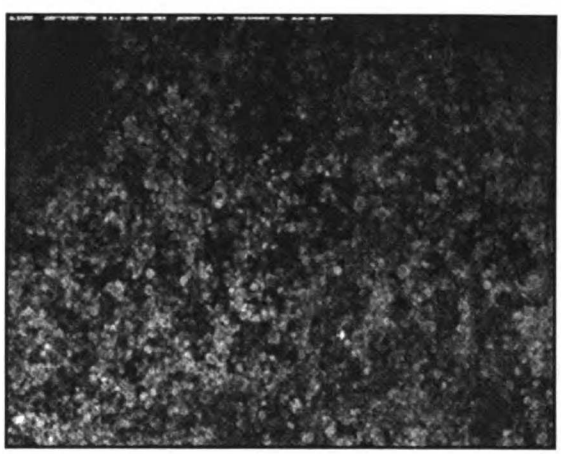

Figure 9.2 Uptake of 4-Di-1-ASP+ (10 µM) at 15 min in hOCT1 DNA-transfected HeLa cells in the absence (*middle panel*) and presence (*bottom panel*) of 2 mM TEA. Control cells (*top panel*) were incubated with PBS buffer only.

The regulation of organic cation transport is poorly understood. Unpublished data from this laboratory indicates that organic cation transport in OK cells can be upregulated after exposure to specific substrates (Chan and Giacomini, 1993). Other studies in non-perfused S2 segments from rabbit kidney (Hohage *et al.*, 1994) as well as in perfused livers from rat (Steen *et al.*, 1993) suggest that protein kinase C (PKC) is involved in regulating the transport of organic cations on the basolateral membrane of the kidney and the brush border membrane of the liver. PKC phosphorylation sites are found on all of the cloned organic cation transport proteins (Gorboulev *et al.*, 1997; Grundemann *et al.*, 1994 and 1997; Kekuda *et al.*, 1998; Okuda *et al.*, 1996; Tamai *et al.*, 1997; Terashita *et al.*, 1998; Wu *et al.*, 1998a and 1998b; Zhang *et al.*, 1997a and 1997b). It is now possible to determine which organic cation transporter is affected directly (or indirectly) by PKC and to determine the detailed mechanisms involved in phosphorylation by PKC.

Tissue specific regulation in the expression of the cloned organic cation transporters has not been studied. Although the kidney, liver and intestine share some common mechanisms of organic cation transport, there are notable differences in the characteristics of transport in each epithelia . These processes are related to the tissue specific expression of different organic cation transporter isoforms. For example, rOCT1 is expressed in all three epithelial tissues in the rat, whereas rOCT2 is more kidney-specific. Genomic studies of these two genes are necessary in order to understand the tissue specific expression of the organic cation transporters. Alternative RNA splicing is likely to be important in defining the tissue specific functions of organic cation transporters.

Understanding pharmacogenetics and pharmacogenomics of metabolizing enzymes as well as transporters is critical for drug development. Discovery of polymorphisms of certain metabolizing enzymes such as CYP2D6 and CYP2C19 revealed that mutations in these genes resulted in poor metabolizer (PM) or extensive metabolizer (EM) phenotypes in different populations of humans. Polymorphisms for transporters such as Glut2, a facilitated glucose transporter, and the sodium-dependent bile acid transporter have also

been identified (Mueckler *et al.*, 1994; Paulusma *et al.*, 1997; Wong *et al.*, 1995). As to organic cation transporters, we identified a methionine deletion located in the 9th transmembrane domain (Met420, Figure 5.1a), which represents a possible polymorphism of hOCT1. This finding was confirmed by another laboratory (Gorboulev *et al.*, 1997). Initial functional characterization was carried out and found that this mutant tends to have a lower transport function, i.e., lower TEA uptake in transfected HeLa cells. Michaelis-Menten studies revealed that the K_m of TEA transport decreased in the mutant hOCT1, whereas the V_{max} was similar in comparison to those of the wild-type hOCT1 suggesting that the mutant hOCT1 has a lower affinity for organic cations leading to lower transport activity (Table 9.4). Further studies are needed to determine the detailed function of the mutant hOCT1, the representation of this mutant in the population and its possible link to xenobiotic disposition in various people.

Table 9.4 Kinetics of TEA transport mediated by wild-type and mutant hOCT1 (ΔMet420)

	K_m	V_{max}
	μM	*pmol/mg protein/20 min*
Wild-type	130 ± 52	2.44 ± 0.27
Mutant	525 ± 74	2.37 ± 0.13

Studies were performed in DNA-transfected HeLa cells. Data are presented as mean ± SD from one experiment.

Despite the exciting molecular studies that have greatly advanced our understanding of organic cation transporters, it will be critical to establish *in vivo* models to fully elucidate the physiological and pharmacological role of organic cation transporters in the intact organism. *In vivo* models such as transgenic animals should be developed and the pharmacokinetics of various organic cations determined in these models. Because organic cation transporters are responsible for the absorption and elimination of a wide array of xenobiotics and may represent potential drug targets, studies in these *in vivo* models will ultimately lead to an enhanced design and development of therapeutic agents.

REFERENCES

Acra, S. A., AND Ghishan, F. K.: Methods of investigating intestinal transport. Jpen. J Parenter Enteral Nutr. **15:** 93S-8S, 1991.

Aronson, P. S.: Kinetic properties of the plasma membrane Na^+-H^+ exchanger. Annu Rev Physiol. **47:** 545-60, 1985.

Balani, S. K., Woolf, E. J., Hoagland, V. L., Sturgill, M. G., Deutsch, P. J., Yeh, K. C., AND Lin, J. H.: Disposition of indinavir, a potent HIV-1 protease inhibitor, after an oral dose in humans. Drug Metab Dispos. **24:** 1389-94, 1996.

Barrand, M. A., Bagrij, T., AND Neo, S. Y.: Multidrug resistance-associated protein: a protein distinct from P-glycoprotein involved in cytotoxic drug expulsion. Gen Pharmacol. **28:** 639-45, 1997.

Bencini, A. F., Mol, W. E., Scaf, A. H., Kersten, U. W., Wolters, K. T., Agoston, S., AND Meijer, D. K.: Uptake and excretion of vecuronium bromide and pancuronium bromide in the isolated perfused rat liver. Anesthesiology. **69:** 487-92, 1988.

Bendayan, R.: Renal drug transport: a review. Pharmacotherapy. **16:** 971-85, 1996.

Benet, L. Z., Wu, C. Y., Hebert, M. F., AND Wacher, V. J.: Intestinal drug metabolism and antitransport processes: A potential paradigm shif in oral drug delivery. J Controlled Release. **39:** 139-43, 1996.

Berry, M. N., Edwards, A. M., AND Barritt, G. J. "Utilizing of hepatocytes for drug studies." In *Isolated Hepatocytes Preparation, Properties and Applications*, edited by R. H. Burdon and P. H. van Knippenberg, 182-4. Amsterdam: Elsevier, 1991.

Berry, M. N., Halls, H. J., AND Grivell, M. B.: Techniques for pharmacological and toxicological studies with isolated hepatocyte suspensions. Life Sci. **51:** 1-16, 1992.

Blaschke, T. F., AND Giacomini, K. M.: "Pharmacodynamic consequences of enantioselective drug disposition." In *Pharmacology*, edited by M. J. Rand and C. Raper, 803-6. Amsterdam: Elsevier Science, 1987.

Blom, A., Scaf, A. H., AND Meijer, D. K.: Hepatic drug transport in the rat. A comparison between isolated hepatocytes, the isolated perfused liver and the liver in vivo. Biochem Pharmacol. **31:** 1553-65, 1982.

Bossuyt, X., Muller, M., Hagenbuch, B., AND Meier, P. J.: Polyspecific drug and steroid clearance by an organic anion transporter of mammalian liver. J Pharmacol Exp Ther. **276:** 891-6, 1996.

Borst, P.: Multidrug resistant proteins. Semin Cancer Biol. **8:** 131-4, 1997.

Boyer, J. L., Ng, O. C., Ananthanarayanan, M., Hofmann, A. F., Schteingart, C. D., Hagenbuch, B., Stieger, B., AND Meier, P. J.: Expression and characterization of a functional rat liver Na^+ bile acid cotransport system in COS-7 cells. Am J Physiol. **266:** G382-7, 1994.

Burg, M. B.: Perfusion of isolated renal tubules. Yale J Biol Med. **45:** 321, 1972.

Burg, M. B., AND Orloff, J.: Oxygen consumption and active transprot in separated renal tubules. Am J Physiol. **203:** 327, 1962.

Busch, A. E., Quester, S., Ulzheimer, J. C., Gorboulev, V., Akhoundova, A., Waldegger, S., Lang, F., AND Koepsell, H.: Monoamine neurotransmitter transport mediated by the polyspecific cation transporter rOCT1. FEBS Lett. **395:** 153-6, 1996a.

Busch, A. E., Quester, S., Ulzheimer, J. C., Waldegger, S., Gorboulev, V., Arndt, P., Lang, F., AND Koepsell, H.: Electrogenic properties and substrate specificity of

the polyspecific rat cation transporter rOCT1. J Biol Chem. **271:** 32599-604, 1996b.

Cacini, W., Keller, M. B., AND Grund, V. R.: Accumulation of cimetidine by kidney cortex slices. J Pharmacol Exp Ther. **221:** 342-6, 1982.

Canton, H., Emeson, R. B., Barker, E. L., Backstrom, J. R., Lu, J. T., Chang, M. S., AND Sanders-Bush, E.: Identification, molecular cloning, and distribution of a short variant of the 5-hydroxytryptamine2C receptor produced by alternative splicing. Mol Pharmacol. **50:** 799-807, 1996.

Carafoli, E.: Biogenesis: plasma membrane calcium ATPase: 15 years of work on the purified enzyme. FASEB J. **8:** 993-1002, 1994.

Cardarelli, C. O., Aksentijevich, I., Pastan, I., AND Gottesman, M. M.: Differential effects of P-glycoprotein inhibitors on NIH3T3 cells transfected with wild-type (G185) or mutant (V185) multidrug transporters. Cancer Res. **55:** 1086-91, 1995.

Cass, C. "Nucleoside transport." In *Drug Transport in Antimicrobial and Anticancer Chemotherapy*, edited by NH Georgopapadakou, 403-51. New York: Marcel Dekker, 1995.

Chan, J. K., AND Giacomini, K. M.: Substrate regulation of the organic cation-H^+ antiporter in OK cells. Pharm Res. **10:** S411, 1993 (Abstr.).

Chan, J. K., Piquette-Miller, M., AND Giacomini, K. M.: Expression of the organic cation transporter for tetraethylammonium in *Xenopus laevis* oocytes. Pharm Res. **12:** S243, 1995 (Abstr.).

Chen, C. J., Chin, J. E., Ueda, K., Clark, D. P., Pastan, I., Gottesman, M. M., AND Roninson, I. B.: Internal duplication and homology with bacterial transport proteins in the mdr1 (P-glycoprotein) gene from multidrug-resistant human cells. Cell. **47:** 381-9, 1986.

Cheng, Y.-C. AND Prusoff, W. H: Relationship between the inhibition constant (K_i) and the concentration of inhibitor which causes 50 per cent inhibition (I_{50}) of an enzymatic reaction. Biochem Pharmacol **22:** 3099-108, 1973.

Chun, J. K., Zhang, L., Piquette-Miller, M., Lau, E., Tong, L.-Q., AND Giacomini, K. M.: Characterization of guanidine transport in human renal brush border membranes. Pharm Res. **14:** 936-41, 1997a.

Chun, J. K., Piquette-Miller, M., Zhang, L., AND Giacomini, K. M.: Expression of human polyspecific renal organic cation transport activity in *Xenopus laevis* oocytes. J Pharm Sci. **86:** 753-5, 1997b.

Clark, J. A., AND Amara, S. G.: Stable expression of a neuronal gamma-aminobutyric acid transporter, GAT-3, in mammalian cells demonstrates unique pharmacological properties and ion dependence. Mol Pharmacol. **46:** 550-7, 1994.

Cole, S. P., Bhardwaj, G., Gerlach, J. H., Mackie, J. E., Grant, C. E., Almquist, K. C., Stewart, A. J., Kurz, E. U., Duncan, A. M., AND Deeley, R. G.: Overexpression of a transporter gene in a multidrug-resistant human lung cancer cell line [see comments]. Science. **258:** 1650-4, 1992.

Dantzler, W. H., Brokl, O. H., AND Wright, S. H.: Brush-border TEA transport in intact proximal tubules and isolated membrane vesicles. Am J Physiol **256:** F290-7, 1989.

Dantzler, W. H., Wright, S. H., Chatsudthipong, V., AND Brokl, O. H.: Basolateral tetraethylammonium transport in intact tubules: specificity and *trans*-stimulation. Am J Physiol. **261:** F386-92, 1991.

Deeks, S. G., AND Volberding, P. A.: HIV-1 protease inhibitors. AIDS Clin Rev. 145-85, 1997.

Dekant, W., AND Vamvakas, S.: Biotransformation and membrane transport in nephrotoxicity. Critic Rev Toxicol. **26:** 309-34, 1996.

Denissen, J. F., Grabowski, B. A., Johnson, M. K., Buko, A. M., Kempf, D. J., Thomas, S.B., AND Surber, B. W.: Metabolism and disposition of the HIV-1 protease inhibitor ritonavir (ABT-538) in rats, dogs, and humans. Drug Metab Dispos. **25:** 489-501, 1997.

Drayer, D. E.: Pharmacodynamic and pharmacokinetic differences between drug enantiomers in humans: an overview. Clin Pharmacol Ther. **40:** 125-33, 1986.

Dudley, A. J., AND Brown, C. D.: Mediation of cimetidine secretion by P-glycoprotein and a novel H(+)-coupled mechanism in cultured renal epithelial monolayers of LLC-PK_1 cells. Br J Pharmacol. **117:** 1139-44, 1996.

Dutt, A., Heath, L. A., AND Nelson, J. A.: P-glycoprotein and organic cation secretion by the mammalian kidney. J Pharmacol Exp Ther. **269:** 1254-60, 1994.

Elsenhans, B., Blume, R., Lembcke, B., AND Caspary, W. F.: *In vitro* inhibition of rat small intestinal absorption by lipophilic organic cations. Biochim Biophys Acta. **813:** 25-32, 1985.

Ernest, S., AND Bello-Reuss, E.: P-glycoprotein functions and substrates: possible roles of MDR1 gene in the kidney. Kidney Int Suppl. **65:** S11-7, 1998.

Evers, R., Kool, M., van Deemter, L., Janssen, H., Calafat, J., Oomen, L. C., Paulusma, C. C., Oude Elferink, R. P., Baas, F., Schinkel, A. H., AND Borst, P.: Drug export activity of the human canalicular multispecific organic anion transporter in polarized kidney MDCK cells expressing cMOAT (MRP2) cDNA. J Clin Invest. **101:** 1310-9, 1998.

Fauth, C., Rossier, B., AND Roch-Ramel, F.: Transport of tetraethylammonium by a kidney epithelial cell line (LLC-PK_1). Am J Physiol. **254:** F351-7, 1988.

Fauth, C., Chabardes, D., Allaz, M., Garcia, M., Rossier, B., Roch-Ramel, F., AND Claire, M.: Establishment of renal cell lines derived from S2 segments of the proximal tubule. Renal Physiol Biochem. **14:** 128-39, 1991.

Ferry, D. R.: Testing the role of P-glycoprotein expression in clinical trials: applying pharmacological principles and best methods for detection together with good clinical trials methodology. Int J Clin Pharmacol Ther. **36:** 29-40, 1998.

Ford, J. M., AND Hait, W. N.: Pharmacology of drugs that alter multidrug resistance in cancer. Pharmacol Rev. **42:** 155-99, 1990.

Fouda, A. K., Fauth, C., AND Roch-Ramel, F.: Transport of organic cations by kidney epithelial cell line LLC-PK_1. J Pharmacol Exp Ther. **252:** 286-92, 1990.

Frohman, M. A., Dush, M. K., AND Martin, G. R.: Rapid production of full-length cDNAs from rare transcripts: amplification using a single gene-specific oligonucleotide primer. Proc Natl Acad Sci U S A. **85:** 8998-9002, 1988.

Ganapathy, V., Ganapathy, M. E., Nair, C. N., Mahesh, V. B., AND Leibach, F. H.: Evidence for an organic cation-proton antiport system in brush-border membranes isolated from the human term placenta. J Biol Chem. **263:** 4561-8, 1988.

Germann, U. A., Pastan, I., AND Gottesman, M. M.: P-glycoproteins: mediators of multidrug resistance. Semin Cell Biol. **4:** 63-76, 1993.

Giacomini, K. M., Markovich, D., Werner, A., Biber, J., Wu, X., AND Murer, H.: Expression of a renal Na(+)-nucleoside cotransport system (N2) in *Xenopus laevis* oocytes. Pflugers Arch. **427:** 381-3, 1994.

Gilsdorf, J. S., Rebbeor, J. F., AND Holohan, P. D.: Evidence that the organic cation/H^+ exchanger in the brush border membrane of dog kidney is a 41-kDa protein. J Pharmacol Exp Ther. **280:** 1043-50, 1997.

Gisclon, L., Wong, F. M., AND Giacomini, K. M.: Cimetidine transport in isolated luminal membrane vesicles from rabbit kidney. Am J Physiol. **253:** F141-50, 1987.

Gorboulev, V., Ulzheimer, J. C., Akhoundova, A., Ulzheimer-Teuber, I., Karbach, U., Quester, S., Baumann, C., Lang, F., Busch, A. E., AND Koepsell, H.: Cloning

and characterization of two human polyspecific organic cation transporters. DNA Cell Biol. **16:** 871-81, 1997.

Gores, G. J., Kost, L. J., AND LaRusso, N. F.: The isolated perfused rat liver: conceptual and practical considerations. Hepatology. **6:** 511-7, 1986.

Gottesman, M. M., Pastan, I., AND Ambudkar, S. V.: P-glycoprotein and multidrug resistance. Curr Opin Genet Dev. **6:** 610-7, 1996.

Gottschalk, C. W., AND Lassiter, W. E. "Micropuncture methodology." In *Handbook of Physiology 8, Renal Physiology*, edited by J. Orloff and R. W. Berliner, 129-43. Washington, D. C.: American Physiological Society, 1973.

Gramatte, T., Oertel, R., Terhaag, B., AND Kirch, W.: Direct demonstration of small intestinal secretion and site-dependent absorption of the beta-blocker talinolol in humans. Clin Pharmacol Ther. **59:** 541-9, 1996.

Grass, G. M., AND Sweetana, S. A.: *In vitro* measurement of gastrointestinal tissue permeability using a new diffusion cell. Pharm Res. **5:** 372-6, 1988.

Grassl, S. M.: Choline transport in human placental brush-border membrane vesicles. Biochim Biophys Acta. **1194:** 203-13, 1994.

Griffith, D. A., AND Jarvis, S. M.: Nucleoside and nucleobase transport systems of mammalian cells. Biochim Biophys Acta. **1286:** 153-81, 1996.

Griffith, J. K., Baker, M. E., Rouch, D. A., Page, M. G., Skurray, R. A., Paulsen, I. T., Chater, K. F., Baldwin, S. A., AND Henderson, P. J.: Membrane transport proteins: implications of sequence comparisons. Curr Opin Cell Biol. **4:** 684-95, 1992.

Groothuis, G. M., AND Meijer, D. K.: Drug traffic in the hepatobiliary system. J Hepatol. **24 Suppl 1:** 3-28, 1996.

Groves, C. E., Evans, K. K., Dantzler, W. H., AND Wright, S. H.: Peritubular organic cation transport in isolated rabbit proximal tubules. Am J Physiol. **266:** F450-8, 1994.

Groves, C. E., Morales, M. N., Gandolfi, A. J., Dantzler, W. H., AND Wright, S. H.: Peritubular paraquat transport in isolated renal proximal tubules. J Pharmacol Exp Ther. **275:** 926-32, 1995.

Groves, C. E., AND Wright, S. H.: Tetrapentylammonium (TPeA): slowly dissociating inhibitor of the renal peritubular organic cation transporter. Biochim Biophys Acta. **1234:** 37-42, 1995.

Grundemann, D., Gorboulev, V., Gambaryan, S., Veyhl, M., AND Koepsell, H.: Drug excretion mediated by a new prototype of polyspecific transporter. Nature. **372:** 549-52, 1994.

Grundemann, D., Babin-Ebell, J., Martel, F., Ording, N., Schmidt, A., AND Schomig, E.: Primary structure and functional expression of the apical organic cation transporter from kidney epithelial LLC-PK_1 cells. J Biol Chem. **272:** 10408-13, 1997.

Hardman, J., Limbird, L., Molinoff, P., Ruddon, R., AND Gilman, A. *Goodman & Gilman's the Pharmacological Basis of Therapeutics*. 9th ed. New York: McGraw-Hill, Health Professions Division, 1996.

Hawley-Nelson, P., Ciccarone, V., Gebeyehu, G., Jessee, J., AND Felgner, P. L.: LipofectAMINE regent: a new, higher efficiency polycationic liposome transfection reagent. Focus. **15:** 73-9, 1993.

Hediger, M., Coady, M. J., and Wright, E. M.: Expression cloning and cDNA sequencing of a Na^+/glucose cotransporter. Nature. **330:** 379-81, 1987.

Higgins, C. F.: ABC transporters: from microorganisms to man. Annu Rev Cell Biol. **8:** 67-113, 1992.

Hilfiker, H., Guerini, D., AND Carafoli, E.: Cloning and expression of isoform 2 of the human plasma membrane Ca^{2+} ATPase. Functional properties of the enzyme and its splicing products. J Biol Chem. **269:** 26178-83, 1994.

Hohage, H., Morth, D. M., Querl, I. U., AND Greven, J.: Regulation by protein kinase C of the contraluminal transport system for organic cations in rabbit kidney S2 proximal tubules. J Pharmacol Exp Ther. **268:** 897-901, 1994.

Hohage, H., Querl, I. U., Morth, D. M., AND Greven, J.: The basolateral organic cation transport system of rabbit kidney proximal tubules. Influence of anorganic anions. J Pharmacol Exp Ther. **279:** 1086-91, 1996.

Holm, J.: Effect of cations on tetraehtylammonium exit from mouse kidney cortex slices. Arch Int Pharmacodyn Ther. **230:** 180-9, 1977.

Holohan, P. D., AND Ross, C. R.: Mechanisms of organic cation transport in kidney plasma membrane vesicles: 1. Countertransport studies. J Pharmacol Exp Ther. **215:** 191-7, 1980.

Holohan, P. D., AND Ross, C. R.: Mechanisms of organic cation transport in kidney plasma membrane vesicles: 2. delta pH studies. J Pharmacol Exp Ther. **216:** 294-8, 1981.

Holohan, P. D., White, K. E., Sokol, P. P., AND Rebbeor, J.: Photoaffinity labeling of the organic cation/H^+ exchanger in renal brush border membrane vesicles. J Biol Chem. **267:** 13513-9, 1992.

Homolya, L., Hollo, Z., Germann, U. A., Pastan, I., Gottesman, M. M., AND Sarkadi, B.: Fluorescent cellular indicators are extruded by the multidrug resistance protein. J Biol Chem. **268:** 21493-6, 1993.

Hori, R., Hirai, M., Katsura, T., Takano, M., Yasuhara, M., Kaneko, S., AND Satoh, M.: Expression of renal organic cation transporter in *Xenopus laevis* oocytes. Biochem J. **283:** 409-11, 1992.

Hsyu, P. H., AND Giacomini, K. M.: The pH gradient-dependent transport of organic cations in the renal brush border membrane. Studies with acridine orange. J Biol Chem. **262:** 3964-8, 1987.

Hsyu, P. H., Gisclon, L. G., Hui, A. C., AND Giacomini, K. M.: Interactions of organic anions with the organic cation transporter in renal BBMV. Am J Physiol. **254:** F56-61, 1988.

Hunt, S. M., AND Groff, J. L. "The digestive system: mechanisms for nourishing the body." In *Advanced Nutrition and Human Metaolism*, edited by S. M. Hunt and J. L. Groff, 25-49. St. Paul/New York: West Publising Company, 1990.

Inui, K., Saito, H., AND Hori, R.: H^+-gradient-dependent active transport of tetraethylammonium cation in apical-membrane vesicles isolated from kidney epithelial cell line LLC-PK_1. Biochem J. **227:** 199-203, 1985.

Iseki, K., Sugawara, M., Saitoh, N., AND Miyazaki, K.: The transport mechanisms of organic cations and their zwitterionic derivatives across rat intestinal brush-border membrane. II. Comparison of the membrane potential effect on the uptake by membrane vesicles. Biochim Biophys Acta. **1152:** 9-14, 1993.

James, D. E., Strube, M., Mueckler, M.: Molecular cloning of an insulin-regulated glucose transporter. Nature. **338:** 83-7, 1989.

Kakuda, T. N., Struble, K. A., AND Piscitelli, S. C.: Protease inhibitors for the treatment of human immunodeficiency virus infection. Am J Health Syst Pharm. **55:** 233-54, 1998.

Kamimoto, Y., Gatmaitan, Z., Hsu, J., AND Arias, I. M.: The function of Gp170, the multidrug resistance gene product, in rat liver canalicular membrane vesicles. J Biol Chem. **264:** 11693-8, 1989.

Kaldor, S. W., Kalish, V. J., Davies, J. F. n., Shetty, B. V., Fritz, J. E., Appelt, K., Burgess, J. A., Campanale, K. M., Chirgadze, N. Y., Clawson, D. K., Dressman, B. A., Hatch, S. D., Khalil, D. A., Kosa, M. B., Lubbehusen, P. P., Muesing, M. A., Patick, A. K., Reich, S. H., Su, K. S., AND Tatlock, J. H.: Viracept (nelfinavir mesylate, AG1343): a potent, orally bioavailable inhibitor of HIV-1 protease. J Med Chem. **40:** 3979-85, 1997.

Kanai, N., Lu, R., Bao, Y., Wolkoff, A. W., AND Schuster, V. L.: Transient expression of oatp organic anion transporter in mammalian cells: identification of candidate substrates. Am J Physiol. **270:** F319-25, 1996.

Karlsson, J., Kuo, S. M., Ziemniak, J., AND Artursson, P.: Transport of celiprolol across human intestinal epithelial (Caco-2) cells: mediation of secretion by multiple transporters including P-glycoprotein. Br J Pharmacol. **110:** 1009-16, 1993.

Katsura, T., Takano, M., Tomita, Y., Yasuhara, M., Inui, K., AND Hori, R.: Characteristics of organic cation transporter in rat renal basolateral membrane. Biochim Biophys Acta. **1146:** 197-202, 1993.

Kekuda, R., Prasad, P. D., Wu, X., Wang, H., Fei, Y., Leibach, F. H., AND Ganapathy, V.: Cloning and functional characterization of a potential-sensitive, polyspecific organic cation transporter (OCT3) most abundantly expressed in placenta. J Biol. Chem **273:** 15971-9, 1998.

Kim, R. B., Fromm, M. F., Wandel, C., Leake, B., Wood, A. J., Roden, D. M., AND Wilkinson, G. R.: The drug transporter P-glycoprotein limits oral absorption and brain entry of HIV-1 protease inhibitors. J Clin Invest. **101:** 289-94, 1998.

Kimura, M., Nabekura, T., Katsura, T., Takano, M., AND Hori, R.: Identification of organic cation transporter in rat renal brush-border membrane by photoaffinity labeling. Biol Pharm Bull. **18:** 388-95, 1995.

Koehler, M. R., Gorboulev, V., Koepsell, H., Steinlein, C., AND Schmid, M.: Roct1, a rat polyspecific transporter gene for the excretion of cationic drugs, maps to Chromosome 1q11-12. Mamm Genome. **7:** 247-8, 1996.

Kozak, M.: The scanning model for translation: an update. J Cell Biol. **108:** 229-41, 1989.

Kozak, M.: Regulation of translation in eukaryotic systems. Annu Rev Cell Biol. **8:** 197-225, 1992.

Krieg, P. A., AND Melton, D. A.: Functional messenger RNAs are produced by SP6 in vitro transcription of cloned cDNAs. Nucleic Acids Res. **12:** 7057-70, 1984.

Krumdieck, C. L., dos Santos, J. E., AND Ho, K. J.: A new instrument for the rapid preparation of tissue slices. Anal Biochem. **104:** 118-23, 1980.

Kuo, S. M., Whitby, B. R., Artursson, P., AND Ziemniak, J. A.: The contribution of intestinal secretion to the dose-dependent absorption of celiprolol. Pharm Res. **11:** 648-53, 1994.

Kyte, J., AND Doolittle, R. F.: A simple method for displaying the hydropathic character of a protein. J Mol Biol. **157:** 105-32, 1982.

Lennernas, H., AND Regardh, C. G.: Regional gastrointestinal absorption of the beta-blocker pafenolol in the rat and intestinal transit rate determined by movement of ^{14}C-polyethylene glycol (PEG) 4000. Pharm Res. **10:** 130-5, 1993a.

Lennernas, H., AND Regardh, C. G.: Dose-dependent intestinal absorption and significant intestinal excretion (exsorption) of the beta-blocker pafenolol in the rat. Pharm Res. **10:** 727-31, 1993b.

Lennernas, H., Nylander, S., AND Ungell, A. L.: Jejunal permeability: a comparison between the Ussing chamber technique and the single-pass perfusion in humans. Pharm Res. **14:** 667-71, 1997.

Leppert, P. S., AND Fix, J. A.: Use of everted intestinal rings for in vitro examination of oral absorption potential. J Pharm Sci. **83:** 976-81, 1994.

Lesage, F., Guillemare, E., Fink, M., Duprat, F., Lazdunski, M., Romey, G., AND Barhanin, J.: TWIK-1, a ubiquitous human weakly inward rectifying K^+ channel with a novel structure. EMBO J. **15:** 1004-11, 1996.

Leveque, D., AND Jehl, F.: P-glycoprotein and pharmacokinetics. Anticancer Res. **15:** 331-6, 1995.

Levinsky, N. G., AND Levy, M. "Clearance techniques." In *Handbook of Physiology 8, Renal Physiology*, edited by J. Orloff and R. W. Berliner, 104-17. Washington, D. C.: American Physiological Society, 1973.

Levy, R. H., AND Boddy, A. V.: Stereoselectivity in pharmacokinetics: a general theory. Pharm Res. **8:** 551-6, 1991.

Lin, J. H., Chiba, M., Balani, S. K., Chen, I. W., Kwei, G. Y., Vastag, K. J., AND Nishime, J. A.: Species differences in the pharmacokinetics and metabolism of indinavir, a potent human immunodeficiency virus protease inhibitor. Drug Metab Dispos. **24:** 1111-20, 1996.

Ling, V.: Multidrug resistance: molecular mechanisms and clinical relevance. Cancer Chemother Pharmacol. **40 Suppl:** S3-8, 1997.

Lingueglia, E., Voilley, N., Waldmann, R., Lazdunski, M., AND Barbry, P.: Expression cloning of an epithelial amiloride-sensitive Na^+ channel. A new channel type with homologies to Caenorhabditis elegans degenerins. FEBS Lett. **318:** 95-9, 1993.

Loe, D. W., Deeley, R. G., AND Cole, S. P.: Biology of the multidrug resistance-associated protein, MRP. Eur J Cancer. **32A:** 945-57, 1996.

Lopez-Nieto, C. E., You, G., Bush, K. T., Barros, E. J., Beier, D. R., AND Nigam, S. K.: Molecular cloning and characterization of NKT, a gene product related to the organic cation transporter family that is almost exclusively expressed in the kidney. J Biol Chem. **272:** 6471-8, 1997.

Maack, T.: Physiological evaluation of the isolated perfused rat kidney. Am J Physiol. **238:** F71-8, 1980.

Malvin, R. L., AND Wilde, W. S. "Stop-flow technique." In *Handbook of Physiology 8, Renal Physiology*, edited by J. Orloff and R. W. Berliner, 119-28. Washington, D. C.: American Physiology Society, 1973.

Marger, M. D., AND Saier, M. H., Jr.: A major superfamily of transmembrane facilitators that catalyse uniport, symport and antiport [see comments]. Trends Biochem Sci. **18:** 13-20, 1993.

Martel, F., Vetter, T., Russ, H., Grundemann, D., Azevedo, I., Koepsell, H., AND Schomig, E.: Transport of small organic cations in the rat liver. The role of the organic cation transporter OCT1. Naunyn Schmiedebergs Arch Pharmacol. **354:** 320-6, 1996a.

Martel, F., Martins, M. J., Hipolito-Reis, C., AND Azevedo, I.: Inward transport of [^{3}H]-1-methyl-4-phenylpyridinium in rat isolated hepatocytes: putative involvement of a P-glycoprotein transporter. Br J Pharmacol. **119:** 1519-24, 1996b.

McDonald, C. K., AND Kuritzkes, D. R.: Human immunodeficiency virus type 1 protease inhibitors. Arch Intern Med. **157:** 951-9, 1997.

McKinney, T. D.: Heterogeneity of organic base secretion by proximal tubules. Am J Physiol. **243:** F404-7, 1982.

McKinney, T. D. "Renal transport of organic anions and cations." In *Diseases of the Kidney*, edited by R. W. Schrier and C. W. Gottschalk, 261-81. Boston: Little, Brown, 1993.

McKinney, T. D., AND Hosford, M. A.: Organic cation transport by rat hepatocyte basolateral membrane vesicles. Am J Physiol. **263:** G939-46, 1992.

McKinney, T. D., AND Hosford, M. A.: ATP-stimulated tetraethylammonium transport by rabbit renal brush border membrane vesicles. J Biol Chem. **268:** 6886-95, 1993.

McKinney, T. D., AND Kunnemann, M. E.: Cimetidine transport in rabbit renal cortical brush-border membrane vesicles. Am J Physiol. **252:** F525-35, 1987.

McKinney, T. D., Scheller, M. B., Hosford, M., AND McAteer, J. A.: Tetraethylammonium transport by OK cells. J Am Soc Nephrol. **1:** 902-9, 1990.

McKinney, T. D., Scheller, M. B., Hosford, M., Lesniak, M. E., AND Haseley, T. S.: Basolateral transport of tetraethylammonium by a clone of LLC-PK_1 cells. J Am Soc Nephrol. **2:** 1507-15, 1992.

Meijer, D. K.: Current concepts on hepatic transport of drugs. J Hepatol. **4:** 259-68, 1987.

Meijer, D. K., AND Molema, G.: Targeting of drugs to the liver. Semin Liver Dis. **15:** 202-56, 1995.

Meijer, D. K. F., Bos, E. S., AND Van der Laan, K. J.: Hepatic transport of mono- and bisquaternary ammonium compounds. Eur J Pharmacol. **11:** 317-7, 1970.

Meijer, D. K., Keulemans, K., AND Mulder, G. J.: Isolated perfused rat liver technique. Methods Enzymol. **77:** 81-94, 1981.

Meijer, D. K., Mol, W. E., Muller, M., AND Kurz, G.: Carrier-mediated transport in the hepatic distribution and elimination of drugs, with special reference to the category of organic cations. J Pharmacokinet Biopharm. **18:** 35-70, 1990.

Meijer, D. K., Smit, J. W., AND Muller, M.: Hepatobiliary elimination of cationic drugs: the role of P-glycoproteins and other ATP-dependent transporters. Adv Drug Del Revs. **25:**159-200, 1997.

Merrick, W.: Mechanism and regulation of eukaryotic protein synthesis. Microbiol Rev. **56:** 291-315, 1992.

Merry, C., Barry, M. G., Mulcahy, F., Ryan, M., Heavey, J., Tjia, J. F., Gibbons, S. E., Breckenridge, A. M., AND Back, D. J.: Saquinavir pharmacokinetics alone and in combination with ritonavir in HIV-infected patients. AIDS. **11:** F29-33, 1997.

Merry, C., Barry, M. G., Mulcahy, F., Tjia, J. F., Halifax, K. L., Heavey, J., Kelly, C., AND Back, D. J.: Ritonavir pharmacokinetics alone and in combination with saquinavir in HIV-infected patients [letter]. AIDS. **12:** 325-7, 1998.

Miller, D. S., Villalobos, A. R., AND Pritchard, J. B.: Organic base transport in rat choroid plexus cells. **6:** 184A, 1995 (Abstr.).

Miyamoto, Y., Ganapathy, V., AND Leibach, F. H.: Transport of guanidine in rabbit intestinal brush-border membrane vesicles. Am J Physiol. **255:** G85-92, 1988.

Miyamoto, Y., Tiruppathi, C., Ganapathy, V., AND Leibach, F. H.: Multiple transport systems for organic cations in renal brush-border membrane vesicles. Am J Physiol. **256:** F540-8, 1989.

Mol, W. E., Fokkema, G. N., Weert, B., AND Meijer, D. K.: Mechanisms for the hepatic uptake of organic cations. Studies with the muscle relaxant vecuronium in isolated rat hepatocytes. J Pharmacol Exp Ther. **244:** 268-75, 1988.

Mol, W. E., Muller, M., Kurz, G., AND Meijer, D. K.: Investigations on the hepatic uptake systems for organic cations with a photoaffinity probe of procainamide ethobromide. Biochem Pharmacol. **43:** 2217-26, 1992.

Moseley, R. H., AND Van Dyke, R. W.: Organic cation transport by rat liver lysosomes. Am J Physiol. **268:** G480-6, 1995.

Moseley, R. H., Morrissette, J., AND Johnson, T. R.: Transport of N^1-methylnicotinamide by organic cation-proton exchange in rat liver membrane vesicles. Am J Physiol. **259:** G973-82, 1990.

Moseley, R. H., Jarose, S. M., AND Permoad, P.: Organic cation transport by rat liver plasma membrane vesicles: studies with tetraethylammonium. Am J Physiol. **263:** G775-85, 1992.

Moseley, R. H., Smit, H., Van Solkema, B. G., Wang, W., AND Meijer, D. K.: Mechanisms for the hepatic uptake and biliary excretion of tributylmethylammonium: studies with rat liver plasma membrane vesicles. J Pharmacol Exp Ther. **276:** 561-7, 1996a.

Moseley, R. H., Takeda, H., AND Zugger, L. J.: Choline transport in rat liver basolateral plasma membrane vesicles. Hepatology. **24:** 192-7, 1996b.

Moseley, R. H., Zugger, L. J., AND Van Dyke, R. W.: The neurotoxin 1-methyl-4-phenylpyridinium is a substrate for the canalicular organic cation/H^+ exchanger. J Pharmacol Exp Ther. **281:** 34-40, 1997.

Mueckler, M., Kruse, M., Strube, M., Riggs, A. C., Chiu, K. C., AND Permutt, M. A.: A mutation in the Glut2 glucose transporter gene of a diabetic patient abolishes transport activity. J Biol Chem. **269:** 17765-7, 1994.

Muller, M., Mayer, R., Hero, U., AND Keppler, D.: ATP-dependent transport of amphiphilic cations across the hepatocyte canalicular membrane mediated by mdr1 P-glycoprotein. FEBS Lett. **343:** 168-72, 1994.

Murer, H., AND Biber, J.: A molecular view of proximal tubular inorganic phosphate (P_i) reabsorption and of its regulation. Pflugers Arch. **433:** 379-89, 1997.

Murer, H., AND Gmaj, P.: Transport studies in plasma membrane vesicles isolated from renal cortex. Kidney Int. **30:** 171-86, 1986.

Nabekura, T., Takano, M., AND Inui, K. I.: Cholesterol modulates organic cation transport activity and lipid fluidity in rat renal brush-border membranes. Biochim Biophys Acta. **1283:** 232-6, 1996.

Nagel, G., Volk, C., Friedrich, T., Ulzheimer, J. C., Bamberg, E., AND Koepsell, H.: A reevaluation of substrate specificity of the rat cation transporter rOCT1. J Biol Chem. **272:** 31953-6, 1997.

Nakamura, H., Sano, H., Yamazaki, M., AND Sugiyama, Y.: Carrier-mediated active transport of histamine H_2 receptor antagonists, cimetidine and nizatidine, into isolated rat hepatocytes: contribution of type I system. J Pharmacol Exp Ther. **269:** 1220-7, 1994.

Neef, C., AND Meijer, D. K.: Structure-pharmacokinetics relationship of quaternary ammonium compounds. Correlation of physicochemical and pharmacokinetic parameters. Naunyn Schmiedebergs Arch Pharmacol. **328:** 111-8, 1984.

Neef, C., Keulemans, K. T., AND Meijer, D. K.: Hepatic uptake and biliary excretion of organic cations--I. Characterization of three new model compounds. Biochem Pharmacol. **33:** 3977-90, 1984a.

Neef, C., Oosting, R., AND Meijer, D. K.: Structure-pharmacokinetics relationship of quaternary ammonium compounds. Elimination and distribution characteristics. Naunyn Schmiedebergs Arch Pharmacol. **328:** 103-10, 1984b.

Ohtomo, T., Saito, H., Inotsume, N., Yasuhara, M., AND Inui, K. I.: Transport of levofloxacin in a kidney epithelial cell line, LLC-PK_1: interaction with organic cation transporters in apical and basolateral membranes. J Pharmacol Exp Ther. **276:** 1143-8, 1996.

Okuda, M., Saito, H., Urakami, Y., Takano, M., AND Inui, K.: cDNA cloning and functional expression of a novel rat kidney organic cation transporter, OCT2. Biochem Biophys Res Commun. **224:** 500-7, 1996.

Ott, R. J., AND Giacomini, K. M.: Stereoselective interactions of organic cations with the organic cation transporter in OK cells. Pharm Res. **10:** 1169-73, 1993.

Ott, R. J., Hui, A. C., Yuan, G., AND Giacomini, K. M.: Organic cation transport in human renal brush-border membrane vesicles. Am J Physiol. **261:** F443-51, 1991.

Ott, R. J., Hui, A. C., AND Giacomini, K. M.: Inhibition of N-linked glycosylation affects organic cation transport across the brush border membrane of opossum kidney (OK) cells. J Biol Chem. **267:** 133-9, 1992.

Ott, R. J., Chan, J. K., Ramanathan, V. K., Hui, A. C., AND Giacomini, K. M.: Effect of phenylisothiocyanate on organic cation transport in opossum kidney cells. J Pharmacol Exp Ther. **269:** 204-8, 1994.

Oude Elferink, R. P. J., Meijer, D. K. F., Kuipers, F., Jansen, P. L. M., Groen, A. K., AND Groothuis, G. M. M.: Hepatobiliary secretion of organic compounds;

molecular mechanisms of membrane transport. Biochim Biophys Acta. **1241:** 215-68, 1995.

Pakyz, A., AND Israel, D.: Overview of protease inhibitors. J Am Pharm Assoc (Wash). **NS37:** 543-51, 1997.

Paulusma, C. C., Kool, M., Bosma, P. J., Scheffer, G. L., ter Borg, F., Scheper, R. J., Tytgat, G. N., Borst, P., Baas, F., AND Oude Elferink, R. P.: A mutation in the human canalicular multispecific organic anion transporter gene causes the Dubin-Johnson syndrome. Hepatology. **25:** 1539-42, 1997.

Peabody, D. S., AND Berg, P.: Termination-reinitiation occurs in the translation of mammalian cell mRNAs. Mol Cell Biol. **6:** 2695-703, 1986.

Peters, L.: Renal tubular excretion of organic bases. Pharmacol Rev. **12:** 1-35, 1960.

Pietruck, F., AND Ullrich, K. J.: Transport interactions of different organic cations during their excretion by the intact rat kidney. Kidney Int. **47:** 1647-57, 1995.

Prasad, P. D., Leibach, F. H., Mahesh, V. B., AND Ganapathy, V.: Specific interaction of 5-(N-methyl-N-isobutyl)amiloride with the organic cation-proton antiporter in human placental brush-border membrane vesicles. Transport and binding. J Biol Chem. **267:** 23632-9, 1992.

Preiano, B. S., Guerini, D., AND Carafoli, E.: Expression and functional characterization of isoforms 4 of the plasma membrane calcium pump. Biochemistry. **35:** 7946-53, 1996.

Pritchard, J. B., AND Miller, D. S.: Mechanisms mediating renal secretion of organic anions and cations. Physiol Rev. **73:** 765-96, 1993.

Pritchard, J. B., AND Miller, D. S.: Intracellular compartmentation of organic anions and cations during renal secretion. Cell Physiol Biochem. **6:** 50-9, 1996a.

Pritchard, J. B., AND Miller, D. S.: Renal secretion of organic anions and cations. Kidney Int. **49:** 1649-54, 1996b.

Pritchard, J. B., Sykes, D. B., Walden, R., AND Miller, D. S.: ATP-dependent transport of tetraethylammonium by endosomes isolated from rat renal cortex. Am J Physiol. **266:** F966-76, 1994.

Pritchard, J. B., Walsh, R. C., AND Sweet, D. H.: Characterization of organic cation transporter 2 (OCT2) isolated from rat kidney. FASEB J. **11:** A278, 1997 (Abstr.).

Proost, J. H., Roggeveld, J., Wierda, J. M., AND Meijer, D. K.: Relationship between chemical structure and physicochemical properties of series of bulky organic cations and their hepatic uptake and biliary excretion rates. J Pharmacol Exp Ther. **282:** 715-26, 1997.

Quick, M. W., AND Lester, H. A. "Methods for expression of excitability proteins in *Xenopus* oocytes." In *Methods in Neuroscience*, edited by P. M. Conn, 261-79. San Diego: Academic Press, 1994.

Rafizadeh, C., Manganel, M., Roch-Ramel, F., AND Schali, C.: Transport of organic cations in brush border membrane vesicles from rabbit kidney cortex. Pflugers Arch. **407:** 404-8, 1986.

Rafizadeh, C., Roch-Ramel, F., AND Schali, C.: Tetraethylammonium transport in renal brush border membrane vesicles of the rabbit. J Pharmacol Exp Ther. **240:** 308-13, 1987.

Reichen, J. "Use of the perfused liver in studies of bile secretion." In *Research in Perfused Liver*, edited by F Ballet and RG Thurman, 149-63. London: John Libbey, 1991.

Rennick, B. R.: Renal tubule transport of organic cations. Am J Physiol. **240:** F83-9, 1981.

Rennick, B. R., Moe, G. K., Lyons, R. H., Hoobler, S. W., AND Neligh, R.: Absorption and renal excretion of the tetraethylammonium ion. J Pharmacol Exp Ther. **91:** 210-7, 1947.

Risso, S., DeFelice, L. J., AND Blakely, R. D.: Sodium-dependent GABA-induced currents in GAT1-transfected HeLa cells. J Physiol (Lond). **490:** 691-702, 1996.

Roch-Ramel, F., Besseghir, K., AND Murer, H. "Renal excretion and tubular transport of organic anions and cations." In *Handbook of Physiology 8, Renal Physiology*, edited by E. E. Windhager, 2189-262. Oxford: Oxford Univ. Press, 1992.

Ross, C. R., AND Holohan, P. D.: Transport of organic anions and cations in isolated renal plasma membranes. Annu Rev Pharmacol Toxicol. **23:** 65-85, 1983.

Rowland, M., AND Tozer, T. N. *Clinical Pharmacokinetics*. 3rd ed. Baltimore: Williams & Wilkins, 1995.

Ruifrok, P. G.: Uptake of quaternary ammonium compounds into rat intestinal brush border membrane vesicles. Biochem Pharmacol. **30:** 2637-41, 1981.

Saito, H., Yamamoto, M., Inui, K., AND Hori, R.: Transcellular transport of organic cation across monolayers of kidney epithelial cell line LLC-PK_1. Am J Physiol. **262:** C59-66, 1992.

Saitoh, H., AND Aungst, B. J.: Possible involvement of multiple P-glycoprotein-mediated efflux systems in the transport of verapamil and other organic cations across rat intestine. Pharm Res. **12:** 1304-10, 1995.

Saitoh, H., Kobayashi, M., Sugawara, M., Iseki, K., AND Miyazaki, K.: Carrier-mediated transport system for choline and its related quaternary ammonium compounds on rat intestinal brush-border membrane. Biochim Biophys Acta. **1112:** 153-60, 1992.

Sandker, G. W., Weert, B., Olinga, P., Wolters, H., Slooff, M. J., Meijer, D. K., AND Groothuis, G. M.: Characterization of transport in isolated human hepatocytes. A study with the bile acid taurocholic acid, the uncharged ouabain and the organic cations vecuronium and rocuronium. Biochem Pharmacol. **47:** 2193-200, 1994.

Schaefer, B. C.: Revolutions in rapid amplification of cDNA ends: new strategies for polymerase chain reaction cloning of full-length cDNA ends. Anal Biochem. **227:** 255-73, 1995.

Schali, C., Schild, L., Overney, J., AND Roch-Ramel, F.: Secretion of tetraethylammonium by proximal tubules of rabbit kidneys. Am J Physiol. **245:** F238-46, 1983.

Schaner, M. E., Wang, J., Zevin, S., Gerstin, K. M., AND Giacomini, K. M.: Transient expression of a purine-selective nucleoside transporter ($SPNT_{int}$) in a human cell line (HeLa). Pharm Res. **14:** 1316-21, 1997.

Schinkel, A. H., Mayer, U., Wagenaar, E., Mol, C. A., van Deemter, L., Smit, J. J., van der Valk, M. A., Voordouw, A. C., Spits, H., van Tellingen, O., Zijlmans, J. M., Fibbe, W. E., AND Borst, P.: Normal viability and altered pharmacokinetics in mice lacking mdr1-type (drug-transporting) P-glycoproteins. Proc Natl Acad Sci U S A. **94:** 4028-33, 1997.

Schoemig, E., Spitzenberger, F., Engelhardt, M., Martel, F., Oerding, N., AND Gruendemann, D.: Molecular cloning and characterization of two novel transport proteins from rat kidney. FEBS Lett. **425:** 79-86, 1998.

Schuetz, E. G., Beck, W. T., AND Schuetz, J. D.: Modulators and substrates of P-glycoprotein and cytochrome P4503A coordinately up-regulate these proteins in human colon carcinoma cells. Mol Pharmacol. **49:** 311-8, 1996a.

Schuetz, E. G., Schinkel, A. H., Relling, M. V., AND Schuetz, J. D.: P-glycoprotein: a major determinant of rifampicin-inducible expression of cytochrome P4503A in mice and humans. Proc Natl Acad Sci U S A. **93:** 4001-5, 1996b.

Schweifer, N., AND Barlow, D. P.: The Lx1 gene maps to mouse chromosome 17 and codes for a protein that is homologous to glucose and polyspecific transmembrane transporters. Mamm Genome. **7:** 735-40, 1996.

Schwenk, M.: Drug transport in intestine, liver and kidney. Arch Toxicol. **60:** 37-42, 1987.

Sekine, T., Watanabe, N., Hosoyamada, M., Kanai, Y., AND Endou, H.: Expression cloning and characterization of a novel multispecific organic anion transporter. J Biol Chem. **272:** 18526-9, 1997.

Shire, D., Carillon, V., Kaghad, M., Calandra, B., Rinaldi-Carmona, M., Le Fur, G., Caput, D., AND Ferrara, P.: An amino-terminal variant of the central cannabinoid receptor resulting from alternative splicing. J Biol Chem. **270:** 3726-31, 1995.

Shull, G. E., AND Greeb, J.: Molecular cloning of two isoforms of the plasma membrane Ca^{2+}-transporting ATPase from rat brain. Structural and functional domains exhibit similarity to Na^+,K^+- and other cation transport ATPases. J Biol Chem. **263:** 8646-57, 1988.

Siebert, P. D., Chenchik, A., Kellogg, D. E., Lukyanov, K. A., AND Lukyanov, S. A.: An improved PCR method for walking in uncloned genomic DNA. Nucleic Acids Res. **23:** 1087-8, 1995.

Sigel, E.: Use of *Xenopus* oocytes for the functional expression of plasma membrane proteins. J Membr Biol. **117:** 201-21, 1990.

Simonson, G. D., AND Iwanij, V.: Genomic organization and promoter sequence of a gene encoding a rat liver-specific type-I transport protein. Gene. **154:** 243-7, 1995

Sohn, Y. J., Bencini, A. F., Scaf, A. H., Kersten, U. W., AND Agoston, S.: Comparative pharmacokinetics and dynamics of vecuronium and pancuronium in anesthetized patients. Anesth Analg. **65:** 233-9, 1986.

Sokol, P. P., AND Gates, S. B.: Effect of endogenous and exogenous polyamines on organic cation transport in rabbit renal plasma membrane vesicles. J Pharmacol Exp Ther. **255:** 52-8, 1990.

Sokol, P. P., AND McKinney, T. D.: Mechanism of organic cation transport in rabbit renal basolateral membrane vesicles. Am J Physiol. **258:** F1599-607, 1990.

Sokol, P. P., Holohan, P. D., AND Ross, C. R.: Electroneutral transport of organic cations in canine renal brush border membrane vesicles (BBMV). J Pharmacol Exp Ther. **233:** 694-9, 1985.

Somogyi, A.: Renal transport of drugs: specificity and molecular mechanisms. Clin Exp Pharmacol Physiol. **23:** 986-9, 1996.

Somogyi, A. A., Rumrich, G., Fritzsch, G., AND Ullrich, K. J.: Stereospecificity in contraluminal and luminal transporters of organic cations in the rat renal proximal tubule. J Pharmacol Exp Ther. **278:** 31-6, 1996.

Sperber, A. M.: A new method for the study of renal tubular excretion in birds. Nature. **158:** 131, 1946.

Stachon, A., Schlatter, E., AND Hohage, H.: Dynamic monitoring of organic cation transport processes by fluorescence measurements in LLC-PK-1 cells. Cell Physiol Biochem. **6:** 72-81, 1996.

Stauffer, T. P., Hilfiker, H., Carafoli, E., AND Strehler, E. E.: Quantitative analysis of alternative splicing options of human plasma membrane calcium pump genes [published erratum appears in J Biol Chem 1994 Dec 16;269(50):32022]. J Biol Chem. **268:** 25993-6003, 1993.

Steen, H., AND Meijer, D. K.: Organic cations. Prog Pharmacol Clin Pharmacol. **8:** 239-72, 1991.

Steen, H., Oosting, R., AND Meijer, D. K.: Mechanisms for the uptake of cationic drugs by the liver: a study with tributylmethylammonium (TBuMA). J Pharmacol Exp Ther. **258:** 537-43, 1991.

Steen, H., Merema, M., AND Meijer, D. K.: A multispecific uptake system for taurocholate, cardiac glycosides and cationic drugs in the liver. Biochem Pharmacol. **44:** 2323-31, 1992.

Steen, H., Smit, H., Nijholt, A., Merema, M., AND Meijer, D. K.: Modulators of the protein kinase C system influence biliary excretion of cationic drugs. Hepatology. **18:** 1208-15, 1993.

Steward, M. C., AND Case, R. M. "Principles of ion and water transport across epithelia." In *Gastrointestinal Secretion.*, edited by J. S. Davison, 1-31. London/Boston: Wright, 1989.

Strehler, E. E., Strehler-Page, M. A., Vogel, G., AND Carafoli, E.: mRNAs for plasma membrane calcium pump isoforms differing in their regulatory domain are generated by alternative splicing that involves two internal donor sites in a single exon. Proc Natl Acad Sci U S A. **86:** 6908-12, 1989.

Suzuki, H., AND Sugiyama, Y.: Kinetic analysis of the disposition of hydrophilic drugs in the central nervous system (CNS): Prediction of the CNS disposition from the transport properties in the blood-brain and blood-cerebrospinal fluid barriers. Yakugaku Zasshi. **114:** 950-71, 1994.

Sweet, D. H., Wolff, N. A., AND Pritchard, J. B.: Expression cloning and characterization of ROAT1. The basolateral organic anion transporter in rat kidney. J Biol Chem. **272:** 30088-95, 1997 (Abstr.).

Takahashi, Y., Itoh, T., Kobayashi, M., Sugawara, M., Saitoh, H., Iseki, K., Miyazaki, K., Miyazaki, S., Takada, M., AND Kawashima, Y.: The transport mechanism of an organic cation, disopyramide, by brush-border membranes. Comparison between renal cortex and small intestine of the rat. J Pharm Pharmacol. **45:** 419-24, 1993.

Takano, M., Inui, K., Okano, T., Saito, H., AND Hori, R.: Carrier-mediated transport systems of tetraethylammonium in rat renal brush-border and basolateral membrane vesicles. Biochim Biophys Acta. **773:** 113-24, 1984.

Takeda, H., Wang, W., AND Moseley, R. H.: Functional expression of a rat liver organic cation transporter in *Xenopus* oocytes. Gastroenterology. **106:** A994, 1994 (Abstr.).

Tamai, I., Yabuuchi, H., Nezu, J., Sai, Y., Oku, A., Shimane, M. AND Tsuji, A.: Cloning and characterization of a novel human pH-dependent organic cation transporter, OCTN1. FEBS Lett. **419:** 107-11, 1997.

Terao, T., Hisanaga, E., Sai, Y., Tamai, I., AND Tsuji, A.: Active secretion of drugs from the small intestinal epithelium in rats by P-glycoprotein functioning as an absorption barrier. J Pharm Pharmacol. **48:** 1083-9, 1996.

Terashita, S., Dresser, M. J., Zhang, L., Gray, A. T., Yost, S. C., AND Giacomini, K. M.: Molecular cloning and functional expression of a rabbit renal organic cation transporter. Biochim Biophys Acta. **1369:** 1-6, 1998.

Tomita, Y., Otsuki, Y., Hashimoto, Y., AND Inui, K.: Kinetic analysis of tetraethylammonium transport in the kidney epithelial cell line, LLC-PK_1. Pharm Res. **14:** 1236-40, 1997.

Turnheim, K., AND Lauterbach, F.: Secretion of monoquaternary ammonium compounds by guinea pig small intestine in vivo. Naunyn Schmiedebergs Arch Pharmacol. **299:** 201-5, 1977a.

Turnheim, K., AND Lauterbach, F.: Absorption and secretion of monoquaternary ammonium compounds by the isolated intestinal mucosa. Biochem Pharmacol. **26:** 99-108, 1977b.

Turnheim, K., AND Lauterbach, F.: Interaction between intestinal absorption and secretion of monoquaternary ammonium compounds in guinea pigs--a concept for the absorption kinetics of organic cations. J Pharmacol Exp Ther. **212:** 418-24, 1980.

Turnheim, K., Lauterbach, F., AND Kolassa, N.: Intestinal transfer of the quaternary ammonium compound N-methyl-scopolamine by two transport mechanisms in series. Biochem Pharmacol. **26:** 763-7, 1977.

Ueda, K., Clark, D. P., Chen, C. J., Roninson, I. B., Gottesman, M. M., AND Pastan, I.: The human multidrug resistance (mdr1) gene. cDNA cloning and transcription initiation. J Biol Chem. **262:** 505-8, 1987.

Ullrich, K. J.: Specificity of transporters for 'organic anions' and 'organic cations' in the kidney. Biochim Biophys Acta. **1197:** 45-62, 1994.

Ullrich, K. J., AND Rumrich, G.: Luminal transport system for choline$^+$ in relation to the other organic cation transport systems in the rat proximal tubule. Kinetics, specificity: alkyl/arylamines, alkylamines with OH, O, SH, NH_2, ROCO, RSCO and H_2PO_4-groups, methylaminostyryl, rhodamine, acridine, phenanthrene and cyanine compounds. Pflugers Arch. **432:** 471-85, 1996.

Ullrich, K. J., Papavassiliou, F., David, C., Rumrich, G., AND Fritzsch, G.: Contraluminal transport of organic cations in the proximal tubule of the rat kidney. I. Kinetics of N^1-methylnicotinamide and tetraethylammonium, influence of K^+, HCO_3^-, pH; inhibition by aliphatic primary, secondary and tertiary amines and mono- and bisquaternary compounds. Pflugers Arch. **419:** 84-92, 1991.

Ullrich, K. J., Rumrich, G., David, C., AND Fritzsch, G.: Bisubstrates: substances that interact with both, renal contraluminal organic anion and organic cation transport systems. II. Zwitterionic substrates: dipeptides, cephalosporins, quinolone-carboxylate gyrase inhibitors and phosphamide thiazine carboxylates; nonionizable substrates: steroid hormones and cyclophosphamides. Pflugers Arch. **425:** 300-12, 1993.

Valdivieso, L., Giacomini, K. M., Nelson, W. L., Pershe, R., AND Blaschke, T. F.: Stereoselective binding of disopyramide to plasma proteins. Pharm Res. **5:** 316-8, 1988.

van Asperen, J., van Tellingen, O., Sparreboom, A., Schinkel, A. H., Borst, P., Nooijen, W. J., AND Beijnen, J. H.: Enhanced oral bioavailability of paclitaxel in mice

treated with the P-glycoprotein blocker SDZ PSC 833. Br J Cancer. **76:** 1181-3, 1997.

Van der Aa, E. M., Wouterse, A. C., Copius Peereboom-Stegeman, J. H., AND Russel, F. G.: Inhibition of choline uptake in syncytial microvillus membrane vesicles of human term placenta. Specificity and nature of interaction. Biochem Pharmacol. **50:** 1873-8, 1995.

Van der Aa, E. M., Wouterse, A. C., Verrijt, C. E., Peereboom-Stegeman, J. H., AND Russel, F. G.: Uptake of cimetidine into syncytial microvillus membrane vesicles of human term placenta. J Pharmacol Exp Ther. **276:** 219-22, 1996.

Van Dyke, R. W., Faber, E. D., AND Meijer, D. K.: Sequestration of organic cations by acidified hepatic endocytic vesicles and implications for biliary excretion. J Pharmacol Exp Ther. **261:** 1-11, 1992.

Varoqui, H., Meunier, F. M., Meunier, F. A., Molgo, J., Berrard, S., Cervini, R., Mallet, J., Israel, M., AND Diebler, M. F.: Expression of the vesicular acetylcholine transporter in mammalian cells. Prog Brain Res. **109:** 83-95, 1996.

Villalobos, A. R., Parmelee, J. T., AND Pritchard, J. B.: Functional characterization of choroid plexus epithelial cells in primary culture. J Pharmacol Exp Ther. **282:** 1109-16, 1997.

von Heijne, G.: Membrane protein structure prediction. Hydrophobicity analysis and the positive-inside rule. J Mol Biol. **225:** 487-94, 1992.

von Heijne, G.: Membrane protein assembly: rules of the game. Bioessays. **17:** 25-30, 1995.

Vonk, R. J., Jekel, P. A., Meijer, K. F., AND Hardonk, M. J.: Transport of drugs in isolated hepatocytes. The influence of bile salts. Biochem Pharmacol. **27:** 397-405, 1978a.

Vonk, R. J., Scholtens, E., Keulemans, G. T., AND Meijer, D. K.: Choleresis and hepatic transport mechanisms. IV. Influence of bile salt choleresis on the hepatic

transport of the organic cations, D-tubocurarine and N4 -acetyl procainamide ethobromide. Naunyn Schmiedebergs Arch Pharmacol. **302:** 1-9, 1978b.

Wacher, V. J., Wu, C. Y., AND Benet, L. Z.: Overlapping substrate specificities and tissue distribution of cytochrome P450 3A and P-glycoprotein: implications for drug delivery and activity in cancer chemotherapy. Mol Carcinog. **13:** 129-34, 1995.

Walsh, R. C., Sweet, D. H., Hall, L. A., AND Pritchard, J. B.: Expression cloning and characterization of a novel organic cation transporter from rat kidney. FASEB J. **10:** A127, 1996 (Abstr.).

Wang, J., Schaner, M. E., Thomassen, S., Su, S.-F., Piquette-Miller, M., AND Giacomini, K. M.: Functional and molecular characteristics of Na^+-dependent nucleoside transporters. Pharm Res. **14:** 1524-32, 1997.

Waser, P. G., Wiederkehr, H., Sin-Ren, A. C., AND Kaiser-Schonenberger, E.: Distribution and kinetics of ^{14}C-vecuronium in rats and mice. Br J Anaesth. **59:** 1044-51, 1987.

Weiner, I. M. "Organic acids and bases and uric acid." In *The Kidney: Physiology and Pathophysiology*, edited by D. W. Seldin and G. Giebisch, 1703-24. New York: Raven, 1985.

Whittico, M. T., Gang, Y. A., AND Giacomini, K. M.: Cimetidine transport in isolated brush border membrane vesicles from bovine choroid plexus. J Pharmacol Exp Ther. **255:** 615-23, 1990.

Whittico, M. T., Hui, A. C., AND Giacomini, K. M.: Preparation of brush border membrane vesicles from bovine choroid plexus. J Pharmacol Methods. **25:** 215-27, 1991.

Wolkoff, A. W., Johansen, K. L., AND Goeser, T.: The isolated perfused rat liver: preparation and application. Anal Biochem. **167:** 1-14, 1987.

Wong, M. H., Oelkers, P., AND Dawson, P. A.: Identification of a mutation in the ileal sodium-dependent bile acid transporter gene that abolishes transport activity. J Biol Chem. **270:** 27228-34, 1995.

Wright, S. H.: Transport of N^1-methylnicotinamide across brush border membrane vesicles from rabbit kidney. Am J Physiol. **249:** F903-11, 1985.

Wright, S. H.: Characterization of renal brush-border and basolateral membrane transporters for organic cations. Cell Physiol Biochem. **6:** 112-22, 1996.

Wright, S. H., AND Wunz, T. M.: Transport of tetraethylammonium by rabbit renal brush-border and basolateral membrane vesicles. Am J Physiol. **253:** F1040-50, 1987.

Wright, S. H., AND Wunz, T. M.: Mechanism of *cis*- and *trans*-substrate interactions at the tetraethylammonium/proton exchanger of rabbit renal brush-border membrane vesicles. J Biol Chem. **263:** 19494-7, 1988.

Wright, S. H., Wunz, T. M., AND Wunz, T. P.: A choline transporter in renal brush-border membrane vesicles: energetics and structural specificity. J Membr Biol. **126:** 51-65, 1992.

Wright, S. H., Wunz, T. M., AND Wunz, T. P.: Structure and interaction of inhibitors with the TEA-H^+ exchanger of rabbit renal brush border membranes. Pflugers Arch. **429:** 313-324, 1995.

Wrighton, S. A., AND Ring, B. J.: Inhibition of human CYP3A catalyzed 1'-hydroxymidazolam formation by ketoconazole, nifedipine, erythromycin, cimetidine, and nizatidine. Pharm Res. **11:** 921-4, 1994.

Wu, X., Ganapathy, M. E., Leibach, F. H., AND Ganapathy, V.: Cloning and functional characterization of an organic cation transporter (OCT3) from mouse kidney. FASEB J. **12:** A1042, 1998a (Abstr.).

Wu, X., Prasad, P. D., Leibach, F. H., AND Ganapathy, V.: cDNA sequence, transport function, and genomic organization of human OCTN2, a new member of the

organic cation transporter family. Biochem Biophys Res Commun. **246:** 589-95, 1998b.

Yamazaki, M., Suzuki, H., AND Sugiyama, Y.: Recent advances in carrier-mediated hepatic uptake and biliary excretion of xenobiotics. Pharm Res. **13:** 497-513, 1996.

Yuan, G., Ott, R. J., Salgado, C., AND Giacomini, K. M.: Transport of organic cations by a renal epithelial cell line (OK). J Biol Chem. **266:** 8978-86, 1991.

Zevin, S., Schaner, M. E., Illsley, N. P., AND Giacomini, K. M.: Guanidine transport in a human choriocarcinoma cell line (JAR). **14:** 401-5, 1997.

Zhang, L., Chan, J. K., Piquette-Miller, M. Giacomini, K. M.: Expression of a rat renal guanidine transporter in *Xenopus laevis* oocyte. Pharm Res. **12:** S352, 1995 (Abstr.).

Zhang, L., Chun, J. K., AND Giacomini, K. M.: Cloning and expression of a rat intestinal organic cation transporter (OCT1) and a novel OCT1 isoform. Pharm Res. **13:** S410, 1996 (Abstr.).

Zhang, L., Dresser, M. J., Chun, J. K., Babbitt, P. C., AND Giacomini, K. M.: Cloning and functional characterization of a rat renal organic cation transporter isoform (rOCT1A). J Biol Chem. **272:** 16548-54, 1997a.

Zhang, L., Dresser, M. J., Gray, A. T., Yost, S. C., Terashita, S., AND Giacomini, K. M.: Cloning and functional expression of a human liver organic cation transporter. Mol Pharmacol. **51:** 913-21, 1997b.

Zhang, L. Chun, J. K., Lau, E. K., AND Giacomini, K. M.: Transport of guanidine in rat renal brush-border membrane vesicles. Pharm Res. **14:** S333, 1997c (Abstr.).

Zhang, L., Brett, C. M., AND Giacomini, K. M.: Role of organic cation transporters in drug absorption and elimination. Ann Rev Pharmacol Toxicol **38:** 431-60, 1998a.

Zhang, L., Schaner, M. S., AND Giacomini, K. M.: Functional characterization of an organic cation transporter (hOCT1) in a transiently transfected human cell line (HeLa). J Pharmacol Exp Ther., **286:** 354-61, 1998b.

Zhang, L., Gorset, W., AND Giacomini, K. M.: The interaction of n-tetraakylammonium compounds with a human organic cation transporer, hOCT1, 1998c (submitted).

Zhang, Y., Guo, X., Lin, E. T., AND Benet, L. Z.: Overlapping substrate specificities of cytochrome P450 3A and P-glycoprotein for a novel cysteine protease inhibitor. Drug Metab Dispos. **26:** 360-6, 1998d.

APPENDIX

INTERACTIONS OF VARIOUS COMPOUNDS WITH hOCT1 IN TRANSFECTED HeLa CELLS

A.1 Objectives

To characterize the role of hOCT1 in the elimination of various drugs, we studied the interactions of various compounds with hOCT1 in transfected HeLa cells. We specifically studied the interactions of (1) β-blockers, (2) azole compounds and (3) stereoisomers with hOCT1.

A.2 Materials and Methods

A.2.1 Construction and Isolation of Plasmid DNA for Transfection

hOCT1 cDNA was obtained by RT-PCR as previously described (Zhang *et al.*, 1997b; Chapter 6). After gel purification, the PCR products were ligated to the mammalian expression vector pTargeT (Promega, Madison, WI) using T4 DNA ligase followed by transformation into DH5α competent cells (Gibco BRL, Gaithersburg, MD). The construct with the cDNA under the CMV promoter (sense orientation), pTargeT-hOCT1, was identified by restriction enzyme analysis and the sequence was confirmed by DNA sequencing (Biomolecular Resource Center, UCSF, CA). The empty vector of pTargeT

was constructed by cutting the hOCT1 insert out of pTargeT-hOCT1 with *Eco*R I followed by gel purification and ligation. The construct of empty vector was confirmed by restriction enzyme analysis.

DNA for transfection was isolated with the QIAGEN Endo-free DNA isolation kit (QIAGEN Inc., Santa Clarita, CA). Several different DNA preparations were carried out for the study. The DNA concentration ranged from 1.7 to 4.0 μg/μl as determined by UV spectroscopy. The DNA was stored in endotoxin-free TE buffer (QIAGEN) at -20°C until use.

A.2.2 HeLa Cell Culture and Transfection

HeLa cells were obtained from the UCSF Cell Culture Facility. Original stocks were from American Type Culture Collection (ATCC, Rockville, MD). Passages from 3 to 18 were used in the studies. The cells were grown at 37°C in a 5% CO_2/95% air humidified atmosphere. The medium was Eagle's minimum essential medium with Earle's balanced salt supplemented with 2 mM glutamine, 100 IU/ml penicillin, 100 μg/ml streptomycin, 0.25 μg/ml fungizone , and 10% (vol/vol) fetal bovine serum. The cells were maintained in Nunc cell culture flasks (Nalge Nunc International, Naperville, IL). The cells were seeded at a density of 1.6-1.8 X 10^5 cells/well in 12-well tissue culture plates (Corning Costar Corp, Cambridge, MA) 24 hours prior to transfection. The cells were transfected with a cationic liposome technique using LIPOFECTAMINE (2 mg/ml, Gibco, BRL) following a modified protocol from Gibco, BRL. For each well, 100 μl Opti-MEM media (Gibco, BRL) was incubated with 1 μg DNA and another 100 μl Opti-MEM media with the lipid (3.25 μl). The two solutions were then mixed together and incubated for 30-35 minutes at room temperature. After incubation, 800 μl Opti-MEM media was added to the previous mixture. The final mixture (1 ml) was applied to each well after rinsing the cells with the Opti-MEM media once. The cells were exposed to the

lipid-DNA complex for 18 hours prior to replacing the transfection media by the fresh standard culture media.

A.2.3 Uptake Measurements

The uptake studies were carried out between approximately 40-44 hours post transfection. Cells were incubated and washed with phosphate buffered saline (PBS) once before the uptake studies. Subsequently, the cells were incubated at room temperature or 4°C (for temperature-dependence study) with 5 or 10 μM ^{14}C-TEA (55 mCi/mmol, American Radiolabeled Chemicals, St. Louis, MO) in 0.5 ml of PBS. For inhibition and IC_{50} studies, various amounts of the tested compounds were included in the reaction mixture. Incubation was stopped by rinsing the cells once with 2 ml of ice-cold PBS and twice with 1 ml of ice-cold PBS buffer. After solubilizing the cells with 1 ml of 0.5% Triton-X 100, 0.5 ml of sample was assayed using liquid scintillation counting (Beckman, Palo Alto, CA).

In *trans*-stimulation studies, each well of cells was preincubated with either 0.5 ml PBS (control) or 0.5 ml PBS plus the indicated concentration of unlabeled compounds at 37°C for one hour. Cells were then rinsed with 1 ml of ice-cold PBS twice before the uptake studies.

A.2.4 Protein Assay

For each plate used in the uptake study, 2 wells were saved for protein analysis. Cells were washed with PBS buffer and then solubilized with 0.5 ml of 1N NaOH. After 2 hours, the solution was neutralized with 0.5 ml of 1N HCl. 100 μl of solubilized cells were used for the protein assay using the Bio-Rad reagent (Bio-Rad, Hercules, CA). Absorbance was read at 595 nm and the amount of protein was calculated from the standard curve generated by using the known amounts of bovine serum albumin as standards.

A.2.5 Data Analysis

Uptake values are presented as mean ± standard deviation (SD). In each experiment, a minimum of two wells was used to generate each data point and each experiment was repeated at least once. The IC_{50} was estimated by a sigmoidal inhibition model and was fit to the equation $V=V_0/(1+(I/IC_{50})^n)$ by nonlinear regression. V is the uptake of TEA in the presence of the inhibitor, V_0 is the uptake of TEA in the absence of inhibitor, I is the inhibitor concentration and n is the Hill coefficient. Data from nonlinear regression are presented as mean ± SD. Statistical analysis was carried out by comparing the treated to the controls from the same experiments using an unpaired Student's *t*-test (Primer of Biostatistics software, Version 3, written by Stanton A. Glantz, McGraw-Hill Companies, 1991), and a value of $p < 0.05$ was considered significant.

A.2.6 Materials

All the media and buffers used to maintain the cells were obtained from the UCSF Cell Culture Facility unless otherwise indicated. All chemicals were obtained from Sigma (St. Louis, MO) or Fisher (Pittsburgh, PA) or as indicated. Stereoisomers, R-, S-verapamil; (+)-, (-)-gallapamil; (+)-, (-)-pindolol; (R)-, (S)-metoprolol; and (+)-, (-)-propranolol were kindly provided by Dr. Wendel Nelson at University of Washington. Azole compounds were kindly provided by Drs. Laurent Salphati and Leslie Benet at UCSF. ^{14}C-TEA (55 mCi/mmol) was purchased from American Radiolabeled Chemicals (St. Louis, MO).

A.3 Results

A.3.1 Inhibition Studies

IC_{50} values of various compounds in inhibiting ^{14}C-TEA uptake mediated by hOCT1 were determined by non-linear regression analysis. Table A.1 listed the IC_{50} values of β-blockers in interacting with ^{14}C-TEA transport mediated by hOCT1 and Table A.2 lists the IC_{50} values for azole compounds in interacting with hOCT1. All of these compounds potently inhibited ^{14}C-TEA transport mediated by hOCT1. It appears that ketoconazole is the most potent inhibitor of TEA transport mediated by hOCT1.

Table A.1 IC_{50} values of β-blockers in inhibiting ^{14}C-TEA uptake in hOCT1 DNA-transfected HeLa Cells

Compound	IC_{50} μM	n
Acebutolol	98 ± 24	0.79 ± 0.15
(±)-Metoprolol	217 ± 44	0.78 ± 0.12
(±)-Pindolol	64 ± 44	0.52 ± 0.18
(±)-Propranolol	22 ± 11	0.55 ± 0.12

Data are presented as mean ± SD from one representative experiment.

Table A.2 IC_{50} values of azole compounds in inhibiting ^{14}C-TEA uptake in hOCT1 DNA-transfected HeLa Cells

Compound	IC_{50} μM	n
Ketoconazole	0.066 ± 0.026	0.75 ± 0.32
(±)-Miconazole	0.59 ± 0.36	0.59 ± 0.36
Terconazole	6.50 ± 3.77	0.71 ± 0.26
Itraconazole	39.7 ± 24.5	0.84 ± 0.40
Clotrimazole	3.37 ± 2.58	1.22 ± 0.96

Data are presented as mean ± SD from one representative experiment.

To test whether there are stereoselective interactions of organic cations with hOCT1, the IC_{50} values of pairs of isomers were determined and compared (Table A.3). IC_{50} values were not significantly different for most of pairs except those for pindolol. Namely, (+)-pindolol is approximately 4-fold more potent than (-)-pindolol in inhibiting TEA transport by hOCT1.

Table A.3 IC_{50} values of stereoisomers in inhibiting ^{14}C-TEA uptake in hOCT1 DNA-transfected HeLa Cell

Compound	IC_{50} μM	n
(R)-Metoprolol	277 ± 126	1.02 ± 0.53
(S)-Metoprolol	231 ± 97	1.19 ± 0.57
(+)-Pindolol	26 ± 8	0.49 ± 0.08
(-)-Pindolol	80 ± 13 *	0.78 ± 0.39
(+)-Propranolol	7.8 ± 1.2	0.48 ± 0.06
(-)-Propranolol	16 ± 9	0.66 ± 0.21
(+)-Verapamil	3.5 ± 1.6	1.14 ± 0.51
(-)-Verapamil	2.0 ± 1.3	0.49 ± 0.14
(+)-Gallapamil	2.3 ± 1.6	0.70 ± 0.29
(-)-Gallapamil	2.2 ± 0.8	1.48 ± 0.68

Data are presented as mean ± SD from one representative experiment. * $p < 0.05$

A.3.2 Trans-Stimulation Studies

To determine whether the compounds inhibited TEA transport by hOCT1 are also translocated by hOCT1, *trans*-stimulation studies were performed. As shown in Figure A.1, after preincubation of the pTargeT-hOCT1-transfected HeLa cells with TEA (2 mM) for one hour at 37°C, ^{14}C-TEA uptake was significantly enhanced ($p < 0.05$). In contrast, preincubation of cells with 200 μM acebutolol, 1 mM (±)-metoprolol, 200 μM (±)-pindolol, 200 μM (±)-propranolol, and (±)-gallapamil did not result in a significant change in ^{14}C-TEA uptake and preincubation of cells with 50 μM (±)-verapamil resulted in a significant decrease (apparent "*trans*-inhibition") of ^{14}C-TEA uptake ($p < 0.05$).

Trans-stimulations studies were also conducted with the azole compounds (Figure A.2). As a positive control, preincubation of the pTargeT-hOCT1-transfected HeLa cells with TEA (2 mM) for one hour at 37°C resulted in enhanced ^{14}C-TEA uptake. In contrast, preincubation of cells with 0.5 μM ketoconazole, 10 μM miconazole and 50 μM terconazole did not result in an enhancement in ^{14}C-TEA uptake.

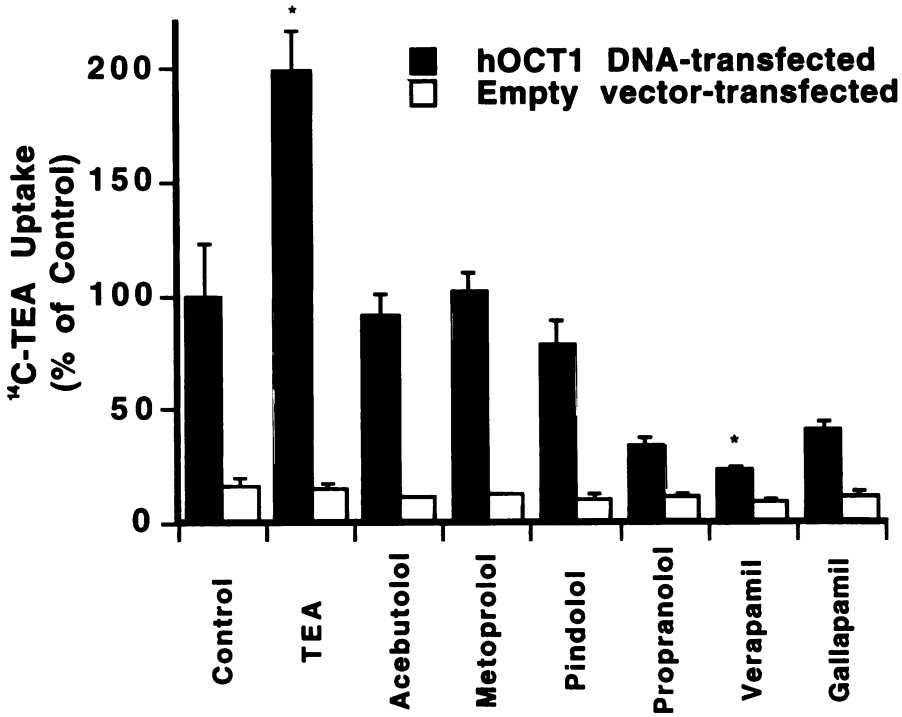

Figure A.1 *Trans*-stimulation of ^{14}C-TEA uptake in pTargeT-hOCT1 transfected HeLa cells. The uptake (at 20 min) of ^{14}C-TEA (10 μM) was measured after 60 min incubation of pTargeT-hOCT1-transfected cells and the empty vector-transfected cells with PBS (control) or PBS containing 2 mM TEA, 200 μM acebutolol, 1 mM (±)-metoprolol, 200 μM (±)-pindolol, 200 μM (±)-propranolol, 50 μM (±)-verapamil and 50 μM (±)-gallapamil, respectively at 37°C. Data represent the mean ± SD (n = 2) from one experiment. * $p < 0.05$ as compared to the uptake value in hOCT1 DNA-transfected cells preincubated with PBS.

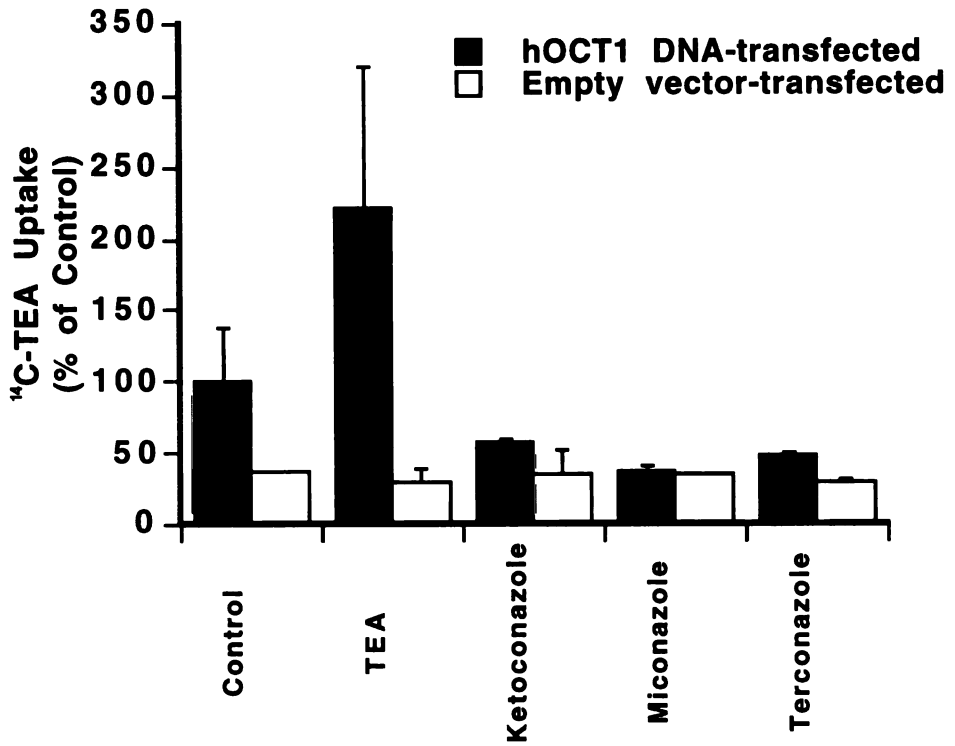

Figure A.2 *Trans*-stimulation of ^{14}C-TEA uptake in pTargeT-hOCT1 transfected HeLa cells. The uptake (at 20 min) of ^{14}C-TEA (10 μM) was measured after 60 min incubation of pTargeT-hOCT1-transfected cells and the empty vector-transfected cells with PBS (control) or PBS containing 2 mM TEA, 0.5 μM ketoconazole, 10 μM miconazole and 50 μM terconazole, respectively at 37°C. Data represent the mean ± SD (n = 2) from one experiment.

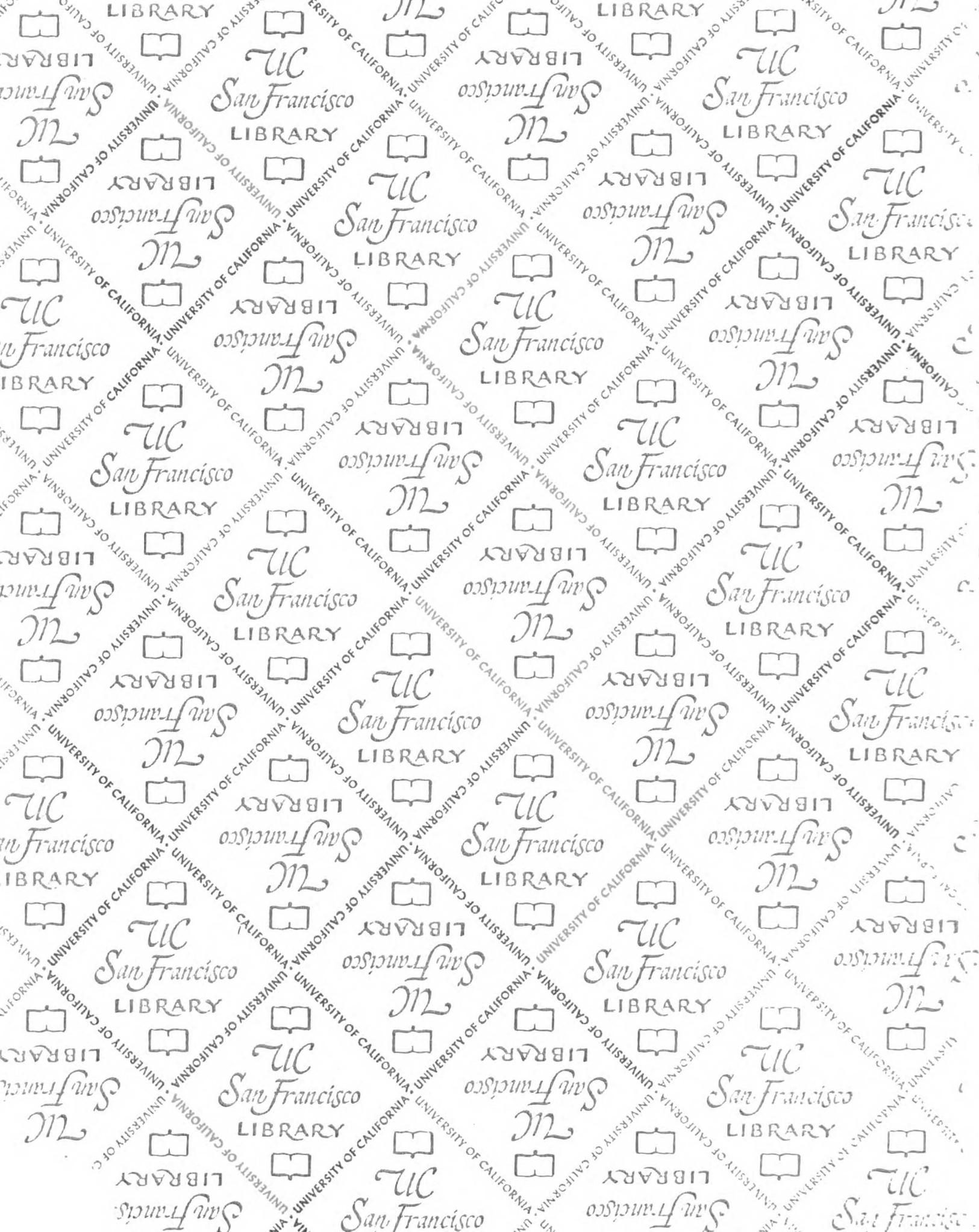
UC
San Francisco
LIBRARY
UNIVERSITY OF CALIFORNIA · UNIVERSITY OF CALIFORNIA